

Electronic Thesis and Dissertation Repository

---

12-13-2013 12:00 AM

## The Development of A New Dry Powder Inhaler

Xi Zhang

*The University of Western Ontario*

Supervisor

Jesse Zhu

*The University of Western Ontario*

Graduate Program in Chemical and Biochemical Engineering

A thesis submitted in partial fulfillment of the requirements for the degree in Doctor of  
Philosophy

© Xi Zhang 2013

Follow this and additional works at: <https://ir.lib.uwo.ca/etd>



Part of the [Biomedical Devices and Instrumentation Commons](#), and the [Pharmaceutical Preparations Commons](#)

---

### Recommended Citation

Zhang, Xi, "The Development of A New Dry Powder Inhaler" (2013). *Electronic Thesis and Dissertation Repository*. 1765.

<https://ir.lib.uwo.ca/etd/1765>

This Dissertation/Thesis is brought to you for free and open access by Scholarship@Western. It has been accepted for inclusion in Electronic Thesis and Dissertation Repository by an authorized administrator of Scholarship@Western. For more information, please contact [wlsadmin@uwo.ca](mailto:wlsadmin@uwo.ca).

THE DEVELOPMENT OF A NEW DRY POWDER INHALER  
(Thesis format: Monograph)

by

Xi Zhang

Graduate Program in Chemical & Biochemical Engineering

A thesis submitted in partial fulfillment  
of the requirements for the degree of  
Doctor of Philosophy

The School of Graduate and Postdoctoral Studies  
The University of Western Ontario  
London, Ontario, Canada

© Xi Zhang 2013

## Abstract

A new dry powder inhaler (DPI) for respiratory drug delivery was developed. This novel device is characterized by a micro-dose, passive delivery and multiple doses individually sealed in one replaceable disk. The micro-dose delivery system uses only a small amount of excipient, such as 2-3mg lactose, thereby improving the drug delivery efficiency. The passive delivery method eliminates the need for coordination between breath and device actuation such as the pressure metered dose inhaler (pMDI). Finally, 14 doses on a disk reduce the need to frequently change dosage disks. In addition, each dose is effectively protected by a blister package to minimize damage from moisture and oxygen.

A comprehensive evaluation on key parameters, including dosage emission, air flow resistance and fine particle fraction, has been conducted. The air resistance of our device is about  $0.06 \text{ kPa}^{0.5}\cdot\text{min/liter}$ , slightly higher than several marketed products but close to Inhalator®. The *in vitro* performance results show that this new dry powder inhaler is able to achieve a high efficiency for drug delivery, with 10% of drug remaining in the device. This device can also effectively disperse drug particles to acquire a high fine particle fraction (FPF) as 50%. A primary stability research demonstrates that the FPF of a formulation containing 5%-fine additive would stay at 40% when being accelerated for 3 months. Furthermore, comparative studies between this novel inhaler and typical marketed products –such as Diskus®, Turbuhaler® and Aerolizer®, show that when combined with suitable formulations, the FPF of our device could be about 25% as Diskus® and Aerolizer®, or above 40% as Turbuhaler® and Clickhaler®. When using the same powder, our device shows a FPF of 50%, similar as Clickhaler® and Aerolizer® and higher than Twister®, indicating similar or better performance of our inhaler device to disperse drug particles.

Because no existing powder filling system could satisfy the filling requirements of this new inhaler, a new powder dispensing and packaging system was developed. The new powder filling system designed and implemented in our lab was evaluated and optimized to improve the uniformity of filling weight and drug content among disks/blisters. The relative standard deviation (RSD) of filling weight among disks and blisters is 1~3% and 6~8% respectively.

The uniformity of drug content among disks, with a RSD from 2~5%, demonstrate the filling system could completely meet the requirements of the inhaler development.

Suitable drug formulations for this new DPI were also developed, including research and optimization of powder composition and processing. The preparation of a uniform drug-lactose blend was investigated, including the mixing method, mixing time & speed, and mixing sequence. The composition studies are conducted to better understand the effect of the drug particle and excipient on the drug delivery. Experiments show that the powder composition and processing have a significant influence on the *in vitro* performance, which can be controlled and adjusted to obtain the desired results. For example, when increasing the ratio of fine additive from 0% to 20%, the FPF is increased from 20% to 45%. Meanwhile, if the mixing time is extended from 2min to 10min, the FPF experiences a drop from 35% to 22%.

With the optimization of powder composition and processing, development of the powder filling system and implement of the new inhaler device, this novel inhaler can deliver 2-3mg powder per dose with an adjustable fine particle fraction from 25%-50%.

## Keywords

Respiratory drug delivery, dry powder inhaler, active pharmaceutical ingredient, lactose, carrier, powder filling, powder formulation, *in vitro* evaluation, delivered drug content uniformity, fine particle fraction, laser diffraction size measurement, air flow resistance, blend content uniformity, powder mixing.



## Acknowledgments

I wish to express my deepest gratefulness to Prof. Jesse Zhu for his encouragement, guidance and continuous support throughout this endeavor. His meticulous supervision not only ensured the successful fulfillment of this study but also brought great improvement of my research skills, which is adequate for me to enjoy forever. Besides his abundant knowledge, his approach to research and solution to problems will be of great value to me in my future work.

Much appreciation is extended to Ms. Ying Ma for her helpful discussion and suggestions on my research and thesis. Thanks for her generous help on the design and manufacture of the critical devices. That ensures this research being able to proceed smoothly. I would also like to express my appreciation to Prof. Fang Jin at Shanghai Institute of Pharmaceutical Industry, for leading me into the field of respiratory drug delivery and supporting me to get this excellent opportunity for further education.

Many thanks go to Mr. Wen for his work and sincere help. I would also like to say thanks to Ms. Hao for her hard work, who worked with me for 2 years. Meanwhile, thanks also go to all members of the project team, since I learned a lot from them.

Last but not least, I would like to express my love and gratitude to my parents for their love and dedication to my education. No words could express my gratitude to my wife who provides continuous support without any reservation.

# Table of Contents

Abstract.....	ii
Acknowledgments .....	iv
Table of Contents.....	v
List of Tables .....	x
List of Figures .....	xvi
Chapter 1.....	1
1 General Introduction .....	1
1.1 Objectives .....	1
1.2 Thesis Overview .....	2
1.3 Major Contributions.....	3
Chapter 2.....	4
2 Literature Review.....	4
2.1 Respiratory Drug Delivery.....	4
2.1.1 The advantages and application of respiratory drug delivery.....	4
2.1.2 Deposition of drug particles in respiratory tract .....	7
2.1.3 Common respiratory drug delivery methods .....	8
2.2 Devices for Dry Powder Inhalation .....	9
2.2.1 Single unit dose DPI .....	10
2.2.2 Multiple unit dose DPI.....	11
2.2.3 Multiple dose DPI.....	12
2.2.4 Active devices.....	13
2.3 Filling Device for Dry Powder Inhaler .....	14
2.3.1 Powder filling by volume .....	14
2.3.2 Powder filling by weight.....	17

2.3.3	Other novel metering device.....	18
2.4	Formulation and Process for Dry Powder Inhaler .....	19
2.4.1	Inter-particle forces in DPI formulation .....	19
2.4.2	Carrier for DPI formulation .....	21
2.4.3	Additives.....	23
2.4.4	Powder preparation.....	23
2.5	<i>In vitro</i> Evaluation for Dry Powder Inhaler.....	24
2.5.1	Inertial impaction method to characterize particle size .....	25
2.5.2	Other particle sizing technologies.....	26
2.5.3	Delivered dose content uniformity tests .....	28
Chapter 3	.....	29
3	Materials and Methods.....	29
3.1	Brief Introduction .....	29
3.2	Analytical Method .....	29
3.2.1	Physical property analysis .....	29
3.2.2	HPLC method for content analysis.....	33
3.2.3	<i>In vitro</i> method for particle Size characterization .....	35
3.3	Dry Powder Inhaler Device .....	41
3.3.1	Evaluation of marketed dry powder inhalers.....	41
3.3.2	Design of a novel dry powder inhaler device .....	44
3.4	Dry Powder Inhaler Filling Device.....	49
3.4.1	Design and implement of packaging system .....	49
3.4.2	Design and implement of powder filling system.....	51
3.4.3	Evaluation of powder filling uniformity.....	53
3.5	Dry Powder Inhaler Formulation.....	55
3.5.1	Powder preparation.....	55

3.5.2	Composition of powder formulation.....	59
3.6	Discussion.....	60
Chapter 4.....		62
4	Validation of Analytical Method .....	62
4.1	Brief Introduction .....	62
4.2	Validation of HPLC Method for Content Analysis .....	62
4.2.1	Validation of suitability, specificity.....	63
4.2.2	Validation of sensitivity and linearity.....	64
4.2.3	Validation of precision, reproducibility and intermediate precision .....	66
4.2.4	Validation of solution stability, accuracy and durability.....	67
4.3	Validation of Size Characterization Methods.....	69
4.3.1	Validation of laser diffraction size measurement .....	69
4.3.2	Validation of inertial impaction size measurement .....	70
4.4	Discussion.....	75
Chapter 5.....		78
5	Evaluation Results of Dry Powder Inhalers.....	78
5.1	Brief Introduction .....	78
5.2	Evaluation of Marketed Dry Powder Inhaler Devices.....	78
5.2.1	The air resistance and delivered dose content uniformity .....	78
5.2.2	The inertial impaction test .....	81
5.3	Primary Evaluation and Design Improvements of the Novel Inhaler.....	84
5.3.1	Primary evaluation.....	84
5.3.2	Design improvement.....	85
5.4	Parallel Comparison with the Marketed Inhalers .....	92
5.5	Discussions .....	94
Chapter 6.....		99

6	Evaluation of Dry Powder Filling Device.....	99
6.1	Brief Introduction .....	99
6.2	Uniformity of Dry Powder Filling Device.....	100
6.2.1	Filling weight uniformity among different disks .....	100
6.2.2	Filling weight uniformity among blisters on one disk.....	104
6.2.3	Drug content uniformity among different disks .....	111
6.2.4	Drug content uniformity among blisters on one disk .....	117
6.2.5	Drug content uniformity of blend during filling process.....	123
6.3	Optimization of Dry Powder Filling process .....	124
6.3.1	Minimization of electrostatic charge .....	124
6.3.2	The role of vacuum in the powder filling .....	126
6.3.3	The role of reducing vibration intensity in the powder filling.....	129
6.3.4	The flowability range suitable for the powder filling.....	132
6.4	Discussion.....	132
	Chapter 7.....	137
7	Research on the formulation for Dry Powder Inhaler.....	137
7.1	Brief Introduction .....	137
7.2	The Compatibility Evaluation.....	138
7.3	Powder Preparation for Dry Powder Inhaler .....	141
7.3.1	Preparation of the API particles and lactose .....	141
7.3.2	Mixing method of the API and lactose .....	146
7.4	Composition Research of Dry Powder Formulation.....	152
7.4.1	The formulation with similar FPF as marketed products .....	153
7.4.2	The influence of the lactose on formulation performance.....	155
7.4.3	The influence of API on formulation performance .....	162
7.5	Orthogonal Experimental Design and Results.....	167

7.6 Stability Evaluation of Dry Powder Inhaler Formulation.....	172
7.6.1 The influence of package on performance stability.....	172
7.6.2 The accelerated stability of different formulations.....	177
7.6.3 The performance stability of under different flow rates .....	184
7.7 Discussion.....	185
Chapter 8.....	190
8 Conclusions and Future Directions .....	190
8.1 Major Conclusions .....	190
8.2 Summary of Key Results .....	191
8.3 Future Directions .....	194
References.....	197

## List of Tables

Table 2.1: A comparison of pMDI and DPI .....	9
Table 2.2: Types of DPIs, formulation and dose system .....	22
Table 3.1: The relationship between Angle of repose and flow properties.....	31
Table 3.2: Cutoff aerodynamic diameter for stages of NGI (US Pharmacopoeia 32).....	39
Table 3.3: Evaluation items of typical marketed products .....	42
Table 3.4: Critical impaction test parameter for the marketed products .....	42
Table 3.5: Primary parameters of HPLC methods for marketed products .....	43
Table 3.6: The material for primary parts of the inhaler-WU2011 .....	48
Table 3.7: The information of lactose used .....	57
Table 4.1: The suitability results.....	63
Table 4.2: Signal-noise ratio of LOD and LOQ .....	64
Table 4.3: The linear range of concentration and corresponding peak area .....	66
Table 4.4: The reproducibility results.....	67
Table 4.5: The intermediate precision results.....	67
Table 4.6: The solution stability result .....	68
Table 4.7: The recovery rate result .....	68
Table 4.8: The calibration criteria and results for laser diffraction sizing.....	70
Table 4.9: The calibration criterion and results for Laser diffraction sizing .....	71
Table 4.10: The research scheme of TI test method validation .....	72

Table 4.11: The TRM and FPF result of TI method validation.....	72
Table 4.12: The research scheme of TI test time point validation.....	73
Table 5.1: The pressure drop in corresponding flow rate of marketed inhalers .....	79
Table 5.2: The airflow resistance of marketed inhalers.....	79
Table 5.3: The FPF and TRR results of TI tests for the marketed inhalers.....	82
Table 5.4: The FPF and TRR results of NGI tests for the marketed inhalers.....	83
Table 5.5: The dimensions of the investigated mouthpieces .....	88
Table 5.6: The air resistance of the new inhaler with different mouthpieces.....	89
Table 5.7: The FPF results of the inhaler with different mouthpieces .....	91
Table 5.8: The TI results of the inhaler when blister at wrong position.....	91
Table 5.9: The TI results of the inhaler when blister at right position .....	91
Table 5.10: The Laser diffraction size measurement results of the marketed products .....	98
Table 6.1: The filling weight and uniformity of disks in Trial A-1.....	100
Table 6.2: The improved uniformity of filling weight between disks in Trial A-2.....	101
Table 6.3: The filling weight uniformity for 100 disks in Trial A-3 .....	103
Table 6.4: The filling weight uniformity of disks using different powders in Trial A-4.....	104
Table 6.5: The initial filling weight uniformity of blisters Trial B-1 .....	106
Table 6.6: The filling weight uniformity among blisters for the powder with improved flowability in Trial B-2.....	107
Table 6.7: The improved filling weight uniformity of blisters in Trial B-3 .....	109
Table 6.8: The final filling weight uniformity of blisters in Trial B-4 .....	110



Table 6.9: The drug content uniformity among disks in Trial C-1 .....	111
Table 6.10: The blend content uniformity of the tested powder in Trial C-1 .....	112
Table 6.11: The drug content uniformity for 100 disks in Trial C-2 .....	114
Table 6.12: The blend content uniformity of the tested powder in Trial C-2.....	115
Table 6.13: The drug content per disk for different powders in Trial C-3 .....	115
Table 6.14: The drug content uniformity among blisters .....	117
Table 6.15: The drug content uniformity among blisters for different powders in Trial D-2.....	118
Table 6.16: The delivered drug content uniformity for different powders .....	120
Table 6.17: The blend content uniformity during filling process .....	124
Table 6.18: The summary of the comparison results for filling with or without vacuum .....	128
Table 6.19: The FPF and blister remains results of filling powder with or without vacuum. ....	129
Table 6.20: The summary of RSD results for filling with normal or reduced vibration.....	131
Table 6.21: The composition and flowability of Blends for filling tests.....	132
Table 6.22: The weight variance of a PVC disk.....	134
Table 7.1: The impurity content of compatibility tests.....	140
Table 7.2: The size results of micronized API.....	142
Table 7.3: The size results of self-made lactose carriers .....	144
Table 7.4: The flowability of self-made lactose carriers .....	144

Table 7.5: The size results of the micronized lactose.....	146
Table 7.6: The blend content uniformity of screening method.....	147
Table 7.7: The blend content uniformity of final mixing method .....	147
Table 7.8: The content uniformity of blend mixed by ultrasonic-sieve.....	148
Table 7.9: The content uniformity of blend by 200-mesh .....	148
Table 7.10: The laser diffraction size results of high and low-speed mixing .....	149
Table 7.11: The comparison of blend content uniformity using different-speed mixing .....	150
Table 7.12: The influence of mixing time on blend drug uniformity .....	151
Table 7.13: The FPF and blister remains results of different mixing time .....	152
Table 7.14: The composition of these formulations with similar FPF as marketed products .....	153
Table 7.15: The angle of repose of blends with different ratio of fine lactose .....	155
Table 7.16: The compression index of blends with different ratio of fine lactose .....	156
Table 7.17: The blend drug content uniformity for formulations containing different fine lactose .....	156
Table 7.18: The FPF and blister remains results of different fine lactose .....	157
Table 7.19: The vibration sieving size and laser diffraction size of the sieved lactose .....	158
Table 7.20: The blend drug content uniformity of formulation with different-size lactose .....	158
Table 7.21: The FPF and blister remains results of formulation with different-size lactose .....	159

Table 7.22: The sieving size and laser diffraction size of lactose from different sources .....	160
Table 7.23: The blend drug content uniformity of formulation with different-source lactose .....	161
Table 7.24: The FPF and blister remains results of different-source lactose .....	161
Table 7.25: The blend drug content uniformity of formulations with different-percentage API. ....	162
Table 7.26: The FPF and blister remains results of the different - percentage API. ....	163
Table 7.27: The blend drug content uniformity of formulation with different-size API.....	164
Table 7.28: The FPF and blister remains results of different-size API .....	165
Table 7.29: The blend drug content uniformity of different mixing sequence for API.....	166
Table 7.30: The FPF and blister remains results of different API mixing sequences .....	167
Table 7.31: The factors and levels in the orthogonal experiments .....	167
Table 7.32: The factors and levels in the orthogonal experiments .....	168
Table 7.33: The FPF results of the orthogonal experiments.....	168
Table 7.34: The signal-to-noise ratios of FPF response .....	170
Table 7.35: The signal-to-noise ratios of blister remain responsive.....	171
Table 7.36: The FPF and blister remains results of the initial and accelerated test for 1 month with/without external foil packages .....	174
Table 7.37: The FPF and blister remains results of stress test for 0/5/10 days with/without desiccant.....	176
Table 7.38: The FPF and blister remains results of accelerated tests for 4 powders.....	182

Table 7.39: The FPF and blister remains results of accelerated tests  
for different-size lactose ..... 184

## List of Figures

Figure 2.1: Illustration of three kinds of dry powder inhaler devices, adapted from Daniher .....	10
Figure 2.2: Common dry powder inhaler products on market. a, Aerolizer®; b, Handihaler®; c, Diskhaler®; d, Diskus®; e, Turbuhaler®; f, Clickhaler®.....	11
Figure 2.3: Active dry powder inhalers. a, Exubera®; b, principle of Microdose® device; c, Microdose® device .....	14
Figure 2.4: Schematic of working principle of the standard dosator technology .....	15
Figure 2.5: Schematic of the working principle of Vacuum drum filler and Xcelodose 600.....	17
Figure 2.6: Schematic of the working principle of Rotation Fluidized bed for filling .....	18
Figure 2.7: Schematic of liquid bridge and mechanical interlocking .....	20
Figure 2.8: Prepared particles. a, particles micronized by a jet mill; b,c particles prepared by spray dry; d, Pulmosphere® particles.....	24
Figure 2.9: A schematic diagram of particle deposition in lung and cascade impactors .....	25
Figure 2.10: Principle of Time of flight sizing and laser diffraction sizing .....	27
Figure 3.1: Pictures of equipment for testing angle of repose (a) and powder density (b) .....	30
Figure 3.2: A picture of SEM (Hitachi S-2600, Japan) .....	32
Figure 3.3: A picture of JCI-150 and JCI-178 (Chilworth Technology Ltd, UK).....	33
Figure 3.4: A picture of HPLC e2695 and 2487 (Waters, USA).....	34

Figure 3.5: A schematic diagram and a picture of twin impinger (Copley, UK) .....	35
Figure 3.6: A picture of Next Generation Impactor with pre-separator (Copley, UK) and a schematic diagram of NGI connected with a flow controller and pump. ....	37
Figure 3.7: A picture of internal structure of Next Generation Impactor and the pre-separator (Copley, UK) .....	38
Figure 3.8: Pictures of Sympatec Helos (a) and Rodos (b) (Sympatec, German) .....	40
Figure 3.9: Pictures of Sympatec Helos and Rodos combination (Sympatec, German) .....	41
Figure 3.10: A schematic diagram and picture of Dose uniformity sampling apparatus connected with a flow controller and pump (Copley, UK) .....	43
Figure 3.11: A schematic diagram of Inhaler-WU2011 working principle.....	44
Figure 3.12: Appearance and primary dimension of the novel inhaler .....	45
Figure 3.13: A schematic diagram of Inhaler-WU2011 upper and lower covers. a&b, upper cover; c&d, lower cover.....	46
Figure 3.14: A schematic diagram of Inhaler-WU2011 inner structure. a, drug disk; b, disk tray; c, combination of the ratchet, trigger and lower cover; d, dimensions of a blister. ....	47
Figure 3.15: A schematic diagram of Inhaler-WU2011. A, cross-section diagram of puncture; b, the shape of the puncture; c, puncture combined with push button; d, combination of puncture, push button and upper cover.....	48
Figure 3.16: A flow chart of filling and packaging. ....	49
Figure 3.17: The whole process of drug disk production .....	50
Figure 3.18: The pictures of equipment for disk formation (a), powder filling (b), hot-pressing sealing (c), punching (d).....	50
Figure 3.19: A schematic diagram of the filling device working principle.....	51

Figure 3.20: A schematic diagram of filling device .....	52
Figure 3.21: A schematic diagram of the metering plate.....	52
Figure 3.22: A picture of a jet-mill and an automatic feeder.....	56
Figure 3.23: A schematic diagram of mixing bed and a picture of the shaker - mixer. ....	58
Figure 3.24: Pictures of the high shear mixer. a, a voltage transformer and the mixer; b, the altered blades. ....	58
Figure 3.25: A picture of vibratory sieve shaker .....	60
Figure 4.1: Pictures of typical salbutamol chromatogram and peak purity .....	63
Figure 4.2: The chromatogram of reference solution, lactose solution, and blank solvent. ....	64
Figure 4.3: The linearity between concentration and peak area. ....	65
Figure 4.4: The cumulative and density distribution results of Sic-F1200'03 for R2 lens....	70
Figure 4.5: The comparison of NGI results for Turbuhaler® Oxis® with the coated and uncoated stages .....	71
Figure 4.6: The <i>in vitro</i> performance of the new inhaler at different intervals between powder preparation and TI test.....	74
Figure 4.7: The <i>in vitro</i> performance of the new inhaler at different intervals between powder filling and TI tests.....	75
Figure 5.1: The linearity between (pressure drop) <sup>0.5</sup> and flow rate for marketed inhalers .....	79
Figure 5.2: The delivered dose content uniformity of Clickhaler® Asmasal®.....	80
Figure 5.3: The delivered dose content uniformity of Turbuhaler® Oxis®.....	81
Figure 5.4: The FPF results of TI test for the marketed inhalers.....	82

Figure 5.5: The TRR results of TI test for the marketed inhalers.....	82
Figure 5.6: The aerodynamic particle size distribution (APSD) for the marketed inhalers .....	84
Figure 5.7: The schematic of the improved puncture design.....	86
Figure 5.8: The linearity between (pressure drop) <sup>0.5</sup> and the flow rate of the improved inhaler .....	86
Figure 5.9: The comparison of delivered efficiency and content uniformity between the old design and new inhaler (n=6) .....	87
Figure 5.10: The airway structure of the mouthpiece .....	87
Figure 5.11: The linearity between (pressure drop) <sup>0.5</sup> and flow rate for different mouthpieces.....	88
Figure 5.12: The APSD of the inhaler with different mouthpieces (mouthpiece 1, 2, 4).....	89
Figure 5.13: The APSD of the inhaler with different mouthpieces (mouthpiece 3, 4, 5).....	90
Figure 5.14: The cumulative distribution of the inhaler with different mouthpieces .....	90
Figure 5.15: The picture and schematic of twister® and Clickhaler® Reservoir .....	92
Figure 5.16: The parallel comparison of FPF with marketed devices by using the same powder.....	93
Figure 5.17: The parallel comparison of remains fraction with marketed devices by using the same powder.....	93
Figure 5.18: The schematic of air flow (blue arrow) and powder metering mechanism.....	96
Figure 5.19: The laser diffraction size result of Diskus® Seretide® .....	97
Figure 5.20: The laser diffraction size result of Turbuhaler® Oxis® .....	97
Figure 6.1: A schematic diagram of the filling uniformity research .....	99



Figure 6.2: The filling weight uniformity between disks in Trial A-1 .....	100
Figure 6.3: The improved uniformity of filling weight between disks in Trial A-2.....	101
Figure 6.4: The descending trend of filling weight for 20 disks in Trial A-2 .....	102
Figure 6.5: The filling weight uniformity among 100 disks in Trial A-3.....	103
Figure 6.6: The filling weight uniformity of disks using different powders in Trial A-4.....	104
Figure 6.7: The initial filling weight uniformity of sequentially numbered blisters in Trial B-1 .....	106
Figure 6.8: The filling weight uniformity among blisters for the powder with improved flowability in Trial B-2.....	108
Figure 6.9: The final filling weight uniformity of blisters in Trial B-4.....	110
Figure 6.10: The filling drug content uniformity among disks in Trial C-1.....	112
Figure 6.11: The filling weight uniformity of the disks for content uniformity evaluation in Trial C-1.....	113
Figure 6.12: The drug content uniformity between 100 disks in Trial C-2.....	114
Figure 6.13: The drug content per disk (n=6) for different powders in Trial C-3.....	116
Figure 6.14: The linear relationship between drug content and filling powder weight per disk in Trial C-3 .....	116
Figure 6.15: The drug content per blisters (6 random blisters from each of the 3 disks) for different powders in Trial D-2. ....	118
Figure 6.16: The drug content per blister (6 random blisters from each of the 3 disks) for 0%-fines and 5%-fines powder in Trial D-2.....	119

Figure 6.17: The drug content per blister (6 random blisters from each of the 3 disks) for 10%-fines and 20%-fines powder in Trial D-2 .....	119
Figure 6.18: The delivered drug content uniformity for 0%-fines and 5%-fines powder .....	120
Figure 6.19: The delivered drug content uniformity for 10%-fines and 20%-fines powder .....	121
Figure 6.20: The drug content for the sequentially numbered blisters in each of the 3 disks of Trial D-3. ....	122
Figure 6.21: The drug percentage for the sequentially numbered blisters in each of the 3 disks of Trial D-3. ....	122
Figure 6.22: The picture of the filled powder for each blister .....	123
Figure 6.23: The comparison of filling disks with (a) or without antistatic treatment (b) .....	125
Figure 6.24: The influence of electrostatic charge on the TI performance of the inhaler .....	126
Figure 6.25: The drug content per blister by filling with vacuum .....	127
Figure 6.26: The drug percentage per blister by filling with vacuum .....	127
Figure 6.27: The comparison of filling powder with (a) without vacuum and (b) with vacuum .....	128
Figure 6.28: The FPF and blister remains of filling powder with or without vacuum. ....	129
Figure 6.29: The picture of the filling powder for each blister with reduced vibration intensity .....	130
Figure 6.30: The drug content per blister of filling with reduced vibration intensity .....	130
Figure 6.31: The drug percentage per blister of filling with reduced vibration intensity ....	131

Figure 6.32: The schematic of principle of an antistatic fan .....	135
Figure 7.1: A schematic diagram of formulation study .....	137
Figure 7.2: The TGA and DSC results. a, lactose. b, the API. c, micronized lactose+API.....	139
Figure 7.3: The XRPD results of lactose, API+lactose, micronized API+lactose, API. ....	139
Figure 7.4: The laser diffraction size distribution of micronized API.....	142
Figure 7.5: The SEM pictures of the micronized API. a, shape of the micronized API; b, cohesive property of the micronized API.....	143
Figure 7.6: The SEM pictures of self-made lactose (a) and the API + lactose mixture (b).....	143
Figure 7.7: The SEM pictures of the commercial lactose and the API-lactose mixture.....	145
Figure 7.8: The cumulative and density volumetric distribution of micronized lactose as fine additives. ....	145
Figure 7.9: A schematic of sampling method for blend content uniformity.....	146
Figure 7.10: The comparison of FPF values for powder pre-sieved by different meshes. ....	148
Figure 7.11: The laser diffraction sizing results for low and high-speed mixing.....	149
Figure 7.12: The comparison of FPF and blister remains by different-speed mixing. ....	151
Figure 7.13: The influence of mixing time on FPF and blister remains.....	152
Figure 7.14: The similar FPF of formulation Rx4/5 as Aerolizer® Foradil® and Diskus® Seretide® .....	154
Figure 7.15: The similar FPF of formulation Rx6/17 as Turbuhaler® Oxis® and Clickhaler® Asmatha®.....	154

Figure 7.16: The FPF and blister remains of formulations containing different fine lactose. ....	156
Figure 7.17: The FPF and blister remains of formulation with different-size lactose. ....	159
Figure 7.18: The FPF and blister remains of formulation with different-source lactose. ....	161
Figure 7.19: The microscope images of different-source lactose. a, SV003; b, LH200 (milled) .....	162
Figure 7.20: The FPF and blister remains of formulation with different-percentage API.....	163
Figure 7.21: The FPF and blister remains of formulation with different-size API. ....	165
Figure 7.22: The FPF and blister remain of formulation with different mixing sequence for the API.....	166
Figure 7.23: The averaged FPF response and various levels of the studied factors. ....	170
Figure 7.24: The averaged blister remains response and various levels of the studied factors. ....	171
Figure 7.25: The FPF and blister remains of initial and accelerated test for 1 month with/without external foil packages. ....	173
Figure 7.26: The FPF and blister remains of initial and accelerated test for 1 month with/without external foil packages. ....	173
Figure 7.27: The FPF and blister remains of stress test for 0/5/10 days with/without desiccant. 0%-fines formulation. ....	175
Figure 7.28: The FPF and blister remains of stress test for 0/5/10 days with/without desiccant. 20%-fines formulation. ....	175
Figure 7.29: The FPF and blister remains of accelerated tests for 0%-fines formulation. ...	177
Figure 7.30: The FPF and blister remains of accelerated tests for 5%-fines formulation. ...	178

Figure 7.31: The uniformity of delivered dose of accelerated tests for 0%- and 5%-fines formulation. ....	178
Figure 7.32: The FPF and blister remains of accelerated tests for 10%-fines formulation. ....	180
Figure 7.33: The FPF and blister remains of accelerated tests for 20%-fines formulation. ....	180
Figure 7.34: The uniformity of delivered dose of accelerated tests for 10% and 20%-fines formulation. ....	181
Figure 7.35: The FPF and blister remains of accelerated tests for lactose <45 $\mu$ m and within 45~75 $\mu$ m. ....	183
Figure 7.36: The FPF and blister remains of accelerated tests for lactose within 75~100 $\mu$ m and 100~150 $\mu$ m.....	183
Figure 7.37: The FPF and blister remains of high and low flow rate.....	185
Figure 7.38: The schematic of disorder and recrystallization on the surface of micronized particle.....	187
Figure 7.39: The schematic particle entrainment in a laminar wall boundary layer. ....	189

### **List of Abbreviations**

ACI	Anderson cascade impactor
API	Active pharmaceutical Ingredients
APSD	Aerodynamic particle size distribution
BCU	Blend content uniformity
CF	Calibration Factor
CFC	Chlorofluorocarbon
CFTR	Cystic fibrosis transmembrane conductance regulator
COPD	Chronic obstructive pulmonary disease
DDCU	Delivered drug content uniformity
DPI	Dry powder inhaler
DSC	Differential Scanning Calorimeter
DUSA	Dose uniformity sample apparatus
ED	Emitted dose
EP	European Pharmacopoeia
FDA	Food and Drug Administration
FPD	Fine particle dose
FPF	Fine particle fraction
GINA	Global Initiative for Asthma
GMP	Good manufacture practice
GOLD	Global initiative for chronic Obstructive Lung Disease
GSD	Geometric standard deviation
HFA	Hydrofluoroalkane
HPLC	High performance liquid chromatography
ICH	International Conference on Harmonisation of Technical Requirements for Registration of Pharmaceuticals for Human Use
LABA	Long Acting Beta Agonist
LPM	Liters per minute
MIC	Maximum inspiratory capacity

MMAD	Mass median aerodynamic diameter
MOC	Micro orifice collector
NGI	Next generation impactor
PIF	Peak inspiratory flow
pMDI	Pressure metered dose inhaler
PVC	Polyvinyl chloride
RPM	Revolution(s) Per Minute
R&D	Research and development
RSD	Relative standard deviation
SABA	Short Acting Beta Agonist
SCF	Supercritical fluid
SD	Standard deviation
SEM	Scanning electron microscope
SFDA	State Food and Drug Administration
TGA	Thermogravimetry analysis
Tg	Temperature of glass transition
TI	Twin impiner
TRM	Total recovery mass
TRR	Total recovery rate
USP	U.S. Pharmacopoeia
UV	Ultraviolet
XRPD	X-ray Powder Diffraction

## Chapter 1

### 1 General Introduction

#### 1.1 Objectives

Respiratory drug delivery is a novel and promising method to treat local and systemic disease, which has attracted increasing attention from pharmaceutical scientists and clinical experts. Among those inhalation drug delivery methods, the dry powder inhaler is particularly attractive. The dry powder inhaler is more and more welcome by patients and clinical experts as a result of its unique advantages. Nevertheless, the welcomed dry powder inhaler products on the market still have some inherent shortcomings from the perspectives of pharmaceutical scientists or patients. Consequently, a novel dry powder inhaler product is designed, manufactured and evaluated in this project. The corresponding powder filling & packaging system and formulation research are also established and carried out to demonstrate the performance of the inhaler and the feasibility of industrialization.

The core targets of this work are listed as follows:

**To develop a novel dry powder inhaler device.** It is characterized by a micro-dose, passive delivery, using an individual blister package and multi-unit doses on one replaceable disk. This device should realize the following targets: high efficiency of drug delivery, effective dispersion of particles, stable performance, convenient and easy to use, and feasible to industrialize.

**To develop a novel powder filling and packaging system.** This system should realize the targets of metering and filling powder accurately, avoiding contamination, feasible to industrialize.

**To develop formulations with similar performance as marketed products.** The influence of formulation process and composition on the inhaler performance should be studied. Furthermore, the influence of packaging and formulation on performance stability should be investigated.



## 1.2 Thesis Overview

This thesis contains eight chapters and follows the “Monograph” format as outlined in the Thesis Regulation Guide by the School of Graduate and Postdoctoral Studies of The Western University. It is organized as follows:

- **Chapter 1** gives a brief introduction of the background of this research and demonstrates the need for this study. Research objectives and thesis structure as well as major contributions of the present work are stated.
- **Chapter 2** reviews the literature related to respiratory drug delivery, dry powder inhaler devices, and powder filling technologies for dry powder inhalers, powder formulation and *in vitro* evaluation of inhalers.
- **Chapter 3** summarizes materials and methods used in this research in four sections: the 1<sup>st</sup> section includes common chemical & physical analysis and special evaluation of inhaler performance; the 2<sup>nd</sup> section covers the powder filling and packaging system; the 3<sup>rd</sup> section focuses on the novel drug powder inhaler device, where both design and working principle of which are described in details; the 4<sup>th</sup> section includes the formulation work like composition and processing of the powder.
- **Chapter 4** provides the validation results of the analytical method, which indicates that the HPLC method for drug content analysis is accurate, durable and reproducible. Furthermore, *in vitro* evaluation methods of inhaler performance are validated.
- **Chapter 5** reports the evaluation results of common marketed dry powder inhalers, modification of the novel dry powder inhaler design and the corresponding improvement. The comparison of the novel inhaler and other commercial products is also presented, demonstrating that the novel inhaler has similar or better *in vitro* performance than others.

- **Chapter 6** introduces the uniformity results of the powder filling system and its optimization, including uniformity of filling weight and drug content among disks and blisters. The results demonstrate that this novel filling and packaging system can meet uniformity requirements and is suitable for the novel inhaler device.
- **Chapter 7** describes the research on formulation composition, powder treatment, and their influence on inhaler performance. After a series of single-factor experiments, a comprehensive orthogonal experiment was designed and carried out to study the influence of formulation factors and their corresponding significance. The stability of formulations is also investigated and presented.
- **Chapter 8** serves as a conclusion to the entire project. It also recommends future research focus and problems to resolve in the future.

### 1.3 Major Contributions

- A novel dry powder inhaler device is designed and implemented. Based on *in vitro* evaluation and improvement work, a better understanding of its critical parameters and working principles has been acquired. This not only lays a solid foundation for future commercialization, but is also helpful for the development of other dry powder inhaler products.
- A novel powder filling and packaging system is designed and made in our lab and Shanghai Institute of Pharmaceutical Industry. A set of quality control criteria and methods are established to ensure inhaler performance. These criteria and test methods can also be used as important intermediate quality controls in large-scale production.
- A comprehensive formulation work has been carried out to study the influence of lactose and drug powder, mixing process on the performance of this inhaler. The innovation of the formulation work is reflected by the small quantity of delivered dose. Specifically, the influence of formulation factors is studied on a scale of 2-3mg rather than 20-30mg commonly studied before.

## Chapter 2

### 2 Literature Review

This chapter reviews the literatures related to the respiratory drug delivery, dry powder inhaler devices, powder filling technologies, powder formulation for dry powder inhaler and *in vitro* evaluation of inhalers.

#### 2.1 Respiratory Drug Delivery

##### 2.1.1 The advantages and application of respiratory drug delivery

The advantage of respiratory drug delivery is determined by the unique physical characteristics of respiratory tract and lung: There are less digestive enzyme in the lung than in the digestive tract and the hydrolytic enzymes show less activities, both of which are helpful to enhance bioavailability of the Active Pharmaceutical Ingredient (API); Second, the respiratory tract and lung have a huge surface area where plenty of capillary vessels exist and carry huge blood flow. Additionally, alveolar epithelial cells are arranged by a monolayer structure which would greatly improve the rate and extent of the API absorption. Third, the API is absorbed into systemic circulation directly, avoiding the hepatic first-pass effect<sup>[1]</sup>. For respiratory disease, besides the advantages mentioned above, inhalation drug delivery could decrease the drug quantity by enhancing therapy efficiency, and decreases systemic side effect by direct action on target cells. As a result, the respiratory drug delivery has been widely used treat respiratory disease by topical therapy and other disease by systemic therapy.<sup>[2]</sup>

Asthma and chronic obstructive pulmonary disease (COPD) are the most common respiratory diseases, and respiratory drug delivery is the first choice to treat both diseases. Asthma is a chronic airway inflammation characterized by reversible airflow limitation. Hence its therapeutic drug could be divided into two categories as anti-inflammatory and relieving symptoms. Glucocorticoids are the most effective anti-inflammatory drugs. When these APIs are administered by inhalation, the therapy amount and systemic side effect are decreased by direct action on the respiratory tract. Therefore, inhaled glucocorticoids are the first choice for treatment of persisting asthma. The contraction of

airway smooth muscle is the primary mechanism of reversible airway narrowing and  $\beta_2$  agonists could prevent and reverse the contraction of airway smooth muscle to relieve symptoms. Consequently, the short-acting  $\beta_2$  agonists (SABA) are the first choice for relieving mild to moderate acute asthma, and long-acting  $\beta_2$  agonists (LABA) are able to maintain their bronchodilator effect more than 12 hours<sup>[3; 4]</sup>. COPD is a preventable and treatable disease characterized by airflow limitation. Inhaled  $\beta_2$  agonists and other bronchodilators are the primary choice to relieve the symptoms of COPD. Meanwhile, long-term and regular corticosteroids administration by inhalation could reduce the incidence of acute exacerbation of COPD, and improve life quality<sup>[5]</sup>. Inhalation therapy is the first recommendation to treat asthma and COPD according to Global Initiative for Asthma (GINA) and Global initiative for chronic Obstructive Lung Disease (GOLD).

In addition to asthma and COPD, the respiratory drug delivery is also used to treat cystic fibrosis. The pathological features of cystic fibrosis include thick secretion, damaged mucociliary and lung infection. Hence, the main treatment is antibiotic therapy, plus bronchodilators and others to alleviate symptoms. Clinical trials demonstrated that inhaled tobramycin could greatly improve lung function, reduce hospitalization and intravenous antibiotic injection<sup>[6]</sup>. By inhalation of hypertonic saline, the hydration of surface liquid of the airway could be enhanced and the clearance of mucosal surface would be increased<sup>[7]</sup>. Because cystic fibrosis is a recessive genetic disease caused by mutations of cystic fibrosis transmembrane conductance regulator (CFTR), the pulmonary delivery of gene therapy has become a hot spot for cystic fibrosis treatment.<sup>[8; 9]</sup>

Other respiratory drug delivery for local treatment include: treatment of neonatal respiratory distress syndrome through inhalation of surfactant<sup>[10]</sup>, avoid acute lung injury caused by hypoxemia through inhalation of prostaglandin E1.

Due to development of modern life science and biotechnology, more and more protein, peptide drugs are widely used in clinical practices. Yet, the easily hydrolysis of protein and peptides would inactivate these macromolecular drugs in the digestive tract. Their large molecular weight would limit their absorption rate and extent in the gastrointestinal

tract. Consequently, most protein, peptide drugs can only be administered by injection, which may cause compliance and convenience problems. Thanks to absorption enhancement, avoiding first-pass effect, bioavailability improvement of inhalation drug delivery, its application in systemic drug delivery, especially for protein and peptides is increasingly attracting attention.<sup>[11; 12]</sup>

Insulin is able to lower blood sugar level, serving as an effective treatment for the type I and type II diabetes. Nevertheless, since insulin is easily digested in the digestive tract, it is usually administered by subcutaneous injection which would bring great inconvenience and pain to patients and result in compliance problems. Therefore, non-invasive administration of insulin, such as respiratory delivery and transdermal delivery has been a hot research field for many years. In 2006, Exubera® became the first FDA-approved inhaled insulin products, developed by Pfizer and Nektar jointly for treatment of type I and type II diabetes. Clinical trials showed that the glycemic control effect of the inhaled product was comparable to injection and superior to oral hypoglycemic drugs<sup>[13; 14]</sup>. Just a year later, Pfizer announced that no production and sales of the inhaled insulin any more for market and safety reasons. Hopefully, other companies are still developing inhaled insulin products, such as Mankind submitting its new drug application to the FDA in 2009. In addition to insulin, other inhaled biological macromolecules like luteinizing hormone-releasing hormone, interferon A, growth hormone had already been in the clinical stages<sup>[15]</sup>.

Respiratory drug delivery is also applied to vaccination. Firstly, immune cells of pulmonary, nasal and oral system account for about 80% of systemic immune cells. Secondly, plenty of macrophages and dendritic cells in respiratory tract could swallow, present antigen to stimulate T cell, induce mucosal and systemic immunity. Finally, the inhaled vaccine could greatly enhance the vaccination speed and reduce the need for health professionals, avoid cross-infection and blood borne diseases. Clinical trials have shown that children vaccinated against measles after inhalation can produce a good immune effect in Mexico.<sup>[16; 17]</sup>

Inhalation drug delivery has become the most popular research topics in the global drug R&D (Research and Development). About 25% of global formulation work is focused on inhalation drug, which is second only to oral preparation.

### 2.1.2 Deposition of drug particles in respiratory tract

There are three primary mechanisms for drug particle depositing on the respiratory tract and lung: inertial impaction, gravitational settling and Brownian diffusion, all of which are closely related to the particle size. When the particle is above a certain size, it is difficult to immediately change particle motion with airflow and particles would impact on airway wall. Consequently, the main deposition mechanism for those particles is inertial impaction mostly in the oropharynx, bronchus and conducting airways. The increase of particles size and velocity would increase the possibility of inertial impaction. [18]

The deposition manner for smaller particles is gravitational settling, which requires longer residence time of particles in airflow. At the first few levels of lung airways, the total cross-section area is small and result in higher flow rate resulting less residence time of particles. Consequently, gravity sedimentation mainly occurs in the small airways and alveolar. This phenomenon also has practical significance for clinical application. When using an inhaler product, enhancing the intake air amount (deep breathing) or holding the breath after administration would increase the particle residence time and deposition in the lung. When particles are smaller than a certain size, the Brownian diffusion would determine the particle precipitation. According to Task Model, when **particles are above 10 $\mu$ m, they would deposit on the oropharynx; for particles between 1~5 $\mu$ m, they would deposit in the bronchi, bronchioles and alveoli. If particles diameter is less than 1 $\mu$ m, they would mainly deposit in alveoli.** [19]

As mentioned above, drug particles of different sizes would deposit in different positions of the respiratory tract, which provides a basis for targeting delivery. Bronchodilators -  $\beta_2$  agonists are mainly used for relaxation of bronchial smooth muscle cells mainly distributing in the large bronchi and smaller bronchi;  $\beta_2$  receptors are mainly distributed in the smaller airways. Therefore, the ideal deposition site of  $\beta_2$  agonists is from

bronchial to bronchioles. The targets of anti-inflammatory drugs are eosinophils or glucocorticoid receptors, locating mainly in the large airway and alveolar wall respectively. For drugs with systemic effect, its ideal deposition targets should be alveoli, since the surface area of the alveoli is the largest, in addition to thinnest cell barrier and lowest mucosal clearance rate. <sup>[20-22]</sup>

### 2.1.3 Common respiratory drug delivery methods

The sufficiently small size ( $<5\mu\text{m}$ ) is the key to respiratory drug delivery. Consequently, the dispersion of drug droplets or powder from bulk liquid or agglomerates is the core part for all respiratory drug delivery methods. Since the surface energy is increased significantly during the dispersion, additional energy should be provided in a short time. According to the energy source and devices, the respiratory drug delivery can be divided into nebulizer, pressure metered dose inhaler (pMDI) and dry powder inhaler (DPI).

Nebulizers apply compressed air, ultrasonic or vibrating sieve to disperse solutions or suspensions into drug droplets of suitable size. The compressed air speed through the nozzle and disperse liquid into droplets by high shear and turbulence, and large droplets would impact on a baffle and return to a liquid reservoir<sup>[23]</sup>. Ultrasonic nebulizers utilize high-frequency vibration of a dielectric unit to atomize the drug solution, which exhibited better atomization efficiency than compressed air nebulizer but may lead to a degeneration of heat-sensitive protein and compound<sup>[24]</sup>. The vibrating-sieve nebulizer is a novel device which uses a sieve with a certain aperture to atomize the drug solution<sup>[25]</sup>.

The advantages of the nebulizer are listed as follows: it could be applied for a wide range of drugs; solution, suspension or emulsion can be atomized; widely used in hospitals, for infants and other patients; compared to pMDI and DPI, patients might feel the administration skills easier. Nevertheless, there are some drawbacks: For the compressed air and ultrasonic atomizer, a large dead volume would remain in the reservoir chamber and the pipe, which may be more than 1ml; longer delivery time decrease patient compliance; devices are too large to carry; vibrating-sieve nebulizer overcome some of above shortcomings, but the price is expensive because of intricate structure.

Pressure Metered Dose Inhalers (pMDI) utilize a propellant with a low boiling point and high vapor pressure to provide droplet dispersion force. All pMDIs are comprised of two parts: device and formulation. The device is comprised of a quantitative valve, pressure containers and an actuator. The formulation includes propellant, latent solvents, drug and surfactant. Based on the dispersed state of drug in the solvent, it can be divided into solution and suspension pMDI. The propellant used to be chlorofluoroalkane (CFC) which has been replaced by hydrofluoroalkane (HFA) in past 20 years because of CFC's destruction effects on the atmosphere ozone.

The DPI will be reviewed in detail in the following sections. Hence, here is a summary table (Table 2.1) to compare the advantage and disadvantage of pMDI and DPI.

**Table 2.1: A comparison of pMDI and DPI**

	Advantages	Disadvantages
DPI	Easy to use, convenient; Compact and portable; No need for "actuation and breath " coordination; Chemically stable for powder state; Larger delivered dose; Environment friendly;	Complicated use for single unit dose DPI; Higher price; Sensitive to moisture; Different usage of different devices; Depending on the inspiratory flow;
pMDI	Easy to use, convenient; Compact and portable; Lower price; Almost the same procedure for different products;	Require the coordination of actuation and breath; Depending on using techniques; Delivered dose is limited; Influence on environment even if HFA is used;

## 2.2 Devices for Dry Powder Inhalation

Unlike oral preparation and injection, the performance of inhaler product is dependent on drug delivery device, which provide energy to overcome the interaction force between particles and make it possible that the fine particle would deposit in the lung. Since the DPI devices are usually used by patients themselves without a doctor's guidance most of the time, the convenience plus excellent aerodynamic performance is important to DPI device design.



After decades of development on DPI device, there are already lots of devices on the market. As Fig.2.1, these devices may be categorized as single unit dose DPI, multiple unit dose DPI and multiple dose DPI (also known as reservoir DPI) according to their dosing principles. Or, DPI devices may also be divided into the passive or active device in terms of driving force to disperse the powder.

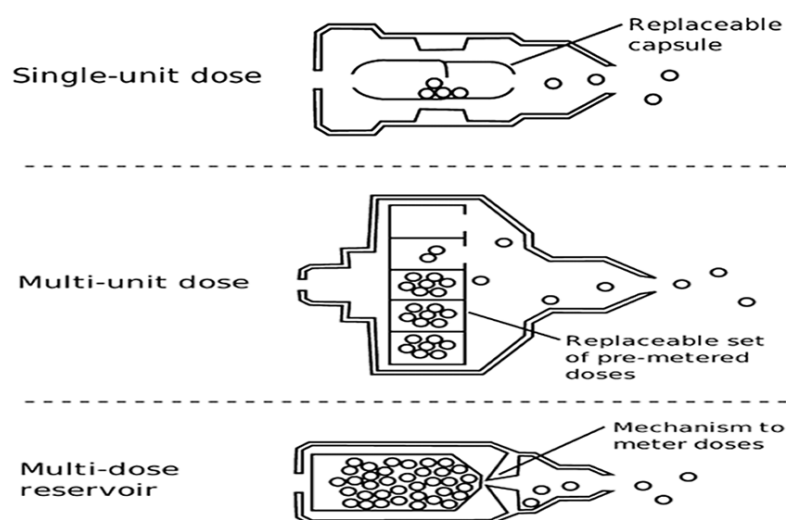


**Figure 2.1: Illustration of three kinds of dry powder inhaler devices, adapted from Daniher<sup>[26]</sup>**

### 2.2.1 Single unit dose DPI

For a single unit dose DPI, the drug powder is metered into a capsule or blister before dispensing to patients. When patients use that kind of device, they must take out a capsule or blister from packages and insert it into the device, and then the device is ready for administration. Aerolizer® (Fig.2.2a) is a famous device marketed in USA market to deliver fumarate formoterol (Foradil®, Novartis). Its working principle is like that: when a capsule is inserted into the bottom, patients push the buttons on both sides of the device to drive needles to pierce the capsule. Then the buttons are released, and patients inhale from the mouthpiece. The inspiratory flow would vibrate the capsule and bring the powder out into the patients' respiratory tract. Meanwhile, a grid above the capsule could prevent large capsule fragments and assist the deagglomeration of particles<sup>[27; 28]</sup>.

Single unit dose DPI is the first DPI device on the market due to its simplicity both on design and formulation, which is still used to develop new DPI products. For example, in 2002, the Boehringer Ingehein introduced Handihaler® (Fig.2.2b) to deliver Tiotropium to treat COPD<sup>[29]</sup>. In 2011, Novartis brings a new compound as Indacaterol for COPD, which also use a single unit dose device<sup>[30]</sup>. Due to their simple design, the single unit dose devices are often employed to study the hydrodynamic of device design<sup>[31]</sup> or used as a model to study computer fluid dynamics<sup>[28; 32; 33]</sup>.



**Figure 2.2: Common dry powder inhaler products on market. a, Aerolizer®; b, Handihaler®; c, Diskhaler®; d, Diskus®; e, Turbuhaler®; f, Clickhaler®.**

However, the disadvantages of the single unit dose device are also obvious. Firstly, usage of the capsule-device is complicated and time-consuming, because a capsule has to be inserted into the device before using and then discarded after administration every time<sup>[34]</sup>. Secondly, the capsule may become fragile under too dry environment<sup>[35]</sup> and produce pieces during piercing which may be inhaled into the respiratory tract causing cough or uncomfortable. To overcome the weakness of single unit dose device, multiple unit dose devices and multiple dose devices are developed.

### 2.2.2 Multiple unit dose DPI

Diskhaler® (Fig.2.2c) is the first multiple unit dose device, marketed in 1988, which has 4-8 dose on one disk. The most commercially successful multiple unit dose devices is Diskus® (Fig.2.2d), marketed by GlaxoSmithKline in 1995 to deliver fluticasone and

salmeterol at the same time for asthma and COPD. There are up to 60 blisters on a long foil strip which curls tightly in the device, and each blister contains the active ingredient for one administration. When a patient use it, they only have to push a lever on one side of the device to open a blister and then push the lever back to make next blister ready for administration. What is better, a counter on the surface of the device would clearly show remaining doses, and remind patients to have a new one before it runs out.<sup>[34; 36]</sup>

Because this kind of device could bring dozens of blisters, it is convenient for usage and carry, making it popular among patients<sup>[37]</sup>. Due to its individual package for each dosage, the powder could be protected rather well against moisture and oxygen<sup>[38]</sup>. Similar as single unit dose inhaler, the dose precision is better than multiple dose DPI, since the drug is pre-metered into individual packages in factories<sup>[39]</sup>. Yet, the metering principle is similar as a single unit dose device, making it necessary to utilize lactose as carrier and result in API and carrier detachment problem.

### 2.2.3 Multiple dose DPI

Multiple dose device, also named as reservoir device, store the drug powder in a reservoir without pre-metering. When it is used, the device could meter a dose accurately and deliver it to patients. Turbuhaler® (Fig.2.2e) is the first device containing more than 100 doses, as convenient as pMDI. By rotating the device bottom, powder flow into a series of very small holes on the metering disk from a reservoir. Simultaneously, a batch of scrapes ripe off excess powder. Since the dose quantity is determined by the volume of the holes on the metering disk, there is no need to employ lactose as carrier as long as the API particles show good flowability. Consequently, the Turbuhaler® could deliver pure API particles with or without carrier, which is a big step forward in the DPI development<sup>[40]</sup>. Clickhaler® (Fig.2.2f) is another example of reservoir device, which is believed as most similar device to the pMDI in terms of shape and operation method. By clicking the top button, the cone rotates to place a dimple filled with powder in respiratory airflow pathway<sup>[41]</sup>.

As a result of less or no carrier, the multiple dose device could achieve a very high drug delivery efficiency than Diskus® at the expense of lower delivery uniformity<sup>[42; 43]</sup>. Yet,

this kind device is more complicated than the other two kinds, and its moisture resistance and delivery uniformity are usually the primary concern for regulatory agencies<sup>[42]</sup>. For example, due to worries on delivered dose content uniformity, the FDA postponed the marketing of Turbuhaler® on the USA market. However, the variance of lung deposition is smaller than pMDI<sup>[44]</sup>. Long-term clinical trials showed that even under hot and humid environment, Turbuhaler® showed good clinical records in adult and child asthma therapy<sup>[45]</sup>.

#### 2.2.4 Active devices

All devices mentioned above would be classified as passive device, which rely on patient inspiratory flow to dispense and detach powder. Dependence on users' airflow is advantageous but also disadvantage of this kind of device at the same time, since persons with different airflow attributes may have different drug delivery results<sup>[46-48]</sup>. As a result, active devices independent of a patient's airflow are developed, which are able to dispense powder by compressed air or vibration produced by the devices themselves.

The most famous active DPI device is Exubera® from Nektar as Fig.2.3a, marketed by Pfizer as the first inhaled insulin product. It has a manual air pump which may produce a compressed air to dispense powder into a transparent chamber, and then patients may inhale drug powder from the chamber<sup>[49]</sup>. Although this device is withdrawn from the market only 1 year after its launch, it greatly expands the potential of the DPI on therapeutic range and device design. After withdraw of the Exubera®-inhaled insulin, there appeared some reluctance to consider the pulmonary delivery for systemically acting agents, as most companies gave up their insulin inhalation product. However, recent R&D and market activities suggest that inhalation for systemic delivery is recovering from the blow<sup>[50]</sup>. Microdose® device (Fig.2.3c) from Microdose Technology utilize vibration (piezoelectric) energy to disaggregate the particles and deliver them into the patient inspiratory flow<sup>[51]</sup>. Corcoran et al utilized this technology for atropine systemic delivery, which obtained rapid and consistent systemic concentrations of atropine<sup>[52]</sup>.



**Figure 2.3: Active dry powder inhalers. a, Exubera®; b, principle of Microdose® device; c, Microdose® device**

## 2.3 Filling Device for Dry Powder Inhaler

A combination and interaction of formulation/inhaler device/powder filling will determine the final product performance, especially for dry powder inhaler. As a result of the high efficiency of inhalation drug delivery and high potency of the API, the delivered amount of API is usually on milligram or microgram scale. Meanwhile, to deliver drugs to bronchi, bronchioles or alveoli, particle size of the API should be in the range of 1~5 $\mu\text{m}$ . When the particle size is so small, the flowability decreases dramatically, making a big challenge for precise filling by volume. Besides, the extra fine particles show strong tendency to form tight agglomerates and prevent particles disaggregation during drug delivery. Although problems mentioned above may be solved partly by adding a carrier, like lactose, the quantity of total powder is still very small. Therefore, the powder filling system for dry powder inhaler is a critical part of whole product development.

### 2.3.1 Powder filling by volume

#### 2.3.1.1 Standard dosator technology

The principle of Standard dosator technology is to utilize a hollow quantitative tube to measure and transfer a certain amount of powder. Accordingly, powder weight is dependant on the volume and compaction extent of powder (density). Its advantage lies in that a quite large amount of powder could be measured precisely, and the amount can be

adjusted in a wide range. The standard dosator technology is most widely used for filling dry powder inhaler. As shown in Fig.2.4, the dosing part comprises a hollow tube with a piston in it. During the dosing process, the hollow tube is inserted into powder bed and taken out with a certain powder in the tube, and then the tube is transferred to a position right above a capsule or reservoir. During the transfer process, a negative pressure may be used to prevent powder falling out. Following that, the piston in the tube pushes powder out and the filling is completed. The powder volume is determined by both the height of the piston in the tube and diameter of the tube. The volume together with powder density as a result of powder compaction extent, determine the dosing weight. Consequently, the powder compaction extent is a critical parameter which should be constant during filling process. The unchanged compaction extent is achieved by keeping powder bed height and tube stroke constant. After filling process, the entire system can be detached for clean, to avoid contamination among different powder<sup>[53]</sup>.

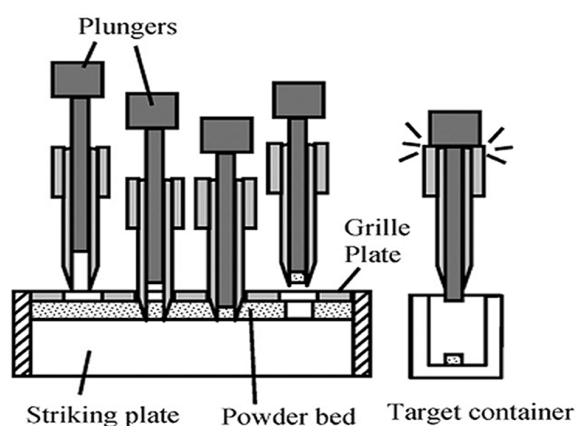


**Figure 2.4: Schematic of working principle of the standard dosator technology<sup>[53]</sup>**

The common parameters for standard dosator technology are listed as follows: the filling quantity is usually between 10 ~ 500 mg and relative standard deviation (RSD) is about 2%. The production capacity may be 3000~200000 capsules per hour dependant on the equipment size. This production capacity can meet requirement of clinical stage I to commercial production<sup>[54]</sup>. Successful marketed equipments include Mod UC Capsule filling and closing machine (German, Harro Hofliker) and G250 Capsule Filling (Italy MG2).

The biggest disadvantage lies in that the lower limit is up to 10mg, implying that lactose must be added as a bulking agent for API to increase filling precision and repeatability. It is commonly believed that lactose would exert a negative influence on delivery efficiency. Besides, an ideal powder state should be free flow, non-agglomerate, but the compaction during the dosing may cause powder agglomeration. At last, most standard dosator units are too large to achieve modular operation, making it impossible to add temperature and humidity control unit<sup>[54]</sup>.

### 2.3.1.2 Vacuum drum filler

The principle of the vacuum drum filler is to utilize a pocket on drum to measure powder. The most impressive advantage is the decreased requirement for powder flowability and much smaller metering quantity. For example, the typical vacuum drum filler as Omnidose® from Harro Hofliger is capable to meter and fill 1mg powder. When it is working, the drum sleeve is rotating under the powder bed and powder would enter the metering hole on the surface of the drum with the assistance of mechanical agitation and vacuum and excess powder would be wiped by a blade. When the metering pocket is rotated to an underneath position, a stream of compressed air come out from air channel instead of vacuum to push powder out (Fig.2.5a). Fadi et al<sup>[55]</sup> evaluated the performance of Omnidose® in tiny dose filling in DPIs by lactose, suggesting that this equipment could be used to meter 1~5mg powder.

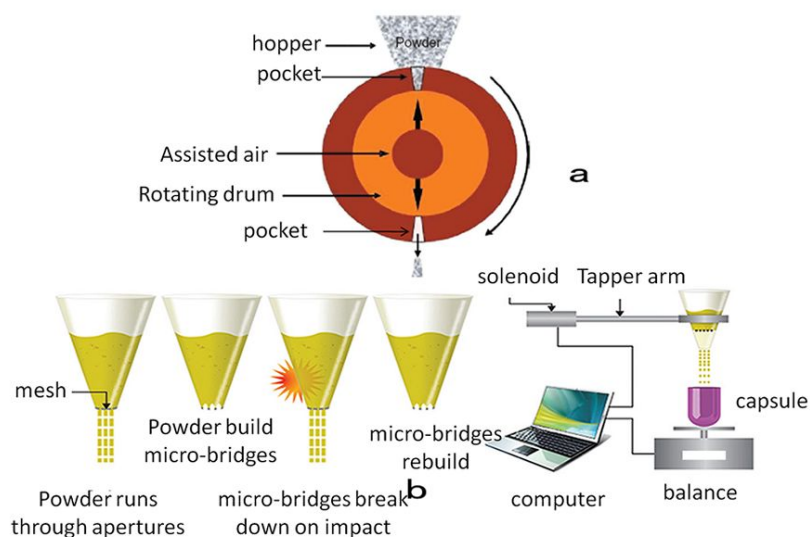


**Figure 2.5: Schematic of the working principle of Vacuum drum filler and Xcelodose 600<sup>[56]</sup>**

### 2.3.2 Powder filling by weight

The most advanced precise & micro metering system is the Xcelodose 600® from Capsule (Fig.2.5b). Its working principle is like a “pepper shaker”: vibration help powder flow out from the hopper, and a balance connected to a computer system would stop the vibration by a feedback system. When the vibration is suspended, the powder would form micro-bridges between holes on the tip of dispensing unit, then the powder flow stop. The metering quantity is dependant on powder flowability, diameter of holes on the dispensing unit and shaking strength and time.

This system can dispense 0.1mg to several hundred milligram powder with about 2% RSD, which is applicable to all kinds of capsule (5#-000#). The production capacity is 600 capsules per hour, suitable for stage I and stage II clinical trial<sup>[56]</sup>. Its most attractive attribute is able to meter extremely tiny powder, for example when metering 1mg sulfate salbutamol, its RSD is about 2.6%. Consequently, it also can be used to meter very expensive drug and high potent compound<sup>[54]</sup>. Additionally, the suitability test by using cohesive starch with 13 micron average volume median diameter (VMD) showed that the RSD is 2.2% when metering 0.5 mg per capsule and 900 capsules, and the metering time for each capsule is 2 second<sup>[57]</sup>.



Another filling by weight technology is Quantos® system by Mettler Toledo. Catalent company used this system to meter mixture of micronized API and lactose, when quantity is between 5~25mg, the RSD is less than 1% and 2.5% for 1~2.5mg. However, its metering process is rather slow, for instance 50mg powder required 20-30 second, which restricts its application in large scale<sup>[58]</sup>.

### 2.3.3 Other novel metering device

Chen et al. reported a vibrating capillary tube to meter powder. The diameter of the capillary was between 0.5~2mm, and lactose particles with 100~200 $\mu$ m VMD would flow in it quantitatively with 0.1-10mg/s flow rate. When an online weight feedback system detected that the metered weight is achieved, the feedback system would send signals to stop powder flow by mechanical blocking or vacuum. Results showed that this system could meter 3mg powder as a low limit with 2.5% RSD<sup>[59; 60]</sup>.

Zhu et al. utilized a rotation fluidized bed to meter tiny and extra-fine particles (Fig.2.6). Firstly, their patented technology achieved the uniform fluidization of particles, and then the particles will be absorbed into metering holes by vacuum. This device could be used to dispense and meter particles under 3 $\mu$ m, and quantity could range from 25 to 2000 $\mu$ g with 2.9% and 3.3% RSD<sup>[61]</sup>.

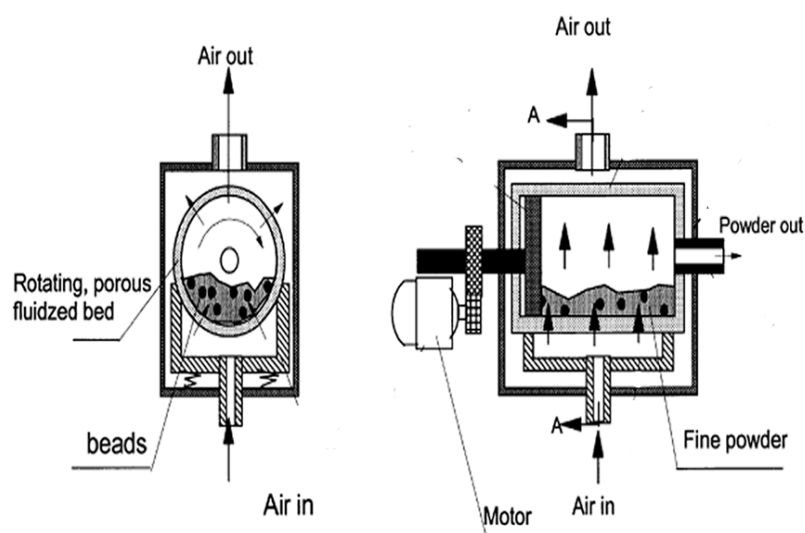


**Figure 2.6: Schematic of the working principle of Rotation Fluidized bed for filling<sup>[62]</sup>**

## 2.4 Formulation and Process for Dry Powder Inhaler

### 2.4.1 Inter-particle forces in DPI formulation

To better understand the composition and processing of DPI formulation, it is necessary to recognize the major inter-particle forces determining the formulation performance and stability. There are mainly four forces between particles.

Van der Waal force is often ignored when we consider large particles. Nevertheless, when particles go down to several microns, the Van der Waal should not be neglected anymore as a result of large specific surface area and small distance between particles<sup>[63]</sup>. If the Van der Waal attraction forces are too strong to impair flowability and dispersibility, it is a wise choice to add large particles into extra-fine ones or make the surface of particle more corrugated since the Van der Waal force of attraction is inversely related to square of inter-particle distance. Then, the Van der Waal forces decrease dramatically and aerosol performance is improved<sup>[64; 65]</sup>.

Capillary force is very important when pharmaceutical scientists consider the stability of DPI formulation. When particles are on micron scale, the pores among particles make water vapor easier to condensate as a result of decreasing saturated vapor pressure. Then, the capillary force would play a dominant role in the adhesion between particles, and significantly reduce the disaggregation and dispersion of a dry powder formulation<sup>[66; 67]</sup>. Once a liquid bridge forms among particles as Fig.2.7, local dissolution and recrystallization of surface material would make a irreversible aggregation through solid bridge between particles, which definitely would decrease the powder dispersibility<sup>[68]</sup>. Consequently, it is very critical to control the humidity of production environment and moisture in the formulation.

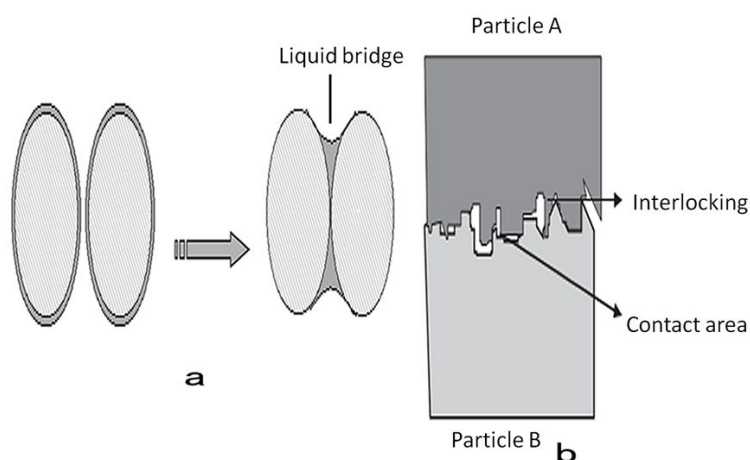


**Figure 2.7: Schematic of liquid bridge and mechanical interlocking**

Electrostatic forces rise mainly from impaction between particles, particles with container wall, during production and transportation<sup>[69]</sup>. Especially, production process would generate much electrostatic charge since a vigorous agitation is often used to obtain a uniform API-lactose blend. Electrostatic force not only has significant influence on drug content uniformity of blend<sup>[70; 71]</sup>, but also on aerosol performance. Pu et al<sup>[70]</sup> reported that uncontrolled electrostatic charge has an adverse effect on powder blend uniformity, meanwhile elimination or minimization of electrostatic charge also appears to have a negative impact on powder blend uniformity. Increasing moisture to a critical point would decrease the electrostatic and hence improve aerosol performance. Yet, when moisture is above a certain value, stability problems such as formation of liquid bridge would become dominate factor for aerosol performance<sup>[72; 73]</sup>.

Mechanical interlocking as Fig.2.7 due to surface features or roughness would increase particulate interaction and prevent particle dispersion<sup>[68]</sup>. The smooth/rough extent of the particle surface determined by the particle preparation method would influence the mechanical interlocking. For example, Raula et al coated sulfate salbutamol particles by L-Leucine to get powder with decreased surface roughness, which greatly improve aerosol performance compared common micronized particle, as a result of decreasing mechanical interlocking<sup>[74]</sup>.

### 2.4.2 Carrier for DPI formulation

DPI formulation is required to exhibit some flowability, which is critical to the production process, e.g. accurately dosing and delivered dose content uniformity (DDCU). Usually, drug particles are micronized by a jet-mill to several microns when high specific surface make particles tend to form agglomerates. Those tight agglomerates are difficult to meter accurately or dispense. The other larger sized particles used to separate those cohesive drug particles are applied into the formulation. Additionally, because of a high efficiency of inhalation drug delivery, the delivered dose is usually dozens to hundred micrograms, as shown in Table 2.2. This makes a big challenge for the pharmaceutical industry, since it is very difficult to meter such a small amount of particle with acceptable speed and accuracy. Consequently, a bulk excipient is required. A common solution is to blend the micronized particle with larger carriers to form interactive mixture. When a patient uses a DPI, the fine drug particles would detach from carriers and penetrate the deep airway. This method is still widely used for DPI development, although it may be somewhat unfavorable for efficient drug delivery. <sup>[75-79]</sup>

**Table 2.2: Types of DPIs, formulation and dose system<sup>[80]</sup>**

DPI	drug	drug: lactose	Total dose weight	Dose system
Spinhaler(Aventis)	20mg sodium cromoglycate	1:1	40mg	Capsule
Rotahaler(GSK)	200µg salbutamol	1:125	25mg	Capsule
Inhalator(Boehringer-Ingelheim)	200µg fenoterol	1:24	5.0mg	Capsule
Diskhaler(GSK)	100µg fluticasone	1:250	25mg	Blister
Diskus(GSK)	50µg salmeterol 100-500µg fluticasone	1:250	12.5mg	Blister
Turbuhaler® (Astrazeneca)	200µg budesonide	No lactose	200µg	Reservoir
Easyhaler(Orion)	100µg salbutamol	1:99	10mg	Reservoir
Twisthaler(Schering-Ploug)	200µg mometasone	1:5.8	1.36mg	Reservoir
Novolizer (ASTA Medica)	200µg budesonide	1:56.5	11.5mg	Reservoir

GSK denote GlaxoSmithKline, fluticasone and mometasone contain acid group respectively.

The most common carrier for DPI is  $\alpha$ -lactose monohydrate for its established safety profile, stable physical and chemical property<sup>[81]</sup>. During the formulation R&D process, the size distribution and surface property of lactose, ratio between lactose and API are important parameters, exerting a great influence on the final product performance<sup>[82-84]</sup>. Alternative carriers like mannitol, glucose, sorbitol, maltitol and xylitol have been studied for their potential use in DPI formulation<sup>[85; 86]</sup>.

To avoid the decline of delivery efficiency, sphere agglomerates formed by fine particles are fabricated purposely with or without carrier<sup>[87; 88]</sup>. Those sphere agglomerates exhibit good flowability as a result of larger size and regular shape. The stability against humidity and mechanical vibration is also improved, since those agglomerates would be treated under specific humidity condition<sup>[89; 90]</sup>. The most important thing for those agglomerates is to remain stable during storage and transportation, but easy to disaggregate during administration<sup>[91; 92]</sup>.

### 2.4.3 Additives

Besides of carrier selection, the fine particles excipient which usually are also lactose with much smaller size, play a key role to enhance the delivery efficiency. One common theory suggests that there are some “high energy” or “active” sites on coarse carriers, especially for carriers with rough surface, and fine drug particles tend to adhere to those sites tightly<sup>[93]</sup>. Those active sites may locate at pores, cracks of carrier and may be caused by amorphous part or powder processing<sup>[94]</sup>. Then, when additive fine particles are introduced into a formulation as competitors for those active sites, it definitely would help drug particle to detach from carrier surface<sup>[95-97]</sup>.

Magnesium stearate is widely studied to improve inhaler performance. Magnesium stearate could not merely increase powder flowability, but also serve to occupy active site on lactose as fine lactose and could stabilize the formulation<sup>[98-100]</sup>. Another additive, leucine could be used in powder processing, serving to decrease the density but enhance flowability and aerosol performance subsequently<sup>[74; 101]</sup>.

### 2.4.4 Powder preparation

In the past, the extra-fine particles are mostly micronized by a jet mill. The particles were produced with sufficiently small size but irregular and fragmented pieces, as Fig.2.8a. Recently, particle engineering like spray drying and super critical fluid (SCF) are used to produce particle with regular shape and favorable size distribution<sup>[102; 103]</sup>. The particles produced by spray drying are usually regularly hollow sphere as Fig.2.8b/c, which not only decrease particles interaction to exhibit better flowability but also decrease particle density to get smaller aerodynamic diameter even if geometric diameter is the same as

micronized flakes<sup>[104-106]</sup>. As is known, the particles produced by spray drying contain amorphous component which may transform to crystal after some time, causing stability problem. Fortunately, when the API is spray dried with carbohydrate, it would enhance the glass transition temperature, indicating that spray-dried powder would remain stable under ambient temperature. A famous example is the Pulmosphere® technology marketed by Nektar (Fig.2.8d). This technology has already been applied in commercial products, e.g. the first marketed inhaled insulin product where the insulin is dispersed in a buffered sugar based matrix<sup>[107; 108]</sup>. In a spray drying process, a blowing agent like fluorocarbon may be used to keep particles inflated and creating pores in their structure, resulting in a better performance<sup>[109]</sup>.

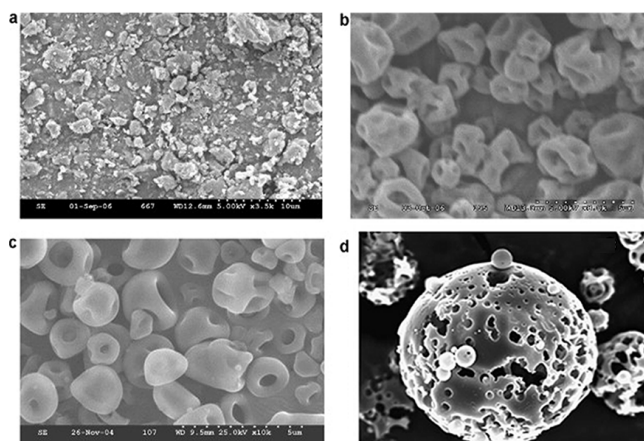


**Figure 2.8: Prepared particles. a, particles micronized by a jet mill; b,c particles prepared by spray dry<sup>[110]</sup>; d, Pulmosphere® particles<sup>[111]</sup>**

## 2.5 *In vitro* Evaluation for Dry Powder Inhaler

The ultimate and perfect assessment of DPI would definitely be a clinical trial. It would provide a definitive result of safety and efficacy, and be employed as the most powerful evidence to get regulatory approval. Unfortunately, unlike oral dose or injection, it is quite difficult to carry out a clinical trial for inhaler products, since the detection method is challenging and results may be confusing due to different airway attributes of subjects. Another point is that the clinical trial is so expensive that it is not suitable for early R&D phase or routine quality control and quality analysis<sup>[112]</sup>.

### 2.5.1 Inertial impaction method to characterize particle size

The primary deposition pattern of drug particle in human airway is an inertial impaction, which could be well reflected by an *in vitro* inertial impaction method. Hence, it should not be too surprising that the impaction method is considered as a “Gold standard” to evaluate inhaler products. Additionally, this method is included in pharmacopoeias of major countries<sup>[113]</sup>.

The principle of the inertial impaction method is shown in Fig.2.9. The larger particles with stronger inertial would impact the surface of collecting stage earlier, behaving similarly as larger particles impacting on primary bronchi. As a contrast, the smaller particles with less inertial are able to change their direction with airflow. Therefore, particles with different sizes could be divided into several sections and the section representing respirable part could be calculated to evaluate the delivery efficiency. What is worthy of attention, the diameter mentioned here is an aerodynamic diameter being correlated with particles’ aerodynamic behavior. Aerodynamic diameter is defined as the diameter of a sphere with unit density, settling in the air with the same velocity as the delivered particles.<sup>[114]</sup>

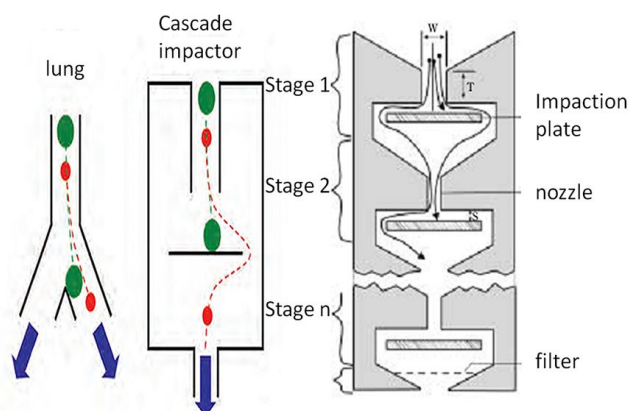


**Figure 2.9: A schematic diagram of particle deposition in lung and cascade impactors<sup>[114]</sup>**

There are several equipments for inertial impaction tests, like Twin impinger (TI), Next Generation Impactor (NGI) and Anderson Cascade Impactor (ACI), and the former two



would be used frequently in this research. Although those equipment outlooks are different, the main information that we get from the experiment is the same, such as the percentage of drug particles under a certain diameter in total drug particles.

As is known, the inertial impaction method is a preferable choice when compared with the clinical trial for inhaler product. Nevertheless, there are still lots of disadvantages for impaction test for *in vitro* evaluation. Firstly, impaction test is a labor-intensive work since analysts should collect and analyze the drug on each plate of the impactors. What is worse, because the quantity of drug collected on each stage is very tiny, high performance liquid chromatography (HPLC) is essential for inhaler analysis. When we consider a cascade impactor, the situation becomes even worse since there are about 10 separate parts requiring rinse and analysis, like NGI or ACI. Therefore, the impaction test is a labor- and time-intensive work. As a solution to this challenge, in the early R&D phase, an impactor with fewer stages like TI are applied to do lots of screen work and then carry out NGI or ACI tests for final quality evaluation. Secondly, impaction tests neglect the size change during flight by only considering particles deposited on stages. Luckily, this drawback is more serious for pMDI rather than DPI.<sup>[115-117]</sup> At last, unlike many other analytical instruments, it is almost impossible to carry out routine calibrations in a pharmaceutical laboratory. As a result, it is hard to distinguish the error from operation or instrument, and it is difficult to train new comers<sup>[118-120]</sup>.

## 2.5.2 Other particle sizing technologies

Thanks to technology progress, other particle sizing techniques have been increasingly used to characterize the aerosol emitted from inhalers. The most exciting one is laser diffraction method as Fig.2.10b, e.g. Sympatec Rodos® & Inhaler®. This technique utilizes a diffraction angle and shape produced when particles fly through a laser beam to calculate the particle size. A laser diffraction method could analyze lots of samples in a short time to accelerate inhalers R&D, and get a full profile of size distribution rather than particle size in a certain range. A laser diffraction method has been recommended by European pharmacopeia as a powerful supplement to test a nebulizer<sup>[121]</sup>. Yet, this method would not replace the impaction tests, since there are some inherent limitations for a laser method. Most important of all, the laser diffraction method could not

distinguish drug from excipient particles; hence it could not provide size distribution of pure drug particles. Another challenge is that laser diffraction result requires intensive calculation and transformation, particle properties like true density and shape factor may significantly affect the final results. At last, this technique could only get volumetric diameter, which further decrease its practicality<sup>[115]</sup>.

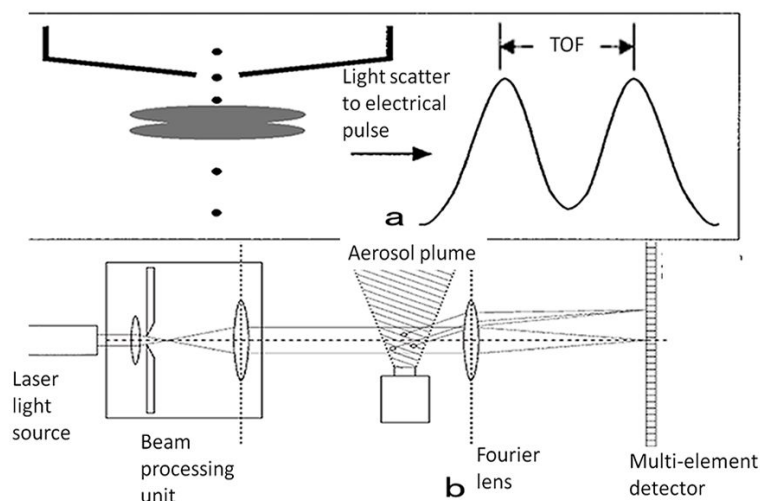


**Figure 2.10: Principle of Time of flight sizing<sup>[122]</sup> and laser diffraction sizing<sup>[23]</sup>**

Another famous particles sizing method for inhalers is Time of Flight technique (Fig.2.10a), e.g. TSI technology, which detect the time of a particle going through 2 adjacent laser beam and then transform the time value to a size by a calibration curve<sup>[123; 124]</sup>. Similarly, this method could not get information of the API size distribution either. Hence, to sum up, those laser sizing techniques may provide useful size information on particles, but could not provide critical data on drug size distribution, so it may just serve as a powerful supplement for impaction test rather than a substitution.<sup>[125]</sup>

Other techniques, like microscope and scanning electron microscope, are also used frequently. Those image results could reflect the size and shape of steady particles, plus particle interaction, like agglomeration and fine particle attaching to large carrier. Once again, people could not tell drug particles from excipients according to images. All particles observed are in static state and only represent a portion of the whole formulation.

### 2.5.3 Delivered dose content uniformity tests

Besides the delivery efficiency, another remarkable parameter of the inhaler product is delivered dose content uniformity. A constant and stable dose emitted from the inhaler device is a prerequisite of delivery efficiency. Only when a uniform delivery is achieved, then we move forward to the respirable fraction of API particle. The inhaler R&D and clinical application allow some drug particles to remain in a blister or capsule after one administration (usually not more than 20%), but the emitted dose should be constant during the whole test and usage.

For pre-metered inhaler devices, like single unit dose inhalers or multiple unit dose inhalers mentioned above, it is relatively simple to achieve the delivery uniformity, since an accurate amount of drugs has been filled into an independent unit package, e.g. a blister or capsule. As long as the powder in a unit package stays physically and chemically stable, the emitted dose would not change significantly. Meanwhile, for a multiple dose inhaler, like Turbuhaler® or Clickhaler®, the delivered dose content uniformity is greatly dependent on the powder metering and filling mechanism of the device, which could be influenced by lots of factors, like patients' operation, the powder remaining in the reservoir and mechanics condition of devices. Another point is that, drug powder stored in a reservoir is more likely influenced by environment moisture than inhaler with independent package.

Therefore, for a pre-metered inhaler device, sometimes regulatory agencies may be satisfied if a supplier proves that the drug content among capsules or blisters is uniform. Nevertheless, for a multiple dose inhaler, the manufacture first need to prove the emitted doses from the same batch or different batches are the same, implying a stable production process. Then, they are required to confirm that the emitted doses are uniform for a product through life, indicating the performance stability at the beginning, middle and end of usage.

## Chapter 3

### 3 Materials and Methods

#### 3.1 Brief Introduction

This chapter describes all methods, devices and equipment used in this project, including analytical methods and equipments, the inhaler devices, a powder filling and packaging system and materials for formulation researches. Some important definitions and calculation methods are also introduced right after corresponding equipments.

#### 3.2 Analytical Method

##### 3.2.1 Physical property analysis

##### 3.2.1.1 Bulk and tapped density

The bulk and tapped density was tested by FT-100A Powder Density Tester (Ningbo Haishu Instrument Ltd, China) as Fig.3.1b, which complied with USA/British/European pharmacopoeia. Because the quantity of powder sample was limited, 10ml cylinder was used. The tapping frequency was set to 100times/min, and the amplitude was 3mm. Firstly,  $m$  grams of powder was taken and poured into the cylinder freely and the volume of powder bed recorded as  $V_0$ . Then the shaking strength was set. After 500 times of shaking, the powder volume  $V_1$  was recorded and compared with the value  $V_2$  of 1250 times to ensure  $V_1$  equal to  $V_2$ .

$$\text{Bulk density } \rho_B = m/V_0$$

$$\text{Tapped density } \rho_T = m/V_1$$

Then compression index, e.g. Carr's index was calculated. It could reflect powder flowability to some extent, since larger compression represented lower flowability and vice versa.

$$\text{Compression index } carr's = (\rho_T - \rho_B) / \rho_T$$

### 3.2.1.2 Angle of repose

The angle of repose was tested by equipment developed in our lab as Fig.3.1a, which was suitable for a small amount of powder. Its principle was the same as a common angle of repose tester. The angles of repose at four directions were calculated and then get the average value  $\theta$ , representing the angle of repose for this powder.

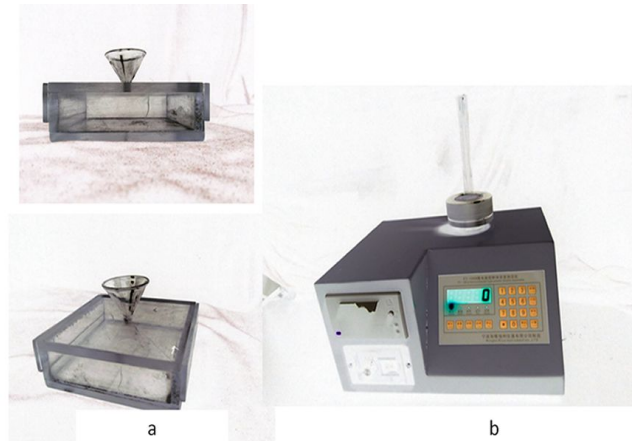


**Figure 3.1: Pictures of equipment for testing angle of repose (a) and powder density (b)**

In general, a smaller angle of repose indicates better flow property as listed in Table 3.1. Powders can be roughly categorized into the following 5 groups according to their angle of repose.

**Table 3.1: The relationship between Angle of repose and flow properties**

Angle of repose	Flow properties
$20^{\circ} < \theta < 30^{\circ}$	Very free-flowing
$30^{\circ} < \theta < 38^{\circ}$	Free-flowing
$38^{\circ} < \theta < 45^{\circ}$	Fair to passable flow
$45^{\circ} < \theta < 55^{\circ}$	Cohesive
$55^{\circ} < \theta < 70^{\circ}$	Very cohesive

### 3.2.1.3 Solid state property

To study the influence of jet mill on the solid state property of particles, Thermogravimetric Analysis (TGA, Netzsch tg 209 f1, German), Differential Scanning calorimeter (DSC, Netzsch dsc 204 f1, German) and X-Ray Polycrystalline Diffractometer (XRPD, D8 Advance, German) were used. TGA was a thermoanalytical technique by which a very small but accurate change of weight of samples was measured as a function of increasing temperature (with constant heating rate). Usually, TGA could effectively provide information on second-order phase transitions, including vaporization, sublimation, and absorption and desorption. During the development of DPI formulation, it was often applied to characterize moisture such as crystallization water and absorbed water<sup>[126]</sup>. During the DSC test, the difference of heat to increase the temperature of the sample and a reference was measured as a function of temperature. This technique could be applied to study polymorphs and content of amorphization during powder preparation<sup>[127; 128]</sup>. XRPD applied X-ray diffraction on powder or microcrystalline samples for structural characterization of materials. This technique could detect the change of polymorphs and content of amorphization during powder preparation<sup>[129; 130]</sup>.

The TGA and DSC took about 2mg sample for each test, with the same temperature program from ambient to 300°C at 10K/10minutes rate, under N<sub>2</sub> atmosphere protection. XRPD was carried out with a condition as: SCAN: 3.0/45.0046/0.01974/23.66 (Sec), Cu

(40kv, 40mA),  $I$  (max) =34988. Yet, those tests were not carried out by us but by a professional analytical center that provided a contracted research service.

#### 3.2.1.4 Scanning electron microscope

Scanning electron microscope (SEM, Hitachi S-2600, Japan, Fig.3.2) was applied to characterize the shape, surface, size of particles and particle interaction. A small amount of sample would be mounted rigidly on a specimen stub. As a result of non-conductivity, specimens were coated first with an ultra-thin coating of electrically conducting gold by low-vacuum sputter coating. Then the pretreated sample would be analyzed by SEM.



**Figure 3.2: A picture of SEM (Hitachi S-2600, Japan)**

#### 3.2.1.5 Electrostatic charge test

As Fig.3.3, a combination of Faraday pail (JCI-150, British) and a charge measurement unit (JCI-178, British) was used to measure the electrostatic charge of powder and package material. When the charged powder was placed in the inner barrel, the surface of inner barrel and outside barrel would generate potential difference. Then, the difference was used to calculate the quantity of charge.

The JCI-178 could detect the charge from  $0 \sim \pm 20\text{nC}$  and  $0 \sim \pm 200\text{nC}$  with a resolution of  $\pm 10\text{pC}$ . Before a test, all cables were connected and JCI-178 was reset to 0. Then, m g sample was carefully transferred into the Faraday pail softly to avoid electrostatic charge caused by the transfer. The charge value was displayed on JCI-178 screen as Q. The most

important thing for this test was that all interference should be eliminated. For example, the JCI-178 should be grounded well; tester wear anti-static clothing and gloves, and tests should be carried out in stable environment. All samples were tested 3 times in parallel but not repeatedly.

The charge-to-mass ratio was calculated as  $e/m = Q/m$ .

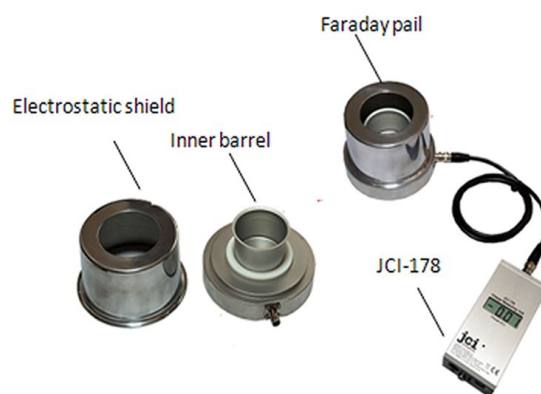


**Figure 3.3: A picture of JCI-150 and JCI-178 (Chilworth Technology Ltd, UK)**

### 3.2.2 HPLC method for content analysis

High-performance liquid chromatography (HPLC) method was the most common analytical equipment in pharmaceutical R&D. This method could effectively isolate a substance from others and accurately quantify its content even. During an analytical process, each analyte interacted differently with the adsorbent material of the solid phase; hence the required elution time for each substance might be different when using the same elution solvent-mobile phase. Its quantitative principle was based on the Lambert–Beer law,

$$A = K \cdot l \cdot c$$

When a beam of UV (Ultraviolet) light passed through the sample solution, the absorbance (A) was proportional to absorption coefficient K of the substance, light path length l and substance concentration C. The former two parameters were constant for the



same substance and the instrument; hence the concentration  $c$  could be calculated from absorbance  $A$  by a calibration curve. Therefore, as a foundational work, the HPLC method had to be validated first for linearity, accuracy, precision, specificity and durability.

The HPLC condition was listed as follows:

Separation module-e2695 (Waters, USA) as Fig.3.4;

UV detector 2487 (Waters, USA);

Solid phase: SUPELCO C18 15cm\*4.6mm, 5 $\mu$ m (Sigma-Aldrich, USA);

Mobile phase: 0.08mol/L  $\text{NaH}_2\text{PO}_4 \cdot 2\text{H}_2\text{O}$  (pH3.11): methanol (HPLC grade) = 85:15;

Detection wavelength: 276nm;

Column temperature: 25°C;

Injection volume: 100 $\mu$ l;

Flow rate: 1ml/min.



**Figure 3.4: A picture of HPLC e2695 and 2487 (Waters, USA)**

During a HPLC analysis, reference samples with known concentration ( $C_0$ ) were analyzed first for the peak area ( $A_0$ ), and then a Calibration Factors (CF) was calculated like this:

$$CF = A_0 / C_0$$

Usually, 2 reference samples were injected twice and 4 CF would be obtained for each content assay. It was required that the relative standard deviation (RSD) of 4 CF values was less than 2% to make sure the HPLC system was stable.

When the peak area ( $A_1$ ) of another sample was acquired, the concentration ( $C_1$ ) and quantity ( $m_1$ ) could be calculated, where  $V_1$  stood for dilution volume.

$$C_1 = CF * A_1$$

$$m_1 = C_1 * V_1$$

### 3.2.3 *In vitro* method for particle Size characterization

#### 3.2.3.1 Inertial impaction tests

Glass twin impinger (TI, also named as TSI) was a simple and convenient impaction equipment for inhalers, especially suitable for early R&D work. As Fig.3.5, this device could be divided into three parts: throat (induction part), stage1 and stage2.

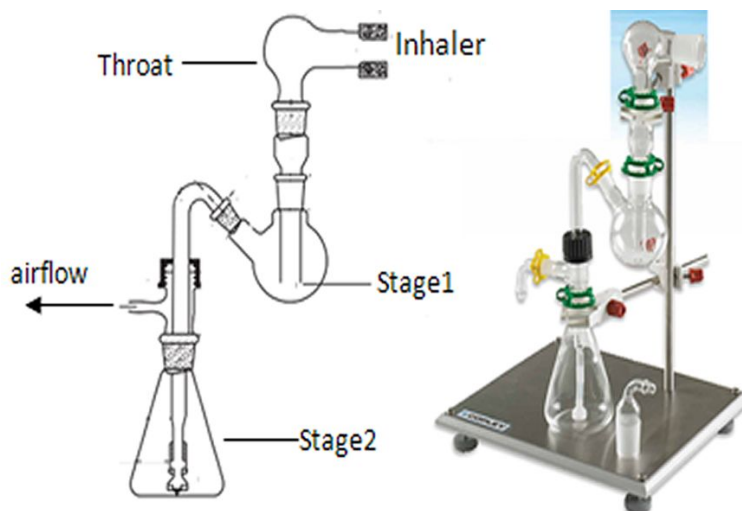


**Figure 3.5: A schematic diagram and a picture of twin impinger (Copley, UK)**

The operations could refer to European Pharmacopoeia 7.0 and China Pharmacopoeia 2010. 1) 7ml receiving solvent was added into stage1 and 30ml to stage2. 2) turn on the vacuum, adjust flow rate to 60L/min and turn off the solenoid valve. 3) Insert a inhaler

into the throat with a suitable adapter; 4) Release a dose and turn on the solenoid valve which would turn off automatically when a set time was over; 5) Repeat above procedures for required doses, 6) Turn off the vacuum, and use a receiving solvent to rinse each part to a set volume; 7) Analyze the drug content by the HPLC. It was noteworthy that the same sampling operation was applied in all in-vitro evaluation as following: the inhaler was actuated first according to its instruction, with the vacuum pump running and the solenoid valve closed; the powder is discharged into the sampling apparatus with the airflow, by activating the timer controlling the solenoid valve.

There are several important definitions which have to be described clearly. The **Total Recovery Mass (TRM)** indicates all drugs recovered from inhaler device, throat, stage1 and stage2. The **Total Recovery Rate (TRR)** is used to evaluate the recovery rate of impaction test, and usually the higher TRR represent a better operation. The **Emitted Dose (ED)** means that all drugs delivered out from the mouthpiece of the inhaler, including drug in adapter/throat, stage1 and stage2. By comparing TRM and ED, it could be calculated that how much drug is left in the inhaler device. The **Fine Particle Dose (FPD)** here refers to drug deposited in stage2 with aerodynamic diameter under  $6.5\mu\text{m}$ . This FPD is proportional to the respirable dose. The **Fine Particle Fraction (FPF)** usually is defined as the ratio of FPD to ED. Similarly, the deposition fraction of each part could be calculated. The **Blister remains** indicates the fraction of powder remains in the blister after a test, which somewhat reflects the delivery efficiency.

$$TRM = m_{device} + m_{throat} + m_{stage1} + m_{stage2}$$

$$TRR = TRM / \text{Labeldose}$$

$$ED = m_{throat} + m_{stage1} + m_{stage2}$$

$$FPD = m_{stage2}$$

$$FPF = FPD / ED$$

$$\text{Fraction of blister remains} = m_{\text{blister remains}} / (m_{\text{blister remain}} + ED)$$

The twin impinger is useful to get a rough deposition profile by dividing particles into two parts: the larger one ( $>6.5\mu\text{m}$ ) and smaller one. But it could not provide more information on particle size distribution. Hence, the Next Generation Impactor (NGI) is applied, as Fig.3.6.

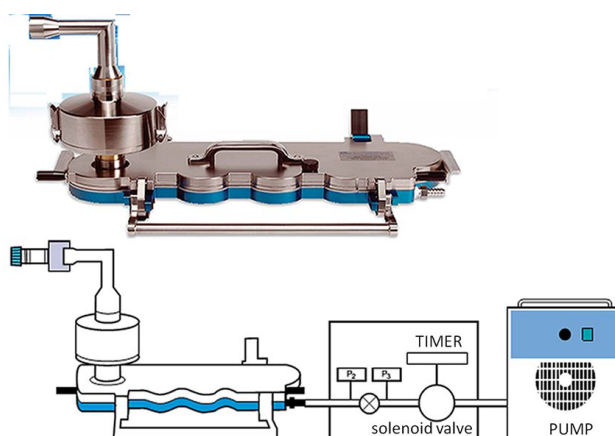


**Figure 3.6: A picture of Next Generation Impactor with pre-separator (Copley, UK) and a schematic diagram of NGI connected with a flow controller and pump.**

The NGI is mainly comprised of three parts: a bottom frame holds the impaction stages, a seal body holds the jets, and a lid that contains the inter-stage passage. The inner structure is shown in Fig.3.7. Particles are blown out from jet nozzles with airflow, then particles within a certain size range would deposit in corresponding stages and smaller particles would fly into the next stage as a result of smaller inertia. Since particles deposit in collection stages, those particles are difficult to fly away during the rinse and collecting process. These collection stages could be moved and replaced as a whole set. As a result of replaceable design, the efficiency of instrument is significantly enhanced. Meanwhile, as all collection stages are placed on the same level without interference, an automatic rinse and sampling become possible.

Unlike NGI used for pMDI, an additional pre-separator is assembled before collection stages for testing a DPI. Since lots of carriers in a DPI formulation could result in overload on collection stages, a pre-separator is essential to avoid particles bounce or reentrainment into the airflow.

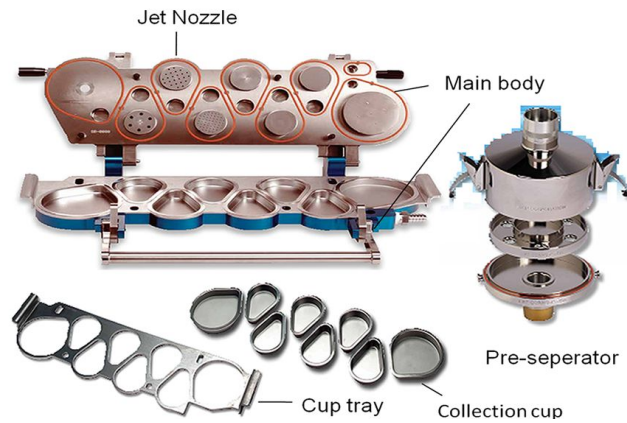


**Figure 3.7: A picture of internal structure of Next Generation Impactor and the pre-separator (Copley, UK)**

The operations was described as follows: 1) Assemble the equipment as instruction, turn on vacuum and set flow rate to a designated value and turn off the solenoid valve; 2) Connect a inhaler to induction port and release a dose, turn on solenoid valve to start flow for a set time; 3) Repeat above operations for designated doses and turn off vacuum; 4) Rinse each part including induction port, pre-separator, stage 1-7 and the last micro-orifice collector (MOC) by suitable solvent; 5) Determine the drug content in each part.

Similar as Twin Impinger, the *in vitro* deposition could be analyzed by following values: **Total Recovery Mass (TRM)**, **Total Recovery Rate (TRR)**, **Emitted Dose (ED)**, **Fine particle dose (FPD)**, **Fine particle Fraction (FPF)** and **Mass Fraction of stage-i (MF<sub>i</sub>)**.

$$TRM = m_{device} + m_{induction} + m_{pre-sep} + \sum_{i=1}^{moc} stage_i$$

$$TRR = TRM / Labeldose$$

$$ED = m_{induction} + m_{pre-sep} + \sum_{i=1}^{moc} stage_i$$

$$MF_i = m_i / TRM$$

A major difference of calculation between TI and NGI is that the FPD would change with flow rate for NGI, since the cutoff diameter  $D_{50}$  of each cup would alter with flow rate. The cutoff diameter at Q flow rate  $D_{50,Q}$  is calculated like following according to U.S pharmacopoeia 32:

$$D_{50,Q} = D_{50,60LPM} * (60/Q)^x$$

**Table 3.2: Cutoff aerodynamic diameter for stages of NGI (US Pharmacopoeia 32)**

To calculate D50, Q for flow rate at Q within 30-100LPM		
Stage	D50,60LPM( $\mu$ m)	x
1	8.06	0.54
2	4.46	0.52
3	2.82	0.50
4	1.66	0.47
5	0.94	0.53
6	0.55	0.60
7	0.34	0.67

When flow rate is 60LPM, then the cutoff diameter of stage2 is 4.46 $\mu$ m. It means that stage2 would capture particles within 4.46~8.06 $\mu$ m and all particles above 4.46 $\mu$ m are captured before stage3. Consequently, the FPD (<4.46 $\mu$ m) under 60LPM is calculated like:

$$FPD(< 4.46\mu m, 60LPM) = \sum_{i=3}^{moc} stage_i$$

$$FPF(< 4.46\mu m, 60LPM) = \sum_{i=3}^{moc} stage_i / ED$$

### 3.2.3.2 Laser diffraction size tests

Laser diffraction was utilized to characterize the particle size of carriers and the API. The laser diffraction sizing was employed as a useful tool for formulation work but not a direct measurement of inhaler performance. Sympatec Helos® (Fig.3.8a) and Rodos® (Fig.3.8b) were combined to test dry powder samples. Helos® is a laser optical system. It could measure particles within different size ranges by corresponding lens with an automatic lens changing system. The R2 and R4 lens were used to characterize particle from 0.25µm to 87.5µm, 0.5µm to 350µm respectively. Specifically, the R2 lens was used to measure fine particles, like API or fine additives. And R4 was used to test lactose carrier. A Rodos® dispersion system with the Vibri feeding system was employed to disperse particles by impaction and friction of particles in high speed airflow. It was claimed by the manufacturer that this system could effectively disperse particles as small as 0.1µm.

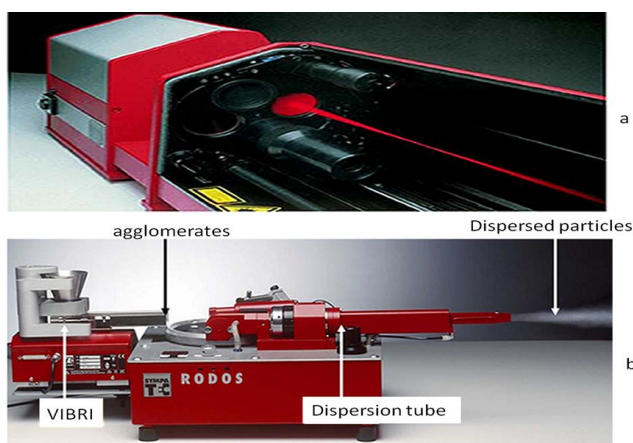


**Figure 3.8: Pictures of Sympatec Helos (a) and Rodos (b) (Sympatec, German)**

The operation parameter:

Assume all particles were sphere and density as unit;

Quantity of sample: ~20mg;

Lens: R2 or R4;

Trigger and termination condition: start when  $C_{opt} \geq 0.5\%$  (optical concentration above 0.5%); stop 4s after  $C_{opt} \leq 0.1\%$  or 4s real time.

Dispersion condition: 3~4bar

Usually, three points on the size distribution profile were taken for analysis: X10, X50 and X90. For example, X10 represented a diameter that 10% of particles by volume accumulation were smaller than it.



**Figure 3.9: Pictures of Sympatec Helos and Rodos combination (Sympatec, German)**

### 3.3 Dry Powder Inhaler Device

#### 3.3.1 Evaluation of marketed dry powder inhalers

Several typical marketed dry powder inhalers as Table.3.3 were evaluated, serving as a comparison with the novel DPI device designed by us. It was noteworthy that dose uniformity was a major concern for reservoir-type device, e.g. Turbuhaler® Oxis® and Clickhaler® Asmasal®. Thereby, a test of delivered dose content uniformity (DDCU) described later was carried out for these two inhalers. Besides, the airflow resistance of all devices was acquired. This resistance was an important parameter of the inhaler device, which would directly influence the feeling and effect when patients use it.



**Table 3.3: Evaluation items of typical marketed products**

Brand name	API	Test Items	Types of device
Aerolizer® Foradil®	Fumarate formoterol 12µg/dose	TI NGI	Capsule
Diskus® Seretide®	Salmeterol&Fluticasone propionate 50µg&250µg/dose	Air resistance Laser diffraction sizing	Multiple blister
Turbuhaler® Oxis®	Fumarate formoterol 6µg/dose	TI NGI Air resistance DDCU Laser diffraction sizing	Reservoir
Clickhaler® Asmasal®	Sulfate Salbutamol 95µg/dose	TI ACI Air resistance DDCU	Reservoir

The operation parameters for TI and NGI are summarized as Table 3.4. Both TI and NGI were carried out under the **same flow rate of 60 LPM and same flow time of 4 seconds**. A certain volume of rinsing solvent was added to each stage of cascade impactor, and the drug content was analyzed by HPLC.

**Table 3.4: Critical impaction test parameter for the marketed products**

Brand name	Delivered dose for TI	Delivered dose for NGI	Rinsing solvent
Aerolizer® Foradil®	2 capsules	2 capsules	Methanol:water=1:1
Diskus® Seretide®	5 blisters	10 blisters	Methanol:water=7:3
Turbuhaler® Oxis®	10 doses	20 doses	Methanol:water=1:1
Clickhaler® Asmasal®	5 doses	10 doses for ACI	Water

Primary parameters of HPLC methods for above 4 products are listed as Table.3.5. The Foradil® and Oxis® had the same condition as a result of the same API—formoterol. The detection method was relatively complicated for Seretide® because of a combination of two APIs. The salmeterol was detected by fluorescence with an excitation wavelength of 225nm and emission wavelength at 305nm.

**Table 3.5: Primary parameters of HPLC methods for marketed products**

Brand name	Mobile phase	Column	Detection wavelength	Injection
Foradil®	Acetonitrile-PBS(3.10)=25:75	ultimate XB-C18 4.6*250mm 5µm	UV 214	100µl
Seretide®	methanol-Acetonitrile-water=30:30:40	Kromail C18 150*4.6mm.5µm	Fluorescence 225nm&305nm UV 239	100µl
Oxis®	Acetonitrile-PBS(3.10)=25:75	Ultimate XB-C18 4.6*250mm 5µm	UV 214	100µl
Asmasal®	methanol-PBS (pH 3.10) =15:85	Waters X-Bridge C18, 150*4.6 mm, 5µm	UV276	50µl

Delivered dose content uniformity and inhaler device air resistance evaluation utilized the Dose Uniformity Sampling Apparatus (DUSA) shown as Fig.3.10.

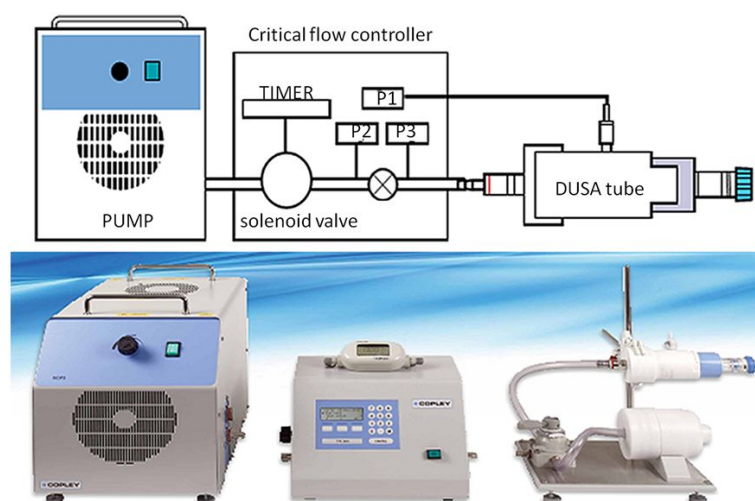


**Figure 3.10: A schematic diagram and picture of Dose uniformity sampling apparatus connected with a flow controller and pump(Copley, UK)**

DDCU test was carried out like that: 1) Adjust the flow rate to 60LPM and set the time to 4s; 2) Insert an inhaler into DUSA tube and release a dose, then turn on solenoid valve which would turn off automatically; 3) Turn off vacuum pump, rinse DUSA tube and analyze the drug content. Since different inhalers had different amount of API, it was better to use the ratio of delivered dose to the labeled dose. Then the RSD of 10 delivered ratio could be calculated to evaluate the uniformity.

$$\text{Delievered Ratio}=\text{Delivered dose}/\text{Labled dose}*100\%$$

The test for air resistance was slightly different: 1) Adjust the flow rate to a series of value (20, 40, 60, 80 LPM); 2) Insert an inhaler into the DUSA tube, make it in the status of releasing doses; 3) Record the pressure drop through the device, reflected by P1 value; 4) Establish a linear regression of the square root of P1 on the flow rate, where slope stood for **device resistance**.

### 3.3.2 Design of a novel dry powder inhaler device

A novel dry powder inhaler device was developed in our group. This device has following characteristics: 1) multiple unit doses, it can be used repeatedly; 2) Passive delivery mode, no need for an operation-inhalation coordination; 3) micro-dose, suitable for 1~5mg powder; 4) blister package, precise dosing and better moisture proof. Because this device has been developed by Western University from 2011, it was named as **Inhaler-WU2011** for short. Its basic principle is shown in Fig.3.11: A hollow acupuncture pieces the drug package. Then a patient inhales from the mouthpiece, and the inspiratory flow would fluidize and entrain powder to form gas-solid aerosols. Simultaneously, the aerosols are delivered to patients' lung with the inspiratory airflow.

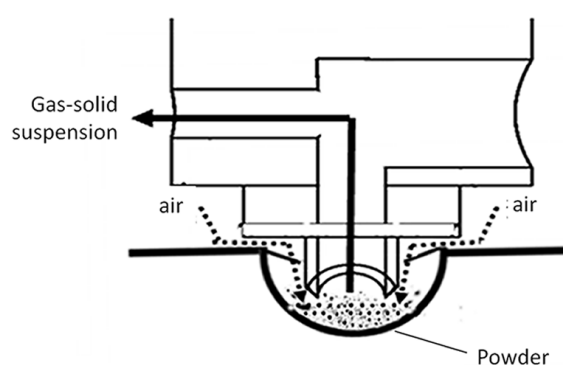


**Figure 3.11: A schematic diagram of Inhaler-WU2011 working principle**

The appearance is shown in Fig.3.12a, b. The inhaler is comprised of an outer shell and an inner functional part. Since the mouthpiece is placed in the mouth when a patient

using this device, a shell is necessary to keep the mouthpiece clean. Besides, the shell can also provide protection against misuse, e.g. pushing down the push button by accident. The basic dimensions are shown in Fig.3.12c&d. The dimensions show that this device is rather compact and portable.

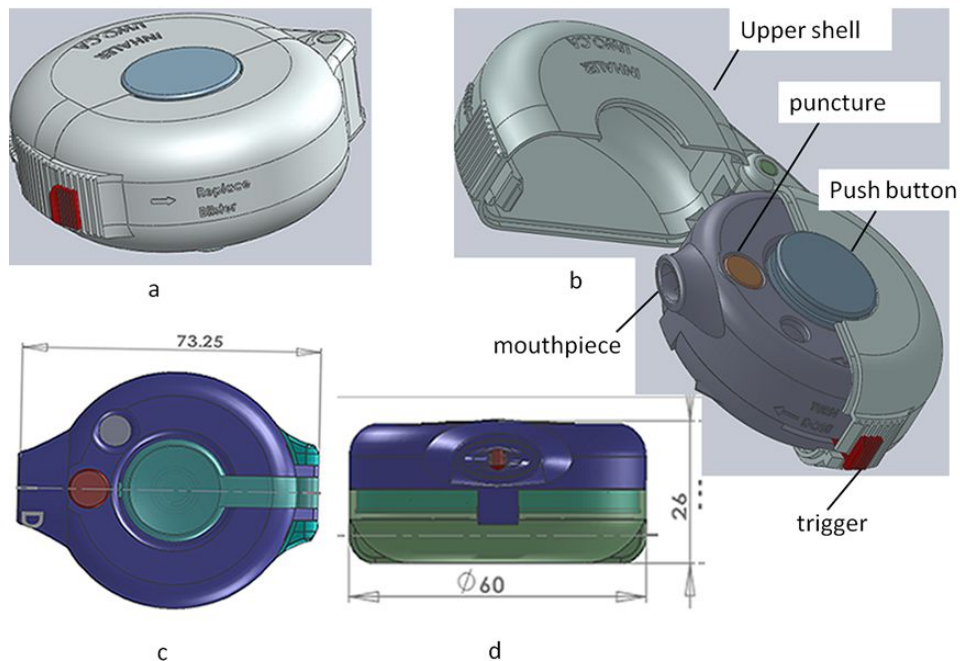
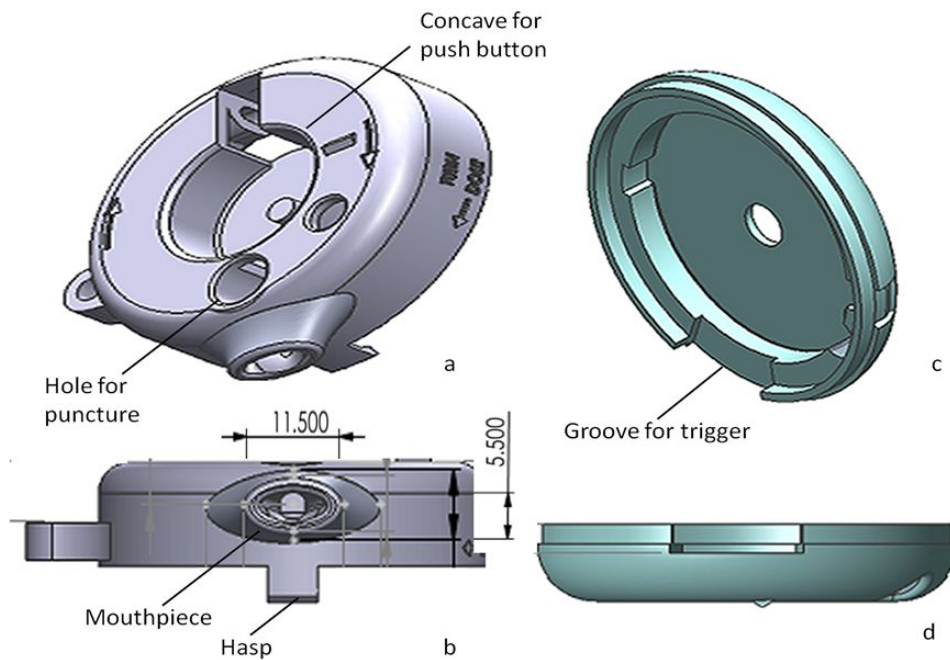


**Figure 3.12: Appearance and primary dimension of the novel inhaler**

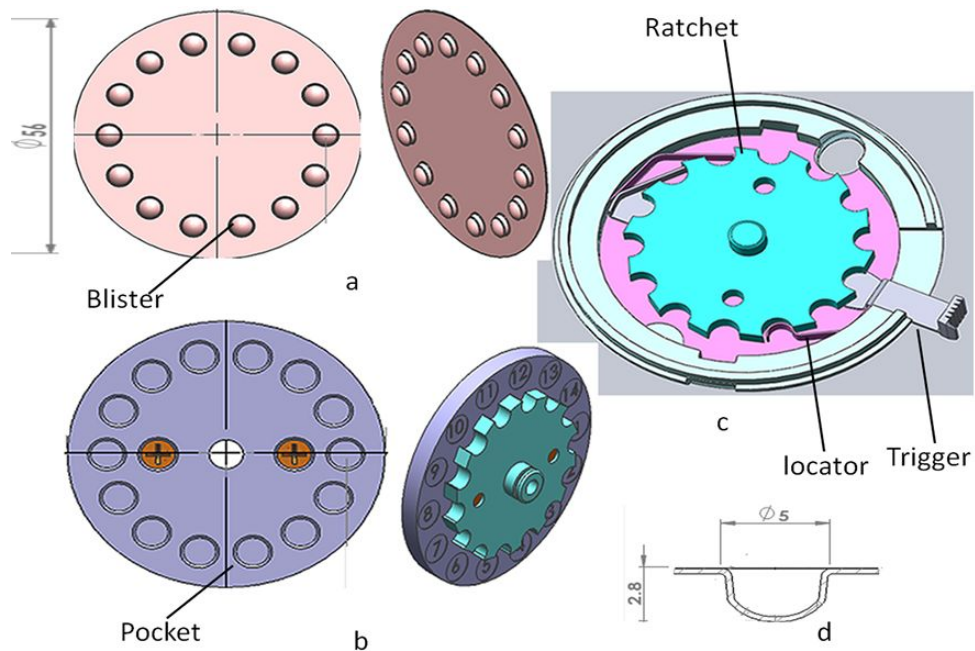
The functional parts of **Inhaller-WU2011** include an upper cover and lower cover. The push button, puncture and mouthpiece are integrated on the upper cover, as shown in Fig.3.13a. The center of the cover and central axis connected with mouthpiece are hollowed out, where the push button and puncture could be placed. The puncture can only move up and down vertically without horizontal movement in a hole. Hence, the vertical motion ensures that the puncture pierces the blister package in the center accurately time by time. As shown in Fig.3.13b, the mouthpiece is rather small, suitable for both children and adults. Two hasps on the upper cover are used to assemble upper and lower cover, which can be opened when replacing a drug disk.

Fig.3.14 displays the inner structure of the inhaler device; a drug disk containing 14 blisters is placed on a circular tray with suitable pockets. The circular tray is bound with a

ratchet underneath, which is driven by a trigger unidirectionally. As shown in Fig.3.14c, when moving the trigger clockwise, the ratchet rotates and makes the circular tray and drug disk rotate for next blister. Meanwhile, when moving the trigger anti-clockwise, the ratchet would remain still as a result of braking effect by the locator.



**Figure 3.13: A schematic diagram of Inhaler-WU2011 upper and lower covers. a&b, upper cover; c&d, lower cover.**



**Figure 3.14: A schematic diagram of Inhaler-WU2011 inner structure. a, drug disk; b, disk tray; c, combination of the ratchet, trigger and lower cover; d, dimensions of a blister.**

As shown in Fig.3.15a&b, a sharp formed by two wedges is located at the bottom of the hollow puncture. When the puncture moves downward, the sharp pierces the package of a blister with a tearing effect. After delivering a dose, the push button would go back as a result of a spring, and brought the puncture to its original position. Some notches are carved on the bottom surface of the puncture, which are designed to introduce airflow through the notches into a blister and produce a better fluidization and entertainment effect.

The air pathway is placed inside the upper part of the puncture. This air passage is comprised of two parts, one connected with push button and the other one connected with the mouthpiece.

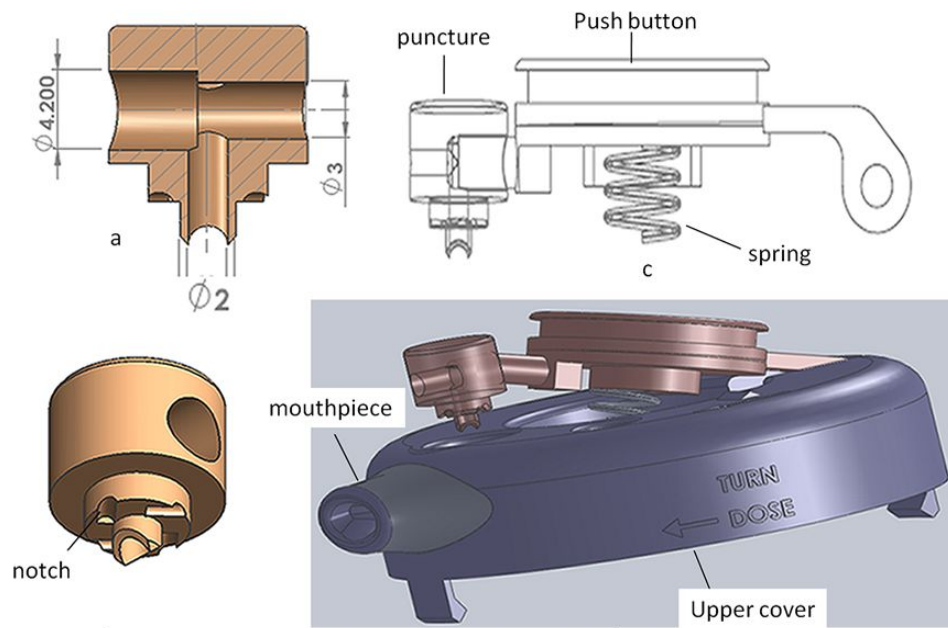


**Figure 3.15: A schematic diagram of Inhaler-WU2011. a, cross-section diagram of puncture; b, the shape of the puncture; c, puncture combined with push button; d, combination of puncture, push button and upper cover**

**Table 3.6: The material for primary parts of the inhaler-WU2011**

Part	Material
Outside shell	Styrene acrylonirile copolymer (AS)
Upper and lower cover	AS
Mouthpiece	Polypropylene (PP)
Ratchet	Polyoxymethylene (POM)
Puncture	Steel, SUS304
Drug disk tray	AS
Trigger	Steel, SUS304
Push button	Steel, SUS304
Locator	Steel, SUS304

The operation of this new inhaler device is described as follows: 1) Open the upper shell; 2) Push down the button and the puncture would pierce top surface of a blister; 3) Keep

the pressed status and put the mouthpiece into mouth and wrap it tightly, then take a deep breath and the inspiratory flow would fluidize particles and take them through the air passage and mouthpiece into the lung; 4) When an administration finished, release the button, then push button and puncture go back to the original position; 5) Move the trigger clockwise once, driving the ratchet and circular-tray rotate for next blister. 6) When a disk is finished, the device could be opened by unlocking the hasps and a new drug disk could be placed into the circular tray. Therefore this device can be used repeatedly.

### 3.4 Dry Powder Inhaler Filing Device

#### 3.4.1 Design and implement of packaging system

As mentioned before, the powder formulation, inhaler device and filling & package equipment constitute a whole system. Based on this principle, a small blister and puncture structure (dimension shown in Fig.3.14&3.15), plus a small amount of powder, determine that the filling technique has to meter and dispense several micrograms powder. Yet, there is no powder filling device on the market, which is able to dispense a small amount of powder into 14 blisters in one disk simultaneously. Consequently, a whole system including blister package formation, powder filling, hot sealing and final punching was established.

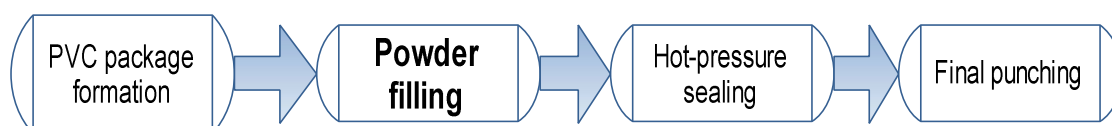


**Figure 3.16: A flow chart of filling and packaging.**

Polyvinyl chloride (PVC) is commonly used for drug package. During production of drug disks, the PVC is pre-heated ( $>150^{\circ}\text{C}$ ) to become soft first, then placed into a special designed mold where pressure air (0.56~0.74Mpa) blow against the soft PVC material to form desired blisters. After filling powder into blisters, the drug disk is sealed with aluminum foil by hot pressing. Following that, the sealed disk is punched to cut off



excessive PVC and foil. If this disk is used for a stability test, one additional foil package is used to wrap the disk for better anti-moisture.

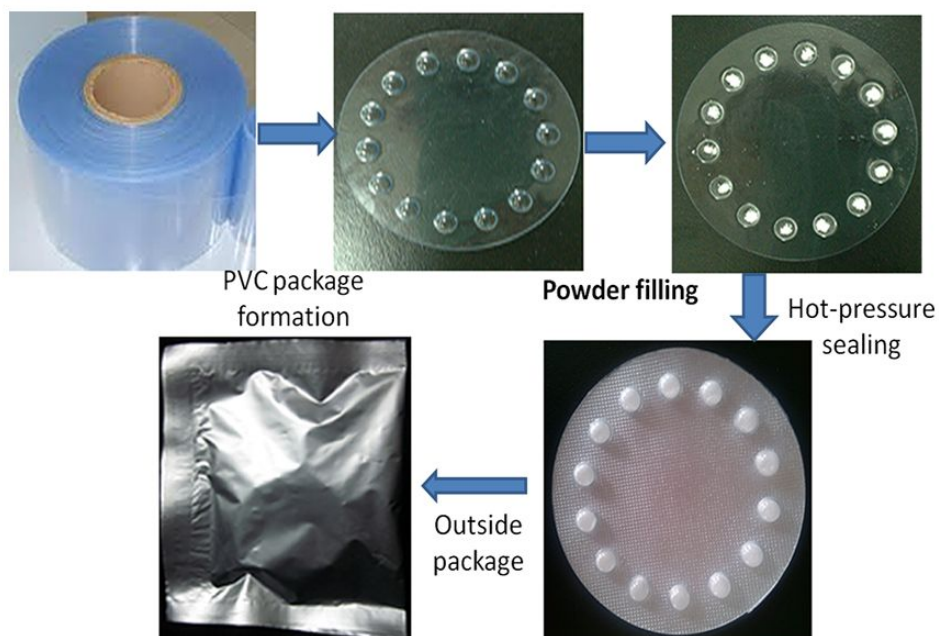


**Figure 3.17: The whole process of drug disk production**

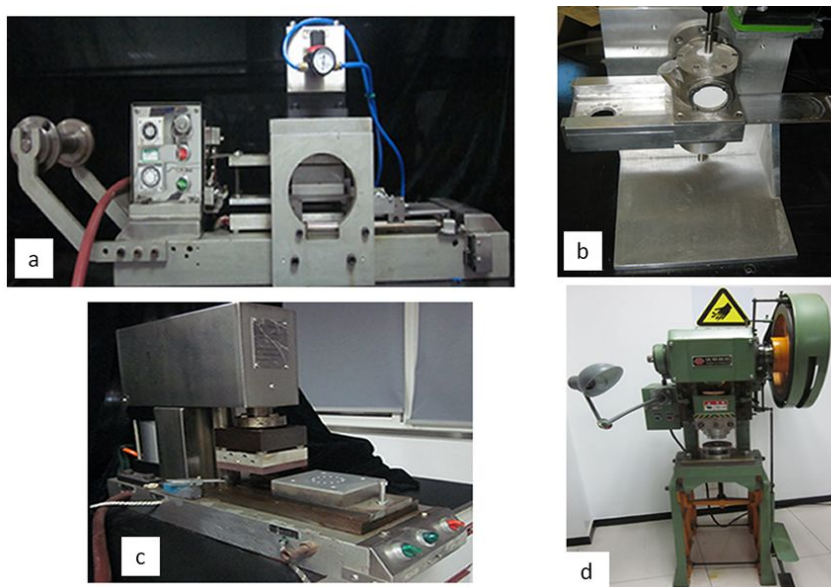


**Figure 3.18: The pictures of equipment for disk formation (a), powder filling (b), hot-pressing sealing (c), punching (d).**

### 3.4.2 Design and implement of Powder Filling system

As shown in Fig.3.19, the principle of filling device is rather simple, using volumetric quantitation. With or without assistance of vacuum, the powder enters into metering pockets as a result of mechanical stirring and form a loose powder “cake”. When the metering plate is moved to the right position where the pockets were vertically above the blisters, the plate is vibrated to make powder in the pockets fall into blisters. The quantity of powder in each blister is determined by the volume of a metering pocket and powder density. This filling device can fill 14 blisters simultaneously as there are 14 metering pockets in the plate.

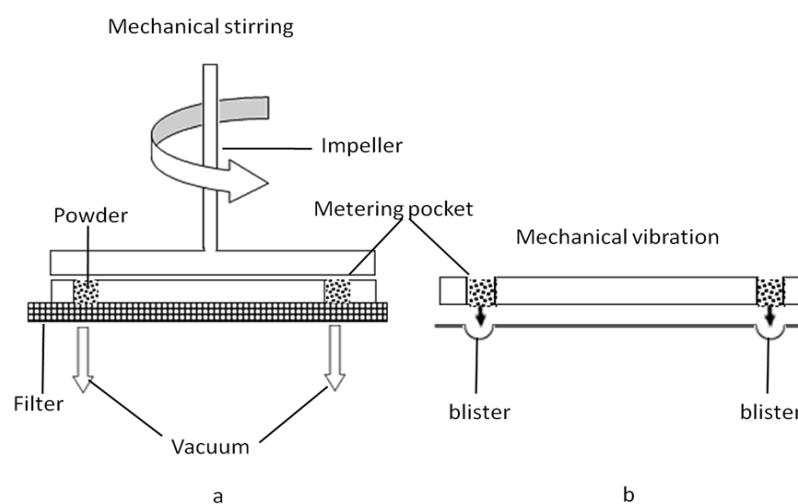


**Figure 3.19: A schematic diagram of the filling device working principle.**

The device design is shown in Fig.3.20. A motor provides the mechanical stirring and a tube can be connected with vacuum. A steel plate with 14 metering pockets at its left end slides in designated grooves. When it slides to the right end, metering pockets are filled with powder in the powder chamber. When the metering plate slides to the left end, metering pockets are vertically above empty blisters. After mechanical vibration, powder falls out of the pockets into blisters. During the plate sliding process, a polymer blade in the chamber wipes powder on the surface of the plate. Two steel bars (Fig.3.21) on both ends of the metering plate help the metering pockets locate accurately.

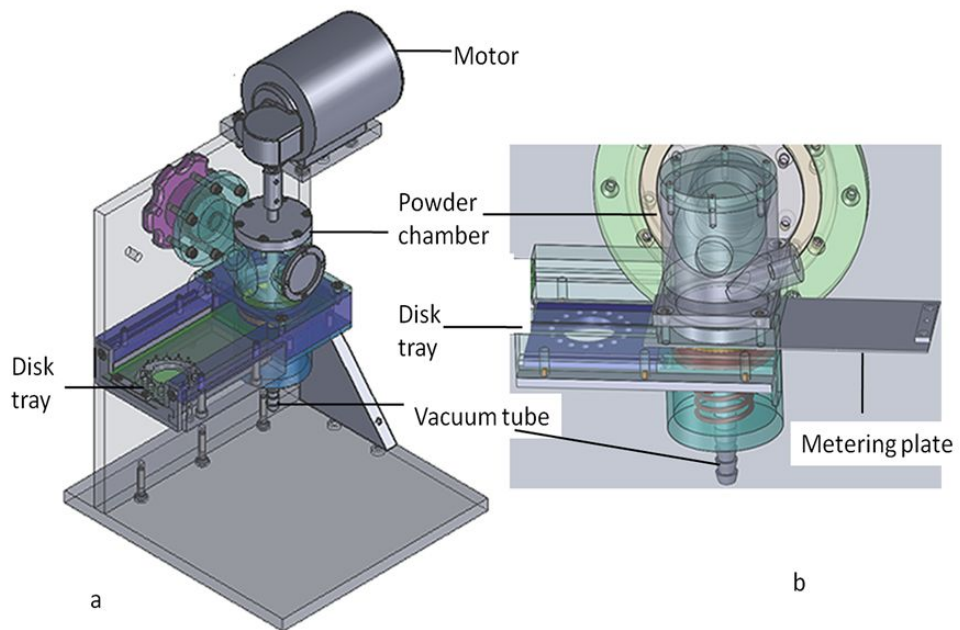


**Figure 3.20: A schematic diagram of filling device**

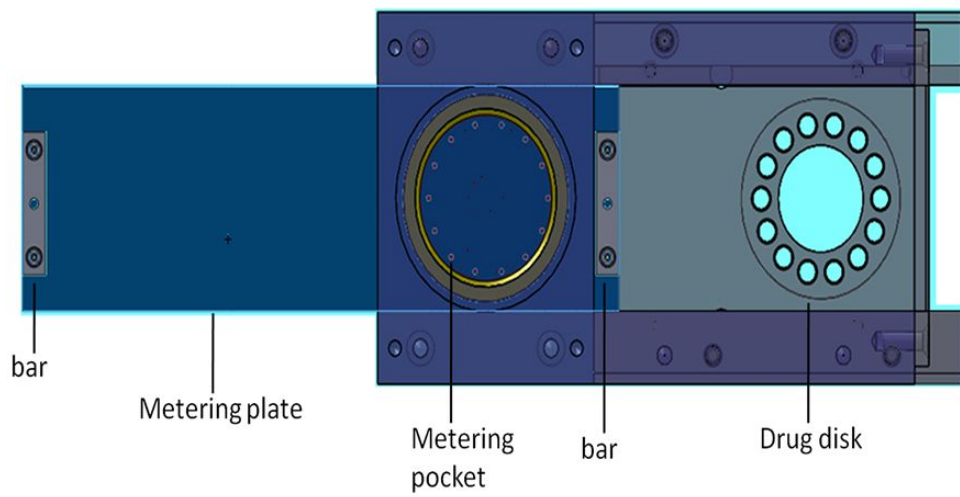


**Figure 3.21: A schematic diagram of the metering plate**

### 3.4.3 Evaluation of powder filling uniformity

When the packaging and filling system is established, its function is validated first, especially for powder filling system. The validation work is focused on powder filling uniformity, which is a prerequisite for the following DPI inhaler evaluation and formulation work. 4 kinds of powder containing 0%, 5%, 10%, 20% fine additives (detailed information is presented in Section 7.4.2) are used in following experiments.

To evaluate the uniformity, including filling weight per disk/blister, drug content per disk/blister, drug content of blend, delivered drug content, the RSD is usually employed to measure the uniformity. RSD can reflect the level of variance even for different average values. Generally, the SD is applied to make sure the inhaler performance is similar or not, such as FPF or blister remains.

#### 3.4.3.1 Filling weight uniformity among different disks

Considering the weight of all powder from 14 blisters in a disk as a whole, the weight uniformity at the beginning, middle and end of the filling process was analyzed to evaluate the filling stability. After powder filling, a drug disk was sealed with aluminum foil and then weighed by a balance (AB135-S, Mettler Toledo, Swiss) to get  $M_{d,0}$ . Then each blister on this disk was opened carefully without foil loss, and all powder was cleaned away completely, then the weight  $M_{d,1}$  of the empty disk was obtained. The filling weight  $M$  for one disk was calculated as this, where  $x$  represented Disk- $x$  and  $d$  for disk.

$$M_d^x = M_{d,0}^x - M_{d,1}^x$$

The uniformity of filling weight among disks was evaluated by RSD of  $M_d^i$ .

#### 3.4.3.2 Filling weight uniformity among blisters in one disk

The uniformity of powder weight among blisters was essential for the delivered dose uniformity. After the powder filling, the drug disk was sealed with aluminum foil and all blisters were numbered. Then a blister on this disk was cut off and weighed ( $M_{b,0}^x$ ).

Following that, this blister was opened carefully without foil loss, and the powder was rinsed by a solvent completely. After air drying of the blister, the weight of an empty blister was obtained ( $M_{b,1}^x$ ).

$$M_b^x = M_{b,0}^x - M_{b,1}^x$$

The uniformity of filling weight among blisters was evaluated by RSD of  $m^x$ .

### 3.4.3.3 Drug content uniformity among different disks

When filling weight uniformity among disks and blisters were validated, we moved on to drug content uniformity. Similarly, the uniformity among different disks was evaluated first. After filling powder, a drug disk was sealed with aluminum foil. Then all blisters on this disk were opened carefully without foil loss, and the powder was rinsed into water of designated volume  $V_x$ . To ensure complete drug dissolution, the disk was immersed into water and sonicated for several minutes. Then the solution was analyzed by HPLC to get the drug concentration  $C_x$ . The drug content of the whole disk was calculated, where  $x$  represented disk  $x$ .

$$M_{API}^x = C^x * V^x$$

The uniformity of drug content uniformity among disks was evaluated by RSD of  $M_{API}^i$ .

### 3.4.3.4 Drug content uniformity among blisters in one disk

After powder filling, a drug disk was sealed with aluminum foil. All blisters of one disk were numbered sequentially first, then cut off and weighed separately. Thereby, we got the weight of each blister  $m_{b,0}$ . Next, each blister was opened carefully without foil loss, and the powder was rinsed into water of volume  $V_i$ . To ensure complete drug dissolution, the blister was immersed into water and sonicated for several minutes. When the solution was analyzed by HPLC to get the drug concentration  $c_i$ , the drug content for each blister was calculated, where  $i$  represented blister  $m_i$ .

$$m_{API}^i = C^i * V^i$$

After drug content analysis, all blisters were taken out and rinsed with ethanol. And those empty blisters were allowed for air-drying until solvent volatilize completely, then corresponding percentage of API for blister (i) could also be calculated based on weight  $m_{b,1}$  of empty blister.

$$API\% = \frac{m_{API}^i}{(m_{b,0}^i - m_{b,1}^i)}$$

Likewise, the drug content and percentage uniformity among blisters in one disk were evaluated by RSD.

In addition to 4 kinds of uniformity described above, the drug content uniformity of the bulk powder blend during filling was also evaluated. Samples were taken out from different positions in the powder chamber (Fig.3.20) to make sure the mechanical stirring and filling process would not cause heterogeneity.

## 3.5 Dry Powder Inhaler Formulation

### 3.5.1 Powder preparation

#### 3.5.1.1 API processing and lactose carrier

The most common micronization method for the API is jet mill. A spiral jet mill (Alpine ® 50 AS, Hosokawa, Japan) with an automatic feeder was applied to micronize API particles as Fig.3.22. Particles were drawn in by a pressure difference resulted from feeding pressure air. Then particles were accelerated to very high speed by grinding pressure air. Because the particles with various sizes exhibited different speeds, then they would impact on each other and walls to become smaller. Until particles were smaller than a cut size when the centripetal force was bigger than centrifugal, those particles would be collected in a filter-bag. Three primary parameters could be adjusted in the jet-milling process: feeding rate, feeding pressure and grinding pressure. For example, decreasing feeding rate would produce smaller particles since a small amount of particles

were accelerated more efficiently and exhibited higher speed and impaction energy. During a jet-milling, the feeding pressure should be smaller than the grinding pressure to avoid flow field interference in the grinding chamber.

The feeder rate was set as 30rpm, and P1 indicating the pressure for grinding was set to 7~8bar and P2 representing the pressure for material feeding was 5~6bar. By controlling the times of micronization, 3 batches of API with different size distribution were obtained. Those batches were used to study the effect of API size on formulation performance.

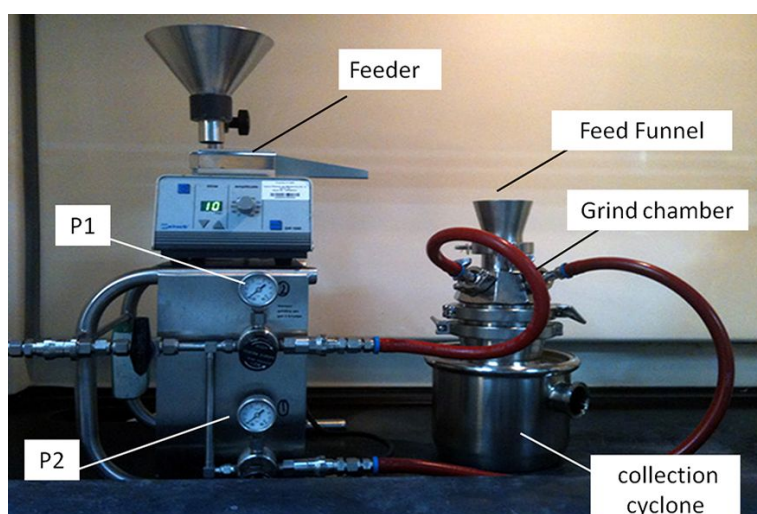


**Figure 3.22: A picture of a jet-mill and an automatic feeder**

The carriers used in this project are listed in Table.3.7, where the size criteria of commercial products are provided by suppliers.

**Table 3.7: The information of lactose used**

Lactose	Source	Size criterion( $\mu\text{m}$ )
Fine lactose	Self-made	D90: <200
Lactose-120504 Lactose-121218 Lactose-121225	Self-made from Lactose 314WG(Kerry)	38.5-74
Inhalac 120	Meggles excipient and technology	D10:70-105, D50:110-155, D90: 160-215
Inhalac 230		D10:30-60, D50:70-110, D90: 110-150
Sorbolac 400		<32
SV003	DFE pharma	D10:19-43, D50:53-66, D90: 75-106
Lactohale LH100		D10:40-80, D50:125-145, D90: 200-250
Lactohale LH200		D10:25-65, D50:80-120, D90: 130-190

### 3.5.1.2 API and lactose mixing method

The powder mixing is a key process of DPI formulation development, since the mixing process determines the uniformity of blend and affects the aerosol performance, like FPF and FPD. The mixing may be considered as energy input process, which not only provides energy to disperse API to bulk carriers, but also changes the interaction between particles, like electrostatic charge and mechanical locking.

Consequently, the methods to mix API and lactose were studied and determined.

After sieving the API by an 100-mesh sieve ( $147\mu\text{m}$ ), the API particles and lactose carrier were added into a steel container as shown in Fig.3.23. The lactose carrier was divided into two layers, one above API particle and the other one under API. This mixture looked like a sandwich. The height of a powder bed should not be more than  $1/3$  of the container. The empty space ensured that enough space existed for particle movement. Then the container was placed in a shaker-mixer (Turbula T2F, WAB, Swiss),



serving as a low shear force mixer. The mixing speed and time was set as 72rpm and 10min respectively.

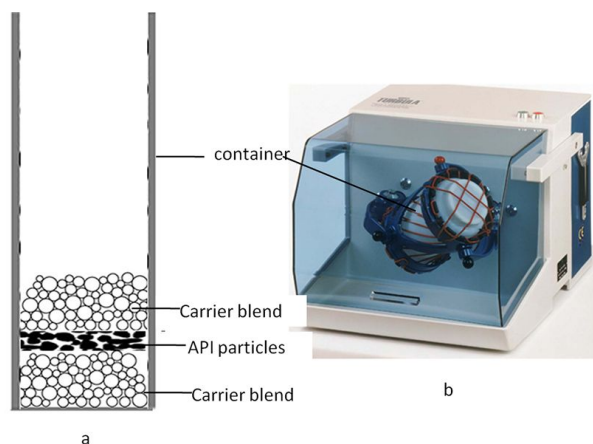


**Figure 3.23: A schematic diagram of mixing bed and a picture of the shaker - mixer.**

After low shear mixing, all powder was transmitted to a high shear mixer (Fig.3.24a) made by ourselves. This device was suitable for a small amount of powder mixing (40-50g), whereas other commercial equipments usually required 200g powder as a minimum for high shear mixing. Large-scale mixing in the primary R&D phase would cause a waste of expensive API and lactose. Consequently, a food mixer was altered for this experiment, the speed of which was controlled by a voltage transformer. The shape and direction of the blades were changed for better agitation effect (Fig.3.24b). By adjusting mixing speed and time, the effect of these two parameters on formulation performance was studied.



**Figure 3.24: Pictures of the high shear mixer. a, a voltage transformer and the mixer; b, the altered blades.**

At last, because ultrasonic vibration was believed to break agglomerates efficiently, an ultrasonic screen (UVS, Shanghai Xuanyi, China) was also applied in the powder mixing research. Its working parameter was set as follows: 60 watts of power, 200-mesh sieve and vibrating 10min with a 4s interval per 30s.

### 3.5.2 Composition of powder formulation

#### 3.5.2.1 API size and proportion

APIs with different size distribution were applied in the formulation research to investigate the effect of API size on formulation performance.

The ratio of API to the formulation was also studied to understand its effect on formulation performance. In most formulation research, the strength of the drug was determined by clinical experiments and the content of API for one administration was fixed. Here, a high and low proportion of the API was studied. The result might expand the application range of **Inhaler-WU2011**, indicating that this device could deliver different doses suitable for various API.

The API mixing sequence was also investigated. One method was to mix fine API particles with fine lactose in the pre-sieving and then this fine mixture with coarse lactose. Another method was to blend fine lactose with coarse carrier first and then carrier as a whole with the API.

#### 3.5.2.2 Lactose composition

Most of the time, the proportion of the API in a specific formulation is fixed and the API particle size is difficult to decrease further by micronization. Hence, the only variable left for pharmaceutical scientists to regulate formulation performance is lactose, including the size distribution, concentration of fine lactose. Consequently, size distribution, the source of lactose, in addition to proportion of fine lactose was investigated.

Using a vibratory sieve shaker (AS 200 control, Retsch, German) as Fig.3.25, the Inhalac 230 was divided into 4 parts: <45 $\mu$ m, 45~75 $\mu$ m, 75~100 $\mu$ m and 100~150 $\mu$ m. The

vibratory amplitude was set as 1.3 mm/”g” and interval time was 10 second. Then API was mixed with these carriers without additional fine lactose.

Similarly, the lactose within the same size range 45~75 $\mu$ m but from different sources (Inhalac230, LH200, SV003) were sieved and applied in formulation to study the effect of lactose source.

When taking Inhalac230 as coarse lactose, the percentage of fine lactose was set to 0%, 5%, 10%, and 20% respectively to study aerosol performance and stability of the formulations.



**Figure 3.25: A picture of vibratory sieve shaker**

## 3.6 Discussion

This chapter can be divided into 4 parts, including the analytical tool, the inhaler device, the powder filling and packaging system, plus materials and methods for formulation work. There are 3 aspects deserving attention especially.

Firstly, the dry powder inhaler developed in this thesis is a completely novel design with an excellent idea. It combines some advantages of other marketed products. For example, the multiple blisters on one disk ensure a uniform delivery because of pre-metered dose, moisture resistance and convenience. It also can relieve the economic burden for patients, since this device can be used repeatedly with replaceable disks. As a result of micro dose, it decreases the quantity of carrier and increases lung delivery efficiency. The inhaler

device, powder filling system and formulation constitutes a whole system. A new powder filling and packaging system is designed and developed, plus comprehensive formulation work is carried out to validate the performance of the novel inhaler. For this thesis, the research is divided into several parts to make it easier to understand, but actually it was impossible to separate those work completely.

Secondly, all analytical methods serve as a tool to facilitate the R&D of inhaler device, powder filling and formulation work. It is difficult to use single equipment for this research. Among all these analytical methods, the most important and difficult one is the inertial impaction test for its key role *in vitro* evaluation and for its complexity. Besides, there are several important definitions and calculation for inertial impaction methods, which are accepted by pharmaceutical scientists and regulatory agencies in many countries.

At last, the methods described in pharmacopoeia to measure delivered drug content and NGI are changed slightly here. According to a pharmacopoeia, the flow rate should be set to a specific value when producing a pressure drop of 4 kPa over the inhaler. When the flow rate is determined according to the pressure drop for a specific inhaler device, then the flow time has to be consistent with a withdrawal of 4L of air from the inhaler. However, all tests of the project are carried out under a flow rate of 60LPM and flow time of 4 s, which also withdraw 4L air from the mouthpiece. There are mainly two reasons to change the test parameters. First, when different inhalers are compared, it would be better to apply the same test parameters since it could eliminate the operation difference and focus on the performance difference between inhalers. For example, If different flow rates or flow time are used in the experiment, then it is difficult to determine the performance difference is caused by test parameters or inhalers. Second, although the 4kPa pressure drop is described in pharmacopoeias for testing a DPI, the 60LPM flow rate is commonly used for many marketed products because of its simplicity.

## Chapter 4

### 4 Validation of Analytical Method

#### 4.1 Brief Introduction

Validation is carried out to ensure accuracy and reproducibility of analytical methods. Firstly, the HPLC method for content assay is validated according to FDA (Food and Drug Administration) and SFDA (State Food and Drug Administration) requirements, as the HPLC provides a basic and reliable tool for other research. Secondly, a validation of laser diffraction size measurement is introduced briefly. At last, a validation of the NGI and TI, serving as the core of *in vitro* evaluation, are completed. Fortunately, this validation work demonstrates that all analytical methods are reliable and precise.

#### 4.2 Validation of HPLC Method for Content Analysis

The HPLC method for sulfate Salbutamol content analysis was established on a method for sulfate Salbutamol tablet in China Pharmacopeia 2010. This work was carried out to validate the suitability of this HPLC method in the DPI formulation.

According to requirements of ICH (International Conference on Harmonization of Technical Requirements for Registration of Pharmaceuticals for Human Use) and SFDA on validation of an assay method, the validation work was consisted of system suitability, specificity, sensitivity, linearity and linear range, precision, reproducibility, intermediate precision, solution stability, accuracy and durability.

About 10mg sulfate Salbutamol was weighed into a 25ml volumetric flask and dissolved by water. Then, the 4 $\mu$ g/ml reference solution was ready.

About 40mg sulfate Salbutamol and corresponding lactose were weighed and dissolved by water to obtain 4 $\mu$ g/ml test solution.

The HPLC method is detailed in Section 3.2.2, and not repeated again.

#### 4.2.1 Validation of suitability, specificity

Repeating 6 times of HPLC assay for reference solution, the chromatogram results are shown in Fig.4.1. A photodiode array detector (PAD2998, Waters, USA) was applied to inspect the peak purity. The results show that the purity angle is smaller than the threshold value, indicating a pure chromatogram peak of sulfate Salbutamol. The shape of the peak is fine without impurity interference. In addition, the RSD of peak area is less than 2.0% and retention time less than 1.0%, shown as Table 4.1.

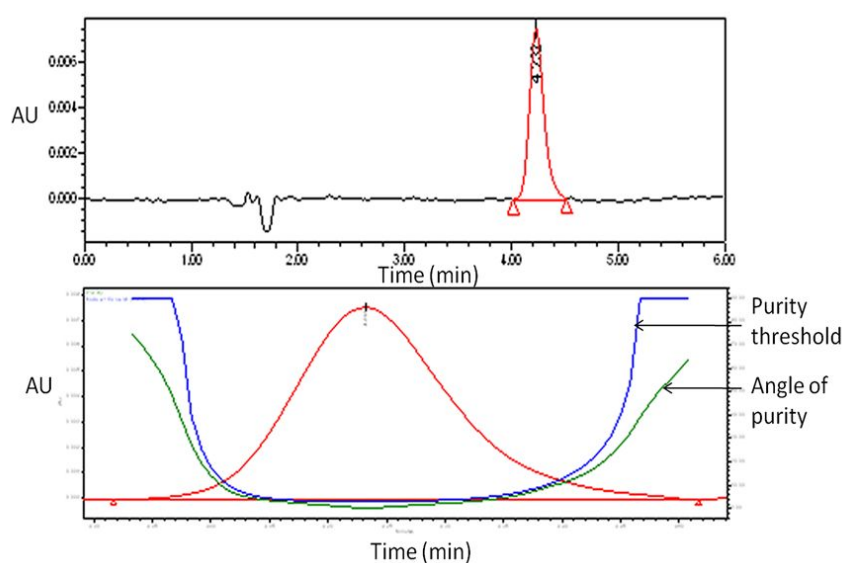


**Figure 4.1: Pictures of typical salbutamol chromatogram and peak purity**

**Table 4.1: The suitability results**

Injection	Peak Area	Retention time (min)
1	70002	4.207
2	68205	4.212
3	71563	4.224
4	70348	4.238
5	70887	4.239
6	71760	4.249
Mean	70461	4.228
RSD (%)	1.84	0.39

A blank solvent of deionized water, a reference solution and lactose solution (about 0.12mg/ml) were injected for HPLC analysis. As shown in Fig.4.2, the blank solvent and excipient do not affect the detection of sulfate salbutamol.

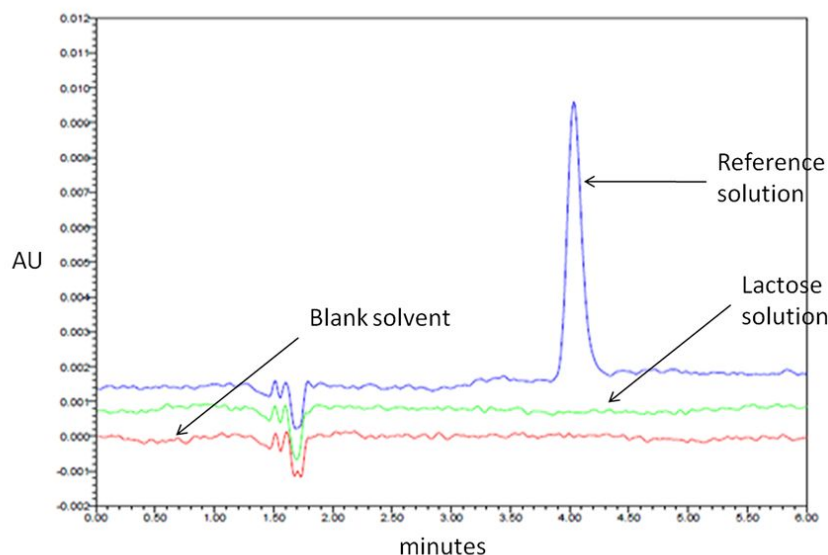


**Figure 4.2: The chromatogram of reference solution, lactose solution, and blank solvent.**

#### 4.2.2 Validation of sensitivity and linearity

The reference solution was diluted gradually and analyzed by the HPCL. When Signal/Noise is closed to 3 ( $S/N \geq 3$ ) and 10 ( $S/N \geq 10$ ), the corresponding concentrations, 300ng/ml and 920ng/ml are the limit of detection (LOD) and limit of quantitation (LOQ). Preparing 6 LOQ and 6 LOD solutions for HPLC, the RSD of retention time of main peak is less than 2.0% as Table 4.2.

**Table 4.2: Signal-noise ratio of LOD and LOQ**

LOQ	RT	S/N	LOD	RT	S/N
LOQ1-1	4.135	11.5	LOD1-1	4.312	3.4
LOQ1-2	4.105	9.6	LOD1-2	4.291	3.2
LOQ2-1	4.149	10.2	LOD2-1	4.350	3.7
LOQ2-2	4.144	10.4	LOD2-2	4.358	3.8
LOQ3-1	4.154	12.5	LOD3-1	4.370	3.5
LOQ3-2	4.194	11.6	LOD3-2	4.401	3.3
RSD (%)	0.70			0.92	

The anticipated linear range was set as 40%~ 300% concentrations of possible samples (samples from tests like blend uniformity, drug content uniformity among disks and blisters, DUSA, TI, and NGI). Corresponding solutions of 7 concentration points within the target range were prepared and analyzed by the HPLC. Then a linear regression was established between the sample concentration ( $\mu\text{g/ml}$ , X-axis) and peak area (AU, Y-axis), and the linear coefficient and range were investigated. The calibration factors (CF), concentration divided by corresponding peak area, were also calculated to evaluate system stability.

An excellent linearity inferred by  $R^2=1$  between sample concentration and peak area is shown in Fig.4.3. Besides, the intercept on the Y-axis is smaller than 2% of complete response and RSD of calibration factors smaller than 2.0% as shown in Table 4.3. As a conclusion, this HPLC method shows a good linearity from 1.63 to 12.22 $\mu\text{g/ml}$ .

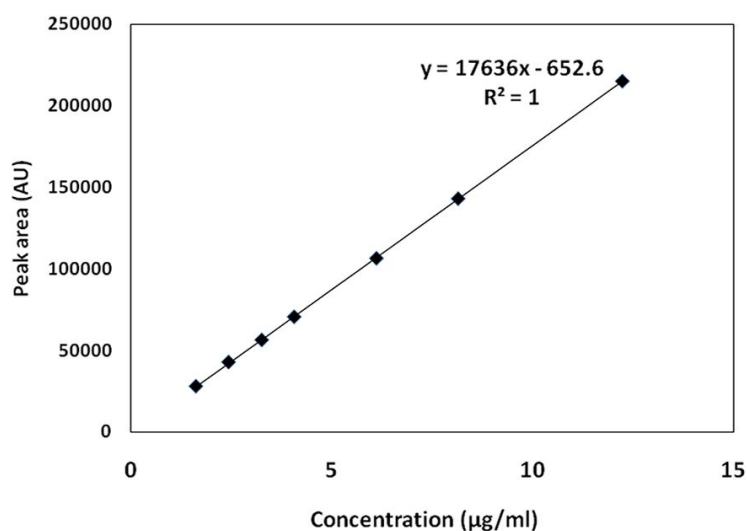


**Figure 4.3: The linearity between concentration and peak area.**



**Table 4.3: The linear range of concentration and corresponding peak area**

Concentration µg/ml	Peak area 1 (AU)	Peak area 2 (AU)	Averaged area (AU)	CF
1.63	27865	28614	28239.5	5.76781E-05
2.44	42692	43343	43017.5	5.67955E-05
3.26	57328	55862	56595.0	5.75599E-05
4.07	70959	70519	70739.0	5.75637E-05
6.11	106590	106553	106571.5	5.73136E-05
8.14	143384	142824	143104.0	5.69097E-05
12.22	215144	214934	215039.0	5.68083E-05
RSD (%)				0.68

#### 4.2.3 Validation of precision, reproducibility and intermediate precision

The reference solution was injected 6 times repeatedly to calculate the RSD of peak area, and results showed that the RSD was less than 2.0%, indicating good precision.

3 powder blends with similar composition as formulations were prepared, and then those blends were dissolved and analyzed by HPLC. The recovery rate was calculated by following formula, where  $m_{i, \text{weighed}}$  stood for the quantity of the API in the blends,  $i$  for blend sample and  $r$  for reference sample. As shown in Table.13, the averaged recovery is 99.66% with 0.71% RSD, indicating good reproducibility.

$$\text{Recovery} = \frac{A_i * C_r / A_r * V_i}{m_{i, \text{weighed}}} * 100\%$$

**Table 4.4: The reproducibility results**

Sample name	Concentration ( $\mu\text{g}/\text{ml}$ )	Peak area	recovery (%)
reference1-1	3.95	68527	
reference1-2	3.95	68486	
reference2-1	4.07	70959	
reference2-2	4.07	70519	
Blend 1-1	3.94	67861	99.25
Blend 1-2	3.94	68629	100.38
Blend 2-1	4.07	70010	99.13
Blend 2-2	4.07	70230	99.44
Blend 3-1	4.00	69918	100.73
Blend 3-2	4.00	68749	99.04
Average			99.66
RSD (%)			0.71

Samples that were similar as reproducibility test were prepared and analyzed by different analysts and HPLC instruments. The total result of 18 tests shows that the average recovery is 99.82% with 0.37% RSD, indicating good intermediate precision.

**Table 4.5: The intermediate precision results**

	Analyst, A HPLC 1#	Analyst, B HPLC 2#	Analyst ,C HPLC 3#
Recovery (%)	98.75	100.96	100.48
	99.87	100.10	100.12
	99.13	99.69	99.22
	99.44	100.01	99.05
	100.73	99.95	99.95
	99.04	100.64	99.72
Average (%)	99.49	100.22	99.75
RSD (%)	0.72	0.47	0.54
Average for all tests: 99.82%                      RSD for all tests: 0.37%			

#### 4.2.4 Validation of solution stability, accuracy and durability

The reference solution was stored in 4°C environment and detected at 0, 2, 4, 6, 8 hour and 15<sup>th</sup> day. Table 4.6 shows that the sample is rather stable under 4°C for 15 days.

**Table 4.6: The solution stability result**

Time (h)	Peak area
0	67986
2	68918
4	67196
6	66453
8	69282
15day	68812
Average	68108
RSD%	1.62

9 samples were prepared by accurately weighing API and setting their concentration at 80%, 100% and 120% level. Then the recovery was calculated in the similar way as reproducibility evaluation. As Table 4.7, the recovery is between 98.0~102.0% for three concentrations, exhibiting excellent accuracy.

**Table 4.7: The recovery rate result**

Sample	Recovery (%)	Average recovery (%)	RSD (%)
Lower concentration-1	100.66	100.66	1.05
Lower concentration-2	101.76		
Lower concentration-3	101.32		
Middle concentration-1	101.73		
Middle concentration-2	100.04		
Middle concentration-3	99.32		
Higher concentration-1	100.76		
Higher concentration-2	98.85		
Higher concentration-3	101.48		

To investigate the durability of HPLC method, different conditions were set: changing the proportion of mobile phase ( $\pm 5\%$ ), pH of mobile phase ( $\pm 0.2$ ), column temperature ( $\pm 5^\circ\text{C}$ ), and flow rate ( $\pm 20\%$ ). Meanwhile, columns of different brands, different HPLC instrument were also studied.

The results show that the tailing factor of primary peak is less than 1.5 and resolution between the API peak and impurity is acceptable. The RSD of concentration results

detected under different conditions is less than 2.0%. To sum up, this HPLC method is durable even if the detection conditions change slightly.

## 4.3 Validation of Size Characterization Methods

### 4.3.1 Validation of laser diffraction size measurement

The operation parameters of laser diffraction size measurement are described in Section 3.2.3. When particles are in the range of 0.25 $\mu\text{m}$  to 87.5 $\mu\text{m}$ , R2 lens should be used and R4 lens for particles from 0.5 $\mu\text{m}$  to 350 $\mu\text{m}$ . At the beginning of each laser sizing, a reference sample provided by the manufacturer should be measured as a calibration, to make sure that operating parameters are suitable and instrument is running well. 2 standard references, Sic-F1200'03 and Sic-P600'06 are applied for R2 lens and R4 lens respectively.

A typical size distribution result is shown in Fig.4.4. From the cumulative distribution, the percentage of particles under a certain size would be known. The type of particle distribution can be inferred from the density distribution graph. A monomodal distribution is exhibited in Fig.4.4, since there is only one peak. As we can see in Table 4.8, the results of reference samples conform to the criteria very well, implying accurate and reliable results for following tests.

$$q_3(x)=dQ_3(x)/dx$$

X represents a diameter value,  $q_3$  and  $Q_3$  represent volumetric density and cumulative distribution respectively.

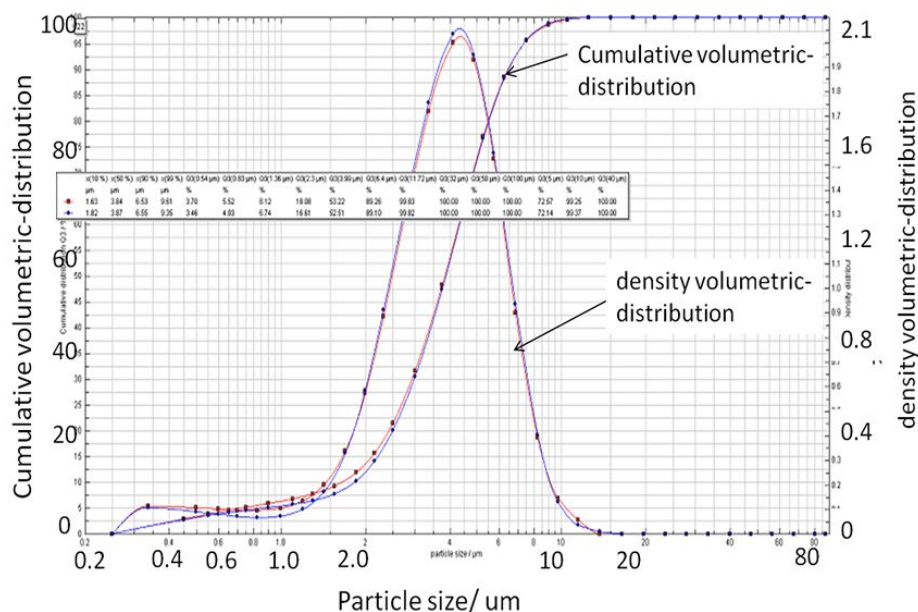


**Figure 4.4: The cumulative and density distribution results of Sic-F1200'03 for R2 lens.**

**Table 4.8: The calibration criteria and results for laser diffraction sizing**

R2 lens	X10( $\mu\text{m}$ )	X50( $\mu\text{m}$ )	X90( $\mu\text{m}$ )
Criterion	1.79-1.98	3.76-3.96	6.30-6.63
Calibration test-1	1.63	3.84	6.53
Calibration test-2	1.82	3.87	6.65
R4 lens	X10	X50	X90
Criterion	15.03-16.62	25.41-26.72	39.23-41.25
Calibration test-1	15.39	26.31	39.99
Calibration test-2	15.38	26.31	40.04

### 4.3.2 Validation of inertial impaction size measurement

#### 4.3.2.1 Validation of NGI test method

The cascade impaction method is a little different for DPIs from pMDIs, which mandates a size distribution comparison between the coated and uncoated stages for DPI test first. Consequently, to investigate the influence of coating stages on NGI (Next Generation Impactor) results, about 50mg surfactant mixture (Tween 80: Glycerin=1: 4) was added

into each stage and then the liquid was smeared evenly with a soft brush. A Turbuhaler® Oxis® inhaler was tested by a coated NGI and an uncoated NGI simultaneously. Other test parameters and data processing method are described in Section 3.2.3 and 3.3.1.

The size distribution results are shown in Table 4.9, presenting similar FPD (fine particle dose) and FPF (fine particle fraction) between the coated and uncoated NGI. When stages are coated, if the detailed particle size distribution is investigated in Fig. 4.5, there are more particles depositing on stage 1-4 and less particles on stage 5-MOC. This phenomenon implies that, if there is no coating, the large particles may bounce and experience reentrainment into stages which should catch small particles. Because of difference of aerodynamic particle size distribution (APSD) between the coated and uncoated NGI, the coating method is used for all following NGI tests to avoid errors from particle bounce and reentrainment.

**Table 4.9: The calibration criterion and results for Laser diffraction sizing**

Turbuhaler® Oxis®	TRM( $\mu\text{g}$ )	ED ( $\mu\text{g}$ )	FPD( $\mu\text{g}$ )	FPF
Coated	105.9	89.7	51.8	57.8%
Uncoated	107.9	95.5	51.3	53.6%

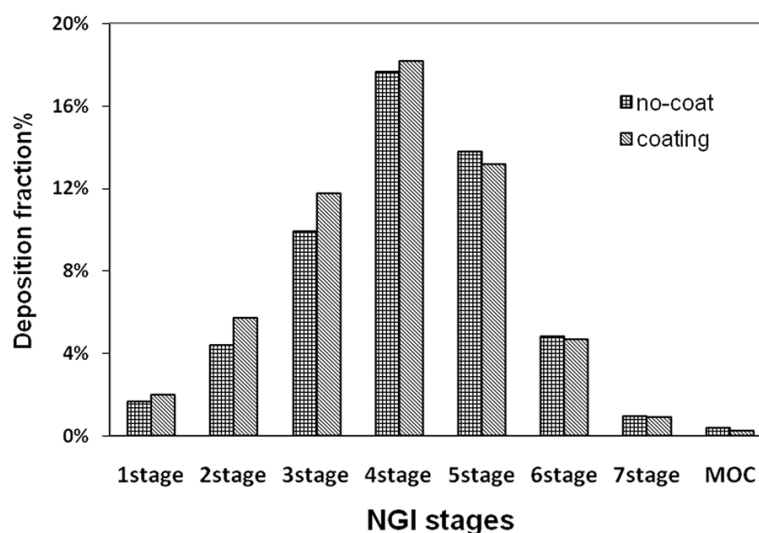


**Figure 4.5: The comparison of NGI results for Turbuhaler® Oxis® with the coated and uncoated stages**

### 4.3.2.2 Validation of TI test method

The TI (Twin impinger) method is described in Section 3.2.3 and 3.3.1 in detail. The TI method is used most in this project for its simplicity and convenience. Therefore, the operation parameters of TI test are validated carefully with a Clickhaler® to make sure that little operation error will not influence the final results. The performance of Clickhaler® is rather stable and suitable for TI method validation. What we have done for the validation is to adjust three critical testing parameters intentionally, and investigate the influence of the alterations on TRR (Total Recovery Rate) and FPF (Fine Particle Fraction). Both values are important for evaluating inhalers performance. In the research scheme as Table 4.10, the higher volume of receiving solvent is excluded, because the receiving solvent only confront the problem of solvent volatilization or solvent loss as a result of fast air flow.

**Table 4.10: The research scheme of TI test method validation**

Clickhaler®	Lower (n=3)	Normal (n=3)	Higher (n=3)
Flow rate (LPM)	58	60	62
Volume of receiving solvent (ml)	25	30	
Flow time (second)	3	4	5

**Table 4.11: The TRM and FPF result of TI method validation**

<b>TRR</b>	Lower (n=3)	Normal (n=3)	Higher (n=3)
Flow rate	99.0%	99.9%	103.7%
Volume of receiving solvent	106.3%	99.9%	
Flow time	101.9%	99.9%	106.6%
<b>FPF</b>			
Flow rate	22.8%	22.2%	23.5%
Volume of receiving solvent	24.9%	22.2%	
Flow time	24.3%	22.2%	24.3%

The validation results are shown in Table 4.11. As we can see in this table, even if there is little alteration of operating parameters, the results are still constant, indicating a stable and reliable TI impaction method.

The electrostatic charge produced in the powder preparation and powder filling exerts a great influence on the inhaler performance, then it would disturb the judgement of researchers in the formulation studies. Consequently, the powders and drug disks should be allowed to stand for a period to dissipate electrostatic and reach a relative stable state.

Hence, two kinds of powder were prepared by 0%w/w and 20%w/w fines with Inhalac 230, representing powder with better and worse flowability respectively. The percentage of the API-sulfate salbutamol was set to 0.72%w/w for both powders and these powder were prepared by the same mixing process, including pre-sieving, low shear and high shear mixing as mentioned as Section 3.5.1. The device used here was Inhaler WU2011.

After powder preparation, the drug powder was sealed and stored in a dryer to get rid of moisture. A certain amount of powder was taken out and filled into disks for TI tests instantly at proposed time points (Table 4.12). This study was used to determine the interval between powder preparation and TI tests required for stable data. After that, when we got the desired information from the above experiments, these two powders were prepared again and allowed to rest for a designated time. And then these powders were filled into drug disks and tested by TI at proposed time points (Table 4.12).

**Table 4.12: The research scheme of TI test time point validation**

Interval between powder preparation-TI test	n=2 for each time point TI test			
	0day	3day	7day	14day
0%fines-100%Inhalac®230	0day	3day	7day	14day
20%fines-80%Inhalac®230	0day	3day	7day	14day
Interval between powder filling-TI test				
0%fines-100%Inhalac®230	0day	3day	7day	14day
20%fines-80%Inhalac®230	0day	3day	7day	14day

The results of interval validation between powder preparation and TI test are shown in Fig.4.6. As we can see in Fig.4.6, the FPF and remains in blisters do not show any obvious trend from 0-day to 14-day for 0%-fines or 20%-fines formulation, implying that the electrostatic charge produced in powder preparation do not influence the aerosol performance.



The result of studies for interval between powder filling and TI test are shown in Fig.4.7. The FPF shows a small raise with increasing rest time of the filled disk. On the contrary, the remains in blisters decrease gradually when increasing the rest time. Both phenomena are more obvious for 0%-fines than 20%-fines formulation.

As shown in these pictures, the composition of formulation has great influence on the FPF and remains in blisters. The 20%-fines formulation exhibits a much higher FPF than 0%-fines and also higher remains in blisters. The influence of fine particles on performance is examined carefully in the formulation part.

As a conclusion for TI test method validation, when powder is prepared, it can be filled into disk without intentional rest for eliminating electrostatic charge. Meanwhile, if these powders are sealed well and kept from moisture, its performance does not change within 2 weeks. What is more important, the fresh drug disk should not be tested immediately, and 1 week of rest time is recommended for TI test after filling disks.

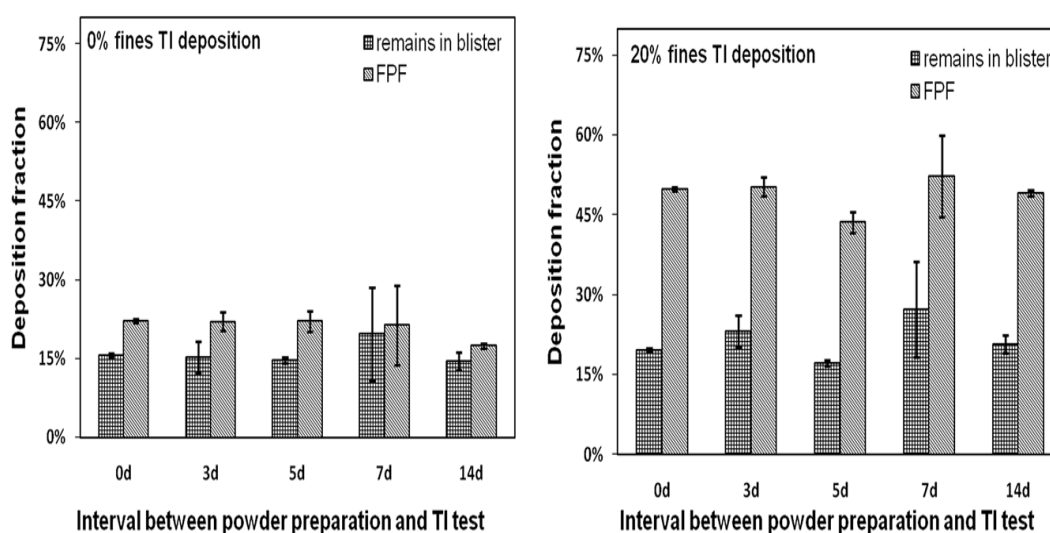


**Figure 4.6: The *in vitro* performance of the new inhaler at different intervals between powder preparation and TI test**

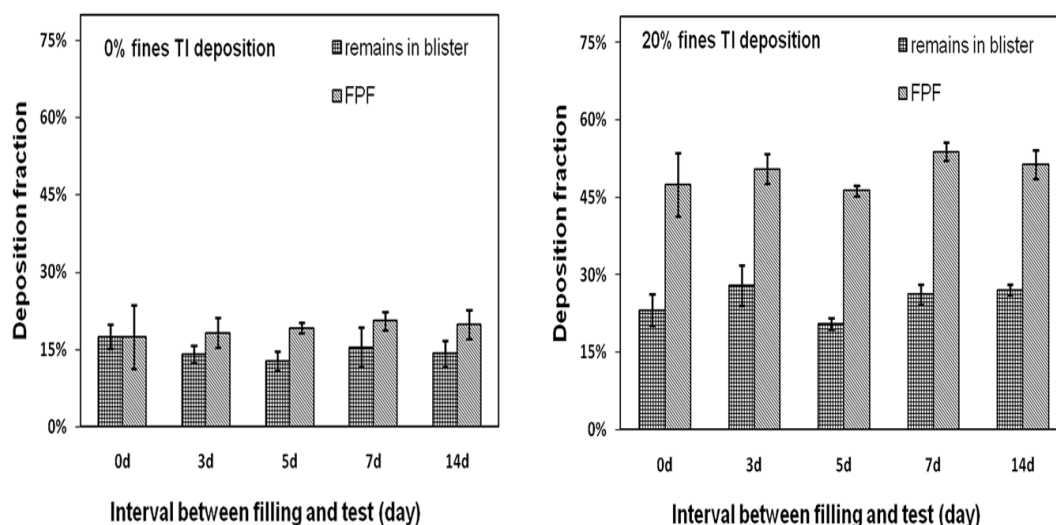


**Figure 4.7: The *in vitro* performance of the new inhaler at different intervals between powder filling and TI tests.**

## 4.4 Discussion

This chapter is mainly focused on validation of analytical methods, including the HPLC method, laser diffraction size measurement, and inertial impaction methods.

The HPLC validation work is carried out according to requirements of ICH (International Conference on Harmonisation of Technical Requirements for Registration of Pharmaceuticals for Human Use) and SFDA. The results have successfully proven that the HPLC method used in this thesis is simple, accurate, precise, durable and specific.

The difference between testing inhalers and other pharmaceutical dosages is that the HPLC method should be very sensitive, since the quantity of the API per dose is very small and is divided into many parts in an impaction test. Meanwhile, this method should be specific to distinguish the API and impurity, excipients, which may become a challenge when the concentration of the API is very low. Additionally, because the analytical work in cascade impaction tests is labor-intensive, the HPLC method should be easy and time saving.

The laser diffraction method should be calibrated before each test, to make sure the detected size results conform to the criteria of reference samples.

The validation of inertial impaction method is the core of this chapter, not only for its importance but also for its susceptibility to the personnel, operation and equipment.

The comparison between the coated and uncoated NGI clearly show that during a NGI test, the stages should be coated. Since scientists do not consider the particle bounce and reentrainment during the design of NGI or other cascade impactor<sup>[131]</sup>, the particle bounce would produce false results. For example, particles with aerodynamic diameter above 4.46 $\mu$ m should be caught on stage2 or even before stage2 at 60 LPM. However, as a result of bounce, these particles are reentrained into the flow and enter next stage. The result would show more fine particles and less large particles, in other words, the particle size distribution moves to the smaller end. Mitchell et al described the common coating material and quantity used in cascade impactor on behalf of members of European Pharmaceutical Aerosol Group<sup>[132]</sup>. Although there are lots of materials available for coating, it is essential that the coating material would affect the detection of the API. Rissler et al reported a methodology to study impactor particle reentrainment, and found that at higher flow rate, like  $\geq 60$  LPM, the particle bounce became even more worse and proposed a soaked filter paper as coating material<sup>[133]</sup>. For high dose DPIs, the situation may become more complicated, because too much powder may result in overload of cascade impactor and make it easier for particle bounce. Consequently, when a high-dose DPI is tested, more attention should be paid to stages coating<sup>[134]</sup>. Nevertheless, for droplet aerosols, like nebulizer or solution-pMDI, the necessity of coating declined as droplets are not so easy to bounce<sup>[135]</sup>.

The validation of TI method is divided into two parts: the first one focuses on operation and parameters. Fortunately, the validation results indicate that even if there is a little error in operation, it does not affect the accuracy of final results. The validation work of a cascade impactor usually refer to validation of its cutoff diameter<sup>[120; 136]</sup>, and there are few studies focusing on the reproducibility and durability of operation and parameters in

TI tests, although the operation and parameters are even more important for industry and formulation scientists.

The second part of TI validation involves the formulation, powder processing and package. The results demonstrate that electrostatic charge produced in powder preparation would not affect the aerosol performance, but charge produced in powder filling and packaging would affect its performance. Adi et al also found that charge induced by different containers during tumbling does not play a significant role in mannitol powder aerosolisation<sup>[137]</sup>. It is recommended that all drug disks should be tested one week after filling. It is inferred that the electrostatic charge produced in particle-PVC interaction is much higher than particle-particle interaction. This assumption is supported by the experiment of Carter et al that PVC could acquire the highest charge compared with lactose and salbutamol and particles. The charge would take a longer time to dissipate charge<sup>[138]</sup>. Ament et al also reported that a coarser aerosol was delivered when the DPI was immediately tested after filling and further testing results confirmed that the particle size distribution would go up and keep stable over a period of 2-3 weeks. The electrostatic charge results showed that relaxed blisters had lower and constant charge<sup>[139]</sup>. What is noteworthy, the longer time required for dissipating charge in that research is related to ultrasonic vibrating of blisters. This high-energy vibration may produce lots of electrostatic charge.

Interestingly, the electrostatic charge has various influences on powders with different fine additives. For 0%-fines formulation, the blisters remain decline but FPF goes up when increasing rest time. This result can be explained that the electrostatic force between particle and PVC decrease with time. As a comparison, the 20%-fines formulation does not show similar trends. It is inferred that since there exist more fine particles in 20%-fines formulation, the cohesive force between the fine API particles and PVC is diluted as a result of fine additives.

## Chapter 5

### 5 Evaluation Results of Dry Powder Inhalers

#### 5.1 Brief Introduction

Several typical marketed inhalers are evaluated first, including airflow resistance, fine particle fraction (FPF) and delivered drug content uniformity. Secondly, an operational state of the inhaler-WU2011 is described. Furthermore, improvements of the inhaler design and corresponding results are presented. At last, the inhaler-WU2011 is compared to several marketed products using the same formulation. This experiment could reflect the performance of inhalers by excluding an interference of different powders.

#### 5.2 Evaluation of Marketed Dry Powder Inhaler Devices

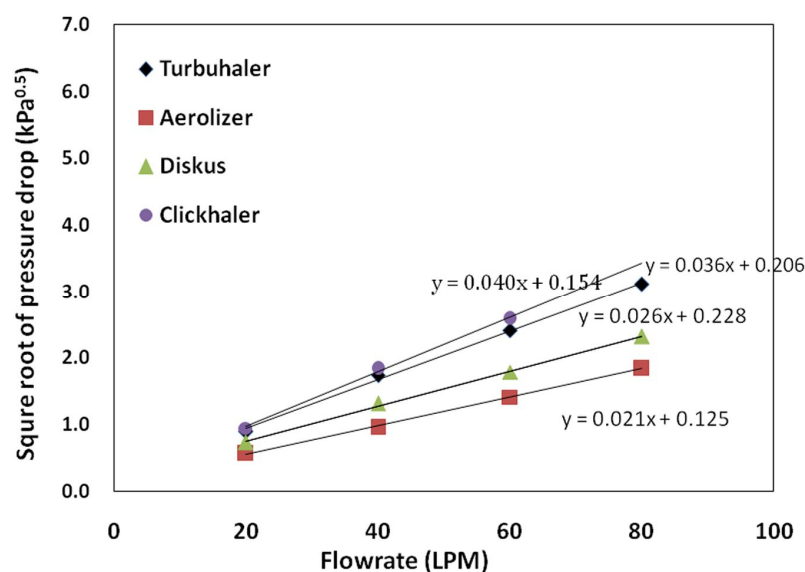
Four typical marketed DPI products are evaluated, including all three categories of DPI device: single unit dose-Aerolizer® Foradil®, multiple unit dose-Diskus® Seretide® and multiple doses (reservoir) -Turbohaler® Oxis® and Clickhaler® Asmasal®. The tested items and operations are described in Section 3.3.1 in detail.

##### 5.2.1 The air resistance and delivered dose content uniformity

The flow rates and corresponding pressure drop are listed in Table.5.1. A linear regression of the square root of pressure drop on the flow rate is established for each device as Fig.5.1. The air resistance of a device is represented by the slope of corresponding curve, as Fig.5.1. All devices show a good linearity between the square root of pressure drop and flow rate with linearity factors above 0.99. The result demonstrates that all airflow resistances are within the range of  $0.02\text{-}0.04\text{kPa}^{0.5}\cdot\text{min/liter}$ . The reservoir device, Clickhaler® Asmasal® show the highest resistance and capsule device Aerolizer® Foradil® has the lowest one.

**Table 5.1: The pressure drop in corresponding flow rate of marketed inhalers**

Flow rate (LPM)	Pressure drop (kPa)			
	Turbuhaler®	Aerolizer®	Diskus®	Clickhaler®
20	0.80	0.32	0.53	0.90
40	3.02	0.92	1.73	3.38
60	5.80	1.99	3.19	6.70
80	9.69	3.40	5.36	Too high

**Figure 5.1: The linearity between (pressure drop)<sup>0.5</sup> and flow rate for marketed inhalers****Table 5.2: The airflow resistance of marketed inhalers**

DPI device	Resistance (kPa <sup>0.5</sup> *min/liter)
Turbuhaler®	0.036
Aerolizer®	0.021
Diskus®	0.026
Clickhaler®	0.04

Usually, the pre-metered device, like single unit dose and multiple unit dose inhalers present a good delivered drug content uniformity (DDCU). Hence, the DCU test is not carried out for Aerolizer® and Diskus® Seretide® but for Turbuhaler®Oxis® and Clickhaler® Asmasal®. The DCU results are shown in Fig.5.2 and Fig.5.3, from which

we can see the delivered dose fluctuating within a certain range. The RSD of Clickhaler® Asmasal® is about 11.6%, much smaller than 22.9% of the Turbuhaler® Oxis®. The fluctuation of Clickhaler® Asmasal® is still acceptable according to US and European Pharmacopeia, but the uniformity of Turbuhaler® Oxis® does not meet the pharmacopeia requirements. Since the pharmacopeias usually requires that the drug content of at least 9 of 10 doses collected from one inhaler should be between 75%-125% of the target-delivered dose, and none is outside the range of 65% to 135% of the target-delivered dose. These requirements are usually considered as the first tier. In consideration of accidental errors, the pharmacopeia also provides a second tier as follows: If the contents of not more than 3 doses are outside the range of 75% to 125%, but within the range of 65% to 135% of the target-delivered dose, 2 additional inhalers are selected, and repeat the prescribed procedure for analyzing 10 doses from each. The requirements are met if not more than 3 results, out of the 30 values, lie outside the range of 75% to 125% of the target-delivered dose, and none is outside the range of 65% to 135% of the target-delivered dose. The results show that the uniformity of Clickhaler® Asmasal® meet the first tier, and Turbuhaler® Oxis does not even comply with the second tier.

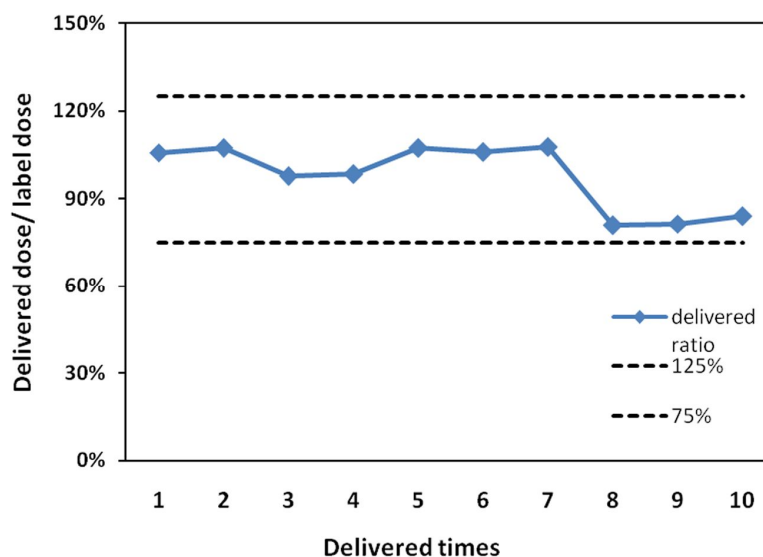


**Figure 5.2: The delivered dose content uniformity of Clickhaler® Asmasal®**

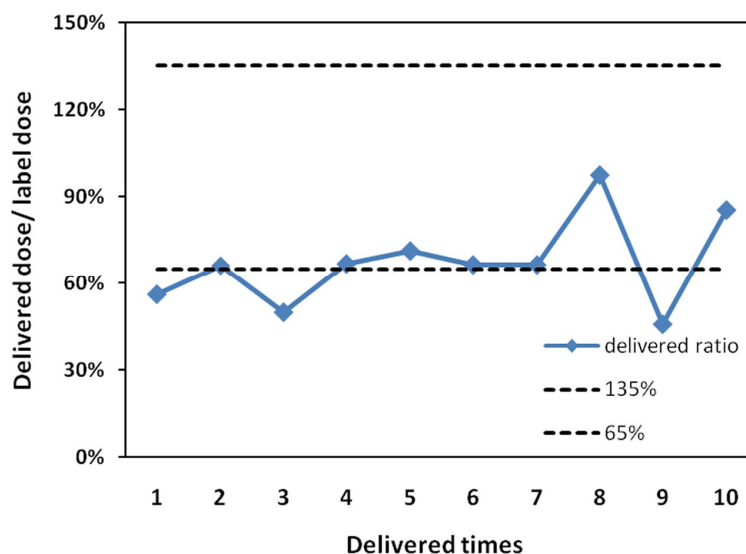


**Figure 5.3: The delivered dose content uniformity of Turbuhaler® Oxis®**

### 5.2.2 The inertial impaction test

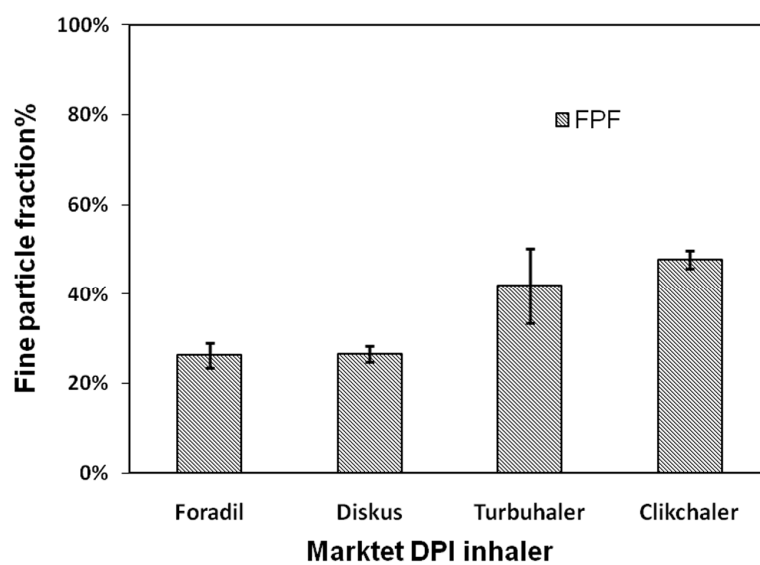
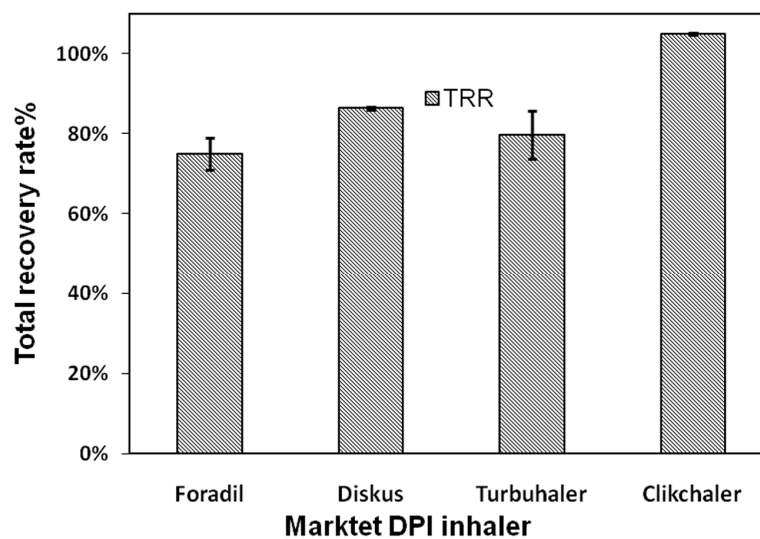
The results of *in vitro* particle size distribution of Aerolizer® Foradil®, Diskus® Seretide®, Turbuhaler® Oxis® and Clickhaler® Asmasal® are first acquired by a TI (Twin Impinger) impaction detailed in Section 3.2.3 and 3.3.1. And all data are processed according to the calculation method in Section 3.2.3. It is noteworthy that there are two APIs, salmeterol and fluticasone in the formulation of Diskus® Seretide®, and the salmeterol is analyzed for convenience.

The result is shown in Table.5.3 and Fig.5.4. The unit dose devices including single unit and multiple-unit device present similar a FPF (fine particle fraction) of about 26%. Due to different device designs, the TRR (total recovery rate) of Diskus® Seretide® is higher than Aerolizer® Foradil®. The reservoir devices, Turbuhaler® Oxis® and Clickhaler® Asmasal® have a much higher FPF value above 40%. The Clickhaler® Asmasal® even has a TRR more than 100%, indicating excellent delivery efficiency. As we can see from Fig.5.4 and Fig.5.5, the Turbuhaler® Oxis® shows the greatest variation in terms of both FPF and TRR. On the contrary, the Diskus® Seretide® and Clickhaler® Asmasal® exhibit the best consistency of FPF and TRR.



**Table 5.3: The FPF and TRR results of TI tests for the marketed inhalers**

Device	FPF(<6.5 $\mu$ m,n=2)	TRR(n=2)
Aerolizer® Foradil	26.3%	75.0%
Diskus®	26.5%	86.4%
Turbuhaler® Oxis	41.9%	79.7%
Clikchaler	47.8%	104.9%

**Figure 5.4: The FPF results of TI test for the marketed inhalers****Figure 5.5: The TRR results of TI test for the marketed inhalers**

These devices are further investigated by cascade impactors with coated stages. The FPF and TRR results are shown in Table 5.4. Aerolizer® Foradil® and Clickhaler® Asmasal® almost have the same FPF values as TI tests. The increasing FPF of Turbuhaler® Oxis might be caused by an abrupt TRR rise. The descending FPF of Diskus® Seretide® might be related to the sensitivity of this device to air flow. Since the dead volume of NGI is larger than the TI, the flow rate would reach 60 LPM slower for NGI than TI. Hence, the flow time is not long enough to produce sufficient airflow through the NGI. Based on this assumption, the flow time is prolonged from 4s to 10s. This NGI test obtains a 30% FPF, being similar to the TI result. To keep test parameters the same for all devices, the result of 4s flow time is presented.

The NGI presents a detailed aerodynamic particle size distribution (APSD) as shown in Fig.5.6. Above 50% of API particles deposit on induction port (throat) and pre-separator, but the Turbuhaler® Oxis® shows less deposition in these two parts. Generally, particles from the single unit dose and multiple unit dose inhalers are caught earlier than reservoir devices. Particularly, Aerolizer® Foradil® and Diskus® Seretide have more particles deposited before stage3 but fewer particles on last 5 stages. On the contrary, the APSD of reservoir devices tends to the smaller end, causing larger FPF values.

**Table 5.4: The FPF and TRR results of NGI tests for the marketed inhalers**

Device	FPF(<4.46µm)	TRR
Aerolizer® Foradil	25.2%	79.5%
Diskus® Seretide	15.7%	86.1%
Turbuhaler® Oxis	57.8%	99.6%
Clickhaler	46.7%	101.1%

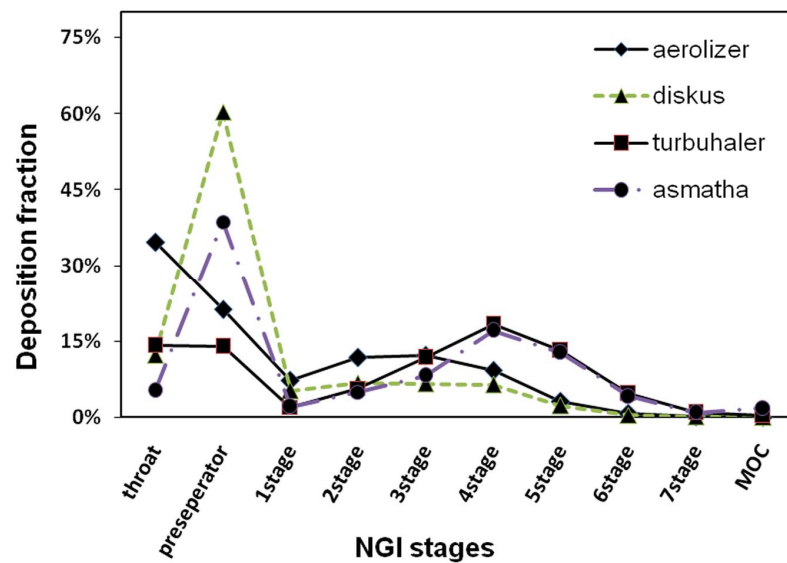


**Figure 5.6: The aerodynamic particle size distribution (APSD) for the marketed inhalers**

## 5.3 Primary Evaluation and Design Improvements of the Novel Inhaler

### 5.3.1 Primary evaluation

A description of the new Inhaler WU2011 is provided to ensure the achievement of designed functions. Nevertheless, detailed performance data is presented mainly in chapter 7.

The external shell can be closed tightly to protect inner structure and mouthpiece from contamination. When the outside shell is closed, the push button and trigger can not move any more to avoid a wrong operation.

When the external shell is open, the push button can be pushed down smoothly and the puncture would pierce into the center of a blister. After an administration or test, releasing the push button, the spring under the push button would help the push button and puncture return to their original positions.

For next dose or blister, the trigger is turned clockwise once to drive the ratchet and circular-tray rotate for one blister, and then a new blister was available for the next administration. People could turn the trigger back immediately or until the next administration. When a disk is finished, the hasps can be unlocked to open the cover, and the exhausted disk can be replaced.

### 5.3.2 Design improvement

During the development of this inhaler device, it is continuously improved based on feedback from experts and testers. Firstly, the number of blisters on a disk is adjusted from 16 to 14, since it is believed that 14 blisters could be used for one or two weeks if two or one blister per day. Besides, decreasing the number of blisters on one disk allow more space between individual blisters, implying possibility of more tight sealing.

The inhaler-WU2011 of initial design is evaluated for its air resistance, delivery uniformity and the proportion of remaining powder in a blister. Firstly, the air resistance is rather high, shown in Fig.5.8. Then the diameter of the puncture (Diameter A, Fig.5.7) was increased from 1.4mm to 2mm, and the diameter of the tube (Diameter B, Fig.5.7) connected to the push button was enhanced from 2.5mm to 3mm. These alterations allow more air to pass through the mouthpiece. Additionally, two very small air holes were placed on the both sides of the mouthpiece, also serving to decrease the resistance.

As shown in Fig.5.8, the air resistance exhibits a significant decline from 0.22 to 0.06  $\text{kPa}^{0.5} \cdot \text{min/L}$  due to the design improvement. The lower resistance of the new design is much closer to marketed products.

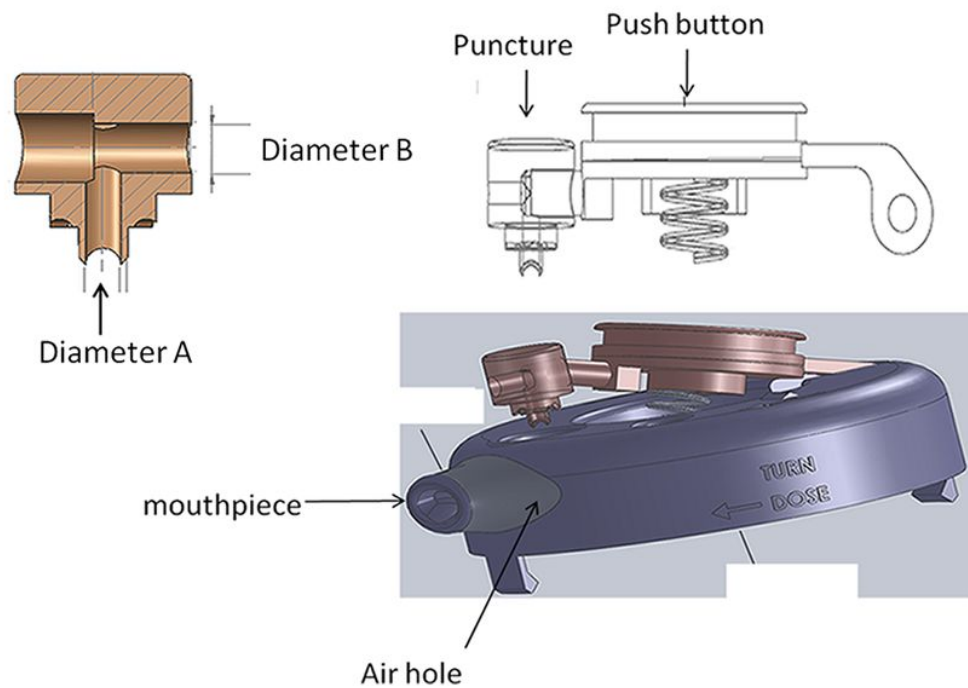


**Figure 5.7: The schematic of the improved puncture design**

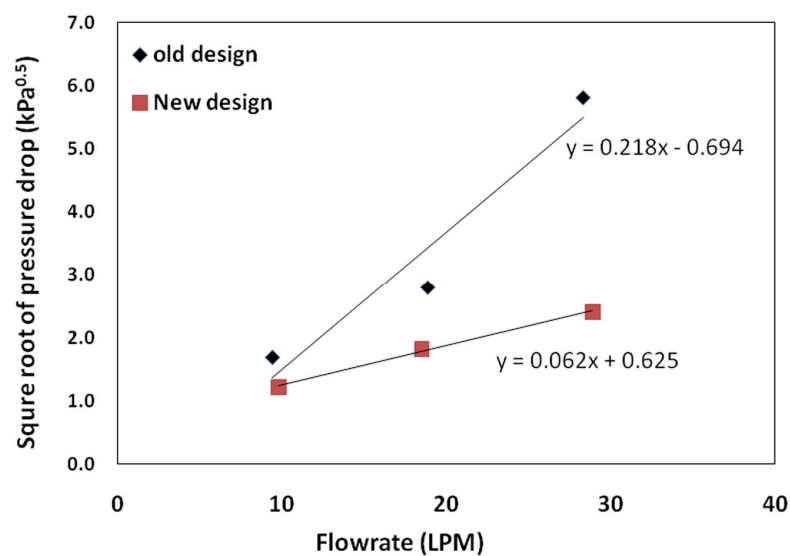


**Figure 5.8: The linearity between (pressure drop)<sup>0.5</sup> and the flow rate of the improved inhaler**

The improvements also exert a beneficial effect on the delivery efficiency and uniformity. As shown in Fig.5.9, the comparison clearly indicates that the new design not only

enhances the delivery rate and decreases the remains in blisters but also reduces the variability.

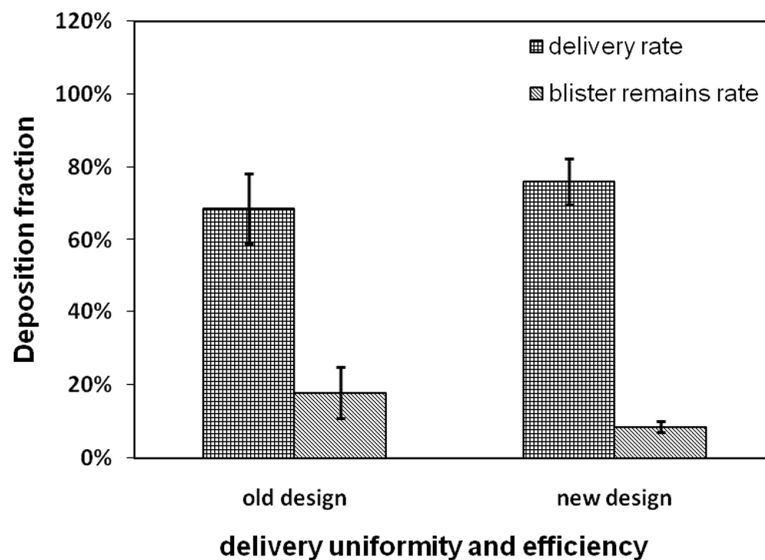


**Figure 5.9: The comparison of delivered efficiency and content uniformity between the old design and new inhaler (n=6)**

The geometry of inhaler mouthpiece is believed to have great influence on the inhaler performance. Consequently, a series of mouthpiece is designed and manufactured to test their performance. The mouthpieces of various interior diameters, length and airway shape are made as Fig.5.10 and Table 5.5 and then tested by the NGI.

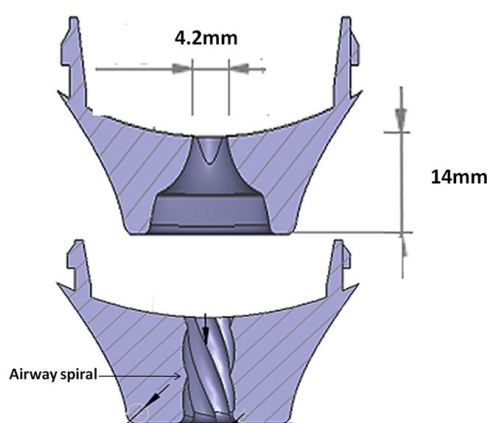
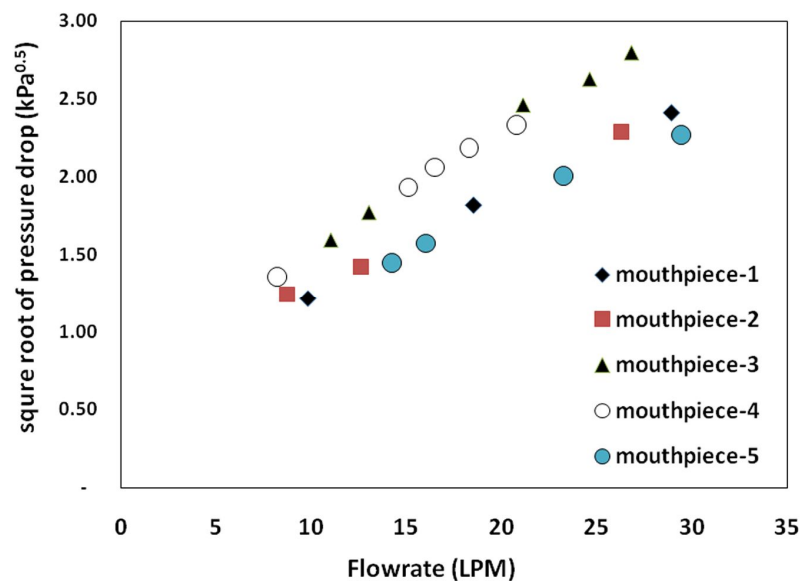


**Figure 5.10: The airway structure of the mouthpiece**

**Table 5.5: The dimensions of the investigated mouthpieces**

Devices	Airway length (mm)	Airway diameter(mm)	Airway spiral
Mouthpiece-1 (Original)	14	4.2	No
Mouthpiece-2	7	4.2	No
Mouthpiece-3	21	2.6	No
Mouthpiece-4	14	2.6	No
Mouthpiece-5	14	4.2	6

In the first test, the influence of mouthpiece geometry on air resistance is studied, and the results are shown in Fig.5.11 and Table.5.6. As we could see in Table.5.6, reduction of the airway length almost do not show any significant effect on air resistance. Yet, the decline of airway diameter greatly raises the resistance. The decline of resistance for spiral airway might be caused by increasing diameter as a result of spiral design.

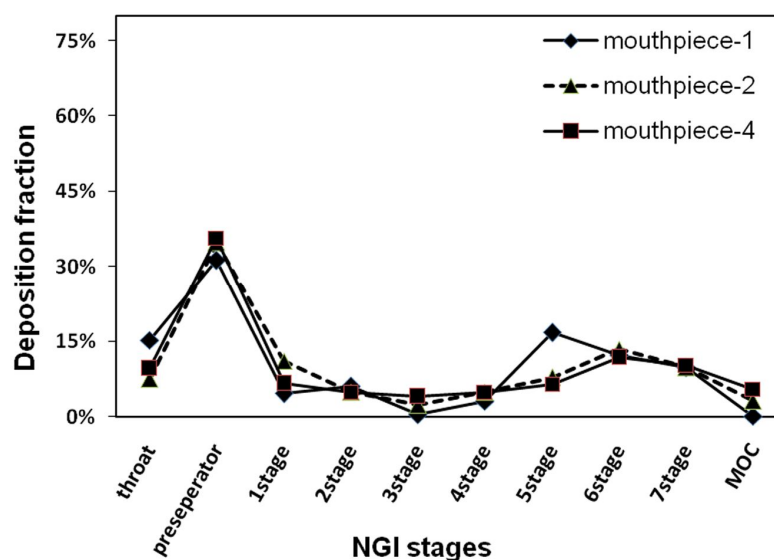


**Figure 5.11: The linearity between (pressure drop)<sup>0.5</sup> and flow rate for different mouthpieces**

**Table 5.6: The air resistance of the new inhaler with different mouthpieces**

Devices	Resistance (kPa <sup>0.5</sup> *min/liter)
Mouthpiece-1 (Original)	0.062
Mouthpiece-2	0.060
Mouthpiece-3	0.076
Mouthpiece-4	0.079
Mouthpiece-5	0.054

To evaluate the influence of the mouthpiece on aerodynamic particle size distribution (APSD), the drug disks containing the same formulation are tested by NGI for mouthpiece 1-5. The APSD result is shown in Fig.5.12, Fig.5.13 and Fig.5.14, and the critical data are presented in Table.5.7. The APSD profiles of different mouthpieces are the same except for one abnormal point of mouthpiece-1. Taking the variation of NGI test into account, the FPF values are the same as shown in Table.5.7. Consequently, the design of the mouthpiece and corresponding slight alteration of air resistance do not exert great influence on the inhaler performance.

**Figure 5.12: The APSD of the inhaler with different mouthpieces (mouthpiece 1, 2, 4)**



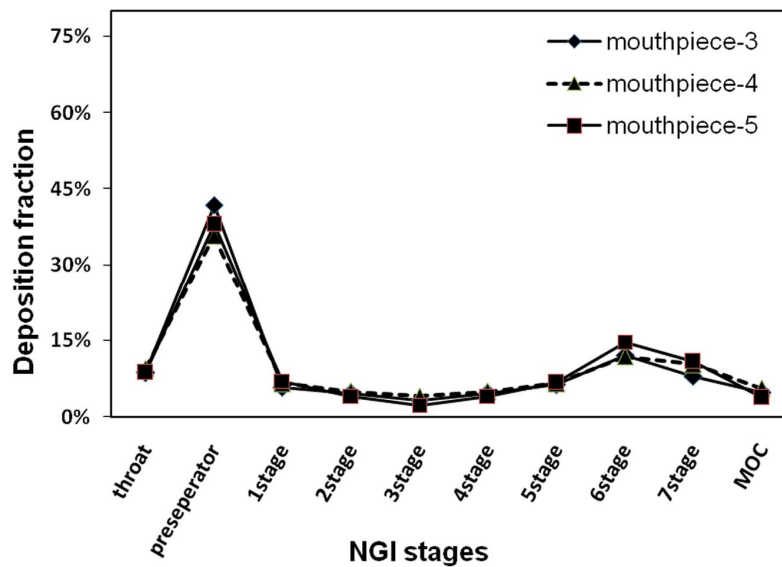


Figure 5.13: The APSD of the inhaler with different mouthpieces (mouthpiece 3, 4, 5)

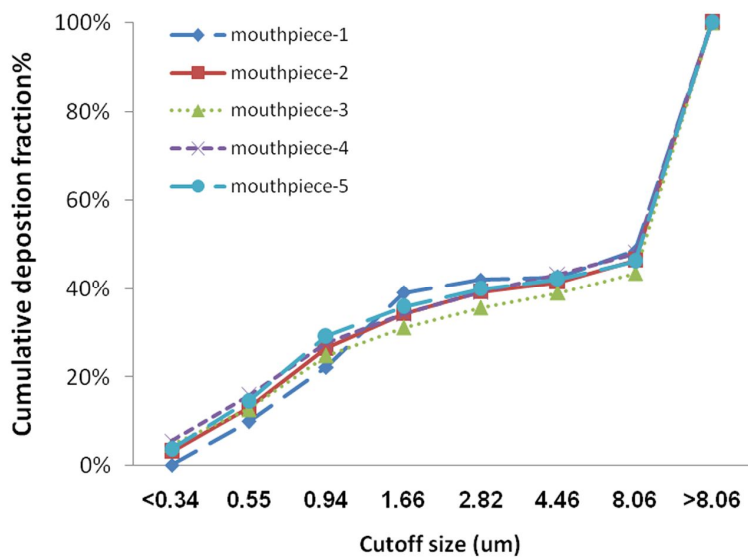


Figure 5.14: The cumulative distribution of the inhaler with different mouthpieces

**Table 5.7: The FPF results of the inhaler with different mouthpieces**

Devices	FPF values	SD (n=3)
Mouthpiece-1(Original)	42.7%	
Mouthpiece-2	41.6%	3.59%
Mouthpiece-3	39.0%	5.30%
Mouthpiece-4	43.2%	0.45%
Mouthpiece-5	42.2%	3.34%

During the evaluation and tests of the Inhaler-WU2011, the accurate position of the blister is very important for the drug delivery. In other words, it is required that the center of a blister should be where the puncture piece into. We compared a good inhaler to an inhaler with the ratchet and locator not working properly. The bad inhaler was tested repeatedly for 3 times using 10%-fines powder. As a comparison, the good inhaler was tested using three kinds of powders including 10%-fines. The results are shown in Table 5.8 and Table 5.9. Although the FPF of both inhalers using 10%-fines powder are almost the same, huge difference of RSD in terms of blister remains and FPF indicates that right position of blisters and accurately puncturing greatly improve the uniformity of drug delivery. Therefore, it is concluded that materials of the ratchet and locator should be carefully studied in the future, and only those exhibiting excellent mechanical properties during a fatigue test are suitable.

**Table 5.8: The TI results of the inhaler when blister at wrong position**

Deposited mass/TRM	1st test	2nd test	3rd test	AVG	RSD
Blister remains	4.1%	17.5%	6.7%	9.5%	75.2%
FPF	54.3%	41.7%	29.6%	41.9%	29.4%

**Table 5.9: The TI results of the inhaler when blister at right position**

Deposited mass/TRM% (n=3)		0fines	5%fines	10%fines
Blister remains	AVG	27.1 %	16.6%	17.2%
	RSD	2.8%	7.3%	1.7%
FPF	AVG	15.8%	33.1%	40.0%
	RSD	5.8%	13.5%	1.3%

## 5.4 Parallel Comparison with the Marketed Inhalers

It is ideal to exclude the formulation effect when we compare the performance of various inhaler devices. Yet, it is difficult to carry out such a research for multiple unit dose devices and reservoir devices. Take Diskus® Seretide® for an example, the drug powder is sealed in an individual blister by special packaging material. Besides, the structure of Diskus® is too complicated to disassemble and assemble. What is even worse for Turbuhaler® Oxis, its unique formulation is composed of sphere agglomerates with superb flowability. Only these sphere agglomerates are suitable for the powder filling and metering mechanism of Turbuhaler®, and other particles would not work properly.

Because the structure and powder filling is relatively easier for Aerolizer®, Twister® and Clickhaler®, they are employed as a comparison with the inhaler-WU2011 using the same powder. The powder was composed of 0.72% sulfate Salbutamol, 20% fine lactose and Inhalac 230. And it was prepared by the method described in Section 3.5.1. Then a certain amount of powder was filled into a 3# capsule for Aerolizer® and Twisthaler®, and the reservoir of Clickhaler®. Then their performance was tested by TI (Twin impinger) method.

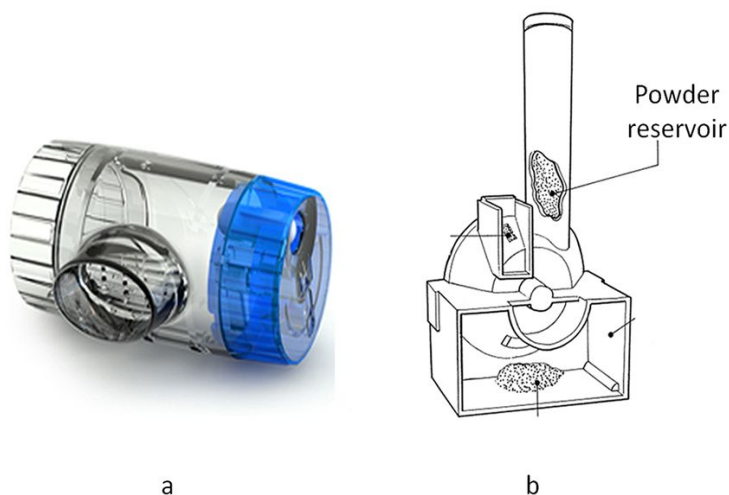


**Figure 5.15: The picture and schematic of twister® and Clickhaler® Reservoir**

The results shown in Fig.5.16 and Fig.5.17 indicate that the Inhaler-WU2011 has similar performance as Aerolizer® and Clickhaler®. Their FPFs are about 50% and higher than the Twister®. When considering the fraction of remains in inhaler devices, Inhaler-WU2011 has the same result as Twister® and similar variations as Aerolizer®. The Clickhaler® do not show remains in the device after drug delivery.

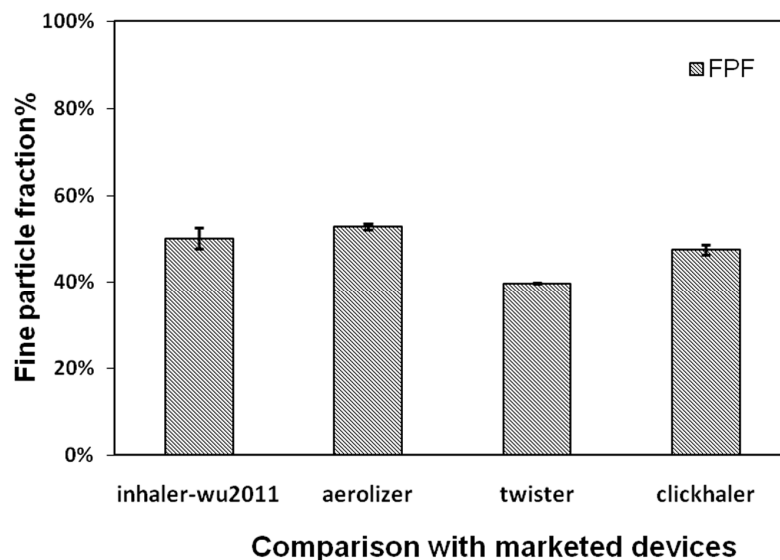


**Figure 5.16: The parallel comparison of FPF with marketed devices by using the same powder.**

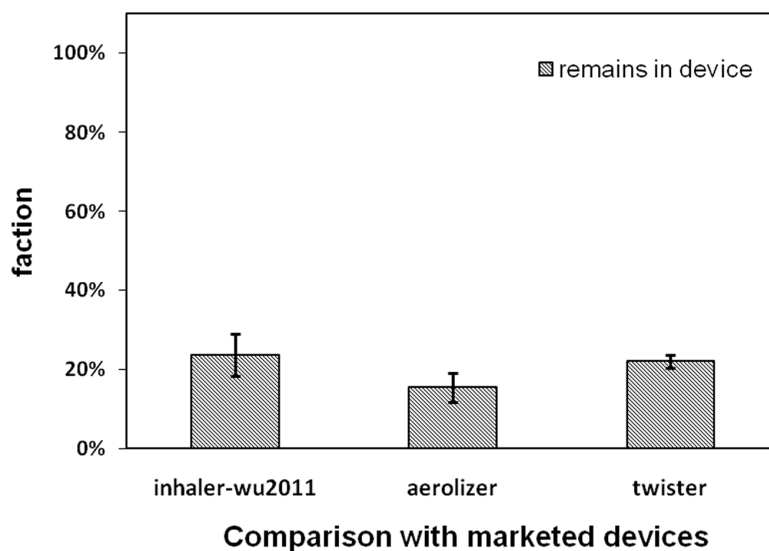


**Figure 5.17: The parallel comparison of remains fraction with marketed devices by using the same powder**

## 5.5 Discussion

Several marketed inhaler products are evaluated for *in vitro* performance. Then, the design improvement of Inhaler-WU2011 and enhanced performance is introduced. At last, the device performance is compared to several inhalers using the same powder formulation. The results indicate that the inhaler-WU2011 has better or similar performance as marketed products.

Without consideration for formulation, the air flow resistance is a critical parameter for inhaler devices. Several marketed DPI device are tested here for resistance, and the results are similar as values mentioned in a review<sup>[140]</sup>. The single and multiple unit dose inhalers have smaller resistance and reservoir devices show higher one. The resistance of Inhaler-WU2011 after design improvement is close to the Inhalator®<sup>[140]</sup>, higher than other marketed devices. As a result of descending resistance, the flow rate increases under the same pressure drop, resulting in a better delivery efficiency and uniformity.

The passive DPI devices are greatly dependent on an inspiratory flow to disperse and deliver powder, and air flow resistance will influence the peak inspiratory flow (PIF) and maximal inspiratory capacity (MIC) directly. If the inspiratory effort is the same, then a bigger resistance results in a lower PIF and MIC<sup>[48; 141]</sup>. During an administration, the total air resistance is equal to the sum of the device ( $R_{\text{inhaler}}$ ) and human airway ( $R_{\text{airway}}$ ). For high resistance device ( $R_{\text{inhaler}} \gg R_{\text{airway}}$ ), the device resistance determines the whole resistance. But for low resistance device, both  $R_{\text{inhaler}}$  and  $R_{\text{airway}}$  would affect the whole resistance. It means that low resistance devices are more sensitive to the bronchi contraction and different patients may produce different aerosol performance.<sup>[142; 143]</sup> Moreover, a high-resistance device may reduce the velocity of the airflow and particles. Then impaction of particle on oropharyngeal would go down as a result of lower velocity and smaller inertia, and deposition of particle in lung would increase.

Nevertheless, the high-resistance device may cause uncomfortable for the patient because it requires a greater effort. Furthermore, the flow rate of high-resistance device would be lower under the same pressure drop. The decline of flow rate might decrease the efficiency of API-carrier detachment as a result of lower airflow energy. For example,

Cegla et al reported that, compared to the patient who used Novolizers, patients had to invest a significantly higher inspiratory effort when they used a Turbuhaler as a result of its higher resistance. And patients had a worse inhalation performance when inhaling through the Turbuhaler than Novolizer<sup>[144]</sup>. On the contrary, Gac et al proposed that a noticeable increase of delivery efficiency and particle detachment was obtained at low airflow rates due to the use of turbulence, which suggested that an appropriate increase of flow resistance is acceptable<sup>[145]</sup>.

As mentioned before, the delivery uniformity of reservoir device is a major concern by the regulatory agency. This problem is confirmed again by the results of this chapter. The uniformity of Clickhaler® Asmasal® is acceptable although there is a tail-off effect at the end of delivery. The tail-off effect is usually used to describe a content drop at the end of a pMDI. The Clickhaler® Asmasal® also experiences drug content decline for its last 3 deliveries. This phenomenon is perhaps caused by its filling and metering mechanism. Particularly, the Clickhaler® must be shaken hard before administration. The shaking operation helps powder flow into a dimple from the reservoir. Then, the powder in that dimple is released when a patient inhaling through the device. Because the powder bed in the reservoir goes down gradually during usage, the density of powder in a dimple decreases and leads to a drug content drop.

We believe that Turbuhaler® Oxis® can achieve its target delivery and meet the uniformity requirements, although the evaluation here shows a disappointing result. Nevertheless, it is doubtless that Turbuhaler® is difficult to operate for satisfying delivery uniformity. Chew et al also reported the problem of delivery efficiency and uniformity for Turbuhaler when they compared the Aerolizer® and Turbuhaler®<sup>[146]</sup>. It is inferred that the poor delivery performance is related to its formulation and filling/metering structure. Firstly, the Oxis® Turbuhaler® only contain 4.5 or 9µg API plus 450µg lactose, and Pulmicort® Turbuhaler® just contain 100 or 200µg API. The extremely small amount of powder makes it a huge challenge to fill and meter powder accurately. Secondly, the metering and filling mechanism of Turbuhaler® is greatly dependent on flowability of the formulation. A dose is loaded into a series of small holes in a dosing disc from the reservoir by twisting the base of the device backwards and

forwards, with a set of scrapers removing excess drug (Fig.5.18). Consequently, the state of agglomerates, fragments of agglomerates and remains in the dosing disk could affect the delivery uniformity.

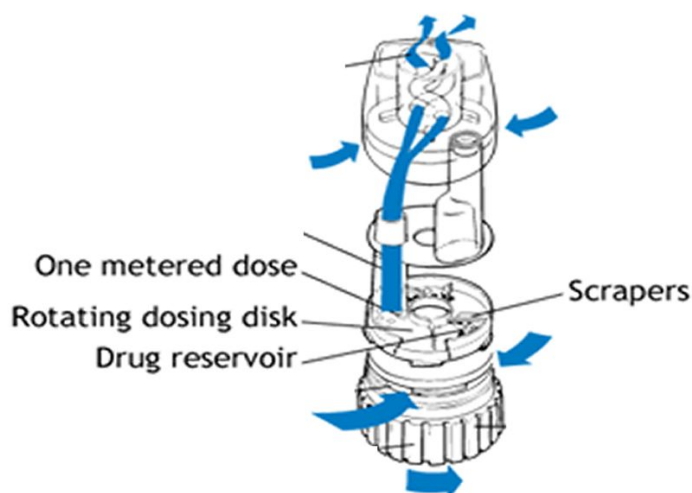


**Figure 5.18: The schematic of air flow (blue arrow) and powder metering mechanism**

When considering the FPF results, the reservoir devices, like Turbuhaler® Oxis® and Clickhaler® Asmasal® have a very high FPF (>40%) compared with Aerolizer® Foradil® and Diskus® Seretide® (~26%). The FPF results are similar to the values described by Frijlink<sup>[140]</sup>. It is inferred that a high FPF of reservoir device is mainly due to the formulation and inhaler devices. First, when testing Aerolizer® with the same powder prepared by ourselves, its FPF also reaches 50%, even higher than Clickhaler®. Secondly, the particle size distribution from laser diffraction sizing. The laser diffraction sizing is carried out immediately after inertial impaction tests to find the deeper reason of different FPF results. These four marketed DPI products are characterized by laser diffraction sizing, and the results are shown in Fig.5.19, Fig.5.20 and Table.5.10. The particle size of Aerolizer® Foradil® and Diskus® Seretide® are much larger than Turbuhaler® Oxis®. Besides, the quantity of lactose would affect the FPF results. The lactose used in Clickhaler® Asmasal® (~5mg) and Turbuhaler® Oxis® (450µg) is significantly less than single and multiple unit does inhaler (~30mg). Less lactose carrier of a reservoir inhaler might make fine drug particles easier to detach from lactose carrier.

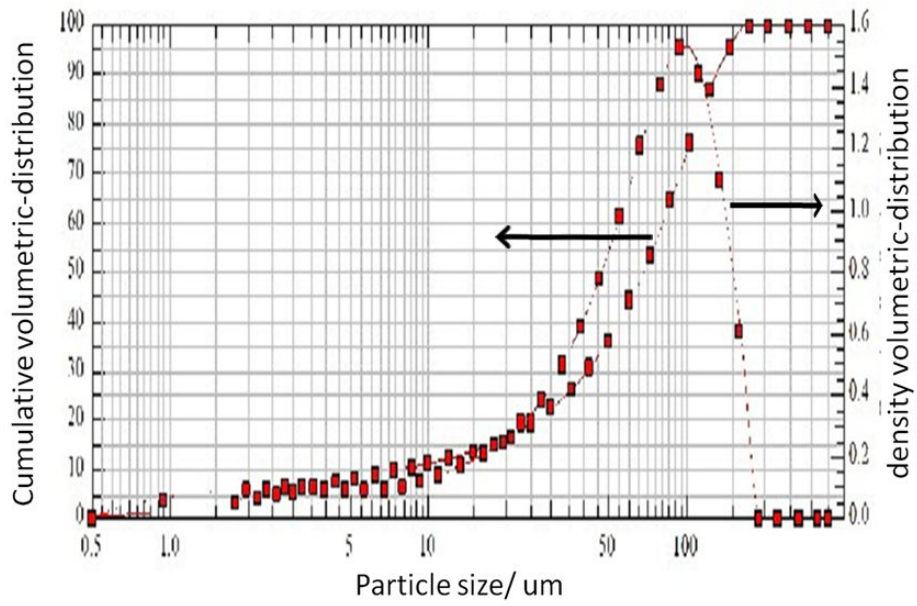


**Figure 5.19: The laser diffraction size result of Diskus® Seretide®**

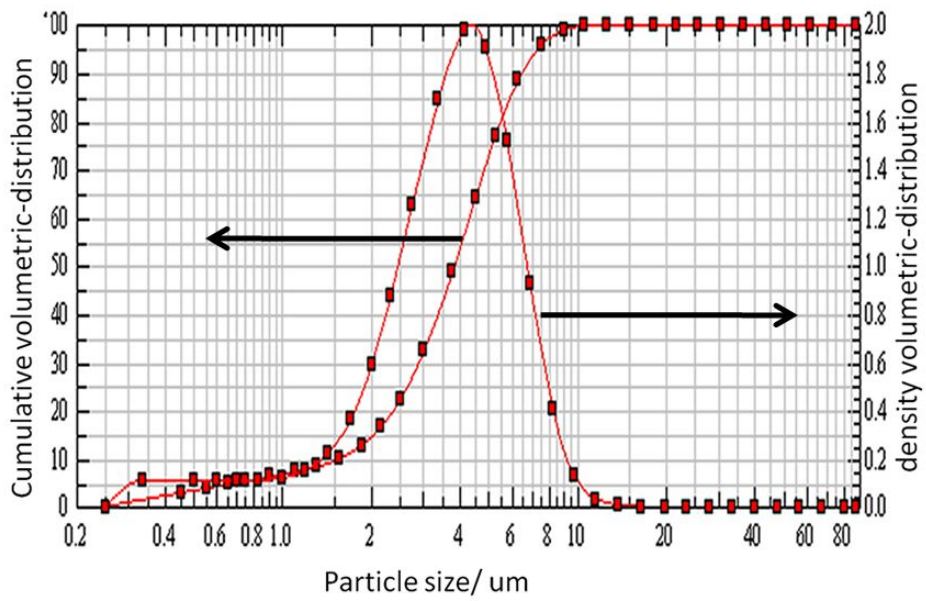


**Figure 5.20: The laser diffraction size result of Turbuhaler® Oxis®**



**Table 5.10: The Laser diffraction size measurement results of the marketed products**

	X10	X50	X90
Aerolizer® Foradil®	3	33	109
Diskus® Seretide®	8	67	131
Turbuhaler® Oxis®	0.6	2.1	5.0
Clickhaler® Asmasal®	30	60	100

The mouthpiece is the part connecting the inhaler to a patient, and it plays an important role in the device design. There are many researches about the influence of mouthpiece shape and geometry on inhaler performance<sup>[28; 31]</sup>. Coates et al studied the influence of mouthpiece geometry on the aerosol delivery performance of Aerolizer®. They found that the geometry had no effect on device retention or dispersion performance, but would affect the local deposition like throat deposition by changing the air flow velocity<sup>[147; 148]</sup>.

It is not very common to compare the performance of inhaler device using the same powder. For one thing, it is difficult to fill and meter powder into the device like Diskus® and Turbuhaler®. On the other hand, the DPI product is usually considered as a whole system including device, formulation and filling system. The result of this chapter demonstrates that the Inhaler-WU2011 has better or similar performance as other marketed products using the same formulation. This conclusion lays a solid foundation for future R&D work in terms of both technology and confidence.

## Chapter 6

### 6 Evaluation of Dry Powder Filling Device

#### 6.1 Brief Introduction

This chapter mainly focuses on the powder filling process. As shown in Fig.6.1, the uniformity of the filling is studied in the following sequence: A) the filling weight uniformity among disks, B) filling weight uniformity among blisters in a given disk, C) drug content uniformity among disks and D) drug content among blisters in a given disk. During the evaluation process, the filling operation and testing methods are improved continually. A vacuum-assisted filling and reduction of vibration strength are applied in the optimization of filling process, which are expected to improve drug content uniformity among blisters.

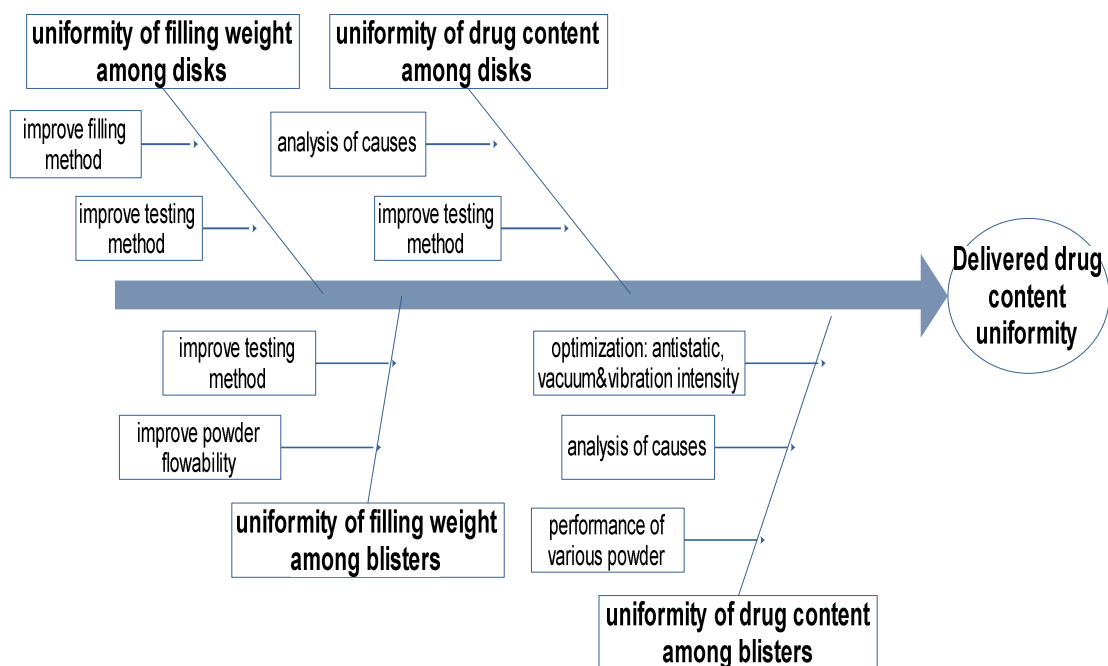


**Figure 6.1: A schematic diagram of the filling uniformity research**

## 6.2 Uniformity of Dry Powder Filling Device

The powder filling techniques and equipment is detailed in Section 3.4.2, and the filling uniformity experiment and method are introduced in Section 3.4.3. The development of uniformity testing method is not described before but in this chapter, and it is greatly helpful for future work.

### 6.2.1 Filling weight uniformity among different disks

In Trial A-1, the quantity of all powder in 14 blisters in a disk was calculated by subtracting the weight of an empty disk from the disk filled with powder. Then, the uniformity was measured by the RSD of filling weight of several disks. The powder was prepared by 10% fine sulfate Salbutamol and 90% Inhalac 230. The results are shown in Table 6.1 and Fig.6.2. An RSD of about 27% indicates a huge variance of filling weight.

**Table 6.1: The filling weight and uniformity of disks in Trial A-1**

	Filling weight mg	AVG(mg)	SD	RSD
disk1	47.9	48.2	13.0	27.0%
disk2	44.7			
disk3	54.4			
disk4	39.9			
disk5	70			
disk6	32.3			

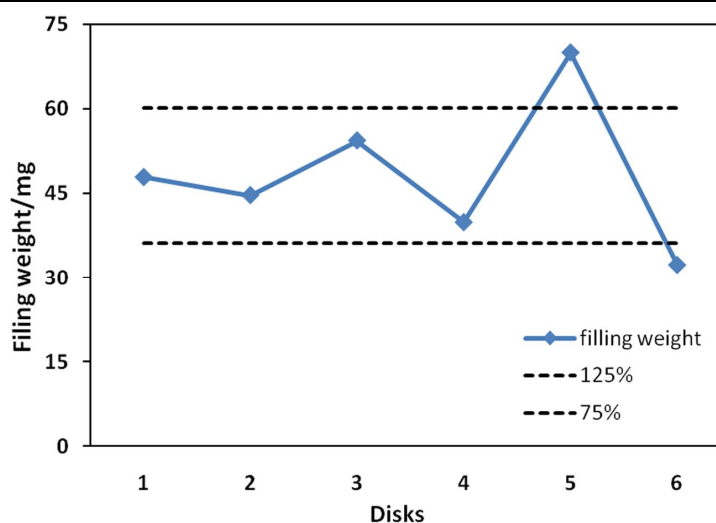


**Figure 6.2: The filling weight uniformity between disks in Trial A-1**

In Trial A-2, the filling process was improved by cleaning the metering plates and pockets every time before filling the next disk. The results are shown in Fig.6.3 and Table 6.2. As we can see, the filling uniformity is significantly improved. The decline of filling weight can be explained by that the powder with smaller density is applied and the variance becomes smaller. Whereas, this filling method would waste some powder on the metering plate and is complicated because of the cleaning procedure. When testing more samples, a downward trend is found despite of an acceptable RSD at 3.73% as Fig.6.4. It is inferred that this problem is due to the testing method rather than filling device. Hence, the evaluating method for the uniformity of filling weight need to be further improved.

**Table 6.2: The improved uniformity of filling weight between disks in Trial A-2**

	M/mg	AVG/mg	SD/mg	RSD%
disk1	25.7	25.76	0.8369	3.25%
disk2	25.1			
disk3	25.1			
disk4	25.6			
disk5	25.0			
disk6	27.9			
disk7	25.8			
disk8	26.2			
disk9	25.6			
disk10	25.6			

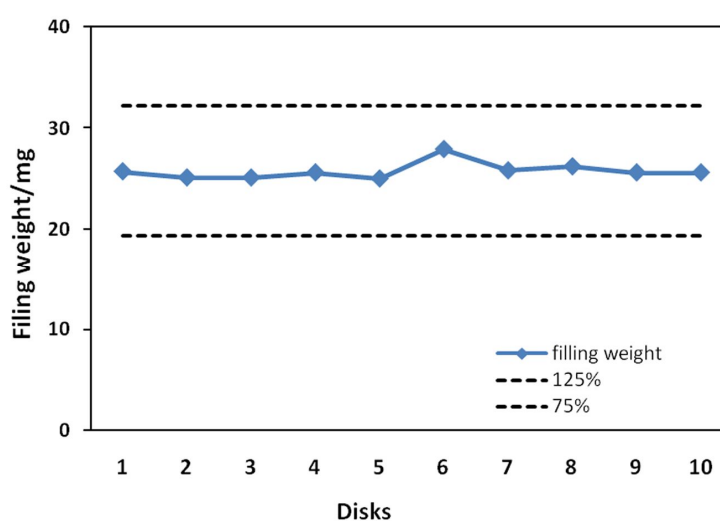


**Figure 6.3: The improved uniformity of filling weight between disks in Trial A-2**

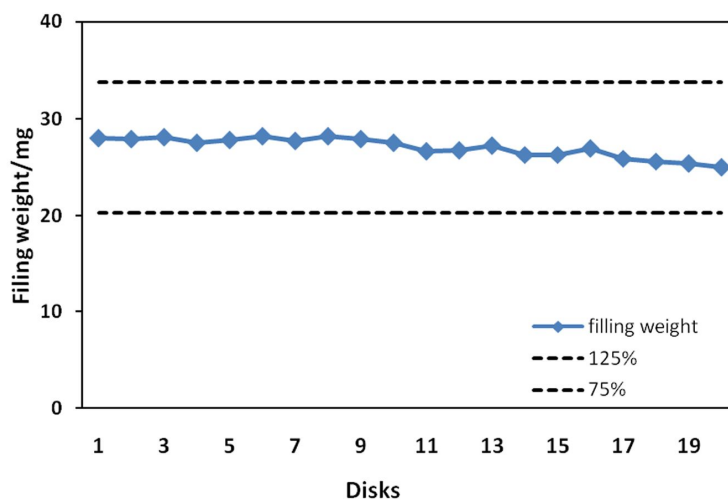


**Figure 6.4: The descending trend of filling weight for 20 disks in Trial A-2**

In Trial A-3, the drug disk was immediately sealed with aluminum foil after filling powder. Then each blister in this disk was opened carefully without foil loss, and all powder was cleaned away completely. The powder weight was calculated by subtracting the weight of a cleaned disk through the disk filled with powder, as mentioned in Section 3.4.3. Then, the number of the filled disks was increased to 100, and 17 disks were analyzed at intervals. The results are shown in Table 6.3 and Fig.6.5, and both demonstrate excellent uniformity.

**Table 6.3: The filling weight uniformity for 100 disks in Trial A-3**

Disk	M/mg	AVG/mg	SD/mg	RSD%
1	25.8	27.8	0.726	2.61
2	28.2			
3	28.5			
11	29.0			
12	28.3			
13	28.3			
20	27.7			
30	27.3			
49	28.3			
50	27.1			
51	28.0			
52	27.6			
70	27.7			
90	27.2			
98	28.3			
99	28.2			
100	27.7			

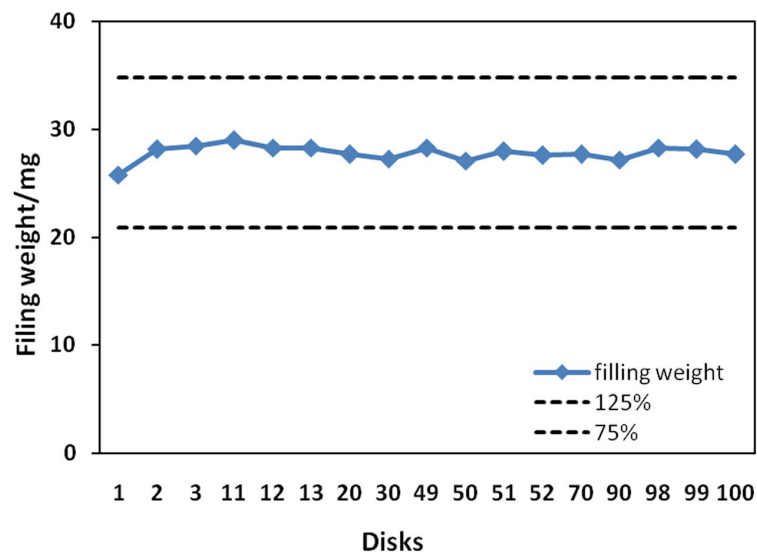


**Figure 6.5: The filling weight uniformity among 100 disks in Trial A-3**

To evaluate the weight uniformity among disks when various powders were used, the powders containing 0%, 5%, 10%, 20% fine lactose and corresponding Inhalac 230 were applied in Trial A-4. The results shown in Table 6.4 and Fig.6.6 clearly demonstrate that the filling weight uniformity among disks for different powders is quite excellent. Moreover, the filling weight per disk goes up with increasing fine lactose, as a result of more condense packing.

**Table 6.4: The filling weight uniformity of disks using different powders in Trial A-4**

n=50		0%-fines	5%-fines	10%-fines	20%-fines
Filling weight per disk	AVG (mg)	25.6	29.4	30.3	30.4
	RSD%	3.18	1.28	1.23	1.81

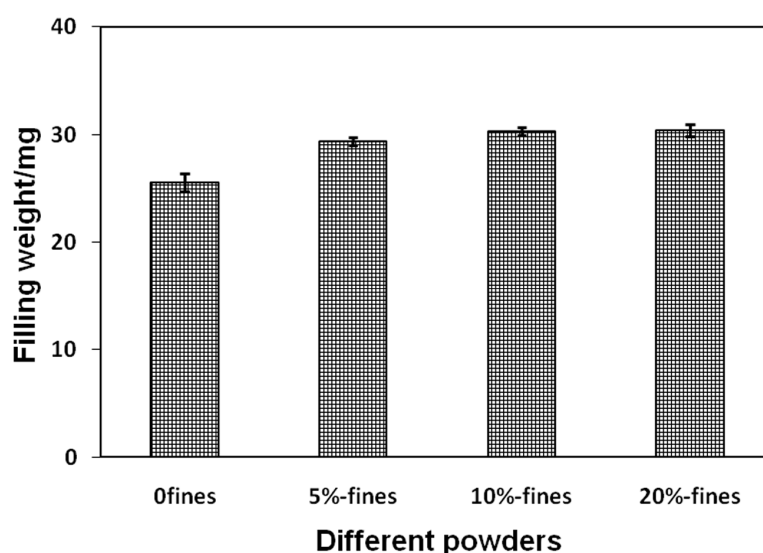


**Figure 6.6: The filling weight uniformity of disks using different powders in Trial A-4**

### 6.2.2 Filling weight uniformity among blisters on one disk

The powder weight uniformity among blisters was a prerequisite for the delivered dose uniformity. All blisters on a disk were numbered sequentially according to their position to the pockets on the metering plates. Thereby, it was possible to find out a pattern of

filling weight for blisters. Initially, the quantity of powder in a blister was calculated by subtracting the weight of the disk through its original one after emptying a specific blister. The powder comprising 10% sulfate Salbutamol and 90% Inhalace 230 were prepared for this filling uniformity test.

After filling powder, a drug disk was weighed to get  $M^{14}$ , where 14 represented 14 blisters. After that, a blister on this disk was opened carefully without foil loss, and the powder was cleaned away completely, and then the weight of the disk  $M^{14-1}$  was obtained. The filling weight  $m^1$  for this blister (1) was calculated. Similarly, filling weight for other blisters (i) was acquired in the same way.

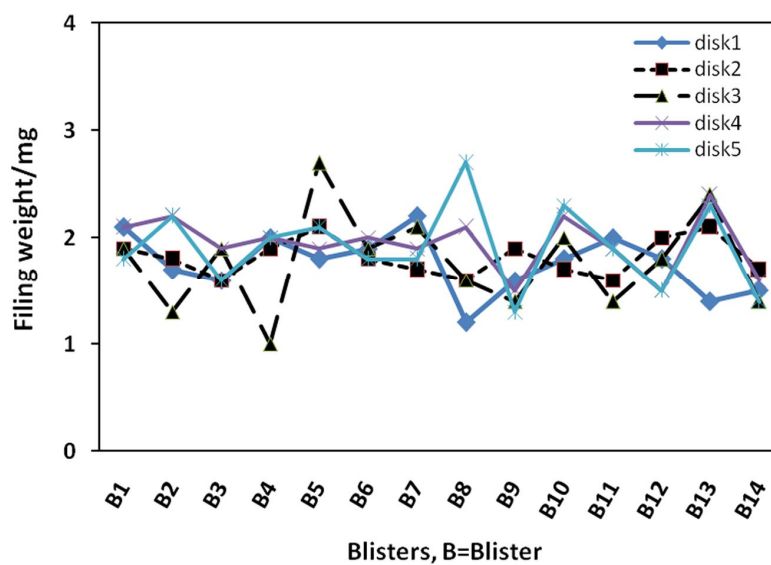
$$M_b^x = M^{15-i} - M^{14-i} \quad (1 \leq i \leq 14)$$

The result of Trial B-1 is shown in Fig.6.7 and Table 6.5. At the first glance, the fluctuation of filling weight for the blisters 1-14 seem to be still acceptable in Fig.6.7 with a SD of about 0.2 mg. Yet, its variation is rather significant actually since the target filling weight is very small. Then, if we consider the uniformity of all blisters from 5 disks, the RSD of 17.8% indicates a unsatisfactory uniformity. As we can see in Table 6.5, the RSD of disk1-5 is from 9.6% to 25%. Those results demonstrate that the uniformity among blisters in single disk also need to be improved. Additionally, if we look at the rows of the table, the quantity of powder metered by the same pocket also exhibit great variance.



**Table 6.5: The initial filling weight uniformity of blisters Trial B-1**

	disk1/mg	disk2/mg	disk3/mg	disk4/mg	disk5/mg	Avg	RSD
blister1	2.1	1.9	1.9	2.1	1.8	1.96	6.9%
blister2	1.7	1.8	1.3	2.2	2.2	1.84	20.6%
blister3	1.6	1.6	1.9	1.9	1.6	1.72	9.6%
blister4	2	1.9	1	2	2	1.78	24.6%
blister5	1.8	2.1	2.7	1.9	2.1	2.12	16.5%
blister6	1.9	1.8	1.9	2	1.8	1.88	4.5%
blister7	2.2	1.7	2.1	1.9	1.8	1.94	10.7%
blister8	1.2	1.6	1.6	2.1	2.7	1.84	31.4%
blister9	1.6	1.9	1.4	1.5	1.3	1.54	15.0%
blister10	1.8	1.7	2	2.2	2.3	2	12.8%
blister11	2	1.6	1.4	1.9	1.9	1.76	14.3%
blister12	1.8	2	1.8	1.5	1.5	1.72	12.6%
blister13	1.4	2.1	2.4	2.4	2.3	2.12	19.8%
blister14	1.5	1.7	1.4	1.6	1.4	1.52	8.6%
AVG/mg	1.81	1.76	1.77	1.94	1.91		
RSD%	9.6%	15.9%	25.9%	13.7%	20.5%		

**Figure 6.7: The initial filling weight uniformity of sequentially numbered blisters in Trial B-1**

In Trial B-2, we tried to change the powder based on an assumption that the improvement of powder flowability would be helpful for the filling uniformity. Hence, the powder was prepared by 5% fine sulfate Salbutamol and 95% Inhalac 230.

The result presented in Table 6.6 and Fig.6.8 shows a slight improvement when compared with Trial B-1. The RSD for 42 blisters from 3 disks is 15%, a little lower than the former result. The maximum RSD for single disk is 17%, which is a little better. Yet, the uniformity is not satisfactory. It is guessed that the variance is also from testing, and the evaluating method is improved in Trial B-3.

**Table 6.6: The filling weight uniformity among blisters for the powder with improved flowability in Trial B-2**

	disk1/mg	disk2/mg	disk3/mg	AVG/mg	RSD%
blister1	1.95	1.74	1.27	1.65	21.06%
blister2	1.64	1.63	1.65	1.64	0.61%
blister3	1.44	1.71	1.43	1.53	10.41%
blister4	1.4	2.01	1.63	1.68	18.34%
blister5	1.51	1.46	1.57	1.51	3.64%
blister6	1.26	1.53	1.3	1.36	10.69%
blister7	1.3	1.3	1.56	1.39	10.83%
blister8	1.33	1.28	1.08	1.23	10.76%
blister9	1.05	1.48	1.49	1.34	18.75%
blister10	1.48	1.69	1.32	1.50	12.40%
blister11	1.45	1.2	1.31	1.32	9.49%
blister12	1.49	1.2	1.2	1.30	12.91%
blister13	1.22	1.24	1.19	1.22	2.07%
blister14	1.23	1.17	1.64	1.35	19.00%
AVG/mg	1.41	1.47	1.40		
RSD%	15.3%	17.4%	13.5%		

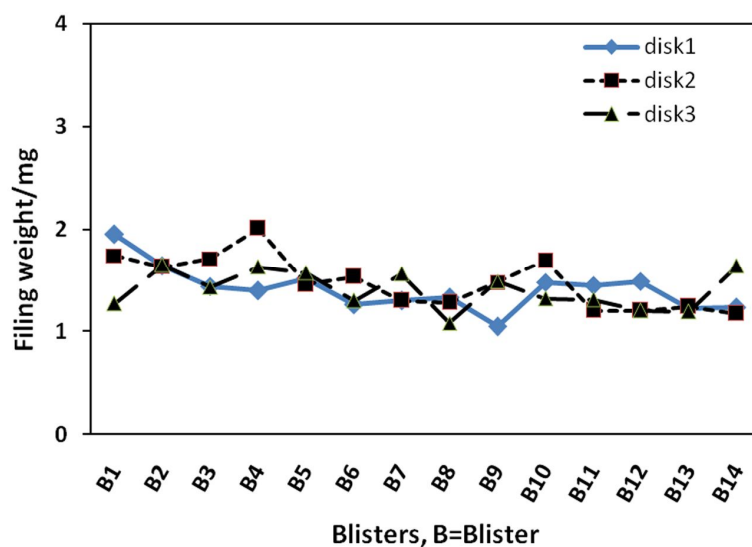


**Figure 6.8: The filling weight uniformity among blisters for the powder with improved flowability in Trial B-2.**

In Trial B-3, empty PVC disks were treated by an antistatic fan for 10min before powder filling. When filled with powder, the disks were sealed with alumina foil by hot-pressing. Then, the blisters were opened sequentially and cleaned by vacuum pump, and were weighed.

The results are shown in Table 6.7. The columns represent all 14 blisters on one disk, while rows stand for corresponding blisters from different disks. The elimination of static electricity and sealing greatly increase the uniformity of filling weight per blister. The RSD for 84 blisters from 6 disks is 7.5%, nearly half of the value of the above research. The maximum RSD for one disk is 9%. The obvious decline of RSD indicates an enhanced uniformity.

**Table 6.7: The improved filling weight uniformity of blisters in Trial B-3**

	1st/mg	2nd/mg	3rd/mg	4th/mg	5th/mg	6th/mg	AVG/mg	RSD%
blister1	1.84	1.72	1.9	1.79	1.91	1.5	1.78	8.6%
blister2	1.66	1.52	1.41	1.66	1.43	1.55	1.54	7.0%
blister3	1.84	1.97	1.73	1.62	1.72	1.49	1.73	9.7%
blister4	1.67	1.75	1.59	1.63	1.89	1.73	1.71	6.2%
blister5	1.83	1.65	1.81	1.96	1.63	1.83	1.79	7.0%
blister6	1.8	1.64	1.52	1.75	1.78	1.74	1.7	6.2%
blister7	1.63	1.67	1.8	1.69	1.65	1.68	1.69	3.5%
blister8	1.64	1.9	1.88	1.71	1.68	1.62	1.74	7.0%
blister9	1.57	1.68	1.9	1.78	1.72	1.76	1.73	6.3%
blister10	1.61	1.73	1.62	1.72	1.73	1.58	1.67	4.1%
blister11	1.71	1.56	1.5	1.6	1.56	1.67	1.6	4.9%
blister12	1.31	2	1.75	1.75	1.79	1.65	1.71	13.3%
blister13	1.72	1.88	1.79	1.74	1.72	1.77	1.77	3.4%
blister14	1.82	1.68	1.8	1.69	1.66	1.63	1.71	4.6%
AVG/mg	1.69	1.74	1.71	1.72	1.71	1.66	1.7	1.7%
SD/mg	0.14	0.15	0.16	0.09	0.12	0.1		
RSD%	8.5%	8.4%	9.3%	5.3%	7.2%	6.2%		

Finally, the test method in Trial B-4 was determined as the final version: After filling powder, the drug disk was sealed with aluminum foil and all blisters were numbered. Then a blister was cut off and weighed. Next, this blister was opened carefully without foil loss, and the powder was rinsed by solvent completely. After air dry, the weight of the empty blister was obtained. The quantity of powder was calculated by subtracting the weight of an empty blister from its original weight.

The result of Trial B-4 is presented in Table 6.8. The RSD of total 42 blisters is 7.5% and maximum RSD of blisters in single disk is 8.1%, which exhibit a further RSD decline and improved uniformity. As shown in Fig.6.9, the filling weight for the sequentially numbered blisters show a very similar trend for all the 3 disks. This result indicates that the filling weight from the same metering pocket is similar, which is also reflected by the relatively lower RSD of each row in Table 6.8. The “consistent” variation of the filling

weight is possible due to a variance of the metering pockets size. In the future, the metering plate will be drilled by laser, and such variance may be reduced.

**Table 6.8: The final filling weight uniformity of blisters in Trial B-4**

	1st/mg	2nd/mg	3rd/mg	Avg	RSD
blister1	2.28	2.39	2.19	2.29	4.4%
blister2	2.16	2.06	1.91	2.04	6.2%
blister3	1.97	2	1.86	1.94	3.8%
blister4	2.33	1.99	1.98	2.10	9.5%
blister5	2.06	1.88	1.94	1.96	4.7%
blister6	2.14	1.92	2.29	2.12	8.8%
blister7	2.22	2.21	2.14	2.19	2.0%
blister8	2.25	2.15	2.18	2.19	2.3%
blister9	2.13	2.02	2.18	2.11	3.9%
blister10	2.03	1.79	1.94	1.92	6.3%
blister11	2.08	1.9	1.91	1.96	5.2%
blister12	1.88	1.87	1.8	1.85	2.4%
blister13	1.91	2.05	1.87	1.94	4.9%
blister14	2.22	2.22	2.11	2.18	2.9%
Avg	2.12	2.03	2.02		
RSD	6.5%	8.1%	7.6%		

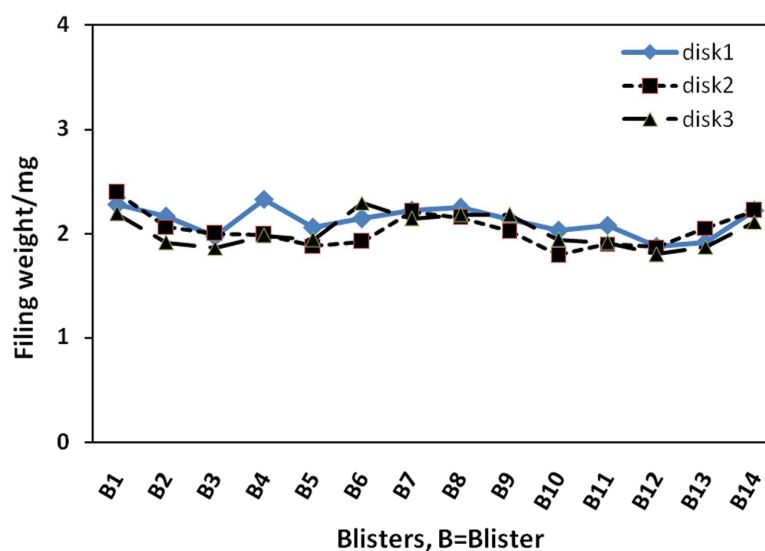


**Figure 6.9: The final filling weight uniformity of blisters in Trial B-4**

### 6.2.3 Drug content uniformity among different disks

After powder filling, the drug content of single disk was measured In Trial C-1 by rinsing the powder of all blisters into a certain volume of solvent first, and then analyzed by HPLC. The uniformity was evaluated by the RSD of drug content. Disk1, Disk5, Disk10, Disk15, Disk20 and Disk25 were sampled from a series of disks. The powder was prepared by 0.74% sulfate Salbutamol, 10% fine lactose as additives and ~90% Inhalac 230.

The result is shown in Table 6.9 and Fig.6.10. As we can see in Table 6.9, the RSD of filling weight is quite small but the RSD of drug content and percentage of API per disk are obviously larger. This table clearly shows that the drug content uniformity is worse than weight uniformity.

**Table 6.9: The drug content uniformity among disks in Trial C-1**

Disk No	Filling weight (mg)	Drug content (ug)	API percentage%
disk1	28.7	251.2	0.88%
disk5	29	220.9	0.76%
disk10	29.1	200.7	0.69%
disk15	28	195.6	0.70%
disk20	29	199.0	0.69%
disk25	29.2	226.0	0.77%
AVG	28.8	215.6	0.75%
RSD	1.5%	6.69%	9.79%

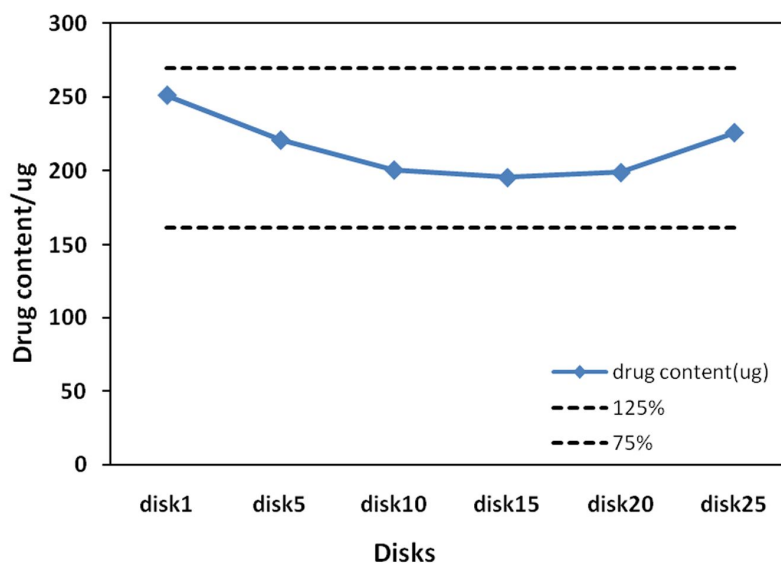


**Figure 6.10: The filling drug content uniformity among disks in Trial C-1**

To investigate the reasons for the high RSD of drug content, two experiments were carried out. First, the filling weight of Disk 1-25 was measured to ascertain the weight variation was the cause of content deviation or not. The results are shown in Fig.6.11. The filling weight of those 25 disks is rather uniform with an RSD at 1.85%, which excludes the possibility that the drug content variation is caused by filling weight. Second, the uniformity of the bulk powder blend was evaluated by analyzing 8 random samples. The results are shown in Table 6.10. The RSD of 1.77% demonstrate that the bulk blend is quite uniform, implying that variation of drug content per disk is not resulted from heterogeneous bulk blend.

**Table 6.10: The blend content uniformity of the tested powder in Trial C-1**

	API percentage	AVG%	RSD%
Blend 1	0.73%	0.74%	1.77%
Blend 2	0.72%		
Blend 3	0.76%		
Blend 4	0.74%		
Blend 5	0.74%		
Blend 6	0.74%		
Blend 7	0.75%		
Blend 8	0.74%		

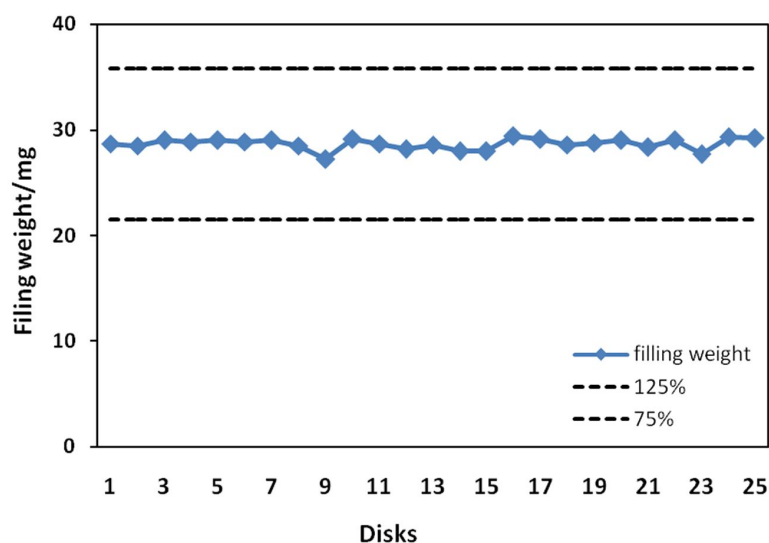


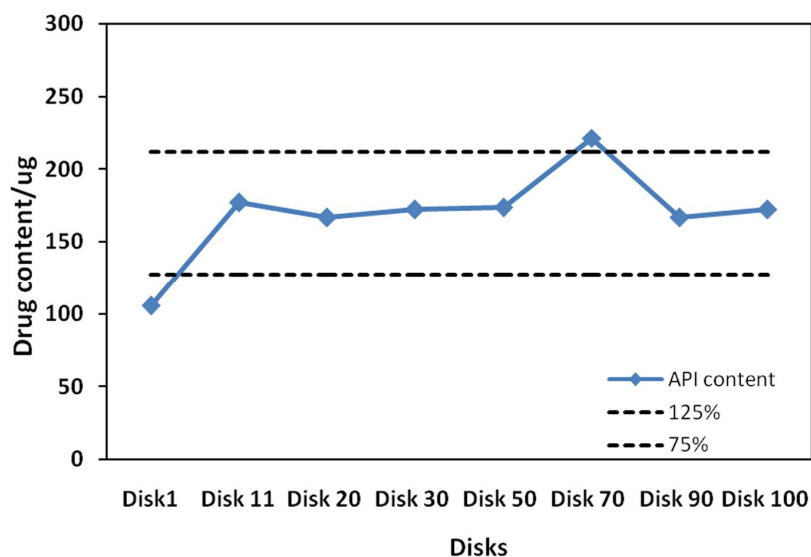
**Figure 6.11: The filling weight uniformity of the disks for content uniformity evaluation in Trial C-1.**

In Trial C-2, 100 disks are analyzed and the uniformity is evaluated every 10 disks, the uniformity declined as shown in Table 6.11. Compared with the drug content uniformity for 25 disks, the uniformity of API content exhibits a disappointing drop from an RSD of 6.7% to 18%. As shown in Fig.6.12, two content points are even outside the  $\pm 25\%$  of the average. Similarly, the percentage of API also shows a strange variation with an RSD of 17%. Nevertheless, if disregarding the first point, then the RSD of drug content uniformity would reach about 10%. This result suggests us to give up several disks at the beginning of the filling process, because the filling device may not achieve a stable working state immediately at the beginning.



**Table 6.11: The drug content uniformity for 100 disks in Trial C-2**

Disk No	Filling weight (mg)	API content ( $\mu\text{g}$ )	API percentage%
Disk1	25.8	105.61	0.41%
Disk 11	29	177.15	0.61%
Disk 20	27.7	166.93	0.60%
Disk 30	27.3	172.04	0.63%
Disk 50	27.1	173.75	0.64%
Disk 70	27.7	221.44	0.80%
Disk 90	27.2	166.93	0.61%
Disk 100	27.7	172.04	0.62%
AVG	27.4	169.5	0.62%
RSD	3.2%	18.5%	17.1%

**Figure 6.12: The drug content uniformity between 100 disks in Trial C-2**

Similarly, the reason for the less satisfactory uniformity is also investigated in two aspects. The filling weight uniformity of disks is shown in Fig.6.5 and Table 6.3. The result demonstrates an excellent uniformity of filling weight with an RSD smaller than 3%. Therefore, this result excludes the possibility that variation of filling weight results in the large RSD of drug content. The blend content uniformity is presented in Table 6.12. It also shows a good uniformity of the bulk powder blend, implying that the

unsatisfactory drug content uniformity among disks is not caused by heterogeneity of this blend.

**Table 6.12: The blend content uniformity of the tested powder in Trial C-2**

	Drug percentage%	AVG	RSD%
Blend 1	0.71	0.69%	1.19
Blend 2	0.7		
Blend 3	0.69		
Blend 4	0.69		
Blend 5	0.7		
Blend 6	0.69		
Blend 7	0.7		
Blend 8	0.68		

Finally, the measurement method of drug content uniformity was determined in Trial C-3 as follows: After filling powder, a drug disk was sealed with aluminum foil. Then all blisters on this disk were opened carefully without foil loss, and the powder was rinsed into waters of designated volume. After complete drug dissolution, the solution was analyzed by HPLC to obtain the drug concentration. Similar as mentioned above, 4 kinds of powder containing 0%, 5%, 10%, 20% fine lactose and corresponding Inhalac 230 were prepared and 50 disks were filled with those powders.

The result is shown in Table 6.13. The drug content uniformity among disks is improved significantly, since all RSD values of drug content for 4 powder compositions are near or smaller than 5%. With increasing fine lactose, the drug content also shows an obviously ascending trend as Fig.6.13. The growth of drug content per disk is directly attributed to an increase of filling weight per disk. As shown in Fig.6.14, the coefficient of regression between drug content and powder weight is close to 0.95, indicating a strong linear relation.

**Table 6.13: The drug content per disk for different powders in Trial C-3**

		0%-fines	5%-fines	10%-fines	20%-fines
Drug content per disk (n=6)	AVG ( $\mu\text{g}$ )	139.3	175.1	194.7	200.6
	RSD	5.66%	2.74%	3.54%	2.87%

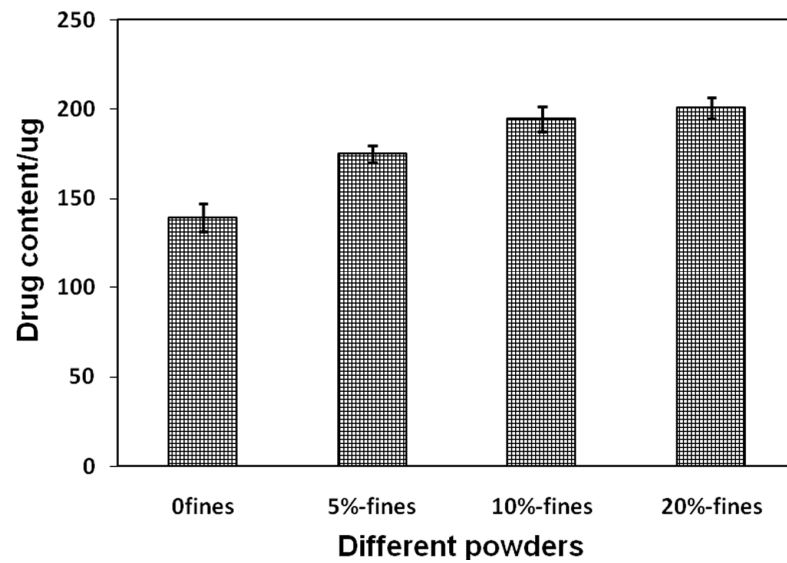


**Figure 6.13: The drug content per disk (n=6) for different powders in Trial C-3**

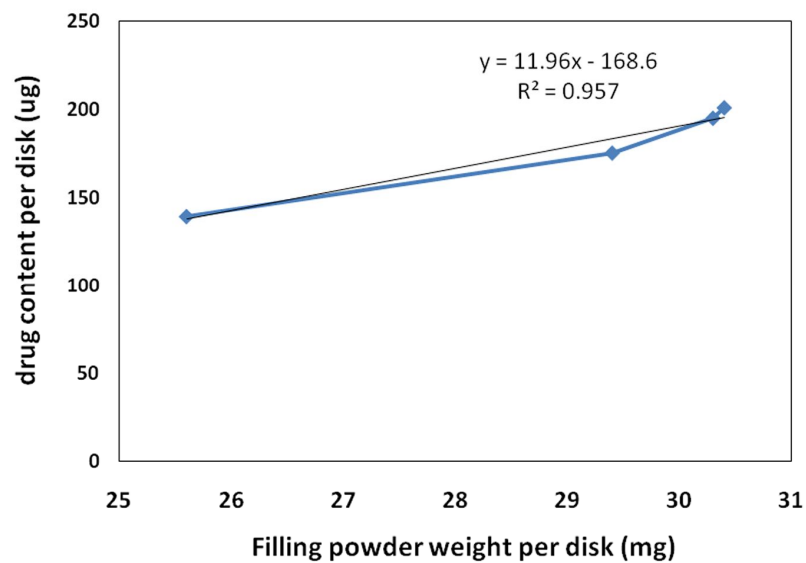


**Figure 6.14: The linear relationship between drug content and filling powder weight per disk in Trial C-3**

#### 6.2.4 Drug content uniformity among blisters on one disk

After evaluating uniformity for filling weight per disk, filling weight per blister, drug content per disk as discussed above, the uniformity work is then focused on the core part and the most difficult one — the uniformity of drug content among blisters.

In Trial D-1, a drug disk was sealed with aluminum foil after powder filling. Each blister was cut off from the disk and weighed separately. Next, each blister was opened carefully without foil loss, and the powder was rinsed into water of a designated volume. Then the solution was analyzed by HPLC to get the drug concentration, and the drug content for each blister was calculated from concentration and the solvent volume. At first, the powder containing 10% fine lactose and 90% Inhalac230 was prepared and applied for this uniformity test. 6 blisters were taken from each disk randomly, and 3 disks were analyzed.

The result of Trial D-1 is shown in Table.6.14. The RSD of drug content in blisters is from 14.1% to 17.7%. Meanwhile, the total RSD for all 18 blisters is 15%, but the RSD of filling weight between blisters is only 4.63%. It is noteworthy that the number of blister here is not related to the sequence in the disk but a random order.

**Table 6.14: The drug content uniformity among blisters**

	disk1	disk2	disk3
blister1	11.1	15.3	16.2
blister2	16.1	15.4	15.8
blister3	16.4	15.1	10.6
blister4	13.8	11.7	15.0
blister5	15.9	17.4	11.0
blister6	16.2	11.6	14.7
AVG	14.9	14.4	13.9
RSD	14.1%	15.8%	17.7%

Then, in Trial D-2, powders with different ratios of fine lactose were tested to investigate the influence of powder composition on drug content uniformity among blisters. 6 blisters were taken from one disk randomly, and 3 disks were analyzed for each powder.

The result is summarized in Table 6.15 and Fig.6.15. The RSD of drug content among blisters for all powders are above 10%, and the 10%-fines shows the worst uniformity.

**Table 6.15: The drug content uniformity among blisters for different powders in Trial D-2**

		0%-fines	5%-fines	10%-fines	20%-fines
Drug content per blister (n=18)	AVG (ug)	9.84	12.54	13.17	14.29
	RSD%	10.07	12.48	17.48	14.83

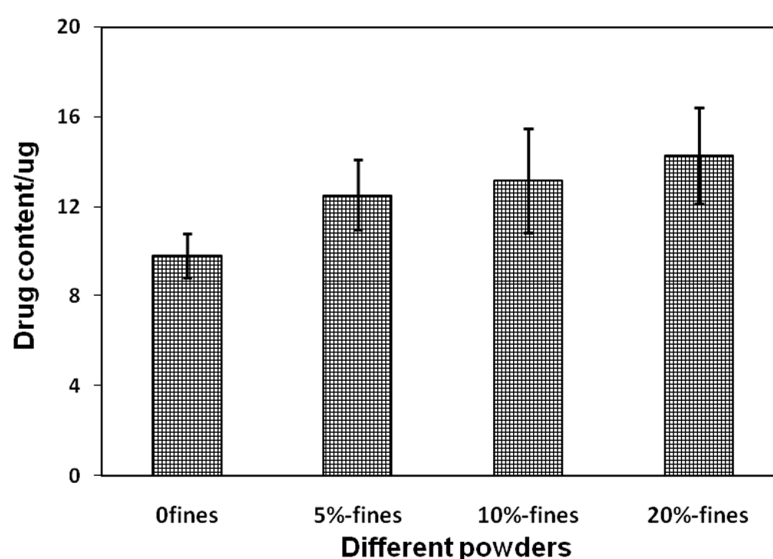


**Figure 6.15: The drug content per blisters (6 random blisters from each of the 3 disks) for different powders in Trial D-2.**

If the drug content per blister for the 4 powders is investigated in detail, the results are shown in Fig.6.16 and Fig.6.17. As we can see from these two figures, the drug content per blister for 0%- and 5%-fines powder are in the range of average $\pm$ 25%. The 0%-fines powder shows a smaller RSD than 5%-fines as Table.6.15, but it has two points on the upper and lower boundary. Consequently, the 5%-fines is better than 0%-fines. As presented in Fig.6.17, the 10%-fines shows the most obvious variance with several points on or even outside the boundary. The 20%-fines powder has fewer points on the boundary than 10%-fines. From these results, it is inferred that the powder property would have an influence on the drug content uniformity among blisters.

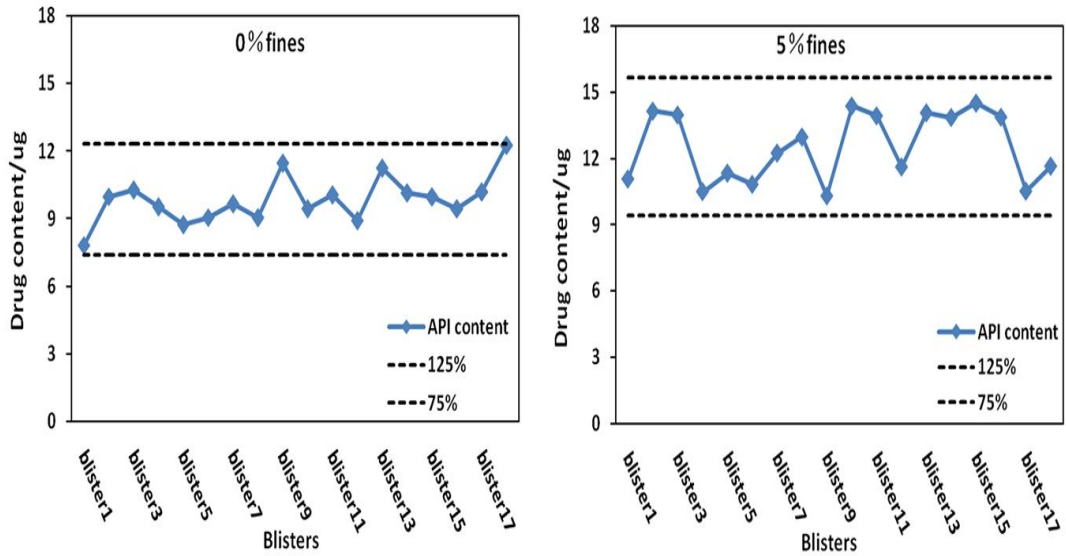


**Figure 6.16: The drug content per blister (6 random blisters from each of the 3 disks) for 0%-fines and 5%-fines powder in Trial D-2**

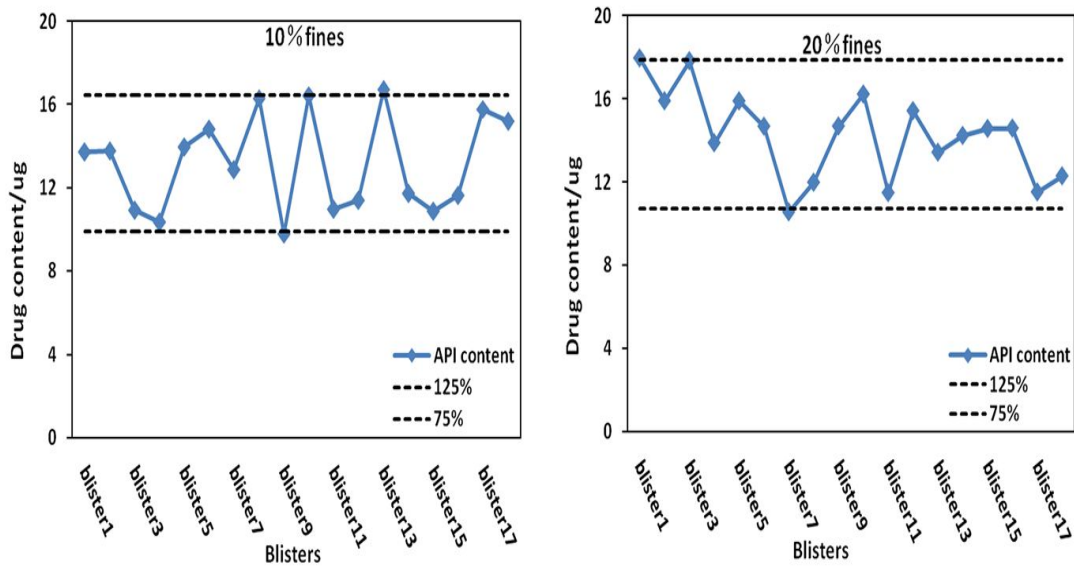


**Figure 6.17: The drug content per blister (6 random blisters from each of the 3 disks) for 10%-fines and 20%-fines powder in Trial D-2**

The emitted dose from Inhaler-WU2011 is studied for the delivered drug content uniformity (DDCU) for those 4 powders.

When comparing RSD of emitted dose with corresponding RSD of drug content among blisters, the RSD of emitted dose increases by 1~2% except for 0%-fines powder. This result means that the variance of delivered drug content is mainly due to the nonhomogeneity in filling process and the inhaler does not greatly increase this variance.

According to US or European pharmacopeias, it is usually required that the drug content of at least 9 of 10 doses collected from one inhaler should be within 75%- 125% of the target-delivered dose. Therefore, according to the results presented in Fig.6.18 and Fig.6.19, we might conclude that the 0%-fines and 10%-fines powder are very likely to fail because 1 of 6 doses is outside the acceptable range and several points approach the boundaries. Meanwhile, 5% and 20%-fines powder are a little better, because there are only several points approaching the limits and no point outside of the range.

**Table 6.16: The delivered drug content uniformity for different powders**

		0%-fines	5%-fines	10%-fines	20%-fines
Delivered drug content per blister (n=6)	AVG (ug)	7.25	10.23	12.01	10.02
	RSD %	17.02	14.76	18.85	15.92

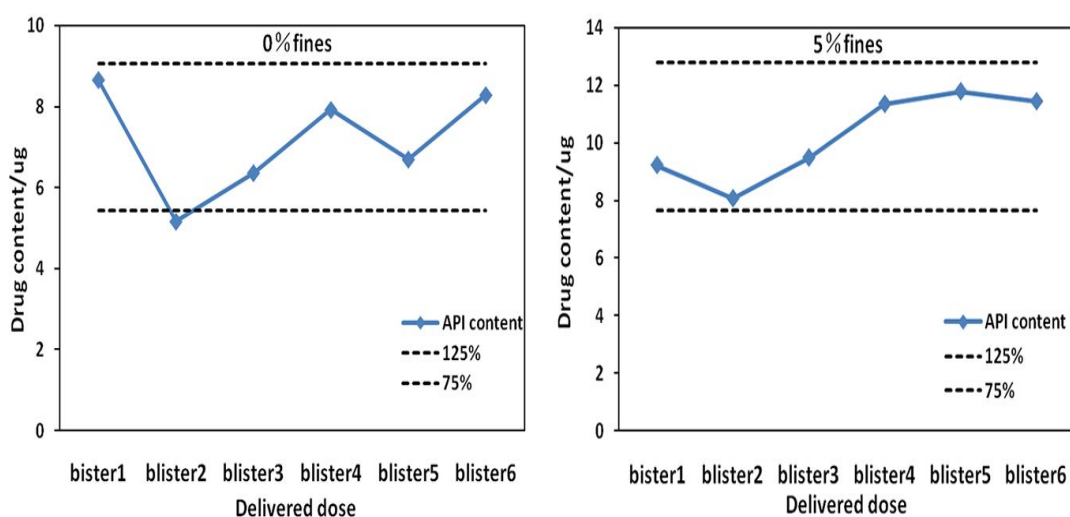


**Figure 6.18: The delivered drug content uniformity for 0%-fines and 5%-fines powder**

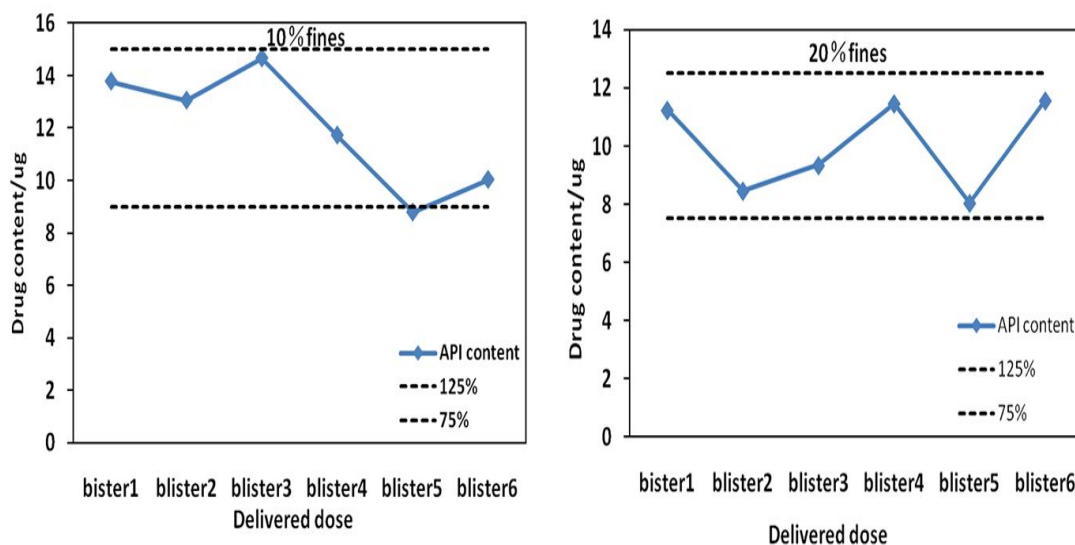


**Figure 6.19: The delivered drug content uniformity for 10%-fines and 20%-fines powder**

In order to further investigate the reason for less satisfactory uniformity among blisters, an experiment (Trial D-3) was carried out as follows: After powder filling and sealing, each blister was numbered according to their position and the number was fixed sequentially for corresponding position. Similarly, the drug content was acquired by rinsing and HPLC analysis. At the same time, the filling powder weight of corresponding blisters was obtained and recorded. And the API percentage of each blister was also calculated from the API content and powder weight. The powder comprised of 0.79% sulfate Salbutamol, 10% fine lactose plus ~90% Inhalac 230 was used in this experiment. And 42 blisters from 3 disks were analyzed.

As shown in Fig.6.20, the first blister usually has more drug content than other blisters and Blister 10-13 experience a strange and sudden drop. Then the filling weight for those blisters is studied to find out the reason for the sudden content drop. The filling weight for those blisters is presented in Fig.6.21. As we can see in Fig.6.9, no obvious drop of filling weight happens for Blister 10-13. This result indicates the abrupt decline of drug content is not due to filling weight change. Following that, the drug percentage of each blister is calculated and presented in Fig.6.21, which also shows a drop for Blister 10-13.



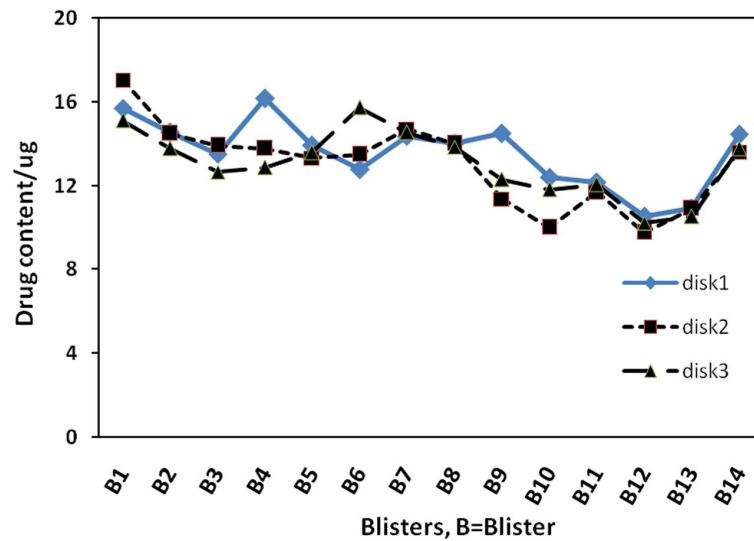


**Figure 6.20: The drug content for the sequentially numbered blisters in each of the 3 disks of Trial D-3.**

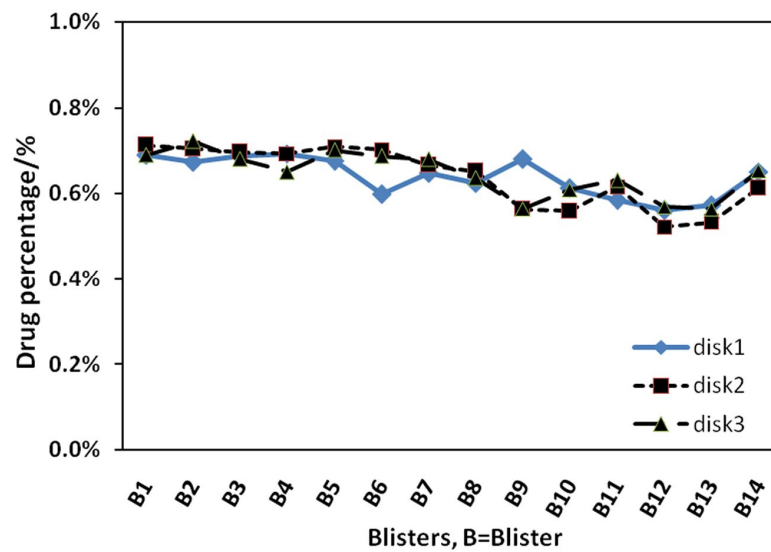


**Figure 6.21: The drug percentage for the sequentially numbered blisters in each of the 3 disks of Trial D-3.**

Then a picture of filling powder is taken to study the reason for the abrupt drop of drug content and percentage, as shown in Fig.6.22. As we can see from Fig.6.22, the powders corresponding to Blister 1-8 and 14 form a cone on the paper, but the powders from

Blister 9-13 are dispersive, especially for Blister 10-12. This phenomenon might explain the drop of drug content and percentage for those blisters. Because the powders from Blister 10-12 are rather dispersive, the fine API particles are much easier to fly away and result in a lower content. More discussion is presented in Section 6.3.2 and Section 6.3.3.

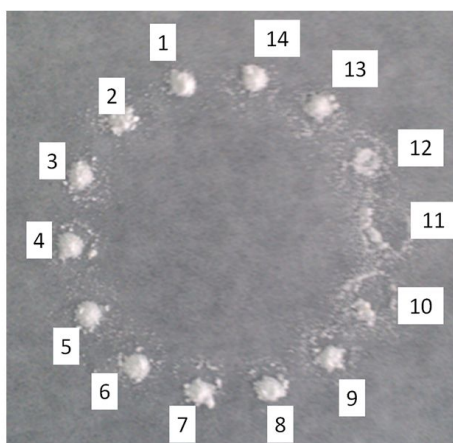


**Figure 6.22: The picture of the filled powder for each blister**

### 6.2.5 Drug content uniformity of blend during filling process

During the filling process, it is necessary to keep the bulk blend in the powder chamber uniform. Because of mechanical stirring or other operation, the powder blend may experience stratification to form an inhomogeneous blend. Hence, the blend content uniformity was validated by taking samples from the top, middle and bottom of the powder chamber for HPLC analysis when 10, 30 and 50 disks were filled.

The result is shown in Table 6.17. The columns represent the sample from different positions but the same time point, and the rows stand for the samples from various time points. As we can see, the uniformity of drug percentage is quite stable for different time points. The uniformity in terms of sampling position is also rather stable. To sum up, the uniformity in the filling process does not change. It is helpful to acquire a drug content uniformity among disks and blisters.

**Table 6.17: The blend content uniformity during filling process**

API percentage	After 10disks	After 30disks	After 50disks	AVG	RSD
Top	0.58%	0.59%	0.60%	0.59%	1.69%
Middle-1	0.60%	0.59%	0.58%	0.59%	3.03%
Middle-2	0.62%	0.58%	0.57%		
Bottom-1	0.60%	0.60%	0.57%	0.59%	2.81%
Bottom-2	0.57%	0.57%	0.60%		
AVG	0.59%	0.59%	0.58%		
RSD	3.3%	1.9%	2.6%		

## 6.3 Optimization of Dry Powder Filling process

### 6.3.1 Minimization of electrostatic charge

The quantity of electricity on a PVC disk is determined by a Faraday pail. After treatment of a PVC disk with an anti-static fan, the quantity of static electricity decreases from -20nc to -0.4nc. Meanwhile, the charge-mass ratio is 0.4~0.8nc/g for powders, which is rather small for several milligrams of powder.

A comparison of filling using antistatic and normal PVC is presented in Fig.6.23. The result clearly shows the necessity to minimize static electricity before filling. A careful observation on the particles dispersing on the disk surface reveals that all particles first fall into the blisters but then “jump out” if the disks are not treated by the antistatic fan. As we can see from the picture, the elimination of electrostatic charge significantly reduce the particles outside of the blisters. It is helpful to improve the drug content uniformity among blisters, since small particles like drug particles are more likely to “jump out” the blisters. Consequently, all PVC disks are treated by the antistatic fan for 10min before powder filling.

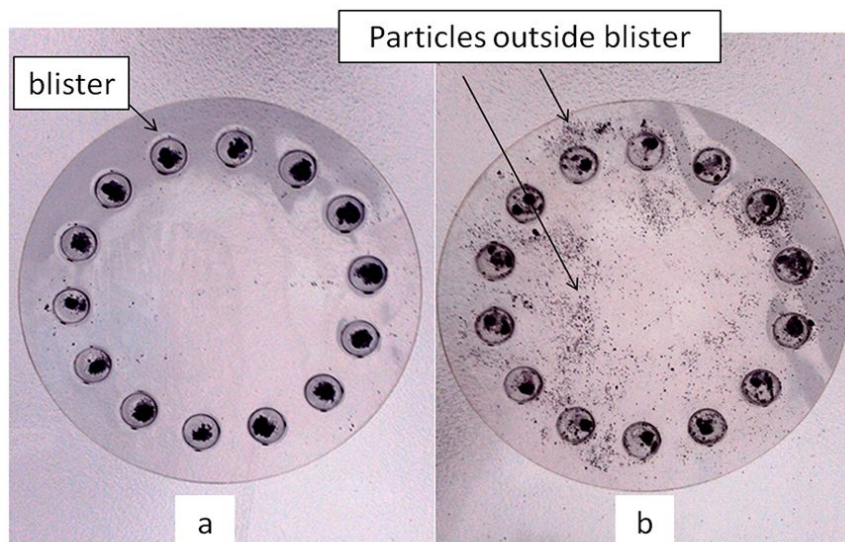


**Figure 6.23: The comparison of filling disks with (a) or without antistatic treatment (b)**

The electrostatic charge not only influences the powder filling, but also affects the drug delivery performance, although this effect was much smaller. The TI (Twin impinger) tests are carried out by using disks with/without an antistatic process. The result is shown in Fig.6.24. Although the FPF (fine particle fraction) values are the same for normal and antistatic disks, the blister remains result shows difference. The higher blister remains of the untreated disks represents more API particles left in the blisters. The phenomenon can be explained by that when particles are delivered out from the inhaler, its aerosol performance would not be influenced by the electrical property of the package. However, the PVC package with a high electrostatic charge would increase the adhesion force between particles and package. Hence, the fraction of the API left in blister goes up. Generally, the higher blister remains result than other results in this chapter is caused by lower flow rate (30LPM) used here.

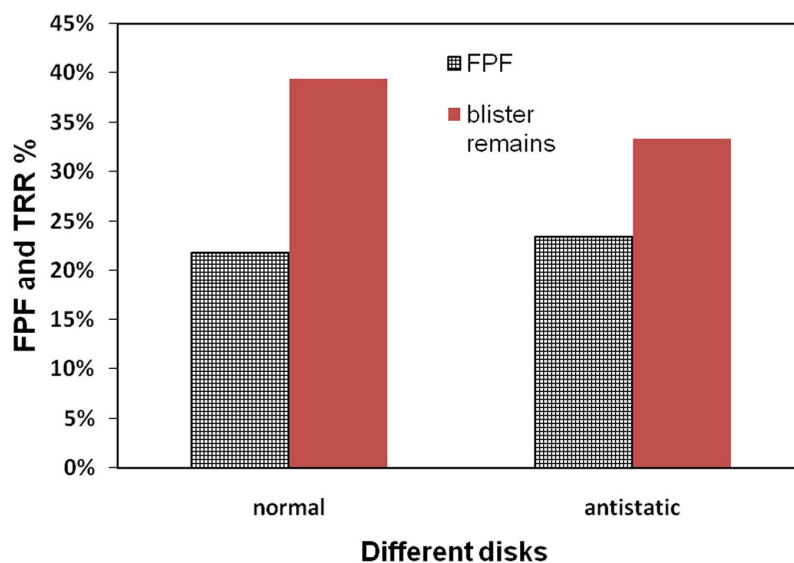


**Figure 6.24: The influence of electrostatic charge on the TI performance of the inhaler**

### 6.3.2 The role of vacuum in the powder filling

As described in Section 3.4.2, vacuum can be applied to help powder flow into the metering pockets. Consequently, vacuum was applied to study its influence on filling results. During the mechanical stirring, a vacuum pump was turned on to form a negative pressure through a tube under the powder chamber. The powder would flow into the metering pockets as a result of stirring and negative pressure. After that, the vacuum was turned off and the metering plate slid out to transfer the powder to drug disks. The flow rate of vacuum pump was set to 30 LPM.

The result of drug content uniformity among blisters is presented in Fig.6.25. As we can see, the fluctuation of drug content among blisters is similar to the results of no vacuum. Especially for the Blister 1 and Blister 14, the drug content is higher than the average level. The good news is that the drug content drop of Blister 10-12 seems not to be as obvious as filling without vacuum. The drug percentage result is shown in Fig.6.26. Similarly, the drop of API percentage for Blister 10-12 is also reduced.

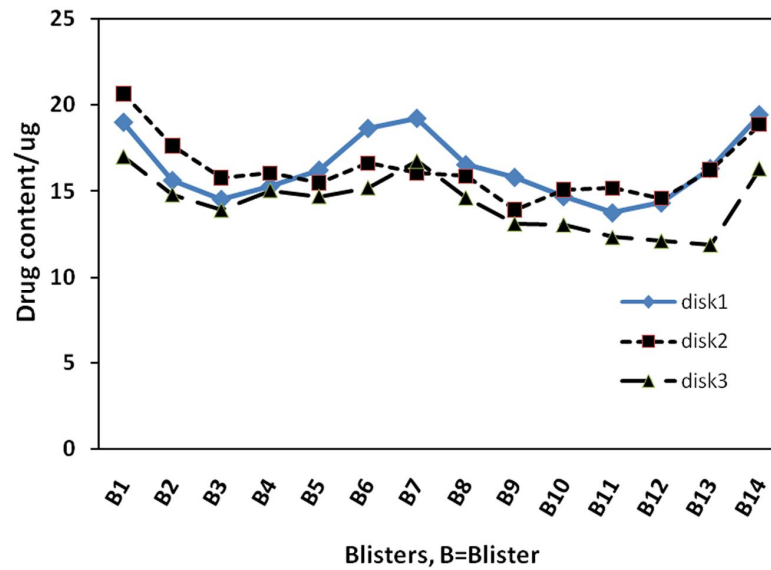


**Figure 6.25: The drug content per blister by filling with vacuum**

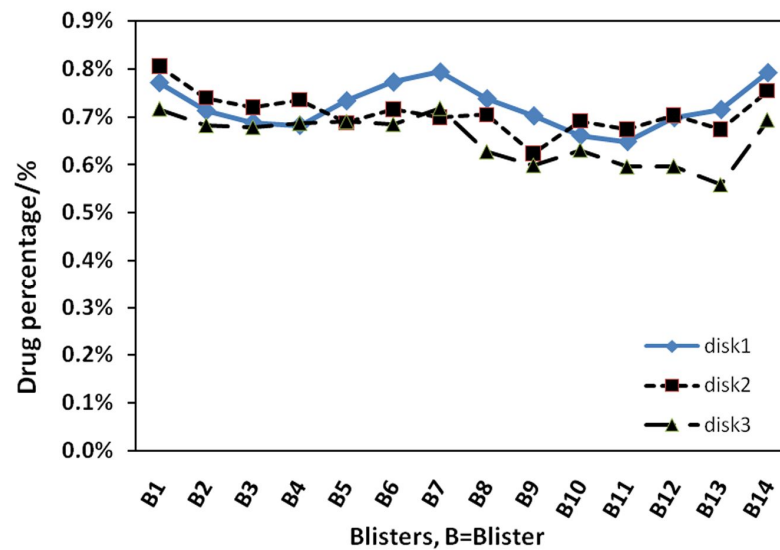


**Figure 6.26: The drug percentage per blister by filling with vacuum**

A picture of filling powder is compared with the filling without vacuum. As we can see in Fig.6.27, the dispersive state of powder in Blister10-12 does not show any obvious improvement.

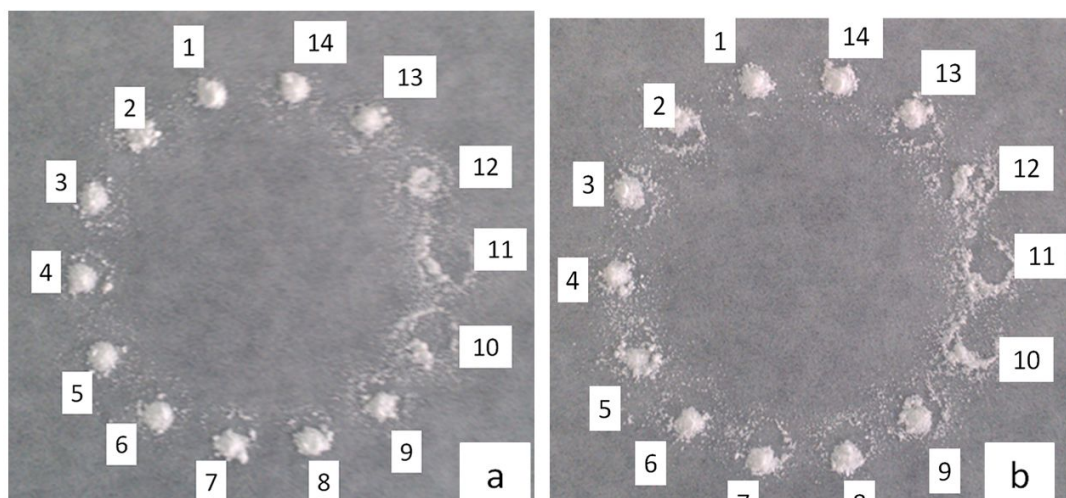


**Figure 6.27: The comparison of filling powder with (a) without vacuum and (b) with vacuum**

Table 6.18 is a summary of comparison between filling with and without vacuum. All uniformity results, including filling weight, drug content and drug percentage are improved when compared with filling without vacuum. The higher filling weight implies that the powders in the metering pockets become tighter as a result of negative pressure. Therefore, the possibility of fine particles flying out decrease, and the loss of fine particles during the powder transfer from metering pockets to blisters decline.

**Table 6.18: The summary of the comparison results for filling with or without vacuum**

		Filling weight (mg)			Drug content (ug)			Drug percentage (%)		
		disk1	disk2	disk3	disk1	disk2	disk3	disk1	disk2	disk3
Without vacuum	AVG	2.12	2.03	2.02	13.57	13.01	13.06	0.64	0.64	0.65
	RSD%	6.50	8.09	7.65	12.06	15.48	12.21	7.29	10.98	8.13
With vacuum	AVG	2.26	2.29	2.19	16.37	16.27	14.33	0.72	0.71	0.65
	RSD%	5.76	5.83	5.37	11.85	10.78	11.68	6.50	6.06	7.86

The application of vacuum in the powder filling also affects the FPF performance of the Inhaler-WU2011. The drug disks filled with/without vacuum are tested by the TI (Twin Impinger) impaction and the results are shown in Fig.6.28 and Table 6.19. As we can see in Table 6.19, the FPF of filling with the vacuum is slightly lower than filling without

vacuum. It is easy to understand that the particles filled with vacuum would become more compact and therefore somewhat more difficult to disperse during aerosolization.

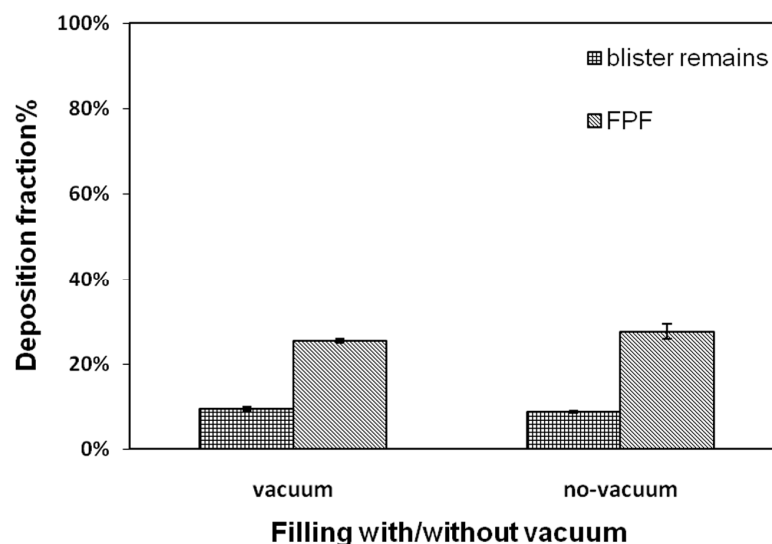


**Figure 6.28: The FPF and blister remains of filling powder with or without vacuum.**

**Table 6.19: The FPF and blister remains results of filling powder with or without vacuum.**

	Vacuum	No-vacuum
FPF-AVG	25.4%	27.6%
SD	0.4%	1.7%
Remains-AVG	9.5%	8.8%
SD	0.6%	0.2%

### 6.3.3 The role of reducing vibration intensity in the powder filling

The research results reported above demonstrate that the drug content uniformity is related to the powder dispersion or flight during the filling process. Therefore, it is a reasonable assumption that reducing the undesired dispersion would improve drug uniformity. For example, increasing the tightness of powder in metering pockets has been proven useful. Hence, a reduction of vibration intensity during the powder transfer is also applied to verify this assumption.



The filling powders with reduced vibration intensity are shown in Fig.6.29. A great improvement in the powder dispersion of Blister 10-12 is observed, since powder from each metering pocket form a cone rather than a dispersed state.

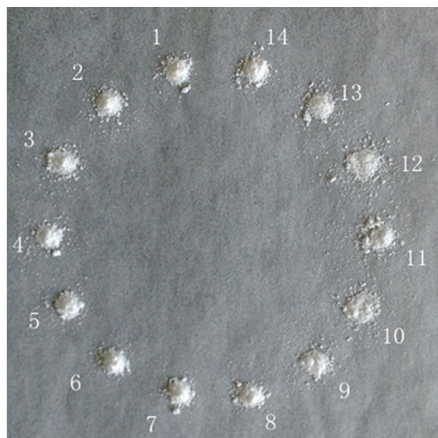


**Figure 6.29: The picture of the filling powder for each blister with reduced vibration intensity**

The results of drug content uniformity and drug percentage are shown in Fig.6.30 and Fig.6.31 respectively. As we can see, although the drug content and percentage of Blister 10, 12 are still a little lower than other blisters, the gap is reduced.

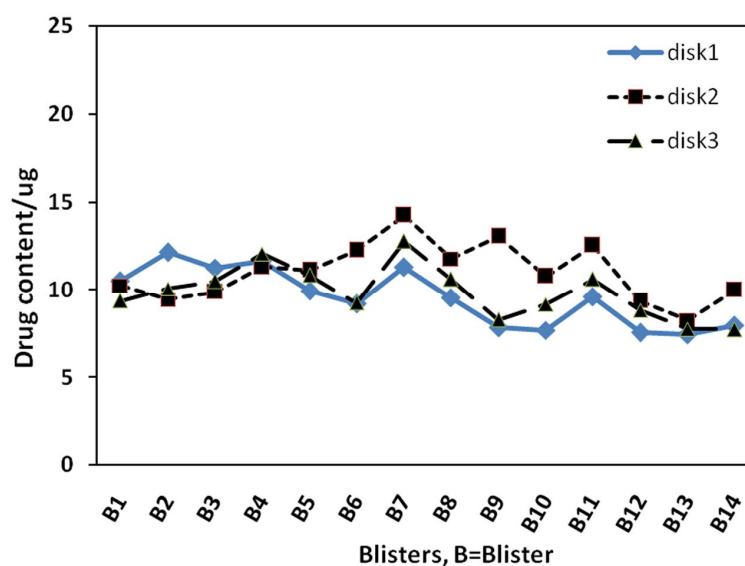


**Figure 6.30: The drug content per blister of filling with reduced vibration intensity**

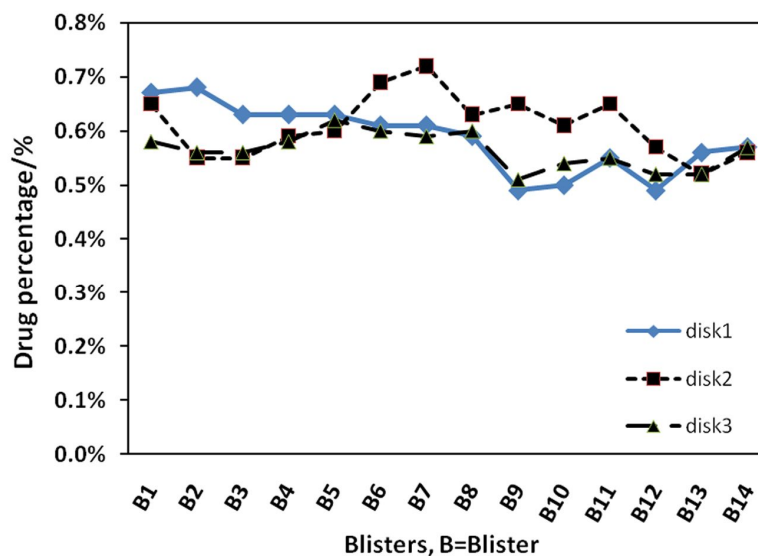


**Figure 6.31: The drug percentage per blister of filling with reduced vibration intensity**

The RSD of filling with normal vibration and the reduced vibration are compared and the results are presented in Table 6.20. As we can see, the RSD of filling weight, drug content and percentage per blister for filling with the reduced vibration are much higher than normal filling. The results indicate the uniformity become even worse, although the abrupt drop of drug content and percentage for Blister 10-12 is improved. Hence, the powder filling is carried out by normal vibration rather than the reduced vibration in the following formulation research.

**Table 6.20: The summary of RSD results for filling with normal or reduced vibration**

		Filling weight per blister(mg)			Drug content per blister (ug)			Drug percentage (%)		
		disk1	disk2	disk3	disk1	disk2	disk3	disk1	disk2	disk3
Normal vibration	RSD %	5.8	5.8	5.4	11.9	10.8	11.7	6.5	6.1	7.9
Reduced vibration	RSD %	10.1	8.0	12.8	17.5	15.0	15.3	10.6	9.6	6.1

### 6.3.4 The flowability range suitable for the powder filling

In the filling experiment, the flowability of powder is important to the powder filling and has to be within a certain range. Specifically, if the flowability is so good, the powder in the metering pockets might fall out easily during the sliding of metering plate. On the contrary, if the flowability is too bad to flow into the metering pockets, it may result in poor uniformity. Meanwhile, the powder might be too cohesive to fall from metering pockets into the blisters by a normal vibration. If a stronger vibration is applied, the particle dispersion and flying away might be more serious. Consequently, a series of blends with different flowability (shown in Table 6.21) are prepared and filled by the filling machine. Then the upper and lower limit of flowability suitable for filling are established.

**Table 6.21: The composition and flowability of Blends for filling tests**

samples	composition	Compression index
Blend-1	0.72%API+LH200(<45 $\mu$ m)+30% fine lactose	49.07%
Blend-2	0.72%API+Inhalac230(<45 $\mu$ m)	44.33%
Blend-3	0.72%API+Inhalac230(45-75 $\mu$ m)	22.06%
Blend-4	0.72%API+Inhalac230(75-100 $\mu$ m)	19.23%
Blend-5	0.72%API+Inhalac230(100-150 $\mu$ m)	18.28%

Based on a careful observation on the filling process, the Blend-1 is difficult to fall into blisters in a drug disk and Blend-4 tends to fall out prematurely during the sliding of the metering plate. Therefore, an approximate flowability range suitable for filling might be 20% to 45% (presented as Compression index).

## 6.4 Discussion

An accurate and reproducible powder filling is a prerequisite for formulation research. Therefore, a powder filling system and uniformity evaluating method are established and developed step by step. The principle of filling is volumetric metering, which is faster than metering by weight. There is no direct displaying of filling weight or automatic feedback system to control filling quantity and the micro-dose filling is a big challenge

for pharmaceutical industry. Consequently, the accuracy and precision of this new filling system require to be validated.

There is an inherent logic in the evaluation of filling uniformity where each step is the prerequisite for the next. Thereby, the uniformity test is carried out by the following sequence: 1) filling weight per disk, 2) filling weight per blister, 3) drug content per disk and 4) drug content per blister. The most important uniformity is the last one, drug content uniformity among blisters which is directly related to treatment effect for the patients. The other three kinds of uniformity not only serve to ensure the last uniformity, but also provide an insight for good or poor drug uniformity among blisters. As these results demonstrate, although the drug content per blister is not very uniform, the possible reasons such as variances of filling weight and blend content are excluded. Theoretically, the drug content per blister should be calculated as

$$\text{Drug content per blister} = \text{Filling weight per blister} * \text{Drug percentage}$$

According to an error calculation method, the relative error of drug content can be

$$\text{calculated as, } E_{\text{drug-content}}^2 = E_{\text{filling-weight}}^2 + E_{\text{percentage}}^2$$

The E stands for relative Error which is represented by the RSD. The results show that the RSD of drug content per blister is higher than a theoretical calculation from the above equation. Consequently, it is inferred that other unknown factors would greatly affect the drug content per blister. The most likely reason is later inferred as a dispersion or flying away during the powder falling out from the metering pockets.

The filling weight uniformity can serve as an intermediate quality control, since the analysis of drug content is rather complicated. This result suggests us to carry out much easier and convenient filling weight tests first. In the section 6.2.1 and 6.2.2, the filling and test methods are modified gradually to the final version. There are many improvements during the method development, and the elimination of electrostatic charge is an impressive one. The electrostatic charge would result in the powder “jumping out” the blisters or flying away. Even worse, it may cause instability of the

weighing balances. The weight of an empty PVC disk is tested by two balances (AB135-S and AL104).

The results are shown in Table 6.22. As we can see, a SD value of about 4mg seems to be rather small to the weight of a disk. Yet, the 4mg of SD value can not be neglected when we calculate a filling weight, because the filling weight is 20-30mg per disk and 2-3mg per blister. At first, we acquire the filling weight by subtracting an empty disk from a filled disk. But this result fluctuates randomly as a result of balance instability. Consequently, this easy method is discarded but a complex test procedure is set up which includes sealing the disks with aluminum foil before the following operations. The sealing of aluminum foil not only protects powder from dispersing, but also stabilizes the weight reading on a balance.

**Table 6.22: The weight variance of a PVC disk**

	AB135-S	AVG (g)	SD (g)
1	2.99796	3.0020	0.0041
2	3.00184		
3	3.00612		
	AL104	AVG (g)	SD (g)
1	2.9790	2.9824	0.0041
2	2.9811		
3	2.9870		

The antistatic fan whose principle is shown in Fig.6.32, is used to reduce the electrostatic effect during filling process. The experiment result shows that the antistatic treatment is important for the filling uniformity as Fig.6.23. The particles deposit on the surface rather than in blisters may influence the sealing effect. The bumps as a result of particles on the surface would provide passage for air and moisture. The electrostatic measurement shows that the charge of powder is much smaller than the charge of PVC disk. It also explains why the particle-PVC interaction is more significant than particle-particle in the TI (Twin Impinger) test. Commonly, there are several methods to control the electrostatic charge of powder. The first one and most effective one is to increase environment humidity, but it is not suitable for DPIs since moisture may bring about stability problems. The second one is to keep the powder still for some time and allow electrostatic charge to dissipate.

Other methods such as additives would not be considered because of safety concern. Consequently, it is very essential to eliminate the electrostatic charge of PVC disks as much as possible. Besides, it is recommended to monitor the environment humidity for each experiment and allow the freshly prepared powder to rest for some time.

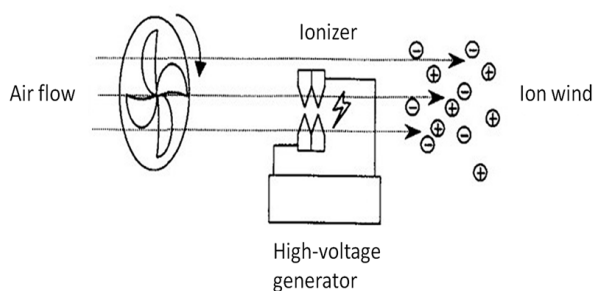


**Figure 6.32: The schematic of principle of an antistatic fan**

Although the uniformity of drug content per blister does not achieve our target value as  $RSD < 5\%$ , some useful information is obtained from the optimization research. When applying a vacuum in the filling process, the filling uniformity is improved. This result can be explained by that powders in the metering pockets become tighter. The tight state keeps fine particles from “jumping out” blisters or flying away during the transfer from metering pockets to blisters. The tight extent of powder in the metering pockets has to be within a reasonable range. When the powder is too tight to fall out, a more intensive vibration is required for the powder transfer. The intensive vibration may result in undesirable dispersion of fine particles during transfer and worse uniformity.

Research result also shows that when reducing the vibration intensity, the shape of filling powder become better than before. It is inferred that the undesired dispersion during powder transfer is reduced. Unfortunately, the uniformity of drug content among blisters and other uniformity results become worse when decreasing the vibration intensity. This result might be explained by that the less intensive vibration cause adherence of powder to metering pockets.

When considering the drug content uniformity, all delivered drug content should be within the range of average  $\pm 25\%$  according to US or European pharmacopoeia. This requirement seems to be satisfied by the results of this chapter. However, this criterion is rather lax since it takes account of possible changes during stability tests or shelf-life. Usually, when a commercial inhaler is produced, its release criterion or internal control in the manufacturer is more stringent than the pharmacopoeia requirements. Consequently, it is difficult to conclude that our filling uniformity is acceptable or not. Even though the drug content uniformity between blisters still needs to be improved, it would not affect the following formulation work at all. The following evaluation of formulations utilizes one disk as a whole to analyze the *in vitro* performance. The results of this chapter show that the drug content uniformity among disks is excellent; hence the formulation work would not be affected. The filling research has validated the content uniformity among disks, which is a solid basis for the following formulation work.

As a conclusion, this chapter provides an effective powder filling system for development of Inhaler-WU2011 and its primary function are validated.

## Chapter 7

### 7 Research on the formulation for Dry Powder Inhaler

#### 7.1 Brief Introduction

The outline of the formulation study is shown in Fig. 7.1. First of all, the compatibility between the API (active pharmaceutical ingredient) and micronization, the API and excipient, formulation and package material is investigated. Then the micronized API and self-made lactose carrier are prepared and evaluated. The mixing process is studied in detail, including the mixing method, mixing speed and time, and mixing sequence. The results demonstrate that all the factors in mixing have an influence on the blend uniformity and the FPF (fine particle fraction). Then, the composition of formulations, like the ratio of fine lactose to powders, size and source of coarse lactose, percentage and size of the API, is investigated. At last, a performance stability test is carried out to study the influence of package, formulation and flow rate of the TI (Twin Impinger) test on the FPF stability.

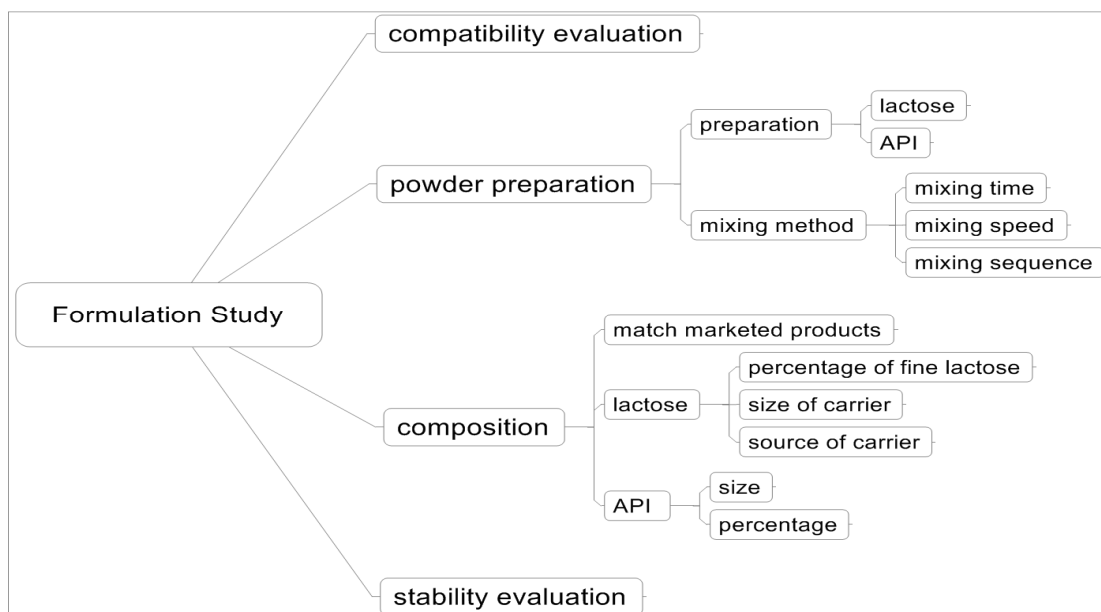


**Figure 7.1: A schematic diagram of formulation study**



## 7.2 The Compatibility Evaluation

Usually, a compatibility evaluation of process, excipient and package materials is the first step in a formulation study. Only if this result demonstrates the compatibility of API with the preparation process, excipient and package materials, the following formulation work will be meaningful. Since no solvent, no heating or other dramatic physical operation is applied in this formulation study, the risk of chemical degradation is minimized. The compatibility test is focused on the micronization, excipient and package material.

Firstly, solid properties of the micronized particles were studied by TGA, DSC and XRPD, as mentioned in Section 3.2.1. The TGA and DSC results are shown in Fig.7.2. As we can see from Fig.7.2b, the TGA curve clearly exhibits a dramatic decline at about 100°C, standing for a weight loss of crystal water evaporation for the API. Because the percentage of API in the micronized mixture is very small, this characteristic peak is not reflected in Fig.7.2c. Additionally, there is no obvious peak of dehydration for lactose and micronized API+lactose, indicating the impossibility to measure the moisture of a formulation by the TGA. As we can see from the DSC results, the peak of micronized API+lactose is the same as lactose. This result demonstrates that there is no significant solid-property alteration during micronization, such as amorphous component increasing

The XRPD results further prove this conclusion. The API+lactose mixture and micronized API+lactose show almost the same diffraction intensity. The diffraction profiles of both are dominated by the lactose as shown in Fig.7.3. When comparing the XRPD results of the mixture and the API, a characteristic peak at 4-5° for the API disappears. It can be explained by that the API only accounted for a very small part of the mixture. Although a violent collision of particles is applied in the jet-mill, the amorphous content only occupy a very small part of the total. Consequently, XRPD, one of the most used methods for quantifying crystallinity, is not sensitive adequately to distinguish the micronized and unmicronized samples<sup>[149]</sup>.

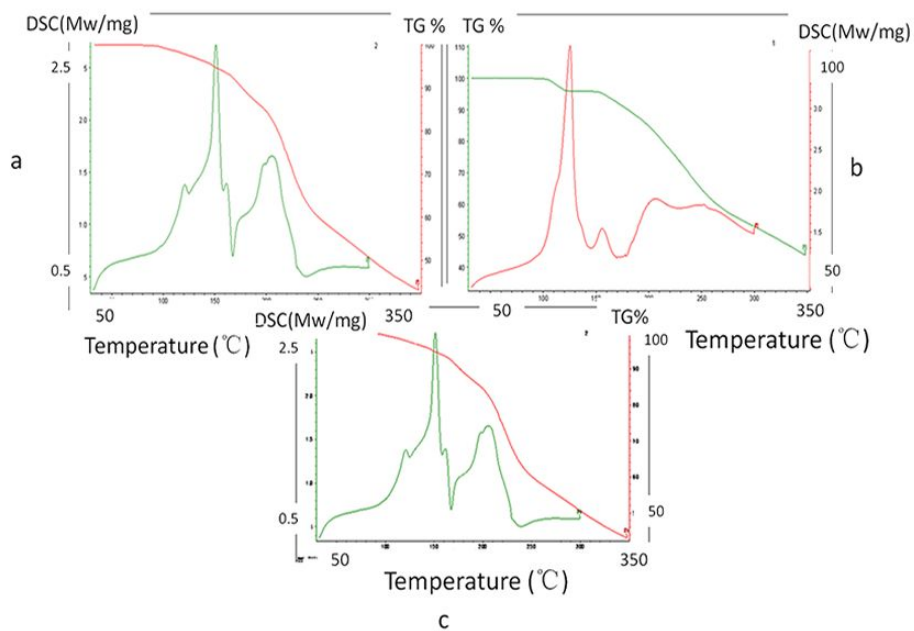


**Figure 7.2: The TGA and DSC results. a, lactose. b, the API. c, micronized lactose+API**

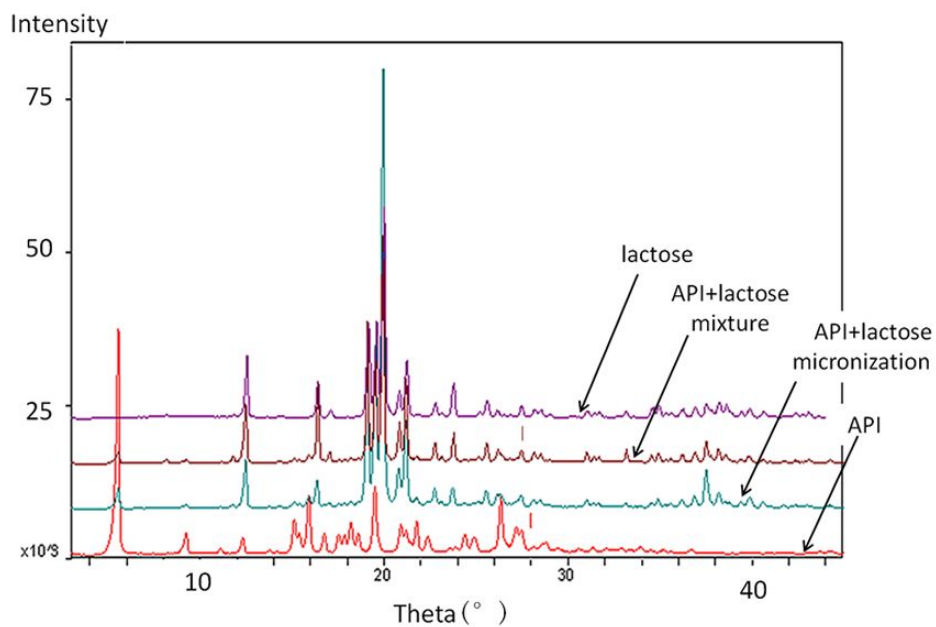


**Figure 7.3: The XRPD results of lactose, API+lactose, micronized API+lactose, API.**

An influence of jet-milling on the API chemical stability is also studied. The impurities of the unprocessed API and micronized API are analyzed by the HPLC. The result shows that the impurity content is 0.50% and 0.41% for the unprocessed API and the micronized API respectively. Hence, the almost same impurity level indicates no degradation of the API caused by micronization.

After that, the compatibility of the API with excipient and packaging material is studied. The API is mixed with lactose for API-excipient compatibility, and then the powder blend is mixed with pieces of PVC and aluminum foil to study the packaging material compatibility. To accelerate a possible degradation, all samples are placed under stress conditions (high temperature, high humidity and intensive light) for 10 days.

The research scheme and result are presented in Table 7.1. As we can see, the lactose and PVC do not significantly accelerate the degradation, since the impurity does not increase obviously even under high humidity (RH92.5%) and high temperature (60°C). The intense light (4500lx) has a larger influence for API+lactose and mixture+PVC. There were two reasons. First, the API is more sensitive to light. The fewer impurity of mixture+foil shows that the foil can prevent light and reduce degradation. Second, when API particles are dispersed in the mixture or mixture+PVC, the total exposure surface is increased and the possibility of degradation goes up. It is noteworthy that the attachment of API to the PVC because of electrostatic charge may enhance the degradation risk. The degradation results of the stress test under intense light imply that the protection of powder from light is necessary.

**Table 7.1: The impurity content of compatibility tests**

Impurity %	Initial	10day		
		RH92.5%	60°C	Intense light (4500lx)
API+lactose	0.58	0.58	0.69	0.90
mixture + PVC		0.57	0.48	1.02
mixture + foil		0.37	0.54	0.63

## 7.3 Powder Preparation for Dry Powder Inhaler

When all the results demonstrate good compatibility of the API with micronization, excipient and the packaging materials, the research then shift to the powder preparation and formulation study.

### 7.3.1 Preparation of the API particles and lactose

The sulfate Salbutamol is micronized to several microns, which is a prerequisite for respiratory delivery. The equipment and parameters of the jet-mill is introduced in Section 3.5.1. To study the effect of multiple micronizations, the API particles are micronized for 1-3 times.

The particle size distribution is measured by laser diffraction sizing, and the results are shown in Fig.7.4 and Table 7.2 As we can see, the particle size decrease gradually with more times of micronization, and the distribution becomes narrower. The reduction of particle size is especially obvious from 1st to 2nd jet-milling. Although more processing times produce smaller particles, the API loss on the wall of equipment increases, causing a problem of low production efficiency. Increasing times of jet-milling may also result in dramatical augment of electrostatic charge. Too much charge is difficult to dissipate and harmful for formulation performance. More importantly, the X90 is under 5 $\mu$ m after 2<sup>nd</sup> micronization, implying that most particles have been already suitable for inhalation delivery. Consequently, the API particles micronized twice are employed in the following experiments unless otherwise specified.

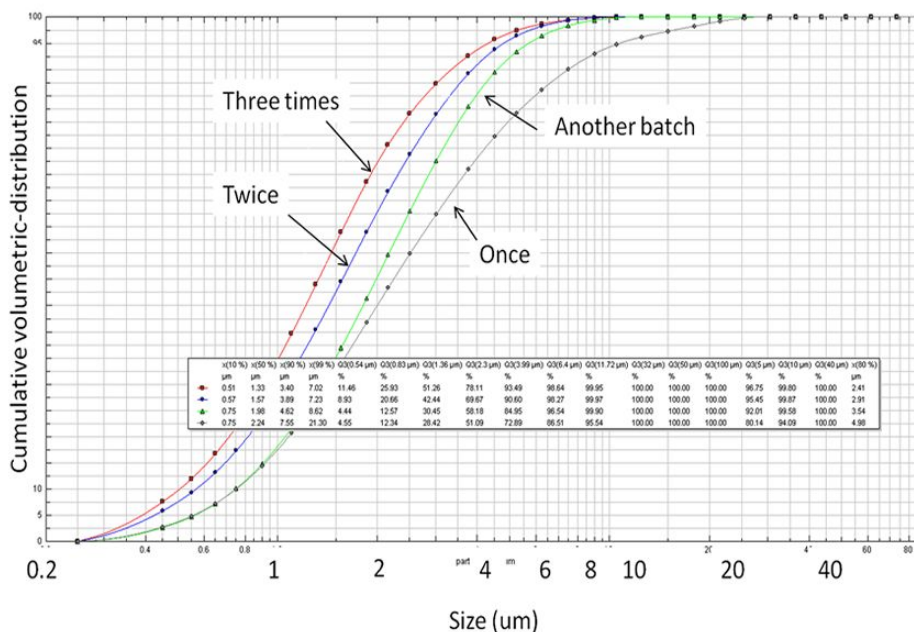


**Figure 7.4: The laser diffraction size distribution of micronized API**

**Table 7.2: The size results of micronized API**

Micronization	X10 (μm)	X50(μm)	X90(μm)	X99(μm)
Once	0.75	2.24	7.55	21.3
Twice	0.57	1.57	3.89	7.23
Three times	0.51	1.33	3.4	7.02

The particles are also characterized by the SEM as shown in Fig.7.5. As we can see in Fig.7.5, the particles are very small strips or sheets, which exhibit a very strong cohesive tendency. As a result of extra small size and strong cohesive force, the addition of lactose as diluents and carrier become essential.

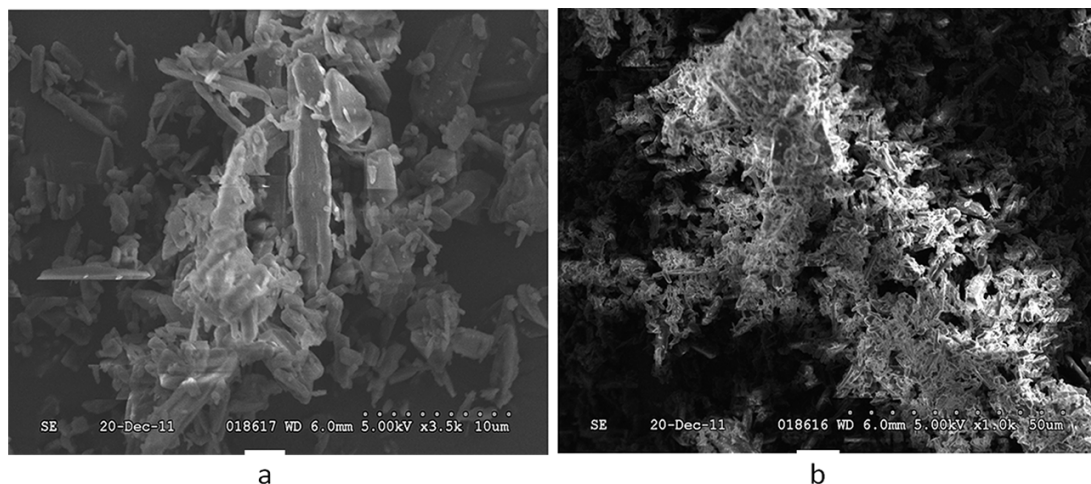


**Figure 7.5: The SEM pictures of the micronized API. a, shape of the micronized API; b, cohesive property of the micronized API.**

At first, the coarse lactose as the carrier is prepared by wet granulation. These carriers exhibit an interesting surface and binding with the fine API. As we can see from Fig.7.6a, the surface of the carrier is rather coarse with lots of caves and crevices. When these carriers are mixed with the extra fine API particles, the fine particles attach to the coarse surface of the carrier as shown in Fig.7.6b. This attachment is an ideal situation anticipated by formulation researchers sometimes.

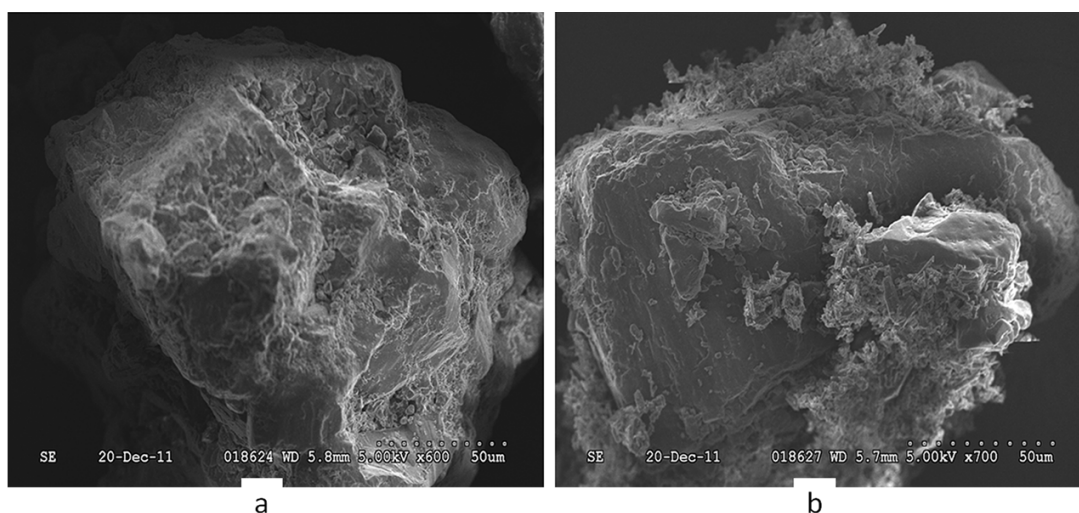


**Figure 7.6: The SEM pictures of self-made lactose (a) and the API + lactose mixture (b).**

Yet, since those carriers are produced manually on a small scale, the size distribution and flowability are not very stable, as shown in Table 7.3 and Table 7.4. The particle size of lactose in terms of X10, X50 and X90 show an obvious difference among three batches. Besides, the angle of repose and compression index also indicate various flowability. It is interesting to notice that the flowability is closely correlated with the particle size. With the decreasing size from Batch 120504 to 121225, especially for X50 and X90, the flowability also exhibit a descending trend reflected by the increasing angle of repose and compression index.

**Table 7.3: The size results of self-made lactose carriers**

Batch No.	Test	X10 / $\mu\text{m}$	X50 / $\mu\text{m}$	X90 / $\mu\text{m}$
120504	1st	18.14	69.89	151.52
	2nd	18.42	70.48	152.90
121218	1st	22.65	61.87	138.11
	2nd	22.75	62.78	140.79
121225	1st	12.58	56.49	138.94
	2nd	12.19	53.88	127.25

**Table 7.4: The flowability of self-made lactose carriers**

Batch No.	Angle of repose	Compression index
120504	37	15.7%
121218	41	26.3%
121225	43	34.3%

Consequently, commercial lactose rather than self-made lactose are used in the following experiments. However, as a result of smooth surface and regular shape, the adhesion of fine API particles to the carrier is much less than self-made lactose as shown in Fig.7.7.

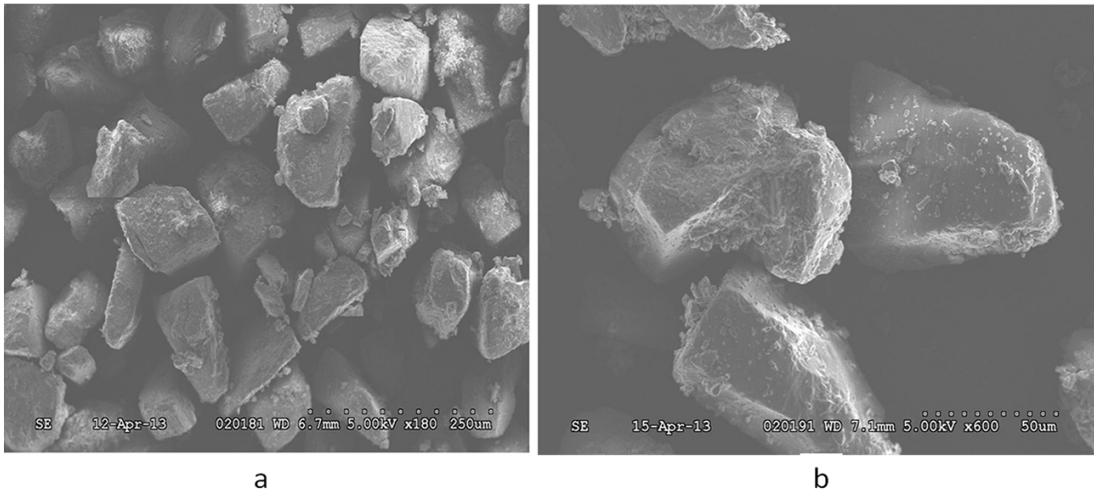


**Figure 7.7: The SEM pictures of the commercial lactose and the API-lactose mixture.**

The fine lactose as additives is micronized in this lab from a common lactose-314WG (Kerry, New Zealand). The particle size distribution is shown in Fig.7.8 and Table 7.5. The fine lactose particles are bigger than the API particles, but much smaller than coarse lactose carriers.

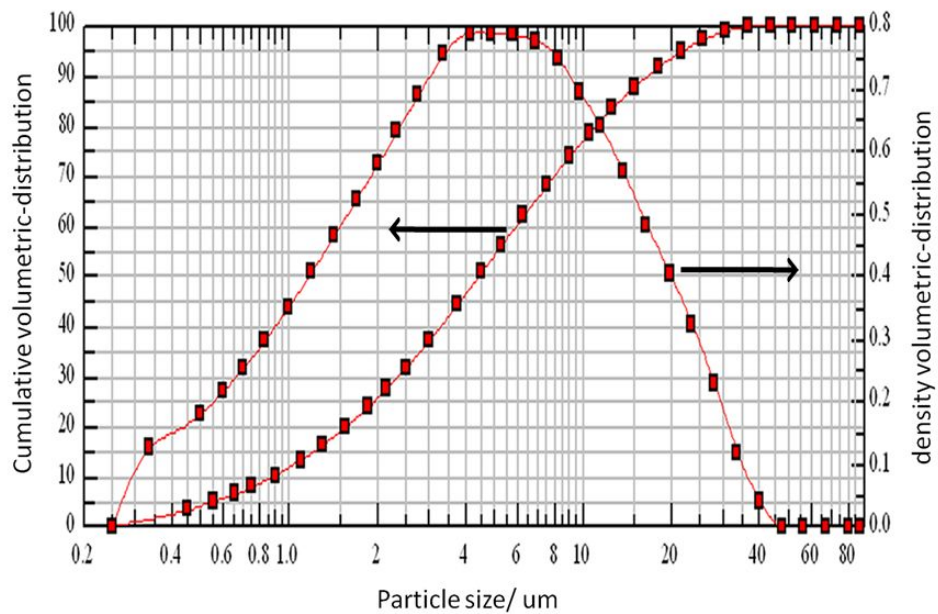


**Figure 7.8: The cumulative and density volumetric distribution of micronized lactose as fine additives.**

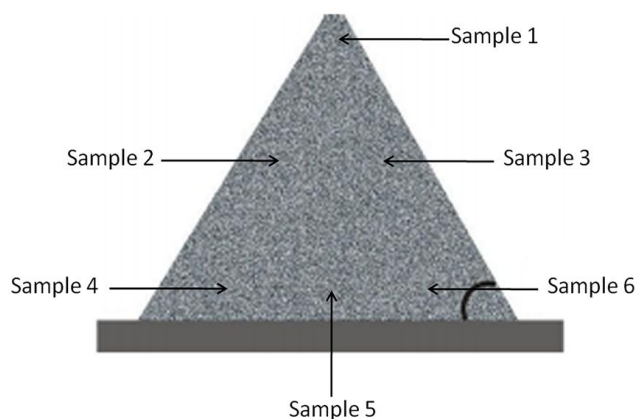


**Table 7.5: The size results of the micronized lactose.**

Sample	Test	X10 / $\mu\text{m}$	X50 / $\mu\text{m}$	X90 / $\mu\text{m}$
Fine lactose	1st	0.89	4.43	16.79
	2nd	0.90	4.40	16.91

### 7.3.2 Mixing method of the API and lactose

When the API and lactose are ready, the mixing method is studied to acquire an optimized process and knowledge of the influence on the content uniformity and FPF performance. In the uniformity tests, taking samples from the bulk powder is a difficult job since these samples have to represent all powder. Here, because the amount of powder is just 40-50g, a simple method is used to sample powders shown as Fig.7.9.

**Figure 7.9: A schematic of sampling method for blend content uniformity.**

At the beginning, the API and lactose particles are mixed by sieving with equivalent addition. This method is commonly used to prepare a uniform blend in oral solid formulations, like tablets and capsules. Its procedure is as follows: when we plan to mixed 1g API with m g lactose, 1g carrier is weighed and mixed with the API first, then the mixture is sieved by an 80-mesh screen (178 $\mu\text{m}$ ). After that, 2g lactose carrier is added into former blend and sieved again. This process is repeated until all powders are mixed.

The uniformity result of the bulk blend shown in Table 7.6 is expressed by the drug percentage since the weight may vary time to time. As we can see from the RSD, the

drug content uniformity of the blend is excellent, implying that the drug particles are evenly distributed in the carriers. Nevertheless, this method is rather complicated and time-consuming. And manual procedures are not suitable for industrial production.

**Table 7.6: The blend content uniformity of screening method**

	sample 1	sample 2	sample 3	sample 4	sample 5	sample 6	AVG	RSD
Drug percentage	0.61%	0.61%	0.62%	0.61%	0.61%	0.62%	0.61 %	0.81 %

The mixing method of a common mechanical stirring after shaking the powder in a container is also used. This method shows poor uniformity performance, for RSD above 10%. Similarly, the uniformity of mixing by low-shear Turbula is terrible.

Then the mixing method is established as Section 3.5.1, including a pre-sieving, low shear mixing by Turbula and high shear mixing. The RSD result shown in Table 7.7 indicates excellent uniformity. Although the final mixing method produces a little higher RSD than the sieving method, it is more mature and can be scaled up for industrial production.

**Table 7.7: The blend content uniformity of final mixing method**

	sample 1	sample 2	sample 3	sample 4	sample 5	sample 6	AVG	RSD
Drug percentage	0.69%	0.69%	0.70%	0.69%	0.70%	0.68%	0.69 %	1.09 %

According to previous experiences, an ultrasonic sieving is able to effectively break agglomerates of extra-fine particles and prepare a homogeneous blend. Hence, the ultrasonic sieving is also applied in the mixing. The fine API particles and part of fine lactose are sieved by ultrasonic vibration through a 200-mesh screen, and then mixed with coarse carriers. However, the results are not good as we expected, shown in Table 7.8. It is inferred that the agglomerates formed in the ultrasonic sieving are too solid to break up. Therefore, the agglomerates of the API and fine lactose are difficult to disperse into the bulk coarse carriers evenly. Consequently, the mixing method is established as 3-steps method without ultrasonic sieving.

**Table 7.8: The content uniformity of blend mixed by ultrasonic-sieve**

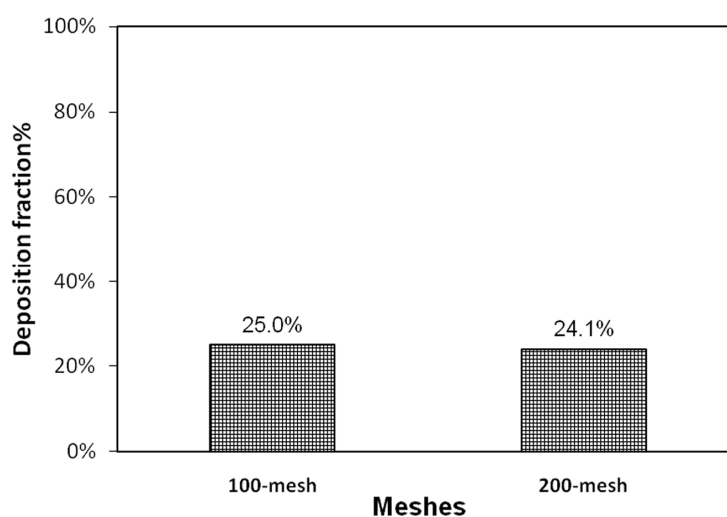
	sample 1	sample 2	sample 3	sample 4	sample 5	sample 6	AVG	RSD
Drug percentage	0.68%	0.83%	0.73%	0.67%	0.67%	0.70%	0.71 %	8.63 %

When the mixing method is established, two critical steps of the mixing are further studied for their influence on blend uniformity and FPF performance. One is the pre-sieving, serving to break API agglomerates. The other one is the high shear mixing.

Two screens with different diameters, 100-mesh (147 $\mu$ m) and 200-mesh (75 $\mu$ m) are used in the pre-sieving, and the uniformity and FPF are compared. The content RSD of the blend pre-sieved by 200-mesh also shows a good results as Table 7.9. The FPF result does not show an obvious difference between 100-mesh and 200-mesh. Therefore, it is concluded that there is no need to replace 100-mesh with 200-mesh, since the latter increases the time.

**Table 7.9: The content uniformity of blend by 200-mesh**

	sample 1	sample 2	sample 3	sample 4	sample 5	sample 6	AVG	RSD
Drug percentage	0.56%	0.59%	0.60%	0.59%	0.60%	0.59%	0.59 %	2.32 %

**Figure 7.10: The comparison of FPF values for powder pre-sieved by different meshes.**

Then, the research is moving on to the high shear mixing. As mentioned in Section 3.5.1, the higher shear blender is revised by us for mixing a small amount of powder. There is no visual display for the mixing speed but the speed can be adjusted by the input voltage. The speeds at 60v and 120v are compared, with an assumption that double voltage may result in double speed.

Since the speed is quite high when using 120v voltage, it is necessary to ensure the particles are not micronized by the mixing. The same Kerry 200 lactose is mixed for 10min under high speed (120v) and low speed (60v). The particle size is shown in Fig.7.11 and Table 7.10. The result demonstrates that the particle size of high-speed mixing is the same as low-speed, and particles are not micronized during the high shear mixing. As Fig.7.11, the size distribution profiles of low-speed and high-speed shear mixing nearly overlap.

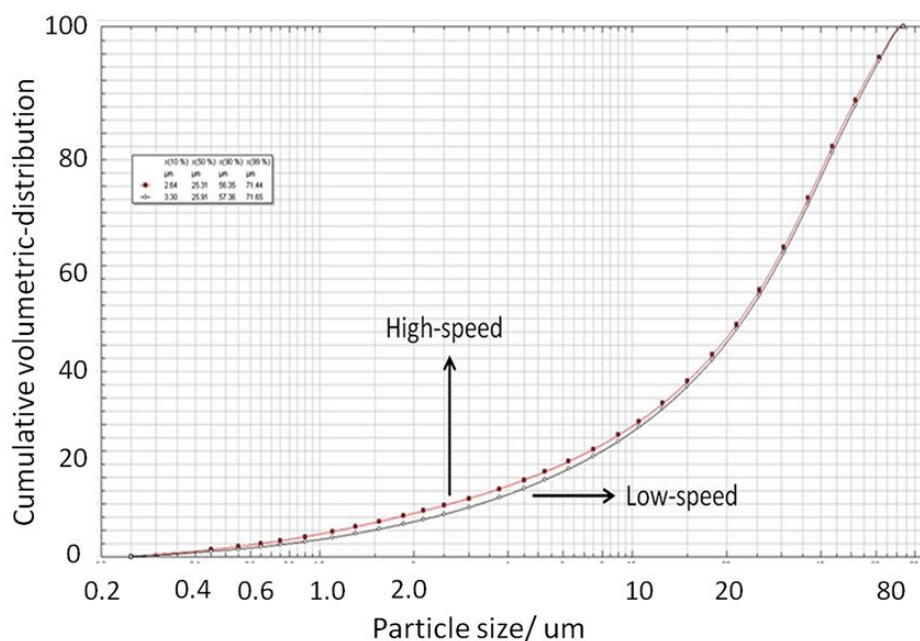


**Figure 7.11: The laser diffraction sizing results for low and high-speed mixing.**

**Table 7.10: The laser diffraction size results of high and low-speed mixing**

	X10	X50	X90
60V	2.70	21.03	47.04
120v	1.54	20.26	47.36

Then the high-speed and low-speed mixing is used to prepare a blend composed of 0.72% sulfate Salbutamol, plus 5% fine lactose and about 94.3% Inhalac 230 respectively. The mixing time is set as 10min. As Table 7.11, the drug percentage and uniformity are almost the same for low-speed and high-speed. This result demonstrates that the speed of mixing do not affect the uniformity of the blend.

**Table 7.11: The comparison of blend content uniformity using different-speed mixing**

Drug percentage	sample 1	sample 2	sample 3	sample 4	sample 5	sample 6	AVG	RSD
Low-speed	0.58%	0.56%	0.58%	0.59%	0.58%	0.58%	0.58 %	1.70 %
High-speed	0.58%	0.56%	0.57%	0.57%	0.57%	0.56%	0.57 %	1.36 %

Then these two powders are filled into blisters and used for TI (Twin impinger) tests to evaluate the influence of mixing speed on FPF. The result is shown in Fig.7.12. The FPF and blister remains are lower for high-speed mixing. This can be explained by that the interaction between API-API and API-carrier are much stronger as a result of high energy input. The strong adhesion force such as electrostatic force or mechanical interlocking makes it difficult to disaggregate agglomerates. Meanwhile, because the interaction between particles increases, the adhesion of particles to the blister wall become smaller accordingly and the blister remains decline. Nevertheless, constant blister remains is acceptable and less important than the FPF. Consequently, a lower mixing speed is selected for following research.

It is reported that high shear mixing increased the FPF values when compared with low shear mixing<sup>[150]</sup>. The different results are caused by an in-situ generation of fine lactose, which is detected during the high-shear mixing in that reference.

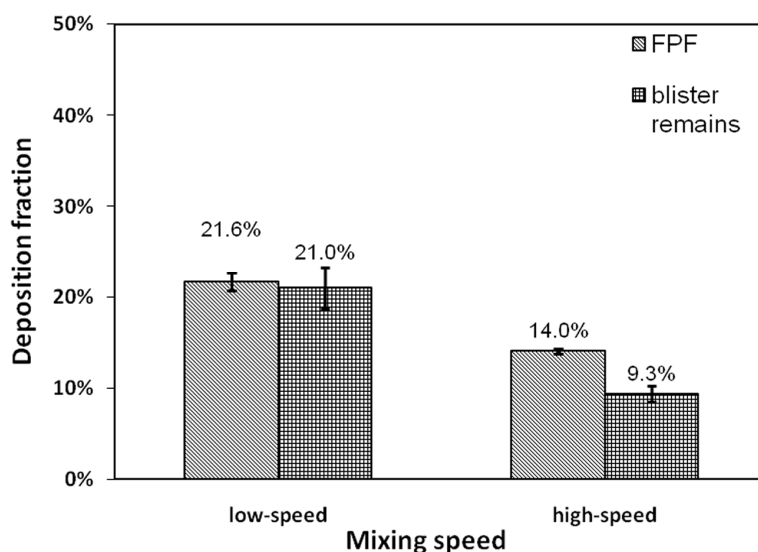


**Figure 7.12: The comparison of FPF and blister remains by different-speed mixing.**

When the mixing speed is determined, the mixing time is optimized as the next step. A powder composed of 0.72% sulfate Salbutamol, 10% fine lactose and about 89.3% Inhalac 230 was mixed at low speed (60v). Then samples were taken out at 5min, 10min and 20min for content analysis. The results are shown in Table 7.12. Actually, no significant difference of uniformity between these time points indicates that 5min of mixing is enough to acquire a homogenous blend. The drug percentages show a drop with increasing mixing time although the decline is not obvious. Despite all that, 10min mixing time is applied to ensure the uniformity.

**Table 7.12: The influence of mixing time on blend drug uniformity**

Drug percentage	sample 1	sample 2	sample 3	sample 4	sample 5	sample 6	AVG	RSD
5min	0.70%	0.67%	0.68%	0.64%	0.67%	0.66%	0.67 %	2.99 %
10min	0.66%	0.64%	0.67%	0.67%	0.68%	0.64%	0.66 %	2.54 %
20min	0.66%	0.66%	0.63%	0.63%	0.61%	0.64%	0.64 %	3.04 %

The powders sampled at different time points are tested by the TI (Twin impinger) to study the effect of mixing time on the FPF. Additionally, the powder at 0min representing

no high shear mixing is also studied. The result is presented in Fig.7.13 and Table 7.13. When increasing the mixing time, the FPF declines gradually with a dramatic drop from 0min to 5min. Meanwhile, the blisters remains do not show obvious changes except for 0min. The drop of FPF can be explained by the higher energy input and increasing loss of fine particles with more mixing time.

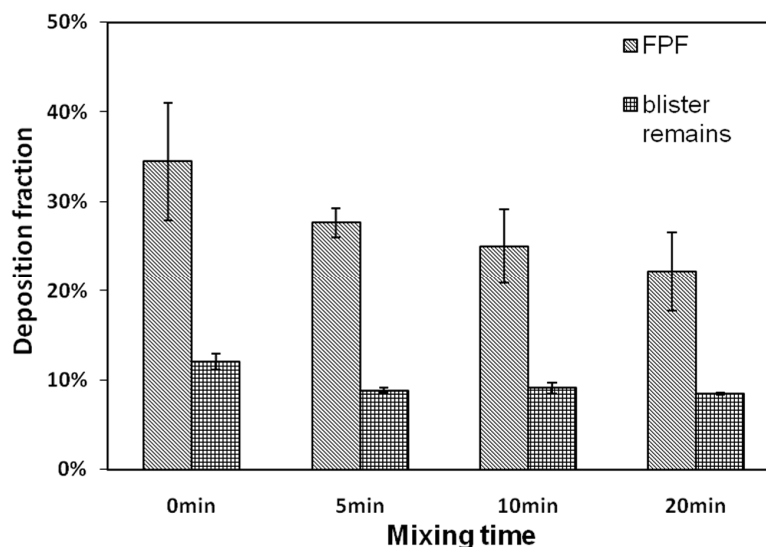


**Figure 7.13: The influence of mixing time on FPF and blister remains.**

**Table 7.13: The FPF and blister remains results of different mixing time**

	0min	5min	10min	20min
FPF-AVG	34.4%	27.6%	25.0%	22.2%
SD	6.6%	1.7%	4.2%	4.5%
Remains-AVG	12.1%	8.8%	9.1%	8.4%
SD	0.9%	0.2%	0.6%	0.1%

## 7.4 Composition Research of Dry Powder Formulation

The composition of a formulation is a field where the pharmaceutical scientists display their talents, when a specific DPI device is given most of the time. Although the available excipients for inhalation drug delivery are limited and the amount of the API for each dose is determined by clinical requirements, the formulation composition is still challenging.

There are several ways to adjust the performance of a DPI formulation, like API size, ratio of fine lactose as additives to the powder, size of coarse lactose carrier and other factors. All those factors are studied in the following experiments.

#### 7.4.1 The formulation with similar FPF as marketed products

Several hopeful formulations are obtained after lots of formulation work. The composition of these formulations is listed in Table 7.14. The powder is mixed by the method mentioned in Section 3.5.1.

**Table 7.14: The composition of these formulations with similar FPF as marketed products**

No.	Lactose-Carrier	Fine lactose	Sulfate Salbutamol
Rx4	SV003	5%	0.72%
Rx5	LH200	0	0.72%
Rx6	Inhalac120	20%	0.72%
Rx17	Inhalac230(<45 $\mu$ m)	0	0.72%

The FPF results are shown in Fig.7.14 and Fig.7.15. As shown in these two figures, the Rx4 and Rx5 have similar or a little higher FPF than Aerolizer® Foradil® and Diskus® Seretide®. And Rx6 and Rx17 have similar or even little higher FPF than Turbuhaler® Oxis® and Clickhaler® Asmatha®. A little higher FPF is acceptable, since the marketed products have been dispersed out for some time and our formulations are freshly prepared. The newly preparation may experience a slight a drop of FPF after storage. Consequently, the FPF of the novel inhaler could match several marketed products by adjusting the composition of a formulation.



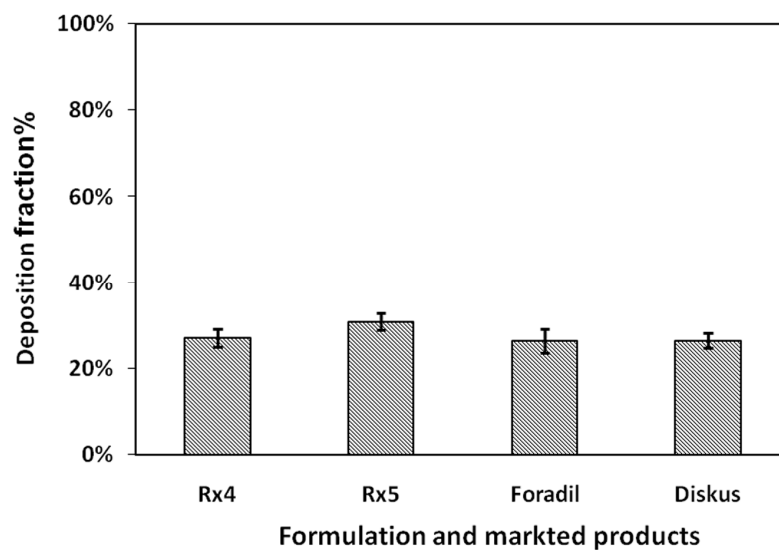


**Figure 7.14: The similar FPF of formulation Rx4/5 as Aerolizer® Foradil® and Diskus® Seretide®**

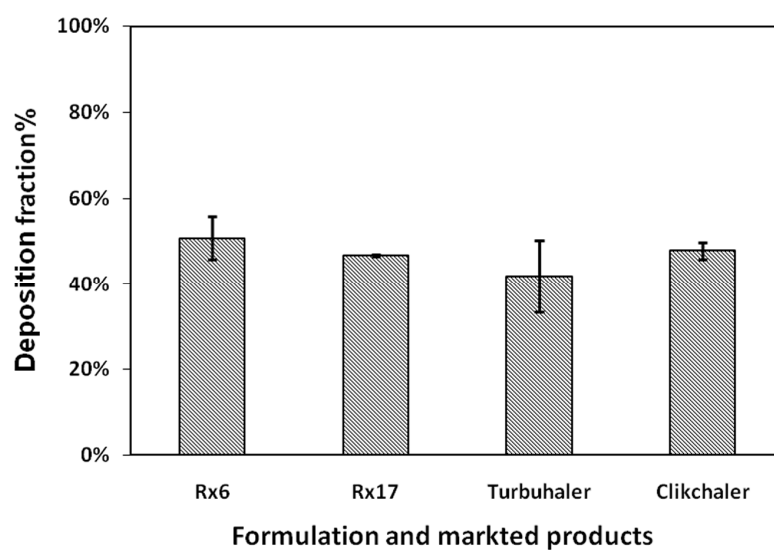


**Figure 7.15: The similar FPF of formulation Rx6/17 as Turbuhaler® Oxis® and Clickhaler® Asmatha®.**

It is noteworthy that the percentages of API for those 4 formulations are the same as 0.72%, delivering about 12µg API by each blister. The dosage is the same as Aerolizer®

Foradil® and Turbuhaler® Oxis®, both of which deliver 12µg fumarate formoterol. But for clickhaler® Asmasal® and Diskus® Seretide®, their delivery dose are at least 100µg/dose. Hence, a capacity to deliver high dose should be validated to evaluate the inhaler performance. This test is carried out in Section 7.4.3 and the result demonstrates the ratio of the API to the total power does not affect the FPF significantly.

#### 7.4.2 The influence of the lactose on formulation performance

Although several formulations with similar FPF as marketed products are acquired, it is necessary to further investigate influences of formulation variables on the inhaler performance.

Firstly, an influence of fine lactose as additives is studied. The blends containing 0%, 5%, 10% and 20% fine lactose are prepared respectively. The percentage of sulfate Salbutamol is set at 0.72% and the Inhalac 230 as coarse lactose. The flowability is evaluated in terms of angle of repose and compression index. The results shown in Table 7.15 and Table 7.16. demonstrate that the flowability decreases gradually with increasing fine lactose. During these tests, it is found that the angle of repose is difficult to measure accurately when the flowability is too bad, thereby the compression index could be used to evaluate the flowability of powders.

**Table 7.15: The angle of repose of blends with different ratio of fine lactose**

Angle of repose	Fraction of fine lactose			
	0%	5%	10%	20%
test1	35.55	42.28	49.64	54.25
test2	34.98	40.54	51.03	53.15
test3	35.94	41.05	47.71	53.15
AVG	35.49	41.29	49.46	53.52

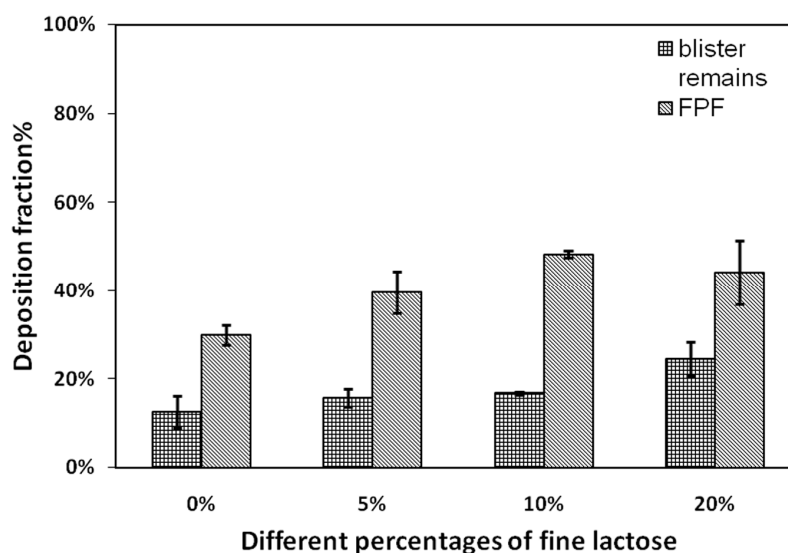
**Table 7.16: The compression index of blends with different ratio of fine lactose**

Compression index	Fraction of fine lactose			
	0%	5%	10%	20%
test1	18.28%	26.37%	34.83%	47.31%
test2	19.32%	25.56%	35.35%	45.16%
test3	17.39%	27.47%	34.07%	46.74%
AVG	18.33%	26.47%	34.75%	46.40%

**Table 7.17: The blend drug content uniformity for formulations containing different fine lactose**

API percentage	Fraction of fine lactose			
	0	5%	10%	20%
AVG	0.53%	0.58%	0.63%	0.63%
RSD	1.89%	0.62%	1.72%	2.03%

As the first step of formulation evaluation, the drug content and uniformity is shown in Table 7.17. This result clearly demonstrates the excellent drug content uniformity for all 4 powders. As we can see from this table, when increasing the percentage of fine lactose, the loss of the API particles decreases slightly. After a uniformity evaluation, the TI (Twin impinger) results are shown in Fig.7.16 and Table 7.18.

**Figure 7.16: The FPF and blister remains of formulations containing different fine lactose.**

As we can see from Fig.7.18, the FPF goes up gradually with the ascending ratio of fine lactose but experiences a slight drop when the fines is increased from 10% to 20%. There are several hypotheses which can explain this phenomenon. For example, the fine lactose would compete against the API for “active or high energy” site on the larger carrier, or the fine lactose act as a diluent to reduce the API-API interaction. Both mechanisms can increase the FPF with more fines. However, there is a critical point between 10% and 20% fines, indicating a turning point or platform for the increasing effect of FPF.

The blister remains also shows a slightly ascending trend with increasing fine lactose. The effect might be explained by the descending flowability as a result of a higher proportion of fine particles. Or it is correlated with an augment of adhesiveness because of the increased contact area<sup>[151; 152]</sup>.

**Table 7.18: The FPF and blister remains results of different fine lactose**

	Fraction of fine lactose			
	0%	5%	10%	20%
FPF-AVG	30.0%	39.7%	48.3%	44.2%
SD	2.2%	4.8%	0.8%	7.3%
Remains-AVG	12.5%	15.7%	16.7%	24.5%
SD	3.6%	2.1%	0.4%	3.9%

The influence of coarse lactose is also studied. The Inhalac 230 is sieved into 4 parts (<45 $\mu$ m, 45-75 $\mu$ m, 75-100 $\mu$ m, 100-150 $\mu$ m) by a vibratory sieve shaker. Then the size distribution of those sieved powders is validated by laser diffraction sizing. For particle smaller than 45 $\mu$ m, the sample is tested by R2 lens and R4 lens for other powders.

The laser diffraction size measurement results are shown in Table 7.19. It is interesting that the laser diffraction size results are not completely consistent with sieving results. As we can see in this table, the X10 standing for small particles is close to the lower limit of sieving, but X90 representing large particles is larger than the upper limit of sieving, especially for particles in 45-75 $\mu$ m and 75-100 $\mu$ m. It is inferred that the shape of the particles caused the size difference. Since the laser diffraction test might take an axial length as particle size for those long-strip particles, it overestimated the particle size. However, those long-strip particles can penetrate the pores of a screen vertically,

exhibiting a smaller diameter. The X90 of 100-150 particles is less than 150 $\mu\text{m}$  and this can be explained by that the original size distribution of Inhalac230 is less than 150 $\mu\text{m}$  as Table 3.7. Generally, the Inhalac 230 lactose is divided into several parts with a desired size range.

**Table 7.19: The vibration sieving size and laser diffraction size of the sieved lactose**

Vibrating sieve	Laser diffraction size		
	X10( $\mu\text{m}$ )	X50( $\mu\text{m}$ )	X90( $\mu\text{m}$ )
<45 $\mu\text{m}$	4.5	27.1	53.4
	4.4	27.0	54.2
45-75 $\mu\text{m}$	42.4	71.5	98.4
	43.2	72.9	100.2
75-100 $\mu\text{m}$	72.6	105.1	137.2
	71.0	104.4	135.7
100-150 $\mu\text{m}$	78.4	116.3	141.7
	77.8	114.0	139.5

Then, the API (0.72%) is mixed with the lactose without fine lactose, avoiding an influence of fines on FPF. The blend drug content uniformity is tested at first. The result shown in Table 7.20 also indicates a good uniformity.

**Table 7.20: The blend drug content uniformity of formulation with different-size lactose**

API percentage(n=6)	The size of lactose			
	<45 $\mu\text{m}$	45-75 $\mu\text{m}$	75-100 $\mu\text{m}$	100-150 $\mu\text{m}$
AVG%	0.68%	0.66%	0.69%	0.67%
RSD%	1.4%	1.4%	2.6%	0.9%

The TI (Twin Impinger) result is shown in Fig.7.17 and Table 7.21. As we can see from this figure, the small carriers (<45 $\mu\text{m}$ ) exhibit the highest FPF and lowest blister remains. And other 3 carriers show a trend that the FPF increase with the decline of carrier size, however this trend is not as obvious as carriers <45 $\mu\text{m}$ . Guenette et al studied an effect of lactose size on the FPF of DPI formulations, and proposed that the fraction of fine lactose was the reason for the difference of FPF<sup>[84]</sup>. Steckel et al used different-size lactose from sieving to study the effect of lactose size on the inhaler performance. Their results also

demonstrated that a smaller lactose (<32 $\mu\text{m}$ ) produced much higher FPF (37%) than larger lactose (125-180 $\mu\text{m}$ ). It was suggested that small particles formed redispersible agglomerates, but the API particle adhered to the larger carrier tightly<sup>[82]</sup>. Another study also demonstrated that smaller lactose carrier (<32 $\mu\text{m}$ ) exhibited better FPF but less emitted dose than larger carriers(~100 $\mu\text{m}$ )<sup>[82]</sup>.

The blisters remains seems to be more complicated. Generally, the larger carrier result in more blister remains.

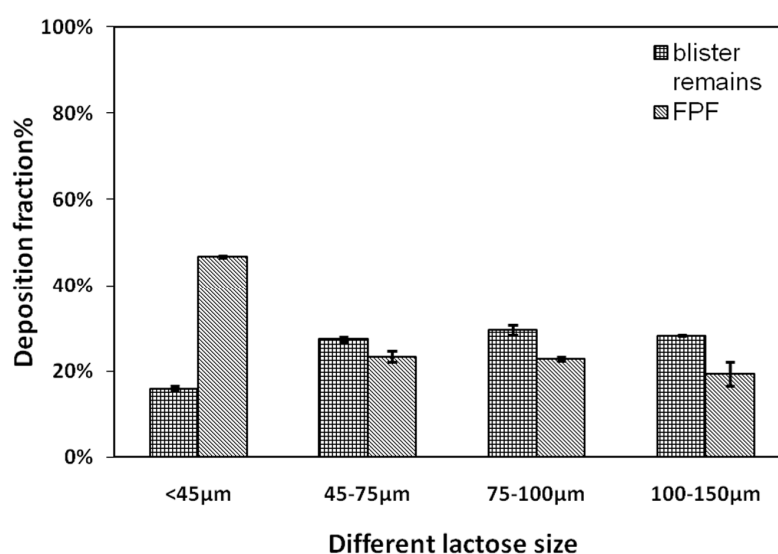


**Figure 7.17: The FPF and blister remains of formulation with different-size lactose.**

**Table 7.21: The FPF and blister remains results of formulation with different-size lactose**

TI test (n=2 )	The size of lactose carrier			
	<45 $\mu\text{m}$	45-75 $\mu\text{m}$	75-100 $\mu\text{m}$	100-150 $\mu\text{m}$
FPF-AVG	46.8%	23.4%	22.8%	19.4%
SD	0.3%	1.4%	0.5%	2.8%
Remains-AVG	15.9%	27.4%	29.6%	28.3%
SD	0.6%	0.5%	1.1%	0.1%

Obviously, the size of lactose carrier exerts a great influence on the inhaler performance. Then, an influence of lactose source on the formulation performance was also studied.

The lactose within the 45-75 $\mu$ m was sieved by vibratory sieving respectively from Inhalac 230, SV003 and LH200 (milled). The size distribution of those lactose carriers was first validated by laser diffraction size measurement.

As we can see from Table 7.22, the particle size is similar for Inhalac230 and SV003. The LH200 (milled) showed a little larger size than the other two. Again, the X90 is higher than the vibration sieving results, which are explained above.

**Table 7.22: The sieving size and laser diffraction size of lactose from different sources**

	Vibrating sieve	Laser diffraction size		
		X10( $\mu$ m)	X50( $\mu$ m)	X90( $\mu$ m)
Inhalac230	45-75 $\mu$ m	42.4	71.5	98.4
		43.2	72.9	100.2
SV003	45-75 $\mu$ m	43.4	67.7	97.2
		43.1	67.1	95.6
LH200 milled	45-75 $\mu$ m	50.2	81.9	119.0
		49.0	81.9	119.4

After that, those powders are tested by the TI impaction method. And the results are shown in Fig.7.18 and Table.7.23. The FFP and blister remains result demonstrate no great difference between Inhalac 230 and SV003. The FPF and blister remains of LH200 (milled) are a little higher than the former two. The result of higher blister remains for LH200 is consistent with an observation above, which shows that larger lactose result in more blister remains when studying different-size lactose. However, the research on lactose size shows that larger lactose may decrease the FPF. That result is contrary to the results of lactose source study. It is infer that the source of lactose outweigh the effect of lactose size on the inhaler FPF. Since the LH200 is prepared by a mill and other two are prepared by sieving, the LH200 may contain more fine particles. And these fines are attached to surface of large particles so tight to be detached during the vibration sieving<sup>[153]</sup>. Another explanation is that the fines in the sieved LH200 are too tiny to be reflected by the Sympatec, but those fines play an important role in the FPF. The microscope observation in Fig.7.19 proves the above inference to some extent, which shows more fines for the LH200 than SV003. Larhrib et al reported that the different

grades of lactose were likely to produce varying delivery profiles of inhaled drug, and the FPF difference mainly stemmed from fraction of fines or the carrier size<sup>[154]</sup>.

**Table 7.23: The blend drug content uniformity of formulation with different-source lactose**

API percentage (n=6)	Lactose (45-75 $\mu$ m)		
	Inhalac230	SV003	LH200 milled
AVG %	0.63	0.68	0.72
RSD %	2.0%	1.0%	1.0%

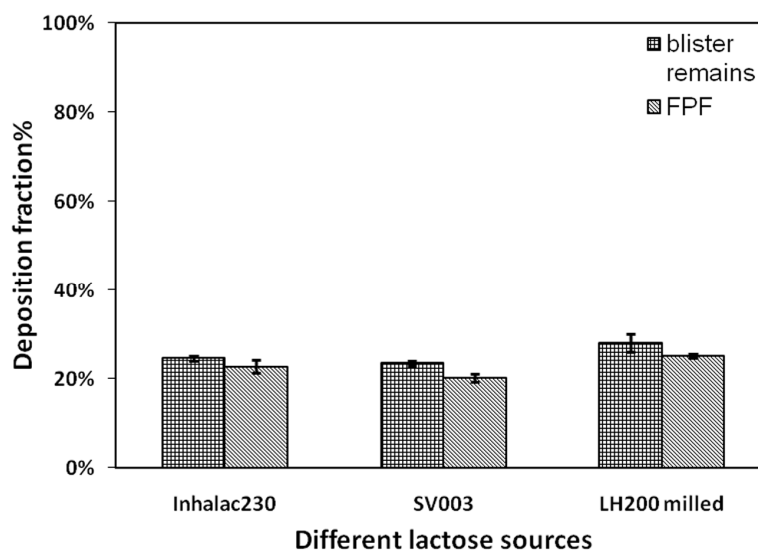


**Figure 7.18: The FPF and blister remains of formulation with different-source lactose.**

**Table 7.24: The FPF and blister remains results of different-source lactose**

TI test (n=2)	Lactose (45-75 $\mu$ m)		
	Inhalac230	SV003	LH200 milled
FPF-AVG	22.8%	20.2%	25.1%
SD	1.4%	0.8%	0.5%
Remains-AVG	24.6%	23.5%	28.0%
SD	0.5%	0.5%	2.1%



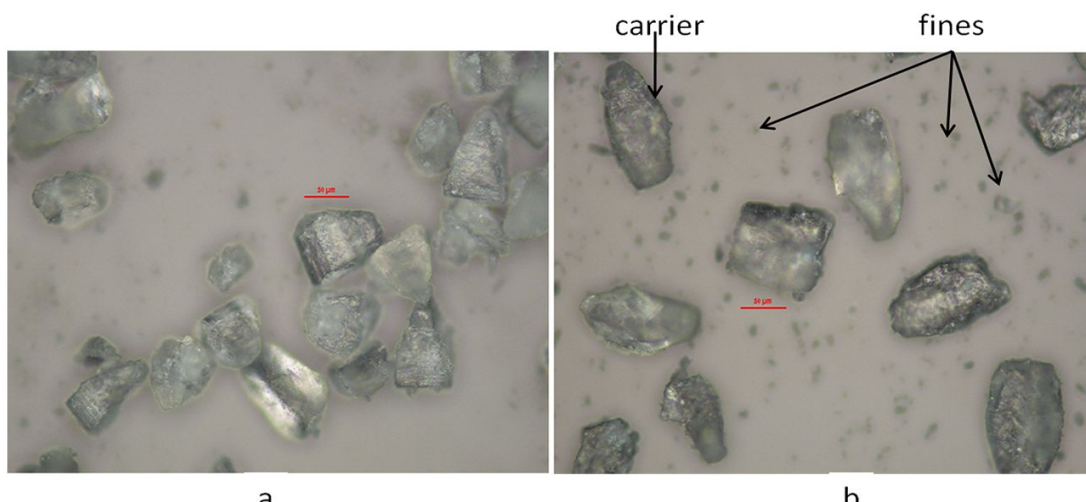


**Figure 7.19: The microscope images of different-source lactose.**  
**a, SV003; b, LH200 (milled)**

### 7.4.3 The influence of API on formulation performance

The percentage of sulfate Salbutamol in the blend is set at 0.72% for most experiments to deliver 12µg drug per dose. Nevertheless, many commercial products deliver 100µg API or even more per dose. Consequently, it is necessary to study the influence of the API percentage on the formulation performance. Two powder formulations were prepared, one of which contained 0.72% fine sulfate Salbutamol and about 20% fine lactose as additives, and the other contained 7.2% fine sulfate Salbutamol and about 13% fine lactose to keep the percentage of fine particles constant. The formulation containing 7.2% sulfate Salbutamol would deliver about 120µg drug per dose. The content uniformity is shown in Table 7.25, indicating uniform blends.

**Table 7.25: The blend drug content uniformity of formulations with different-percentage API.**

API percentage(n=6)	API=0.72%	API=7.2%
AVG %	0.62	5.74
RSD %	2.9%	4.4%

The TI performance result is shown in Fig.7.20 and Table 7.26. As we can see from the results, the percentage of API does not affect the FPP values but the blister remains

slightly. The high percentage of the API in formulation results in a larger fraction of blister remains, because more API particles mean more adherences to the blister wall. More fine drug particles do not affect a disaggregation of agglomerates or detachment of fine particle from carriers. This result is especially meaningful for the Inhaler-WU2011, since it greatly expands device application to match different marketed products but not only the fumarate formoterol inhalers. Although the fraction of blister remains is a little higher than low-API formulation, it is still acceptable as long as the value remain constant during storage and transportation.

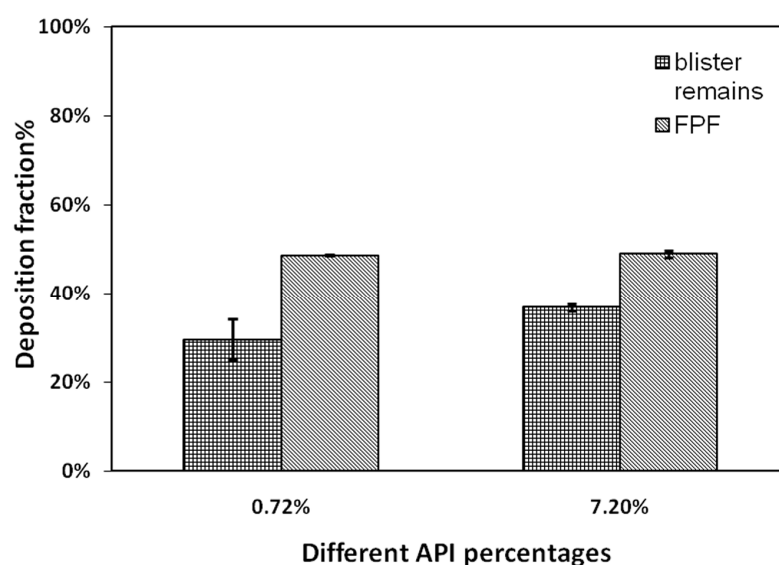


**Figure 7.20: The FPF and blister remains of formulation with different-percentage API.**

**Table 7.26: The FPF and blister remains results of the different - percentage API.**

TI test (n=2)	Percentage of API	
	0.72%	7.20%
FPF-AVG	48.6%	49.0%
SD	0.1%	0.8%
Remains-AVG	29.5%	36.8%
SD	4.5%	0.8%

The influence of API size on formulation performance is studied. The sulfate Salbutamol particle is micronized by a jet-mill to produce API with different size distribution. The size distribution results are shown in Table 7.2. Then formulations containing 0.72% of these API, about 5% fine lactose and 94% Inhalac 230 were prepared. The drug content uniformity result shown in Table 7.27 demonstrates an excellent uniformity.

**Table 7.27: The blend drug content uniformity of formulation with different-size API**

API percentage(n=6)	API size ( $\mu\text{m}$ )		
	X50=1.33	X50=1.57	X50=2.24
AVG %	0.61	0.60	0.59
RSD %	1.5%	0.8%	0.8%

As shown in Fig.7.21 and Table 7.28, the FPF and blister remains are not sensitive to the API particle size. This result not only provides an investigation into the influence of API size on the formulation performance, but also demonstrates that even if the size of API fluctuates within a certain range, the performance does not change obviously. This conclusion is greatly useful for large-scale production. Usually, some critical parameters of commercial production should be set in a range rather than a specific value. A lot of work should be carried out to validate the acceptable range for the critical parameters. This is a core viewpoint in the Common Technical Document (CTD) by the International Conference on Harmonisation of Technical Requirements for Registration of Pharmaceuticals for Human Use (ICH).

There is some literature focusing on the influence of the API particle size on the inhaler performance. Yet, most of the API particles are prepared by spray-drying; hence they can not provide plenty of useful information for jet-milled particles. For instance, Chew reported that the spray-dried disodium cromoglycate with  $2.3\mu\text{m}$  of MMD exhibited lower FPF than particles with  $3.7$  or  $5.2\mu\text{m}$  of MMD<sup>[155]</sup>. When considering the jet-milled API particles, it was reported that the larger size would decrease the FPF and performance stability in pMDI<sup>[156]</sup>.

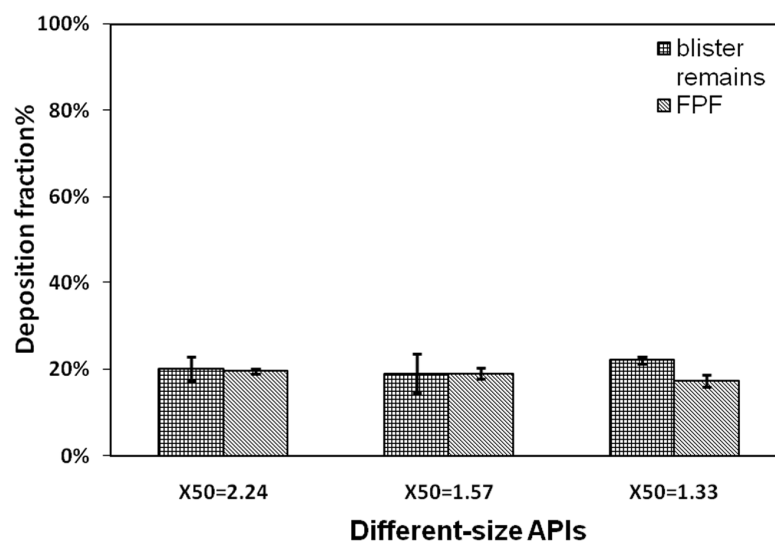


**Figure 7.21: The FPF and blister remains of formulation with different-size API.**

**Table 7.28: The FPF and blister remains results of different-size API**

	API size ( $\mu\text{m}$ )		
	X50=2.24	X50=1.57	X50=1.33
Tl test (n=2)			
FPF-AVG	19.6%	19.0%	17.3%
SD	0.6%	1.2%	1.4%
Remains-AVG	20.1%	19.1%	22.1%
SD	2.8%	4.5%	0.8%

The mixing sequence of API is further investigated to study the mechanism of performance improvement by fine lactose. One method is to mix the fine lactose with coarse lactose first, and then the API is added into the lactose system. This procedure is based on an assumption that the fine lactose would occupy the active site on the large carriers and assist the detachment of API from carriers. Another method is to blend the API and fine lactose first and then fine particle system is added into coarse lactose and mixed. The percentage of the API is 0.72%, with 5% fine lactose and about 94% Inhalac 230 for both methods. As shown in Table 7.29, the mixing sequence does not affect the blend drug content uniformity and both mixtures show good uniformity.

**Table 7.29: The blend drug content uniformity of different mixing sequence for API**

API percentage(n=6)	API mixing sequence	
	(API+fines) +coarse	API+(fines+coarse)
AVG %	0.58	0.59
RSD %	1.9%	1.1%

According to Fig.7.22 and Table 7.30, the (API+Fines) +Coarse mixing sequence exhibit a little higher FPF and less blister remains than the other one. This observation is contradictory to the common “active site” or “high-energy site” hypothesis. It is inferred that the API-fines agglomerates are formed in the (API+Fines) +Coarse method. And those agglomerates can be dispersed easily during delivery. As a result of API-Fines agglomerates formation, the adhesion of API to blister wall decreased.

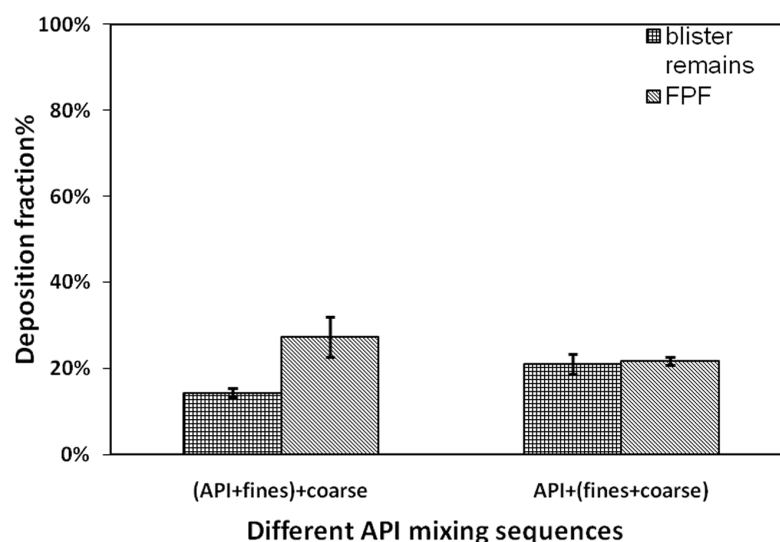


**Figure 7.22: The FPF and blister remain of formulation with different mixing sequence for the API.**

**Table 7.30: The FPF and blister remains results of different API mixing sequences**

	API mixing sequence	
	(API+finer)+coarse	API+(finer+coarse)
TI test (n=2)		
FPF-AVG	27.2%	21.6%
SD	4.6%	1.0%
Remains-AVG	14.3%	21.0%
SD	1.0%	2.3%

## 7.5 Orthogonal Experimental Design and Results

Many factors in the DPI formulation process and composition have been studied by the single-factor method. However, when considering all those factors at the same time, orthogonal experimental design is a wise choice to decrease the times of experiment, obtain evenly distributed data and more reliable conclusion.

As shown in Table 7.31, four factors with mixed level are studied, including the ratio of fine lactose, mixing time, mixing speed and mixing sequence. Since there are only two levels for mixing speed and sequence, a Taguchi design of L16 ( $4^2 \times 2^2$ ) is obtained from Minitab 16 software. The orthogonal experiment design is shown in Table 7.32

**Table 7.31: The factors and levels in the orthogonal experiments**

Level	A	B	C	D
	Percentage of fines	Mixing time	Mixing speed	Mixing sequence
1	20%	2min	60V	(F-lac+API) +Inhalac230
2	10%	5min	100V	(F-lac+Inhalac 230) +API
3	8%	8min		
4	5%	10min		

**Table 7.32: The factors and levels in the orthogonal experiments**

Formulation No.	A	B	C	D
1	1	1	1	1
2	1	2	2	2
3	1	3	1	1
4	1	4	2	2
5	2	1	2	1
6	2	2	1	2
7	2	3	2	1
8	2	4	1	2
9	3	1	1	2
10	3	2	2	1
11	3	3	1	2
12	3	4	2	1
13	4	1	2	2
14	4	2	1	1
15	4	3	2	2
16	4	4	1	1

16 formulations are prepared and content uniformity of these blends is evaluated first. The result indicates that all blends are uniform with RSD of the API percentage around 2-3%. Then, each formulation is tested by the TI (Twin impinger) twice and FPF (fine particle fraction) result is calculated as shown in Table 7.33.

**Table 7.33: The FPF results of the orthogonal experiments**

Formulation No.	Averaged FPF % (n=2)	Percentage of blister remains %	Formulation No.	Averaged FPF% (n=2)	Percentage of blister remains %
1	51.4	29.4	9	39.7	20.3
2	46.0	33.3	10	18.8	16.0
3	42.8	32.6	11	23.9	20.4
4	32.0	15.1	12	16.5	12.5
5	32.4	20.4	13	25.7	15.4
6	39.4	21.0	14	22.5	21.4
7	20.7	18.6	15	12.8	15.7
8	30.0	20.6	16	13.9	18.2

After that, the FPF is set as “response data” and the signal-to-noise ratio as “large expectation” by the Taguchi analysis using Minitab 16. The results are shown in Fig.7.23 and Table 7.34. As we can see in Fig.7.23, the FPF increases with more fine lactose, less mixing time and lower mixing speed. All these results are perfectly consistent with former results of single-factor experiments. The results of mixing sequence are opposite the previous study. The orthogonal experiment indicates that mixing fine and coarse lactose first and then with the API is better for higher FPF results, which is more reliable than the previous study. And the contradiction with former result might be explained by the lowest ratio of signal to noise for the mixing sequence presented in Table 7.34. The smaller ratio of signal to noise implies that this factor would be more vulnerable to interference. To sum up, the optimized parameters for the best FPF are 20%-fines, 2min of mixing time, 65v of mixing speed and (fine lactose+Inhalac 230)+API of mixing sequence.

When considering the ratio of signal to noise presented in Table 7.34, the percentage of fine lactose exhibits the largest ratio and mixing time presents the second largest one. This result implies that the percentage of fines has the greatest and most definite influence on the FPF and the mixing time occupies the second place. Consequently, when carrying out a formulation project, the percentage of fines and mixing time should be considered and adjusted first.



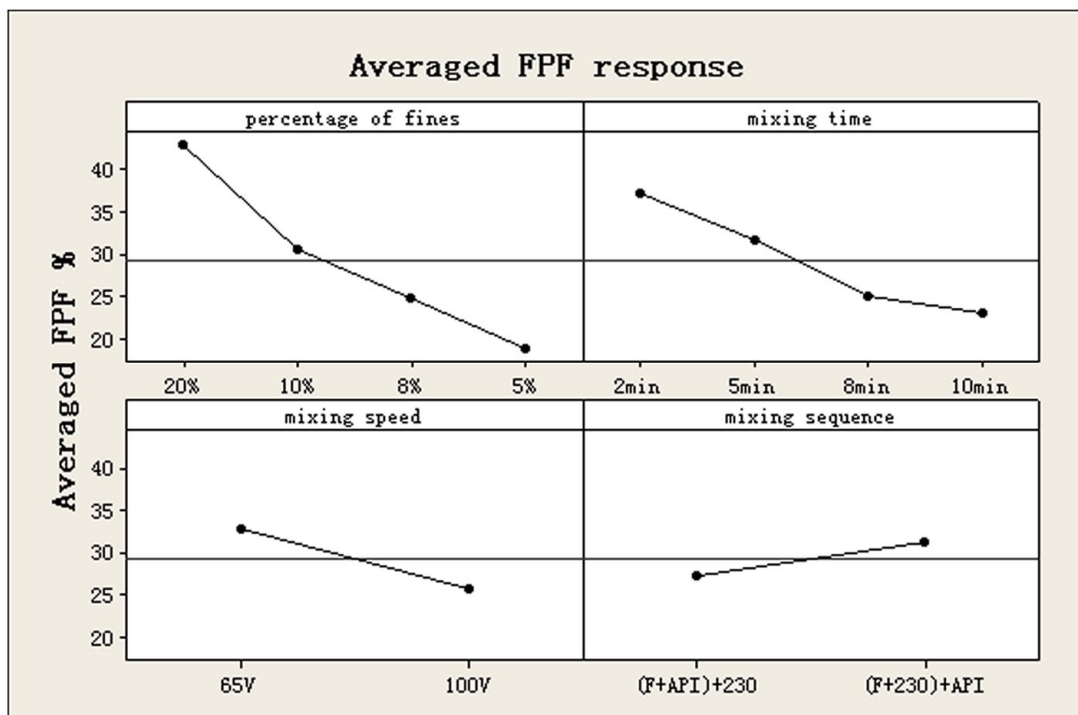
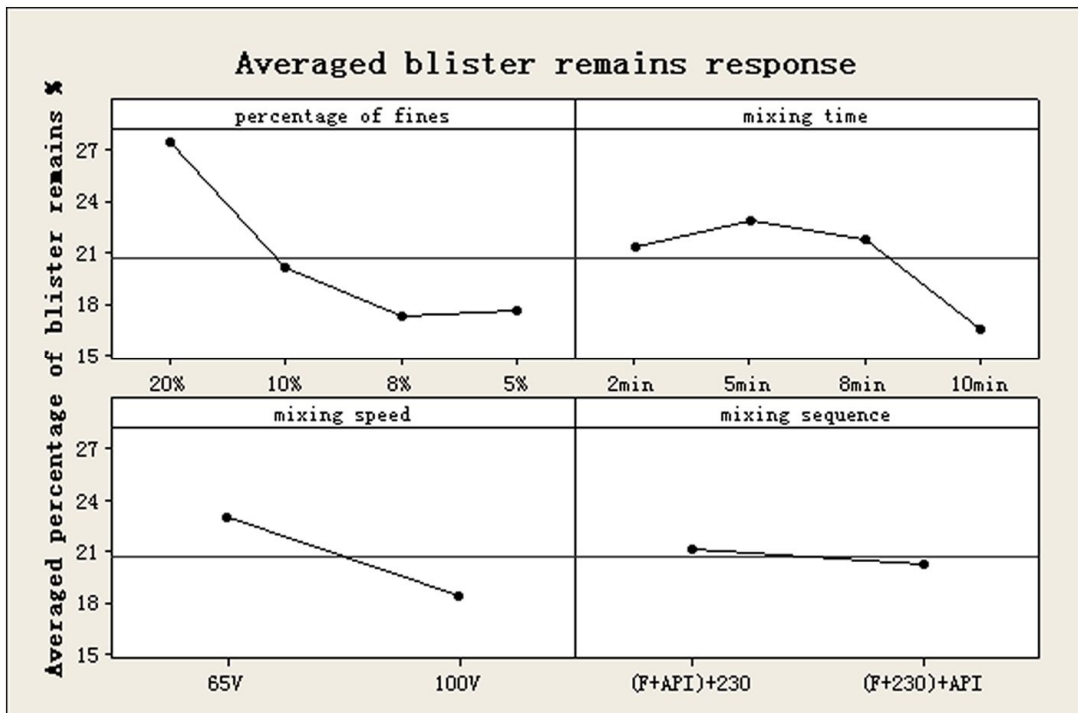


Figure 7.23: The averaged FPF response and various levels of the studied factors.

Table 7.34: The signal-to-noise ratios of FPF response

Level	Percentage of fines	Mixing time	Mixing speed	Mixing sequence
1	32.56	31.16	29.73	27.90
2	29.50	29.43	27.52	29.34
3	27.35	27.17		
4	25.07	26.73		
Delta	7.48	4.43	2.21	1.44
Ranking	1	2	3	4

The blister remain results of this orthogonal experiment are shown in Fig.7.24 and Table 7.35. As we can see in Fig.7.24, the percentage of blister remains experiences a decline with less fines, longer mixing time and higher mixing speed. It is inferred that these three factors result in a decline of fines in the formulation and then the decrease of blister remains. This inference is consistent with the results of single-factor results above. The mixing sequence shows a negligible effect on the blister remains.



**Figure 7.24: The averaged blister remains response and various levels of the studied factors.**

The signal to noise ratios of blister remains are listed as Table 7.35, presenting the same ranking of factors as FPF response. This result implies that the percentage of fines has the greatest and most definite influence on the blister remains and mixing sequence exert the smallest effect on the blister remains. Consequently, when we want to adjust the blister remains, the percentage of fines and mixing time should be considered first

**Table 7.35: The signal-to-noise ratios of blister remain responsive**

Level	Percentage of fines	Mixing time	Mixing speed	Mixing sequence
1	28.41	26.36	27.06	26.12
2	26.07	26.9	24.91	25.85
3	24.6	26.45		
4	24.86	24.24		
Delta	3.81	2.66	2.15	0.28
Ranking	1	2	3	4

## 7.6 Stability Evaluation of Dry Powder Inhaler Formulation

### 7.6.1 The influence of package on performance stability

As mentioned above, four kinds of powder containing 0%, 5%, 10% and 20% fine lactose were prepared, and the percentage of the API was 0.72% for all 4 powders. Then the powders were filled into PVC disks and sealed with aluminum foil, and those drug disks were divided into two groups: one was wrapped by foil outside the disks and the other was treated without additional package. Both groups were placed under 40°C, RH75% for 1 month. Then the FPF performance and blister remains were compared.

The results are shown in Fig 7.25, Fig.7.26 and Table 7.36. First of all, the external foil package is very useful to maintain the FPF performance. The packaged disks show similar or a little lower FPF than the initial value after 1 month. The disks without an additional foil package experience a dramatic decline of the FPF when compared to initial values. Besides, the foil package is helpful to decrease the blister remains. When comparing the blister remains, the results of disks with the external foil package are less than disks without external package, except for powder containing 20% fines. It is believed that the external foil package can provide better protection against moisture. Under high humidity environment, a capillary force plays a dominating role in the particle interactions and it will greatly affect the dispersibility of API particles. What is worse, if a liquid bridge forms between particles, then the dispersibility would decrease to a very low level. The descending dispersibility of particles not only reduce the FPF, but also is unfavourable for the fluidization and entrainment of particles into the flow. Consequently, the drop of the dispersibility would increase blister remains. It is also inferred that the moisture would raise the interaction force between particle and PVC wall.

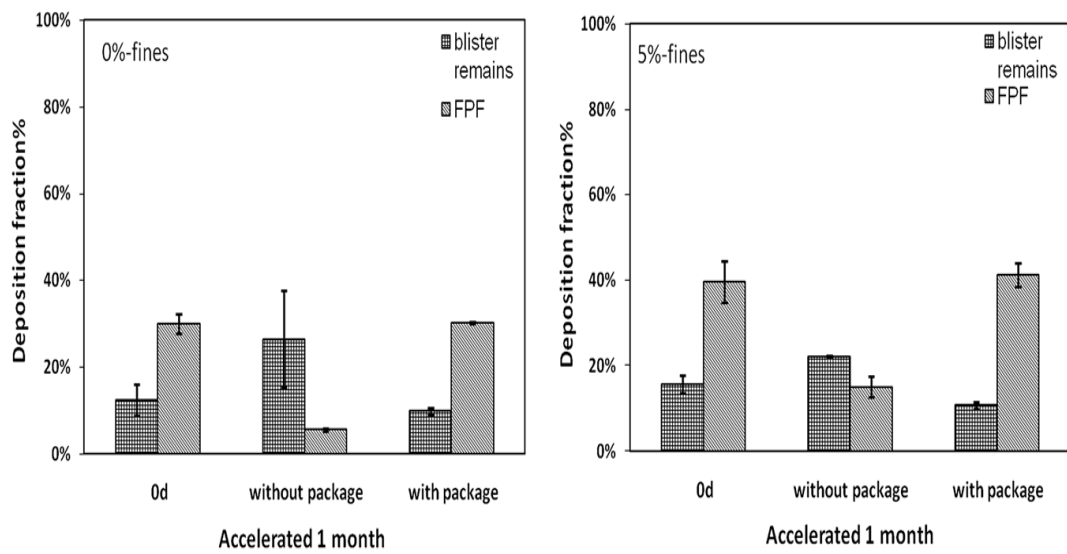


**Figure 7.25: The FPF and blister remains of initial and accelerated test for 1 month with/without external foil packages.**

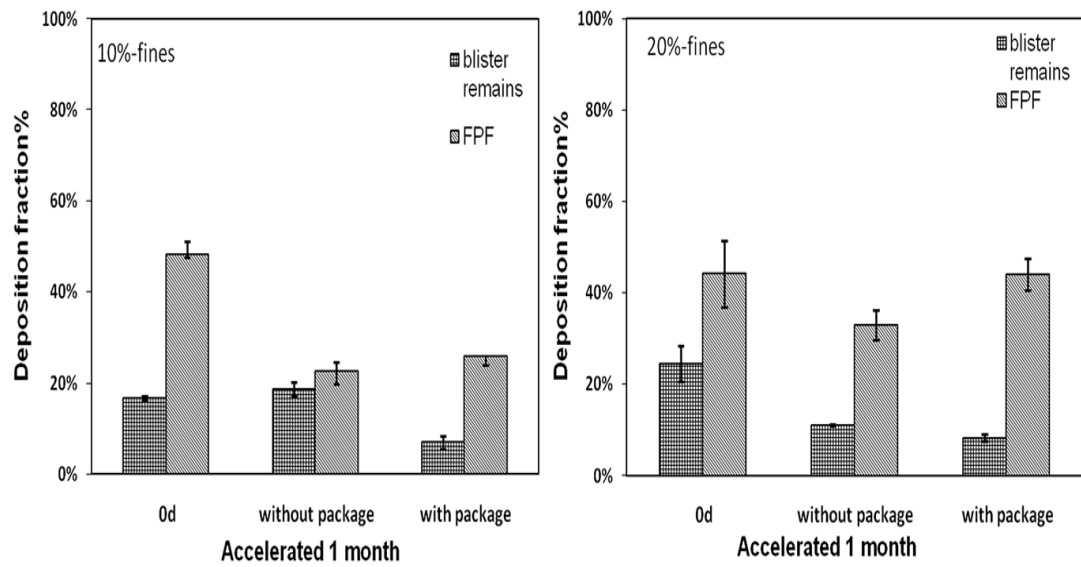


**Figure 7.26: The FPF and blister remains of initial and accelerated test for 1 month with/without external foil packages.**

**Table 7.36: The FPF and blister remains results of the initial and accelerated test for 1 month with/without external foil packages**

TI test (n=2)		40°C, RH75%, 1month		
		Oday	Without packaging	With package
0%	FPF-AVG	30.0%	5.5%	30.2%
	SD	2.2%	0.2%	0.2%
	Remains-AVG	12.5%	26.5%	9.9%
	SD	3.6%	11.2%	0.8%
5%	FPF-AVG	39.7%	15.0%	41.2%
	SD	4.8%	2.3%	2.7%
	Remains-AVG	15.7%	22.2%	10.7%
	SD	2.1%	0.3%	0.8%
10%	FPF-AVG	48.3%	22.6%	25.9%
	SD	0.8%	2.9%	2.0%
	Remains-AVG	16.7%	18.6%	7.0%
	SD	0.4%	1.5%	1.4%
20%	FPF-AVG	44.2%	33.0%	43.9%
	SD	7.3%	3.2%	3.5%
	Remains-AVG	24.5%	11.0%	8.3%
	SD	3.9%	0.2%	0.7%

It is interesting to find that various powders show different anti-moisture performance, since these 4 powders without external package experience dissimilar FPF declines from the initial value. The powder containing 20% fines exhibits the best stability without external package, and 0%-fines powder shows the worst stability by contrary. Consequently, the stability performance is speculated to be related to the percentage of fine lactose in a formulation. The formulation would be more stable with more fine lactose. As a conclusion of this experiment, an external foil package is essential to ensure product stability.

Following that, the influence of desiccant on the FPF performance was also investigated. One group of disks was wrapped by an external foil package with a certain amount of desiccant in it and the other group was wrapped by foil without desiccant. Here, the representative powders containing 0% and 20% fines were tested under 25°C, RH92.5% for 5/10 days which was a typical humidity condition for a stress test.

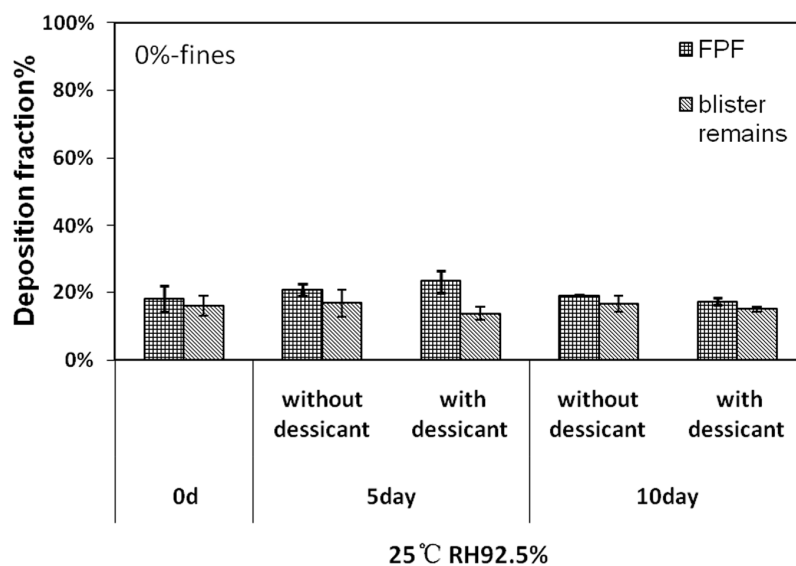


**Figure 7.27: The FPF and blister remains of stress test for 0/5/10 days with/without desiccant. 0%-fines formulation.**

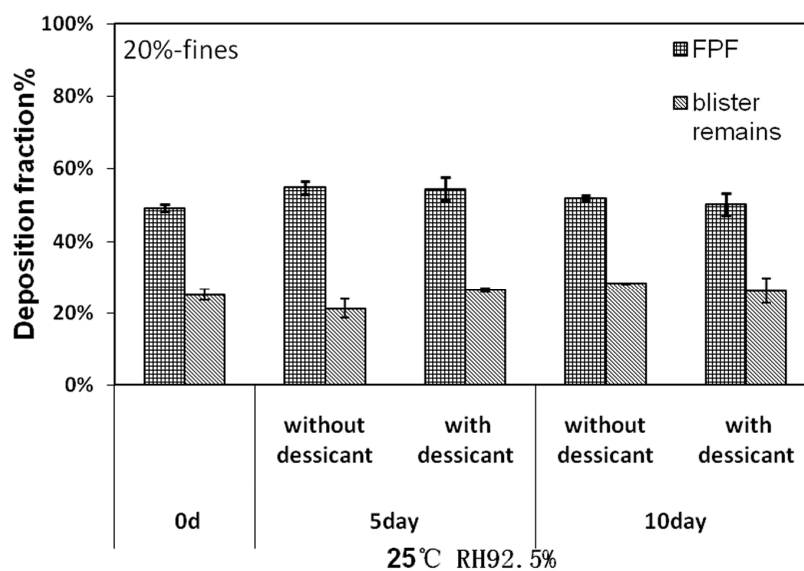


**Figure 7.28: The FPF and blister remains of stress test for 0/5/10 days with/without desiccant. 20%-fines formulation.**

**Table 7.37: The FPF and blister remains results of stress test for 0/5/10 days with/without desiccant**

TI test (n=2)		0day	25°C, RH92.5%			
			5day		10day	
			Without desiccant	With desiccant	Without desiccant	With desiccant
0%	FPF-AVG	18.0%	20.6%	23.2%	19.0%	17.3%
	SD	3.9%	1.8%	3.3%	0.2%	1.0%
	Remains-AVG	15.9%	16.7%	13.7%	16.6%	15.0%
	SD	2.9%	4.1%	1.9%	2.4%	0.8%
20%	FPF-AVG	49.2%	54.8%	54.5%	52.0%	50.3%
	SD	1.0%	1.7%	3.2%	0.7%	3.1%
	Remains-AVG	25.1%	21%	26%	28.3%	26.2%
	SD	1.5%	2.7%	0.5%	0.1%	3.4%

As we can see from Fig.7.27, Fig.7.28 and Table 7.37, the FPF is relatively stable under the high humidity environment for both 0%- and 20%-fines formulation. Besides, the desiccant seems to be useless, since the samples without desiccant also show good stability of FPF. Consequently, this experiment does not display desiccant's influence on keeping DPI stability. As mentioned above, the humidity exert a great influence on the FPF performance of a DPI, therefore the extreme humidity (RH92%) is expected to affect the FPF significantly. Yet, the results do not comply with the expectation. Firstly, it is inferred that the external foil package provides good protection against humidity. Secondly, the time for this stress test is not long enough to allow ingress of moisture into packages. Or, the influence of moisture on interactions between particles may require a longer time than 10 days. Similar results are obtained during the development of other DPI inhaler products in our group. When the inhalers are exposed to RH92% for 10 days, the FPF performance does not show any decline but experiences an obvious decrease when exposed to RH75% for 1 month. Therefore, it is inferred that not only the relative humidity but also the equilibrium time influence the stability of FPF performance. The invasion of moisture into the foil package, the absorption of moisture on the particle surface, and capillary force working require a relatively long time. Consequently, the FPF

performance stability need to be studied in a long term but not in a stress test. For example, the result of a high humidity test may lead to a false prediction of stability.

### 7.6.2 The accelerated stability of different formulations

Usually, a stress test including high temperature, high humidity, and intense light is used to study which factor may greatly influence the stability of the formulation. Then those stability data are more meaningful for selecting package and storage condition. As a contrast, an accelerated test is commonly applied to speculate the product shelf life, as it can reflect the product stability much better. For this reason, some different formulations are placed under 40°C, RH75% and tested by TI (Twin Impinger) impaction. At first, the formulations containing 0, 5, 10, and 20% fines are studied.

As Fig.7.29 and Fig.7.30, the 0%-fines and 5%-fines formulation show a similar stability trend under an accelerated condition. At first month, the FPF does not show obvious change but blister remains are decreased. Then the FPF decreases a little and blister remains experience a dramatic rise. Generally speaking, the FPF is relatively stable with an acceptable drop. The blister remains go up remarkably and it may influence the delivery uniformity. Consequently, the delivered dose results at each time point are collected and presented in Fig.7.31.

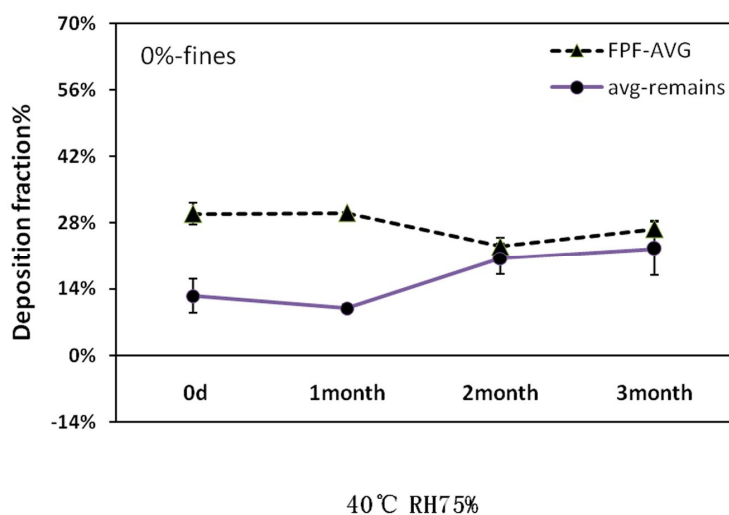


**Figure 7.29: The FPF and blister remains of accelerated tests for 0%-fines formulation.**



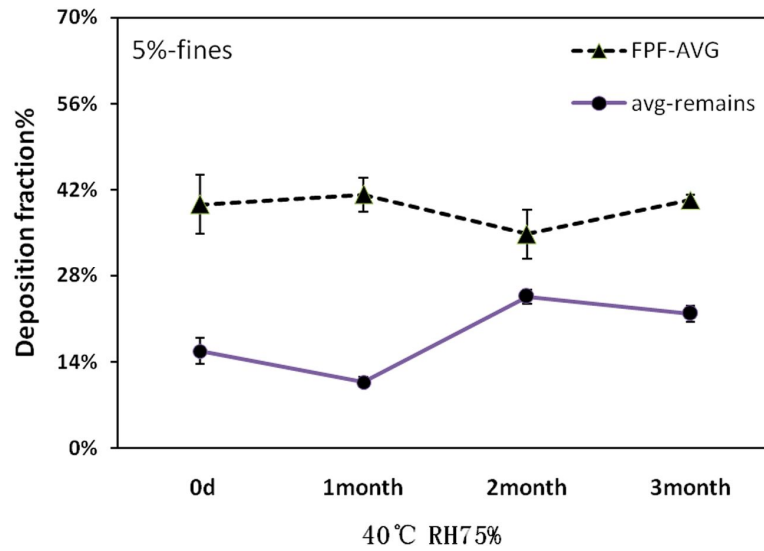


**Figure 7.30: The FPF and blister remains of accelerated tests for 5%-fines formulation.**

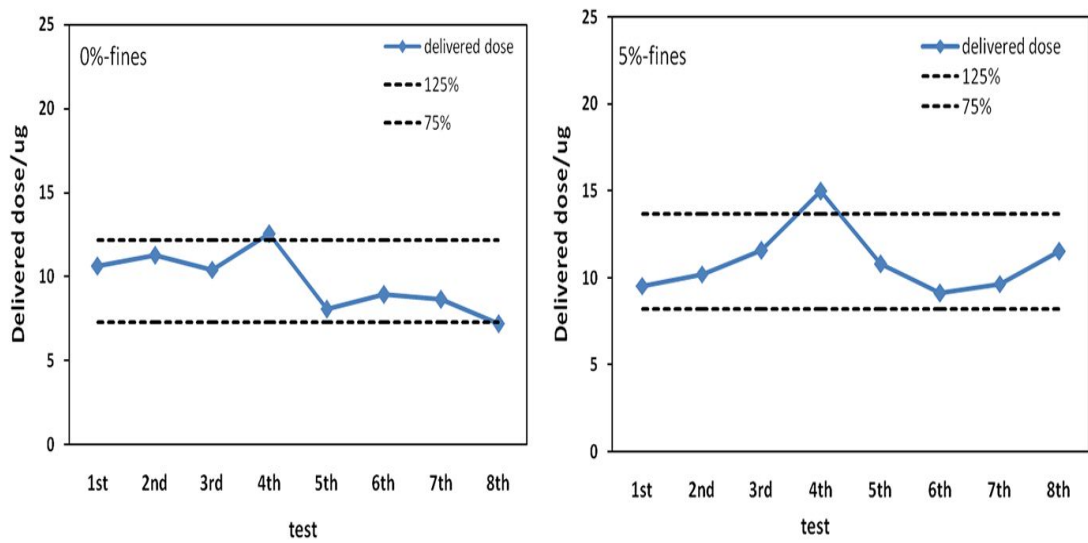


**Figure 7.31: The uniformity of delivered dose of accelerated tests for 0%- and 5%-fines formulation.**

The delivered dose uniformity of 0% and 5%-fines formulation is presented in Fig.7.31. Most delivered doses are within the acceptable range except for the 4<sup>th</sup> point where the delivered dose is higher than the upper limit.

The trends of blister remains for 10%-fines and 20%-fines are similar as 5% and 10%-fines. The ratio of the blister remains experiences a decline at the first month and then a rise. Nevertheless, the blister remains for 10% and 20%-fines formulation are relatively constant when comparing the 3month values to the initial values. The phenomenon of blister remains going down first and then up is rather confusing. Above all, an accidental error should be excluded, since all samples tested at 1<sup>st</sup> month show a decline and the results of two repeated tests present a very small variation. Then, an assumption is proposed. After the first month, the electrostatic force between particle and PVC disk decrease a lot. The descending electrostatic force results in less adhesion and smaller blister remains. But for next 2 months, the adhesion caused by capillary force becomes the dominant and results in the growth of blister remains.

When considering the FPF performance, the 10% and 20%-fines formulation show a completely opposite trend as Fig.7.32 and Fig.7.33. The FPF of 10%-fines formulation presents an abrupt drop at first month, and then is almost stable for next 2 months. The FPF of 20%-fines is stable at first month and then shows a gradually rising trend for following months. The results are rather confusing, which require further research and more stability data. However, it is conclusive that the ratio of fine lactose exert a great influence on the performance stability.

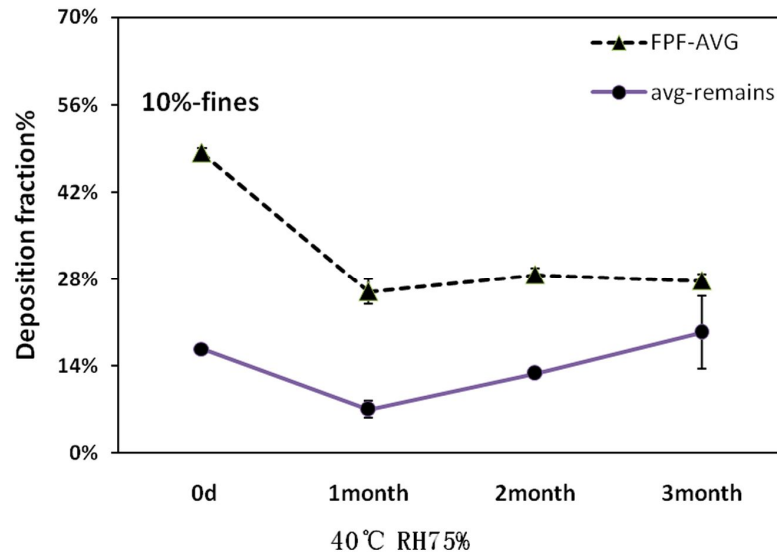


**Figure 7.32: The FPF and blister remains of accelerated tests for 10%-fines formulation.**

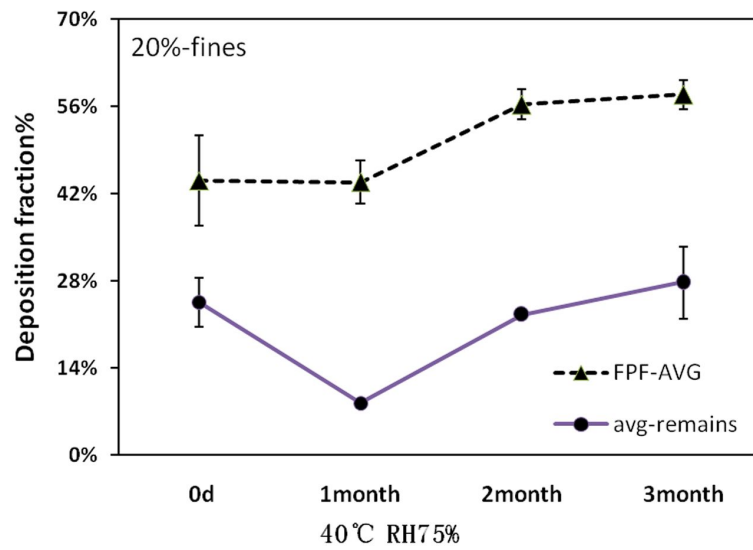


**Figure 7.33: The FPF and blister remains of accelerated tests for 20%-fines formulation.**

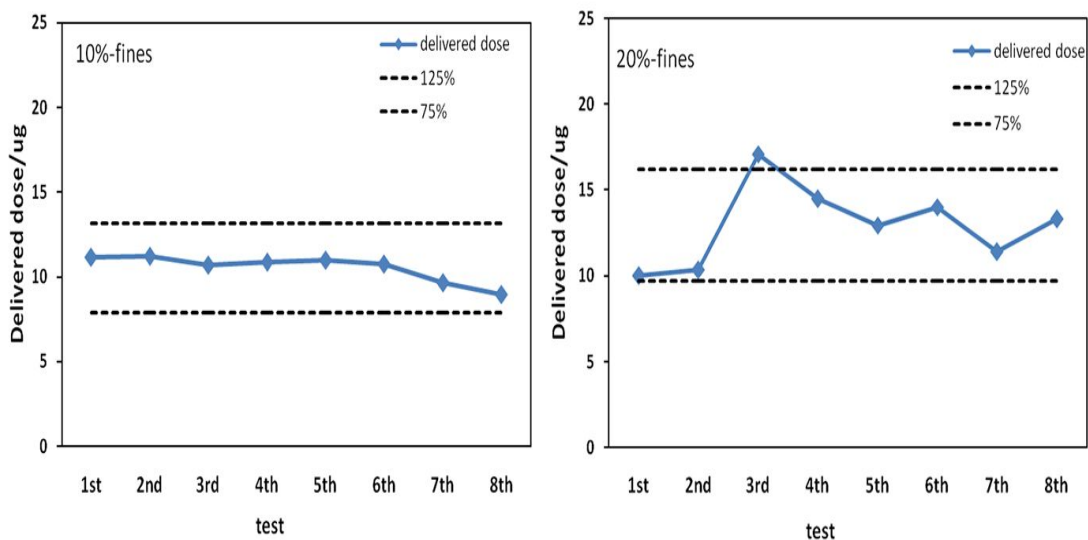


**Figure 7.34: The uniformity of delivered dose of accelerated tests for 10% and 20%-fines formulation.**

The delivered dose uniformity of 10% and 20%-fines formulation is presented in Fig.7.34. The result of 20%-fines is similar as 0% or 5%-fines formulation. The delivered doses of 20%-fines formulation are within the acceptable range except for one point. The delivered dose of 10%-fines is quite excellent, with all doses in the acceptable range.

**Table 7.38: The FPF and blister remains results of accelerated tests for 4 powders**

TI test (n=2)		Accelerated test, 40°C RH75%			
		0d	1month	2month	3month
0%fines	FPF-AVG	30.0%	30.2%	23.1%	26.8%
	SD	2.2%	0.2%	1.9%	1.7%
	Avg-remains	12.5%	9.9%	20.5%	22.6%
	SD	3.6%	0.8%	3.3%	5.6%
5%fines	FPF-AVG	39.7%	41.2%	34.8%	40.4%
	SD	4.8%	2.7%	4.0%	0.8%
	Avg-remains	15.7%	10.7%	24.5%	21.8%
	SD	2.1%	0.8%	1.1%	1.3%
10%fines	FPF-AVG	48.3%	25.9%	28.7%	27.7%
	SD	0.8%	2.0%	1.1%	1.0%
	Avg-remains	16.7%	7.0%	12.8%	19.4%
	SD	0.4%	1.4%	0.1%	5.8%
20%fines	FPF-AVG	44.2%	43.9%	56.4%	57.9%
	SD	7.3%	3.5%	2.4%	2.3%
	Avg-remains	24.5%	8.3%	22.6%	27.7%
	SD	3.9%	0.7%	0.1%	5.9%

As a conclusion of these stability experiments, the 0% and 5%-fines formulation show the FPF stability after 3 month in the accelerated tests. The 20%-fines powder experiences a slow rise during accelerated test, which is also observed in other stability tests for powders with more fine particles. The 10%-fines formulation is also acceptable, because accelerated results are quite stable after 1<sup>st</sup> month. This phenomenon provides a possible solution to the dramatic decline at first month, which is to place the products under a certain environment for some time. When the FPF becomes stable, those products can be tested or dispersed to patients.

In addition to the influence of fine-lactose percentage on stability, the size of carrier lactose is studied preliminarily. The sieved lactose from Inhalac 230 with 4 different sizes (<45µm, 45-75µm, 75-100µm, 100-150µm) is further studied for stability. These samples are placed under 40°C, RH75% for 1 month.

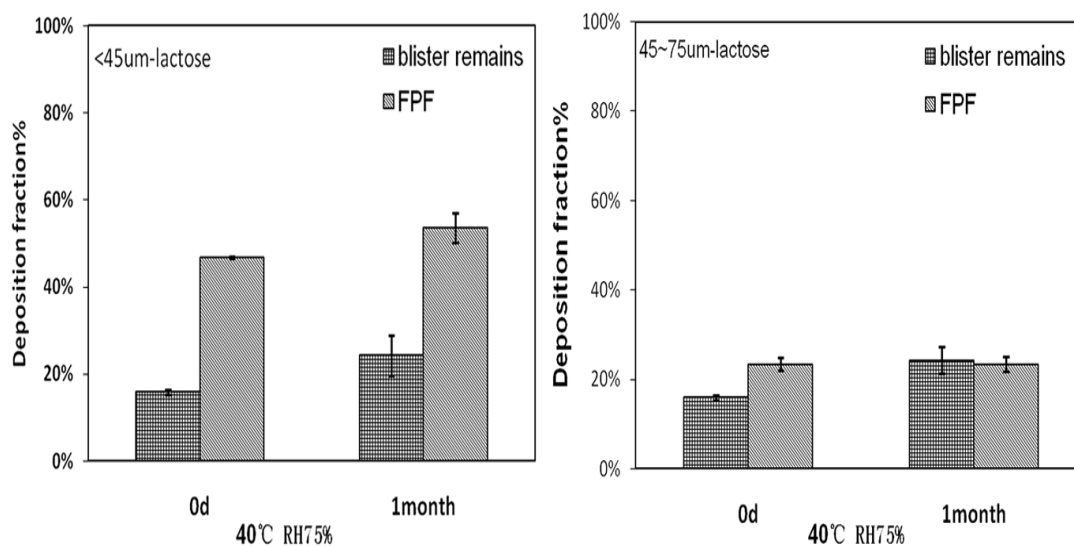


**Figure 7.35: The FPF and blister remains of accelerated tests for lactose <45µm and within 45~75µm.**

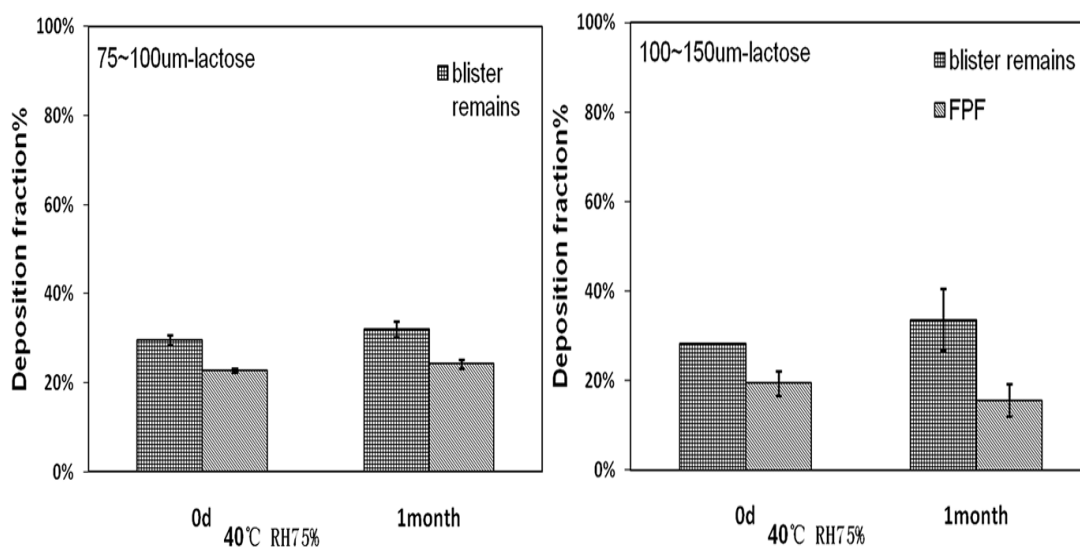


**Figure 7.36: The FPF and blister remains of accelerated tests for lactose within 75~100µm and 100~150µm.**

The results are shown in Fig.7.35, Fig.7.36 and Table 7.39. These results demonstrate that different-size lactose exhibit various stabilities. Specifically, the FPF of smallest

lactose (<45 $\mu$ m) experiences a little rise after 1 month whereas the largest lactose (100~150 $\mu$ m) shows a slight decline after 1 month. Meanwhile, the FPF of lactose within 45~75 $\mu$ m and 75~100 $\mu$ m almost do not show any alteration. It is relatively easy to explain the FPF decline or constant FPF values, but it is difficult to guess the reason for FPF raise. Here, the ascending of FPF after 1 month is explained by that fine particles formed tight agglomerates initially as a result of electrostatic force or other forces, and those interaction forces become weaker after a month. Yet, this assumption is difficult to validate. The increasing FPF for lactose <45 $\mu$ m is consistent with stability results of 20%-fines formulation, which has the most fine particles. The latter one also shows an upward trend during the accelerated test. The decline of FPF for lactose within 100~150 $\mu$ m is similar as the FPF drop of formulations without fines. Different-size lactose present different FPF stability, which may be helpful to understand the confusing stability results of formulations with different amount of fine lactose.

**Table 7.39: The FPF and blister remains results of accelerated tests for different-size lactose**

TI test (n=2)	<45 $\mu$ m		45-75 $\mu$ m		75-100 $\mu$ m		100-150 $\mu$ m	
	0d	1month	0d	1month	0d	1month	0d	1month
FPF-AVG	46.8%	53.6%	23.4%	23.4%	22.8%	24.2%	19.4%	15.6%
SD	0.3%	3.5%	1.4%	1.6%	0.5%	1.0%	2.8%	3.6%
Avg-remains	15.9%	24.3%	27.4%	27.0%	29.6%	32.1%	28.3%	33.6%
SD	0.6%	4.6%	0.5%	2.9%	1.1%	1.8%	0.1%	7.0%

### 7.6.3 The performance stability of under different flow rates

One important characteristic of an ideal DPI is to exhibit similar FPF performance under different flow rates. The formulation including 0.72% sulfate Salbutamol and about 99% lactose (45~75 $\mu$ m) was tested for TI (Twin Impinger) impaction under 30LPM and 60LPM respectively.

The result is shown in Fig.7.37. It is reasonable that the larger flow rate produces a better fluidization and entrainment effect. As a result, more particles are taken into the air flow, and the blister remains decrease correspondingly. The FPF values of high and low flow rate are similar, implying that the inhaler can be operated under high or low flow rate.

This result is an attractive characteristic for a DPI. The lower FPF produced by the higher flow rate can be explained by that impaction of particles on the throat part of TI become more serious under high flow rate. When tested at high flow rate, the particles acquire a higher initial speed and larger inertia when particle size does not change. As a result of larger inertia, the particles cannot change direction immediately and impact on the throat part. This assumption is proven by the fraction of API deposited on the throat part, which is 20% for low flow rate and 30% for the high one. This result implies the particles are effectively dispersed under 30 LPM as a sign for an excellent inhaler.

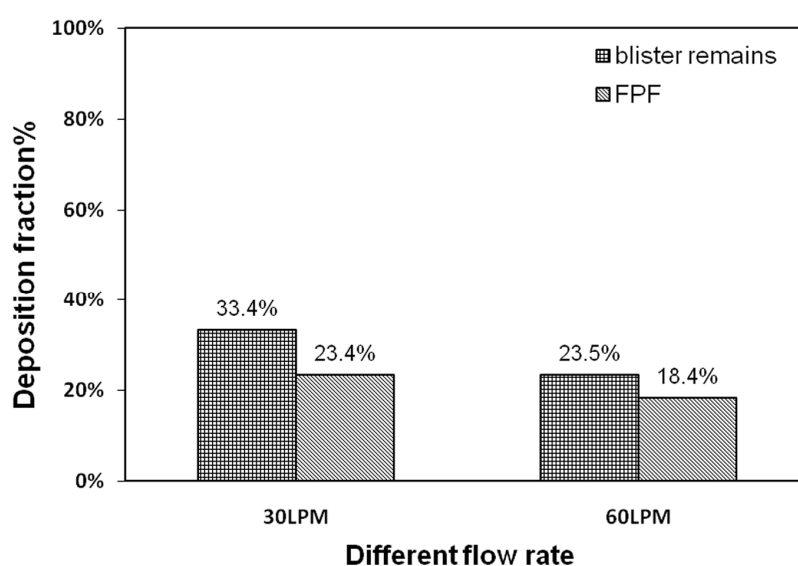


**Figure 7.37: The FPF and blister remains of high and low flow rate.**

## 7.7 Discussion

In recent years, the particle engineering is increasingly popular among pharmaceutical scientists to develop dry powder formulation for macromolecules. The common particle engineering technologies include a spray drying, spray freeze-drying and supercritical fluid (SCF). The spray drying is studied most extensively and has been applied in some marketed products, such as Nektar's Pulmosol®. <sup>[103]</sup>

There are some impressive advantages for particle engineering. For example, the shape, size and density of particles can be controlled by adjusting atomization parameters like



inlet/outlet temperature, feeding rate. Mostly important, sphere and hollow particles produced by the spray-drying present smaller aerodynamic diameter as a result of less density. These engineered particles can penetrate into the deep lung and keep good flowability at the same time<sup>[157; 158]</sup>. Additionally, the porous and hollow particles exhibit low inter-patient variability and flow rate independence<sup>[109]</sup>.

Nevertheless, the application of particle engineering is still limited for its stability problems. The instability may be caused by a transient exposure of API to high temperature and high flow jet, or a physical alteration like a transformation of crystalline phase. Due to a rapid precipitation process in the spray-drying or SCF, there is not enough time for the nucleation of API. Therefore, the spray-dried substance exist mainly in amorphous state, making it a big challenge for physical stability. First of all, the amorphous state is metastable with excess entropy and free energy which may experience “annealing” or “aging” during storage. The amorphous particles are transformed slowly to crystalline and the surface change from smooth to rough during storage<sup>[159]</sup>. Secondly, an amorphous material is more sensitive to moisture for its larger surface area. And a small amount of moisture may decrease the glass transition temperature (T<sub>g</sub>) greatly, resulting in a dramatic drop of stability<sup>[160]</sup>. To improve the T<sub>g</sub> of an amorphous formulation, other glass-forming agents are required. However, these agents may increase the complexity of formulation research as a result of safety and compatibility concerns<sup>[161; 162]</sup>. At last, small molecules with smaller configurational entropy are much easier to transform from amorphous to crystallization<sup>[163]</sup>. Consequently, a jet-mill micronization is still the most common method to prepare the API particles for respiratory drug delivery, especially for small molecules.

The API particles are micronized for several times. The results show that the particle size decrease with increasing times of jet-milling. Despite of various API sizes, the FPF performance does not show a great difference. Hence, the twice of jet-milling is applied for economic and stability consideration. As Fig.7.38, after a micronization, surface layers of particles become disrupted, leaving a small amount amorphous area. That amorphous content may go up with more times of micronization. Then, when these particles are exposed to water vapor and/or heat, the amorphous part may experience a

conversion to crystalline which result in inter-particle bridging or fusion shown in Fig.7.38. The formation of tight connection between particles will greatly influence the FPF performance<sup>[149; 164]</sup>.

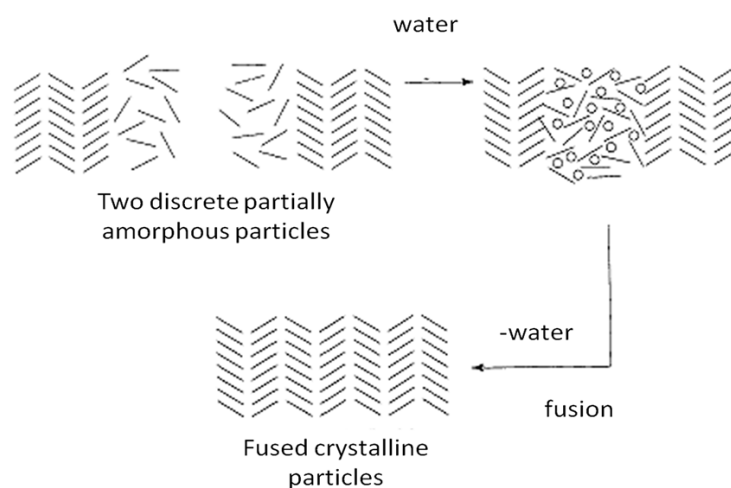


**Figure 7.38: The schematic of disorder and recrystallization on the surface of micronized particle.**

The intentional addition of a small amount of fine particle excipient into coarse lactose is a well developed technique to improve formulation performance and is applied widely in the development of dry powder formulation. This application of fine lactose is originated from the phenomenon that removal of intrinsic fines from a lactose carrier may decrease formulation performance, whereas adding fines of various materials into formulations can improve performance. There are two primary hypotheses to explain the role of fines. The first one suggests that the fines compete against the API particles for the “active” or “high energy” site on the coarse carrier. Hence, the fine additives may assist the detachment of API from carrier. The other one proposes that the fine lactose serve as a diluent to reduce the API-API interaction, and the fine lactose form agglomerates with the API which are easy to disperse during aerolization<sup>[95]</sup>.

The first hypothesis is supported by findings that the mixing sequence is important for enhancing FPF. This theory requires that the fine lactose should be mixed with coarse carrier first to occupy the “active” sites. For example, Zeng et al reported that mixing fine

and coarse lactose first showed higher FPF<sup>[165]</sup>, or the mixing sequence would affect the FPF<sup>[166]</sup>. However, there is also some literature reporting that the mixing sequence would not influence the final FPF results. The second hythe fine lactose

Lucas et al reported that when fine particle lactose was increased from 2.5% to 10%, the FPF showed a gradually but obvious increase. They also found that the improvement in performance was independent of the addition order of fine particle lactose<sup>[167]</sup>. Louery et al proposed a novel hypothesis involving competitive and multilayer adhesion when they found that a higher FPF obtained from the addition of fines. This improvement was independent of the mixing order<sup>[168]</sup>. On the other hand, it was reported that more API and fine lactose increased the API dispersion in carrier-based system. And the agglomeration as a result of high fine-particle load coincided with increased dispersion, which directly supported the second hypothesis.<sup>[169; 170]</sup>

When considering the effect of flow rate on the *in vitro* performance, the inertia of the particles determines their deposition. Usually, the inertia of a particle can be evaluated by a stop distance shown as the following formula.  $\rho$ 、 $v$ 、 $d$  represented the density, velocity and diameter of a moving particle respectively and  $\eta$  for viscosity. This equation is able to explain why larger particles impact on the earlier stages of cascade impactors. It also provides an interpretation why more particles deposit in the throat part of TI under a higher flow rate as we find. When the particle velocity is similar, the stop distance is proportional to the square of diameter. Hence, the difference of particle size is amplified and then distinguished by the stop distance. Meanwhile, when the particles size and density are similar, the higher flow rate makes the particle exhibit higher velocity, then the stop distance is increased and particles impact on the corner of the throat part<sup>[171]</sup>.

$$D_s = \frac{\rho * v * d^2}{18\eta}$$

The influence of flow rate on the blister remains can be explained by particle entrainment in a laminar wall boundary layer as Fig.7.39. The drag force ( $F_{drag}$ ) can be calculated by following formula, where  $C_D$  is drag coefficient,  $\rho$  for fluid density,  $A_f$  for cross area of a particle,  $U$  for fluid velocity. Based on an approximation that the  $C_D$  is constant, the

higher fluid velocity may produce a larger drag force. The lift force is similar as drag force. Consequently, the increase of drag force and lift force result in a better entrainment effect and reduce the blister remains<sup>[171; 172]</sup>.

$$F_{drag} = 0.5C_D * \rho_{fluid}A_fU^2$$

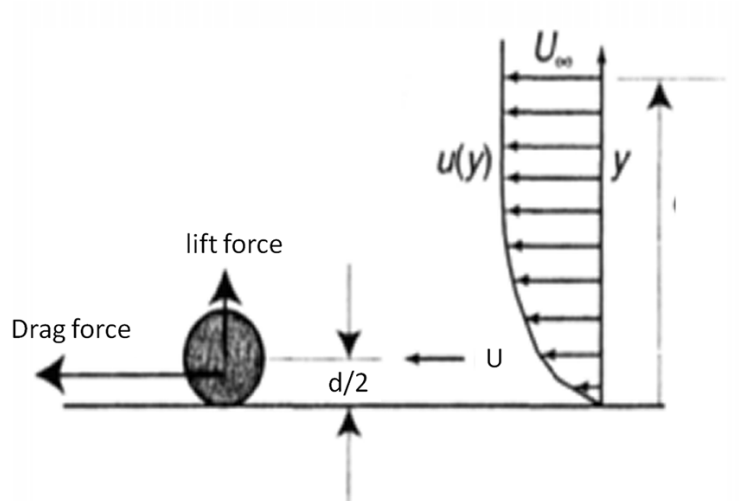


**Figure 7.39: The schematic particle entrainment in a laminar wall boundary layer.**

## Chapter 8

### 8 Conclusions and Future Directions

#### 8.1 Major Conclusions

A new dry powder inhaler device is designed, manufactured and evaluated. This device is characterized by micro-dose, passive drug delivery and multiple doses in one replaceable disk with each dose individually packaged. The evaluation results show that this device can deliver 2-3mg powder each time, disperse the powder effectively and obtain ideal *in vitro* depositions with suitable drug formulations.

A novel powder filling and packaging system is established specifically for this inhaler. This system can dispense a small amount of drug powder into blisters of a drug disk quickly and accurately. The uniformity evaluation demonstrates that the filling is rather uniform among disks and blisters, except for drug content among blisters of a disk. This uniformity problem does not affect the evaluation of inhaler at present and should be solved in the future.

Through a formulation study, it is found that the *in vitro* performance of this new inhaler can match different marketed products. Furthermore, the influence of various factors on the inhaler performance is clarified by a comprehensive and systemic formulation research.

The novel dry powder inhaler is the core part of this project, and the powder filling & packaging system and formulation research are designed and carried out based on the inhaler. Specifically, because the delivered dose is rather small for each blister, the filling system should be able to meter a small amount of powder accurately. Additionally, the arrangement of 14 blisters in one disk determines the mode of powder metering and filling. Meanwhile, the formulation has to be consistent with the inhaler and filling system. For example, the quantity of formulation is also small and flowability of the powder is suitable for filling. Most importantly, the formulation should be dispersed effectively by this novel inhaler device when administered.

Although the novel inhaler device is the key to the project, its performance is greatly dependent on other two components. For instance, the powder filling system would greatly affect the delivered drug uniformity, and packaging system would determine the performance stability. The drug delivery efficiency and uniformity are also determined by the formulation process and composition. Moreover, the formulation is the easiest variable and most convenient one to adjust to acquire a desired fine particle dose.

## 8.2 Summary of Key Results

During the establishment and validation of analytical methods, the HPLC method is validated according to the ICH requirements. All validation results demonstrate that the HPLC method is accurate, precise, sensitive, durable and reproducible. In addition, the methods of Twin Impinger (TI) and Next Generation Impactor (NGI) are also validated. The validation data show that the TI is accurate and durable. Besides, the stages of NGI need to be coated before an NGI test according to pharmacopoeias, since the APSD (Aerodynamic particle size distribution) of coated and uncoated NGI present a difference. Therefore, the impaction tests provide a reliable and widely accepted tool to study inhaler performance. Following that, the calibration of laser diffraction size measurement is also mentioned. This sizing method is applied as a fast, convenient and reliable method to analyze the formulation powder.

In chapter 5, typical marketed products including unit-dose inhaler (Aerolizer®), multiple unit-dose inhaler (Diskus®) and reservoir inhalers (Turbuhaler® and Clickhaler®) are evaluated first. The results of air flow resistance, DDCU (delivered drug content uniformity) and the FPF (fine particle fraction) of those marketed products are obtained and provide a comparison to the new inhaler designed by us.

When considering the novel inhaler of this project, the designated and mechanical functions are confirmed first. After design improvement, a dramatic drop of resistance from 0.218 to 0.062 kPa<sup>0.5</sup>\*min/l is observed. Meanwhile, the delivery efficiency is increased as the blister remains experience an obvious decline from 20% to 10%. Mouthpieces with different geometries are manufactured and tested. The result shows that air resistance is negatively correlated with the diameter of airway, but the APSD and

FPF are the same for 5 mouthpieces. Consequently, the original geometry of the mouthpiece is adopted. Through a parallel comparison with the marketed inhalers using the same formulation, the novel inhaler shows similar FPF as Aerolizer® and Clickhaler®, and better performance than Twister®.

The powder filling system is established and validated. The filling uniformity is studied in following sequence: 1) the filling weight uniformity among the disks, 2) filling weight uniformity among blisters of a disk, 3) drug content uniformity among disks and 4) drug content uniformity among blisters of a disk. During the uniformity evaluation, not only the filling operation but also the test methods influence the results. The RSD of filling weight and drug content among disks is about 1~3% and 3~5% respectively even for different powders. The RSD of filling weight among blisters of a disk is 6~8%, but the RSD is 10%~17% for drug content among blisters. Through a detailed investigation of drug content of each blister in one disk, it is suggested that dispersion of fine API particles during the powder transfer from metering pockets to blisters is the main reason for the slightly higher RSD of drug content among blisters. This assumption is verified by the experiment of vacuum-assisted filling and reduction of vibration strength in the powder transfer. As mentioned in the discussion part of chapter 6, the drug content uniformity among blisters do not affect the following research at present, since one disk is tested as a whole for inhaler evaluation. At last, a sketchy flowability range suitable for powder filling is set up, represented by compression indices from 20-45%.

When the novel inhaler device and filling system are ready, the formulation work is carried out thoroughly. The compatibility between powders and processing, the API and excipient, formulations and package is confirmed.

The API is micronized in our laboratory and the size distribution is acquired by laser diffraction sizing. The API particles are suitable for inhalation drug delivery since all X90 values are under 5 $\mu$ m. Following that, a mixing method including pre-sieving at first, then low shear and high shear mixing is established. This mixing method can obtain a powder with RSD<2% of drug content. Then, several critical parameters of the mixing are investigated. With increasing mixing speed and mixing time, the blend uniformity

does not show obvious improvement but the FPF experiences a decline. Specifically, when the mixing speed is doubled, the FPF decreases from 22% to 14%. The study of mixing time shows that, when the mixing time is increased from 0 to 20min, the FPF exhibit a decline from 34% to 22%.

During a composition research, the formulations containing SV003 and LH200 show similar FPF as Aerolizer® Foradil® and Diskus® Seretide®. The formulations containing Inhalac120 and Inhalac230 (<45µm) exhibit similar FPF as Turbuhaler® Oxis® and Clickhaler® Asmatha® respectively. The ratio of fine lactose and the API to the total powder, size and source of the coarse lactose, and size of the API particles are all studied. Different ratios of fine lactose to the whole powder exert a great influence on the FPF and the following performance stability. An exciting result is that the ratio of API to the powder does not affect the FPF, implying that the novel inhaler can be used to deliver various APIs for different delivered doses. Additionally, the FPF is rather stable for different-size API, indicating the durability and reproducibility of the inhaler performance.

An orthogonal experiment is completed after a series of sing-factor experiments. This statical result further proves the conclusion of single-factor tests. Meanwhile, because of the ratios of signal to noise obtained in this experiment, it is found that the percentage of fine lactose has the most significant effect on both FPF and blister remains. Consequently, the percentage of fines should be considered first in the future formulation work.

Through a stress test and accelerated test, the package form is determined. The drug disk should be wrapped with an aluminum foil as an external package without desiccant. Then, some formulations show satisfying stability under an accelerated condition for several months. The performance stability under different flow rates also demonstrates good FPF consistency.



### 8.3 Future Directions

Since the target of this project is to develop an inhaler product which can be commercialized some day, there will be some industrialization research required in the future.

For the inhaler device:

A fatigue test would be necessary to study and validate the mechanical property, such as how many times the device can be used without influence on drug delivery.

The materials of the device have to be chosen carefully. The ideal materials should exhibit a good mechanical property, lightweight and an acceptable price. Most importantly, the material should be approved by the regulatory agency for application in medical devices or health products.

Some volunteers and clinicians should be called together to use this device, and suggestions from them will be important for further improvement of device design.

For the powder filling:

First of all, the drug content uniformity among blisters should be enhanced by improving the design of filling machine. This filling uniformity is the prerequisite for the delivered drug content uniformity. If possible, the filling quantity should be adjusted conveniently.

Secondly, the operation of filling should be automated as much as possible; hence it can satisfy the requirements of a pilot-scale production. More importantly, an automated filling process is easier to comply with Good Manufacture Practice (GMP), and will minimize the possibility of contamination and operational errors.

At last, if possible, a monitoring system should be applied to monitor the filling weight online, which could detect the wrong filling and discard it immediately. To achieve those functions, it will be a complicated system requiring cooperation between pharmaceutical scientists and engineers.

For the powder formulation:

Most formulation research is carried out on a small scale here, and it should be scaled up to a pilot production. Then, the optimized formulation should be repeated for 3 batches. The performance and stability of 3 batch sample will be studied carefully for application documents of a drug product. A systematic evaluation should be carried out, including appearance, delivered drug content uniformity, FPF, moisture, degradation impurities and so on.

After formulation work, an acute toxicity and irritating experiment should be carried out on animals to demonstrate the safety of the inhaler. Both the API and excipient are quite safe since they have been applied in the commercial products for a long time. When the safety is established, a bioequivalence or clinical trial is required to demonstrate its efficacy, serving as an ultimate evaluation of the inhaler performance.

From a viewpoint of basic research, there are also some interesting topics deserving further investigations.

The computational fluid dynamic has been increasingly popular in the design of inhaler device. The entrainment of powder into airflow, dispersion of aerosol in the device could be treated as an air-solid interaction. The kinetic energy of turbulence, energy and times of particle impaction could be calculated and analyzed to find the relationship between the disaggregation of agglomerates and the aerodynamic design of the inhaler device.

The electrostatic property of powder and packaging material could be studied deeply, since there are few reports in that field. If possible, the unexpected dispersion of particles during powder transfer in the filling process could be related to the quantity of electricity of particles and PVC disks. Furthermore, the generation and dissipation of electrostatic charge of powder in the PVC blister could be studied, and it might explain why the freshly filled drug disk should be kept still for some time before tests.

During this research, commercial lactose is used as carriers, although the self-made lactose show interesting adhesion of fine particles. If possible, the effect of this adhesion on formulation performance should be studied. Most literature on the mixing process

utilize low shear mixing equipment to study the influence of mixing speed or time. If an appropriate high shear mixer is available which could process a small amount of powder and adjust/display the mixing speed, the relation between speed/time of high shear mixing and formulation performance can be studied in detail.

The novel inhaler device also provides a good platform to deliver other inhaled powders. Consequently, engineering powders like spray-drying particles could also be applied in this device. Then, the application range of the inhaler device may be expanded greatly.

## References

- [1] Yu, J., & Chien, Y. W. (1997). Pulmonary drug delivery: physiologic and mechanistic aspects. *Crit Rev Ther Drug Carrier Syst*, 14, 395-453.
- [2] Groneberg, D. A., Witt, C., Wagner, U., et al. (2003). Fundamentals of pulmonary drug delivery. *Respir Med*, 97, 382-387.
- [3] Anderson, G. P. (1993). Formoterol: pharmacology, molecular basis of agonism, and mechanism of long duration of a highly potent and selective beta 2-adrenoceptor agonist bronchodilator. *Life Sci*, 52, 2145-2160.
- [4] Donohue, J. F., & Fromer, L. (2006). Long-acting beta-agonists role in asthma management. *J Fam Pract, Suppl*, 1-6.
- [5] Nagai, A. (2007). [Guideline for COPD management and prevention]. *Nihon Rinsho*, 65, 594-598.
- [6] Smyth, A., Touw, D., Tan, K. H., et al. (2005). Tobramycin dosing in cystic fibrosis. *Lancet*, 365, 1767-1768.
- [7] Kuver, R., & Lee, S. P. (2006). Hypertonic saline for cystic fibrosis. *N Engl J Med*, 354, 1848-1851; author reply 1848-1851.
- [8] Griesenbach, U., Geddes, D. M., & Alton, E. W. (2004). Gene therapy for cystic fibrosis: an example for lung gene therapy. *Gene Ther*, 11 Suppl 1, S43-50.
- [9] Ibrahim, B. M., Park, S., Han, B., et al. (2011). A strategy to deliver genes to cystic fibrosis lungs: a battle with environment. *J Control Release*, 155, 289-295.
- [10] Sweet, D., Bevilacqua, G., Carnielli, V., et al. (2007). European consensus guidelines on the management of neonatal respiratory distress syndrome. *J Perinat Med*, 35, 175-186.

- [11] Shoyele, S. A., & Slowey, A. (2006). Prospects of formulating proteins/peptides as aerosols for pulmonary drug delivery. *International Journal of Pharmaceutics*, 314, 1-8.
- [12] Patton, J. S., & Byron, P. R. (2007). Inhaling medicines: delivering drugs to the body through the lungs. *Nature Reviews Drug Discovery*, 6, 67-74.
- [13] Strack, T. R. (2006). Inhaled human insulin. *Drugs Today (Barc)*, 42, 207-221.
- [14] Jani, R., Triplitt, C., Reasner, C., et al. (2007). First approved inhaled insulin therapy for diabetes mellitus. *Expert Opin Drug Deliv*, 4, 63-76.
- [15] Vanbever, R. (2005). Performance-driven, pulmonary delivery of systemically acting drugs. *Drug Discovery Today: Technologies*, 2, 39-46.
- [16] Ekunwe, E. O. (1990). Immunization by inhalation of aerosolized measles vaccine. *Ann Trop Paediatr*, 10, 145-149.
- [17] Sabin, A. B., Flores Arechiga, A., Fernandez de Castro, J., et al. (1983). Successful immunization of children with and without maternal antibody by aerosolized measles vaccine. I. Different results with undiluted human diploid cell and chick embryo fibroblast vaccines. *Jama*, 249, 2651-2662.
- [18] Bisgaard, H. (2002). *Drug Delivery to the Lung*. New York: Marcel Dekker.
- [19] Hickey, A. J. (2004). *pharmaceutical inhalation aerosol technology*. New York: Marcel Dekker.
- [20] Lipworth, B. J. (1996). Pharmacokinetics of inhaled drugs. *Br J Clin Pharmacol*, 42, 697-705.
- [21] Usmani, O. S., Biddiscombe, M. F., & Barnes, P. J. (2005). Regional lung deposition and bronchodilator response as a function of beta(2)-agonist particle size. *American Journal of Respiratory and Critical Care Medicine*, 172, 1497-1504.

- [22] Labiris, N. R., & Dolovich, M. B. (2003). Pulmonary drug delivery. Part I: physiological factors affecting therapeutic effectiveness of aerosolized medications. *Br J Clin Pharmacol*, 56, 588-599.
- [23] Mitchell, J. P., Nagel, M. W., Nichols, S., et al. (2006). Laser diffractometry as a technique for the rapid assessment of aerosol particle size from inhalers. *Journal of aerosol medicine*, 19, 409-433.
- [24] Yeo, L. Y., Friend, J. R., McIntosh, M. P., et al. (2010). Ultrasonic nebulization platforms for pulmonary drug delivery. *Expert Opin Drug Deliv*, 7, 663-679.
- [25] Skaria, S., & Smaldone, G. C. (2010). Omron NE U22: Comparison between vibrating mesh and jet nebulizer. *J Aerosol Med Pulm Drug Deliv*, 23, 173-180.
- [26] Daniher, D. I., & Zhu, J. (2008). Dry powder platform for pulmonary drug delivery. *Particuology*, 6, 225-238.
- [27] Wong, W., Fletcher, D. F., Traini, D., et al. (2011). Particle aerosolisation and break-up in dry powder inhalers: evaluation and modelling of the influence of grid structures for agglomerated systems. *J Pharm Sci*, 100, 4710-4721.
- [28] Zhou, Q. T., Tong, Z., Tang, P., et al. (2013). Effect of device design on the aerosolization of a carrier-based dry powder inhaler--a case study on Aerolizer((R)) Foradile ((R)). *Aaps J*, 15, 511-522.
- [29] Dahl, R., Backer, V., Ollgaard, B., et al. (2003). Assessment of patient performance of the HandiHaler compared with the metered dose inhaler four weeks after instruction. *Respir Med*, 97, 1126-1133.
- [30] Pavkov, R., Mueller, S., Fiebich, K., et al. (2010). Characteristics of a capsule based dry powder inhaler for the delivery of indacaterol. *Curr Med Res Opin*, 26, 2527-2533.
- [31] Jiang, L., Tang, Y., Zhang, H., et al. (2012). Importance of powder residence time for the aerosol delivery performance of a commercial dry powder inhaler Aerolizer((R)). *J Aerosol Med Pulm Drug Deliv*, 25, 265-279.

- [32] Wong, W., Fletcher, D. F., Traini, D., et al. (2012). The use of computational approaches in inhaler development. *Adv Drug Deliv Rev*, 64, 312-322.
- [33] Coates, M. S., Chan, H. K., Fletcher, D. F., et al. (2006). Effect of design on the performance of a dry powder inhaler using computational fluid dynamics. Part 2: Air inlet size. *J Pharm Sci*, 95, 1382-1392.
- [34] Chrystyn, H. (2007). The Diskus: a review of its position among dry powder inhaler devices. *Int J Clin Pract*, 61, 1022-1036.
- [35] Kontny, M. J., & Mulski, C. A. (1989). Gelatin capsule brittleness as a function of relative humidity at room temperature. *International Journal of Pharmaceutics*, 54, 79-85.
- [36] Ronmark, E., Jogi, R., Lindqvist, A., et al. (2005). Correct use of three powder inhalers: comparison between Diskus, Turbuhaler, and Easyhaler. *J Asthma*, 42, 173-178.
- [37] Van Der Palen, J., Eijsvogel, M. M., Kuipers, B. F., et al. (2007). Comparison of the Diskus inhaler and the Handihaler regarding preference and ease of use. *J Aerosol Med*, 20, 38-44.
- [38] Fuller, R. (1995). The Diskus: a new multi-dose powder device--efficacy and comparison with Turbuhaler. *J Aerosol Med*, 8 Suppl 2, S11-17.
- [39] Sumby, B., Slater, A., Atkins, P. J., et al. (1997). Review of dry powder inhalers. *Adv Drug Deliv Rev*, 26, 51-58.
- [40] Wetterlin, K. (1988). Turbuhaler: a new powder inhaler for administration of drugs to the airways. *Pharm Res*, 5, 506-508.
- [41] Smith, I. J., & Parry-Billings, M. (2003). The inhalers of the future? A review of dry powder devices on the market today. *Pulm Pharmacol Ther*, 16, 79-95.
- [42] Borgstrom, L., Asking, L., & Thorsson, L. (2005). Idealhalers or realhalers? A comparison of Diskus and Turbuhaler. *Int J Clin Pract*, 59, 1488-1495.

- [43] Bisgaard, H., Klug, B., Sumby, B. S., et al. (1998). Fine particle mass from the Diskus inhaler and Turbuhaler inhaler in children with asthma. *Eur Respir J*, *11*, 1111-1115.
- [44] Borgstrom, L., Bengtsson, T., Derom, E., et al. (2000). Variability in lung deposition of inhaled drug, within and between asthmatic patients, with a pMDI and a dry powder inhaler, Turbuhaler. *Int J Pharm*, *193*, 227-230.
- [45] Selroos, O., Borgstrom, L., & Ingelf, J. (2006). Performance of Turbuhaler((R)) in Patients with Acute Airway Obstruction and COPD, and in Children with Asthma : Understanding the Clinical Importance of Adequate Peak Inspiratory Flow, High Lung Deposition, and Low In Vivo Dose Variability. *Treat Respir Med*, *5*, 305-315.
- [46] Martin, G. P., Marriott, C., & Zeng, X. M. (2007). Influence of realistic inspiratory flow profiles on fine particle fractions of dry powder aerosol formulations. *Pharm Res*, *24*, 361-369.
- [47] Rau, J. L. (2006). Practical problems with aerosol therapy in COPD. *Respir Care*, *51*, 158-172.
- [48] De Boer, A. H., Gjaltema, D., & Hagedoorn, P. (1996). Inhalation characteristics and their effects on *in vitro* drug delivery front dry powder inhalers Part 2: Effect of peak flow rate (PIFR) and inspiration time on the *in vitro* drug release from three different types of commercial dry powder inhalers. *International Journal of Pharmaceutics*, *138*, 45-56.
- [49] Harper, N. J., Gray, S., De Groot, J., et al. (2007). The design and performance of the exubera pulmonary insulin delivery system. *Diabetes Technol Ther*, *9 Suppl 1*, S16-27.
- [50] Hickey, A. J. (2013). Back to the future: inhaled drug products. *J Pharm Sci*, *102*, 1165-1172.
- [51] Donovan, M. J., Gibbons, A., Herpin, M. J., et al. (2011). Novel dry powder inhaler particle-dispersion systems. *Ther Deliv*, *2*, 1295-1311.



- [52] Corcoran, T. E., Venkataramanan, R., Hoffman, R. M., et al. (2013). Systemic delivery of atropine sulfate by the MicroDose Dry-Powder Inhaler. *J Aerosol Med Pulm Drug Deliv*, 26, 46-55.
- [53] Yang, J. R. G. E. (2007). Metering and dispensing of powder; the quest for new solid free forming techniques. *Powder Technology*, 56-72.
- [54] David, E. (2010). Applications of capsule dosing techniques for use in dry powder. *Therapeutic Delivery*, 1, 195-201.
- [55] Fadi, E., Morgane, L., & Stephen, E. (2011). Low powder mass filling of powders inhalation formulations. *Drug Development and Industrial Pharmacy*, 37, 24–32.
- [56] Edwards, D., & Johnston, J. (2011). Maximising effectiveness of DPI capsules. *Pharmaceutical Manufacturing and Packing Sourcer*, 86-87.
- [57] Simon, B., Imogen, G., David, E., et al. (2002). Advance in powder dosing technology. *Innovations in Pharmaceutical Technology*, 95-100.
- [58] Craig, J. (2010). Considerations and Approaches for Filling Dry-Powder Inhalers. *Pharmaceutical Technology*, s21-s25.
- [59] Chen. (2012). Development of a micro dosing system for fine powder using a vibrating capillary Part 1: The investigation of factors influencing on the dosing performance. *International Journal of Pharmaceutics*, 34- 41.
- [60] Chen, X., Seyfang, K., & Steckel, H. (2012). Development of a micro-dosing system for fine powder using a vibrating capillary. Part 2. The implementation of a process analytical technology tool in a closed-loop dosing system. *International Journal of Pharmaceutics*, 433, 42-50.
- [61] Zhu, J., & Ma, Y. (2006). A new breath-activated, excipient-free dry powder inhaler and a rotating fluidized bed powder dispenser for pulmonary drug delivery [C]. In *Respiratory Drug Delivery X* (pp. 925–930).

- [62] Zhu, J., Wen, J., Ma, Y., et al. (2004). Apparatus for volumetric metering of small quantity of powder from fluidized beds [P]. U.S. Patent 6,684,917. In.
- [63] Begat, P., Morton, D. A., Staniforth, J. N., et al. (2004). The cohesive-adhesive balances in dry powder inhaler formulations I: Direct quantification by atomic force microscopy. *Pharm Res*, 21, 1591-1597.
- [64] Atkins, P. J. (2005). Dry powder inhalers: an overview. *Respir Care*, 50, 1304-1312; discussion 1312.
- [65] Chew, N. Y. K., Tang, P., Chan, H. K., et al. (2005). How much particle surface corrugation is sufficient to improve aerosol performance of powders? *Pharmaceutical Research*, 22, 148-152.
- [66] Price, R., Young, P. M., Edge, S., et al. (2002). The influence of relative humidity on particulate interactions in carrier-based dry powder inhaler formulations. *Int J Pharm*, 246, 47-59.
- [67] Berard, V., Lesniewska, E., Andres, C., et al. (2002). Dry powder inhaler: influence of humidity on topology and adhesion studied by AFM. *Int J Pharm*, 232, 213-224.
- [68] Telko, M. J., & Hickey, A. J. (2005). Dry powder inhaler formulation. *Respir Care*, 50, 1209-1227.
- [69] Watanabe, H., Ghadiri, M., Matsuyama, T., et al. (2007). Triboelectrification of pharmaceutical powders by particle impact. *Int J Pharm*, 334, 149-155.
- [70] Pu, Y., Mazumder, M., & Cooney, C. (2009). Effects of electrostatic charging on pharmaceutical powder blending homogeneity. *J Pharm Sci*, 98, 2412-2421.
- [71] Zhu, K., Tan, R. B., Chen, F., et al. (2007). Influence of particle wall adhesion on particle electrification in mixers. *Int J Pharm*, 328, 22-34.

- [72] Zhu, K., Ng, W. K., Shen, S., et al. (2008). Design of a device for simultaneous particle size and electrostatic charge measurement of inhalation drugs. *Pharm Res*, 25, 2488-2496.
- [73] Young, P. M., Sung, A., Traini, D., et al. (2007). Influence of humidity on the electrostatic charge and aerosol performance of dry powder inhaler carrier based systems. *Pharm Res*, 24, 963-970.
- [74] Raula, J., Lahde, A., & Kauppinen, E. I. (2009). Aerosolization behavior of carrier-free L-leucine coated salbutamol sulphate powders. *Int J Pharm*, 365, 18-25.
- [75] Saint-Lorant, G., Leterme, P., Gayot, A., et al. (2007). Influence of carrier on the performance of dry powder inhalers. *Int J Pharm*, 334, 85-91.
- [76] Pilcer, G., & Amighi, K. (2010). Formulation strategy and use of excipients in pulmonary drug delivery. *International Journal of Pharmaceutics*, 392, 1-19.
- [77] Smyth, H. D. C., & Hickey, A. J. (2005). Carriers in drug powder delivery: Implications for inhalation system design. *American Journal of Drug Delivery*, 3, 117-132.
- [78] De Boer, A. H., Chan, H. K., & Price, R. (2012). A critical view on lactose-based drug formulation and device studies for dry powder inhalation: Which are relevant and what interactions to expect? *Advanced Drug Delivery Reviews*, 64, 257-274.
- [79] Pilcer, G., Wauthoz, N., & Amighi, K. (2012). Lactose characteristics and the generation of the aerosol. *Advanced Drug Delivery Reviews*, 64, 233-256.
- [80] Newman, S. P., & Busse, W. W. (2002). Evolution of dry powder inhaler design, formulation, and performance. *Respir Med*, 96, 293-304.
- [81] Kou, X., Chan, L. W., Steckel, H., et al. (2012). Physico-chemical aspects of lactose for inhalation. *Adv Drug Deliv Rev*, 64, 220-232.

- [82] Donovan, M. J., & Smyth, H. D. (2010). Influence of size and surface roughness of large lactose carrier particles in dry powder inhaler formulations. *Int J Pharm*, 402, 1-9.
- [83] Flament, M. P., Leterme, P., & Gayot, A. (2004). The influence of carrier roughness on adhesion, content uniformity and the *in vitro* deposition of terbutaline sulphate from dry powder inhalers. *Int J Pharm*, 275, 201-209.
- [84] Guenette, E., Barrett, A., Kraus, D., et al. (2009). Understanding the effect of lactose particle size on the properties of DPI formulations using experimental design. *Int J Pharm*, 380, 80-88.
- [85] Steckel, H., & Bolzen, N. (2004). Alternative sugars as potential carriers for dry powder inhalations. *Int J Pharm*, 270, 297-306.
- [86] Kaialy, W., Larhrib, H., Martin, G. P., et al. (2012). The effect of engineered mannitol-lactose mixture on dry powder inhaler performance. *Pharm Res*, 29, 2139-2156.
- [87] Ikegami, K., Kawashima, Y., Takeuchi, H., et al. (2003). A new spherically agglomerated drug composite system with lactose for dry powder inhalation. *Advanced Powder Technology*, 14, 215-229.
- [88] Karpel, J. P. (2000). An easy-to-use dry-powder inhaler. *Adv Ther*, 17, 282-286.
- [89] Trofast. (1993). Process for conditioning substances In. CN1133004.
- [90] Yang. (1997). Preparation of powder agglomerates In. CN1552310.
- [91] Yang, T. T., Kenyon, D. (2000). Use of an agglomerate formulation in a new multidose dry powder inhaler. *Respiratory Drug Delivery VII, Vol 2, pp 503-506*.
- [92] Adi, S., Adi, H. (2010). Agglomerate Strength and Aerosol Performance of API-Only Powders. *Respiratory Drug Delivery 2010 (2010), Vol 3, pp 865-870*.
- [93] Staniforth, J. N. (1996). Pre-Formulation Aspects of Dry Powder Aerosols. *Respiratory Drug Delivery V, Vol 1, pp 65-74*.

- [94] Young, P. M., Chan, H., Chiou, H., et al. (2007). The influence of mechanical processing of dry powder inhaler carriers on drug aerosolization performance. *Journal of Pharmaceutical Sciences*, *96*, 1331-1341.
- [95] Jones, M. D., & Price, R. (2006). The influence of fine excipient particles on the performance of carrier-based dry powder inhalation formulations. *Pharm Res*, *23*, 1665-1674.
- [96] Iida, K., Leuenberger, H., Fueg, L. M., et al. (2000). Effect of mixing of fine carrier particles on dry powder inhalation property of salbutamol sulfate (SS). *Yakugaku Zasshi*, *120*, 113-119.
- [97] Young, P. M., Edge, S., Traini, D., et al. (2005). The influence of dose on the performance of dry powder inhalation systems. *International Journal of Pharmaceutics*, *296*, 26-33.
- [98] Zhou, Q. T., Armstrong, B., Larson, I., et al. (2010). Understanding the influence of powder flowability, fluidization and de-agglomeration characteristics on the aerosolization of pharmaceutical model powders. *Eur J Pharm Sci*, *40*, 412-421.
- [99] Guchardi, R., Frei, M., John, E., et al. (2008). Influence of fine lactose and magnesium stearate on low dose dry powder inhaler formulations. *Int J Pharm*, *348*, 10-17.
- [100] Kumon, M., Machida, S., Suzuki, M., et al. (2008). Application and mechanism of inhalation profile improvement of DPI formulations by mechanofusion with magnesium stearate. *Chem Pharm Bull (Tokyo)*, *56*, 617-625.
- [101] Lucas, P., Anderson, K., Potter, U. J., et al. (1999). Enhancement of small particle size dry powder aerosol formulations using an ultra low density additive. *Pharm Res*, *16*, 1643-1647.
- [102] Chow, A. H. L., Tong, H. H. Y., Chattopadhyay, P., et al. (2007). Particle engineering for pulmonary drug delivery. *Pharmaceutical Research*, *24*, 411-437.

- [103] Shoyele, S. A., & Cawthorne, S. (2006). Particle engineering techniques for inhaled biopharmaceuticals. *Advanced Drug Delivery Reviews*, 58, 1009-1029.
- [104] Dellamary, L. A., Tarara, T. E., Smith, D. J., et al. (2000). Hollow porous particles in metered dose inhalers. *Pharm Res*, 17, 168-174.
- [105] Hirst, P. H., Pitcairn, G. R., Weers, J. G., et al. (2002). In vivo lung deposition of hollow porous particles from a pressurized metered dose inhaler. *Pharm Res*, 19, 258-264.
- [106] Bosquillon, C., Lombry, C., Preat, V., et al. (2001). Influence of formulation excipients and physical characteristics of inhalation dry powders on their aerosolization performance. *J Control Release*, 70, 329-339.
- [107] White, S., Bennett, D. B., Cheu, S., et al. (2005). EXUBERA: pharmaceutical development of a novel product for pulmonary delivery of insulin. *Diabetes Technol Ther*, 7, 896-906.
- [108] Sadrzadeh, N., Miller, D. P., Lechuga-Ballesteros, D., et al. (2010). Solid-state stability of spray-dried insulin powder for inhalation: chemical kinetics and structural relaxation modeling of Exubera above and below the glass transition temperature. *J Pharm Sci*, 99, 3698-3710.
- [109] Duddu, S. P., Sisk, S. A., Walter, Y. H., et al. (2002). Improved lung delivery from a passive dry powder inhaler using an Engineered PulmoSphere powder. *Pharm Res*, 19, 689-695.
- [110] Zhang, X., Ma, Y., Zhang, L., et al. (2012). The development of a novel dry powder inhaler. *Int J Pharm*, 431, 45-52.
- [111] Geller, D. E., Weers, J., & Heuerding, S. (2011). Development of an inhaled dry-powder formulation of tobramycin using PulmoSphere technology. *Journal of aerosol medicine and pulmonary drug delivery*, 24, 175-182.

- [112] Byron, P. R., Hindle, M., Lange, C. F., et al. (2010). In vivo-*in vitro* correlations: predicting pulmonary drug deposition from pharmaceutical aerosols. *J Aerosol Med Pulm Drug Deliv*, 23 Suppl 2, S59-69.
- [113] Fuglsang, A. (2012). The US and EU regulatory landscapes for locally acting generic/hybrid inhalation products intended for treatment of asthma and COPD. *J Aerosol Med Pulm Drug Deliv*, 25, 243-247.
- [114] Mitchell, J. P., & Nagel, M. W. (2004). Particle size analysis of aerosols from medicinal inhalers. *Kona*, 22, 32-65.
- [115] de Boer, A. H., Gjaltema, D., Hagedoorn, P., et al. (2002). Characterization of inhalation aerosols: a critical evaluation of cascade impactor analysis and laser diffraction technique. *Int J Pharm*, 249, 219-231.
- [116] Mitchell, J. P., & Nagel, M. W. (2003). Cascade impactors for the size characterization of aerosols from medical inhalers: their uses and limitations. *Journal of aerosol medicine*, 16, 341-377.
- [117] Agu, R. U., & Ugwoke, M. I. (2011). *In vitro* and in vivo testing methods for respiratory drug delivery. *Expert Opin Drug Deliv*, 8, 57-69.
- [118] Chambers, F., Ali, A., Mitchell, J., et al. (2010). Cascade impactor (CI) mensuration--an assessment of the accuracy and precision of commercially available optical measurement systems. *AAPS PharmSciTech*, 11, 472-484.
- [119] Nichols, S. C., Mitchell, J. P., Shelton, C. M., et al. (2013). Good Cascade Impactor Practice (GCIP) and considerations for "in-use" specifications. *AAPS PharmSciTech*, 14, 375-390.
- [120] Marple, V. A., Olson, B. A., Santhanakrishnan, K., et al. (2003). Next generation pharmaceutical impactor (a new impactor for pharmaceutical inhaler testing). Part II: Archival calibration. *J Aerosol Med*, 16, 301-324.

- [121] Vecellio None, L., Grimbert, D., Becquemin, M. H., et al. (2001). Validation of laser diffraction method as a substitute for cascade impaction in the European Project for a Nebulizer Standard. *Journal of aerosol medicine*, 14, 107-114.
- [122] Stein, S. W., Myrdal, P. B., Gabrio, B. J., et al. (2003). Evaluation of a new Aerodynamic Particle Sizer spectrometer for size distribution measurements of solution metered dose inhalers. *Journal of aerosol medicine*, 16, 107-119.
- [123] Nagel, M. W., Wiersema, K. J., Bates, S. L., et al. (2002). Size analysis of a pressurized metered dose inhaler-delivered solution formulation by an Aerosizer-LD time-of-flight aerosol particle size spectrometer. *J Aerosol Med*, 15, 75-85.
- [124] Mitchell, J. P., Nagel, M. W., & Archer, A. D. (1999). Size analysis of a pressurized metered dose inhaler-delivered suspension formulation by the API Aerosizer time-of-flight aerodynamic particle size analyzer. *J Aerosol Med*, 12, 255-264.
- [125] Mitchell, J. P., & Nagel, M. W. (1999). Time-of-flight aerodynamic particle size analyzers: their use and limitations for the evaluation of medical aerosols. *Journal of aerosol medicine*, 12, 217-240.
- [126] Najafabadi, A. R., Gilani, K., Barghi, M., et al. (2004). The effect of vehicle on physical properties and aerosolisation behaviour of disodium cromoglycate microparticles spray dried alone or with L-leucine. *Int J Pharm*, 285, 97-108.
- [127] Giry, K., Pean, J. M., Giraud, L., et al. (2006). Drug/lactose co-micronization by jet milling to improve aerosolization properties of a powder for inhalation. *Int J Pharm*, 321, 162-166.
- [128] Larhrib, H., Martin, G. P., Prime, D., et al. (2003). Characterisation and deposition studies of engineered lactose crystals with potential for use as a carrier for aerosolised salbutamol sulfate from dry powder inhalers. *European Journal of Pharmaceutical Sciences*, 19, 211-221.



[129] Naini, V., Byron, P. R., & Phillips, E. M. (1998). Physicochemical stability of crystalline sugars and their spray-dried forms: dependence upon relative humidity and suitability for use in powder inhalers. *Drug Dev Ind Pharm*, 24, 895-909.

[130] Buckton, G. (1997). Characterisation of small changes in the physical properties of powders of significance for dry powder inhaler formulations. *Advanced Drug Delivery Reviews*, 26, 17-27.

[131] Marple, V. A., Roberts, D. L., Romay, F. J., et al. (2003). Next generation pharmaceutical impactor (a new impactor for pharmaceutical inhaler testing). Part I: Design. *J Aerosol Med*, 16, 283-299.

[132] Mitchell, J. P. (2003). PRACTICES OF COATING COLLECTION SURFACES OF CASCADE IMPACTORS:

A SURVEY OF MEMBERS OF THE EUROPEAN PHARMACEUTICAL AEROSOL GROUP (EPAG) *Drug Delivery to the Lungs-14*, 75-78.

[133] Rissler, J., Asking, L., & Dreyer, J. K. (2009). A methodology to study impactor particle reentrainment and a proposed stage coating for the NGI. *J Aerosol Med Pulm Drug Deliv*, 22, 309-316.

[134] Grasmeijer, F., Hagedoorn, P., Frijlink, H. W., et al. (2012). Characterisation of high dose aerosols from dry powder inhalers. *Int J Pharm*, 437, 242-249.

[135] Berg, E., Lamb, P., Ali, A., et al. (2008). Assessment of the need to coat particle collection cups of the NGI to mitigate droplet bounce when evaluating nebuliser-produced droplets. *Pharmeur Sci Notes*, 2008, 21-25.

[136] Marple, V. A., Olson, B. A., Santhanakrishnan, K., et al. (2004). Next generation pharmaceutical impactor: a new impactor for pharmaceutical inhaler testing. Part III. extension of archival calibration to 15 L/min. *J Aerosol Med*, 17, 335-343.

- [137] Adi, H., Kwok, P. C. L., Crapper, J., et al. (2010). Does electrostatic charge affect powder aerosolisation? *Journal of Pharmaceutical Sciences*, 99, 2455-2461.
- [138] Carter, P. A., Rowley, G., Fletcher, E. J., et al. (1998). Measurement of electrostatic charge decay in pharmaceutical powders and polymer materials used in dry powder inhaler devices. *Drug Development and Industrial Pharmacy*, 24, 1083-1088.
- [139] Brian Ament, K. U., Nagaraja Rao. (2012). Mitigation of Particle Tribo-Charging Effect on Dry Powder Inhaler Performance. *Respiratory Drug Delivery 2012, Vol 2, pp 623-626*.
- [140] Frijlink, H. W., & De Boer, A. H. (2004). Dry powder inhalers for pulmonary drug delivery. *Expert Opin Drug Deliv*, 1, 67-86.
- [141] De Boer, A. H., Winter, H. M. I., & Lerk, C. F. (1996). Inhalation characteristics and their effects on *in vitro* drug delivery from dry powder inhalers Part 1. Inhalation characteristics, work of breathing and volunteers' preference in dependence of the inhaler resistance. *International Journal of Pharmaceutics*, 130, 231-244.
- [142] Tiddens, H. A., Geller, D. E., Challoner, P., et al. (2006). Effect of dry powder inhaler resistance on the inspiratory flow rates and volumes of cystic fibrosis patients of six years and older. *Journal of aerosol medicine*, 19, 456-465.
- [143] Clark, A. R., & Hollingworth, A. M. (1993). The relationship between powder inhaler resistance and peak inspiratory conditions in healthy volunteers implications for *in vitro* testing. *Journal of aerosol medicine*, 6, 99-110.
- [144] Cegla, U. H. (2004). Pressure and inspiratory flow characteristics of dry powder inhalers. *Respir Med*, 98 Suppl A, S22-28.
- [145] Gac, J., Sosnowski, T. R., & Grado, L. (2008). Turbulent flow energy for aerosolization of powder particles. *Journal of Aerosol Science*, 39, 113-126.

- [146] Chew, N. Y., & Chan, H. K. (2001). *In vitro* aerosol performance and dose uniformity between the Foradile Aerolizer and the Oxis Turbuhaler. *J Aerosol Med*, *14*, 495-501.
- [147] Coates, M. S., Chan, H. K., Fletcher, D. F., et al. (2007). Influence of mouthpiece geometry on the aerosol delivery performance of a dry powder inhaler. *Pharm Res*, *24*, 1450-1456.
- [148] Coates, M. S., Fletcher, D. F., Chan, H. K., et al. (2004). Effect of design on the performance of a dry powder inhaler using computational fluid dynamics. Part 1: Grid structure and mouthpiece length. *J Pharm Sci*, *93*, 2863-2876.
- [149] Ward, G. H., & Schultz, R. K. (1995). Process-induced crystallinity changes in albuterol sulfate and its effect on powder physical stability. *Pharm Res*, *12*, 773-779.
- [150] Shur, J., Harris, H., Jones, M. D., et al. (2008). The role of fines in the modification of the fluidization and dispersion mechanism within dry powder inhaler formulations. *Pharm Res*, *25*, 1631-1640.
- [151] Murakoshi, H., Saotome, T., Fujii, Y., et al. (2005). Effect of physical properties of carrier particles on drug emission from a dry powder inhaler device. *Journal of drug delivery science and technology*, *15*, 223-226.
- [152] Podczeck, F. (1999). The influence of particle size distribution and surface roughness of carrier particles on the *in vitro* properties of dry powder inhalations. *Aerosol Science & Technology*, *31*, 301-321.
- [153] Steckel, H., Markefka, P., teWierik, H., et al. (2006). Effect of milling and sieving on functionality of dry powder inhalation products. *Int J Pharm*, *309*, 51-59.
- [154] Larhrib, H., Zeng, X. M., Martin, G. P., et al. (1999). The use of different grades of lactose as a carrier for aerosolised salbutamol sulphate. *International Journal of Pharmaceutics*, *191*, 1-14.

- [155] Chew, N. Y., Bagster, D. F., & Chan, H. K. (2000). Effect of particle size, air flow and inhaler device on the aerosolisation of disodium cromoglycate powders. *Int J Pharm*, 206, 75-83.
- [156] Berry, J., Kline, L. C., Sherwood, J. K., et al. (2004). Influence of the size of micronized active pharmaceutical ingredient on the aerodynamic particle size and stability of a metered dose inhaler. *Drug Dev Ind Pharm*, 30, 705-714.
- [157] Edwards, D. A., Hanes, J., Caponetti, G., et al. (1997). Large porous particles for pulmonary drug delivery. *Science*, 276, 1868-1871.
- [158] Edwards, D. A., Ben-Jebria, A., & Langer, R. (1998). Recent advances in pulmonary drug delivery using large, porous inhaled particles. *Journal of Applied Physiology*, 85, 379-385.
- [159] Lahde, A., Raula, J., Kauppinen, E. I., et al. (2006). Aerosol synthesis of inhalation particles via a droplet-to-particle method. *Particulate science and technology*, 24, 71-84.
- [160] Zeleznak, K. J., & Hosenev, R. (1987). The Glass Transition in Starch1. *Cereal Chem*, 64, 121-124.
- [161] Weers, J. G., Tarara, T. E., & Clark, A. R. (2007). Design of fine particles for pulmonary drug delivery. *Expert Opin Drug Deliv*, 4, 297-313.
- [162] Vehring, R. (2008). Pharmaceutical particle engineering via spray drying. *Pharm Res*, 25, 999-1022.
- [163] Zhou, D., Zhang, G. G., Law, D., et al. (2002). Physical stability of amorphous pharmaceuticals: Importance of configurational thermodynamic quantities and molecular mobility. *J Pharm Sci*, 91, 1863-1872.
- [164] Ticehurst, M. D., Basford, P. A., Dallman, C. I., et al. (2000). Characterisation of the influence of micronisation on the crystallinity and physical stability of revatropate hydrobromide. *Int J Pharm*, 193, 247-259.

- [165] Zeng, X. M., Martin, G. P., Tee, S. K., et al. (1999). Effects of particle size and adding sequence of fine lactose on the deposition of salbutamol sulphate from a dry powder formulation. *Int J Pharm*, 182, 133-144.
- [166] Zeng, X. M., Pandhal, K. H., & Martin, G. P. (2000). The influence of lactose carrier on the content homogeneity and dispersibility of beclomethasone dipropionate from dry powder aerosols. *Int J Pharm*, 197, 41-52.
- [167] Lucas, P., Anderson, K., & Staniforth, J. N. (1998). Protein deposition from dry powder inhalers: fine particle multiplets as performance modifiers. *Pharmaceutical Research*, 15, 562-569.
- [168] Louey, M. D., & Stewart, P. J. (2002). Particle interactions involved in aerosol dispersion of ternary interactive mixtures. *Pharm Res*, 19, 1524-1531.
- [169] Adi, H., Larson, I., Chiou, H., et al. (2006). Agglomerate strength and dispersion of salmeterol xinafoate from powder mixtures for inhalation. *Pharm Res*, 23, 2556-2565.
- [170] Adi, H., Larson, I., Chiou, H., et al. (2008). Role of agglomeration in the dispersion of salmeterol xinafoate from mixtures for inhalation with differing drug to fine lactose ratios. *J Pharm Sci*, 97, 3140-3152.
- [171] Finlay, W. H. (2001). *The mechanics of inhaled pharmaceutical aerosols: an introduction*: Access Online via Elsevier.
- [172] Zeng, X. M. (2001). *Particulate interactions in dry powder formulations for inhalation*: CRC Press LLC.

## Curriculum Vitae

**Name:** Xi Zhang

**Place of Birth** Hunan, China

**Post-secondary Education:** Department of Chemical and Biochemical Engineering,  
University of Western Ontario, London, Ontario, Canada  
2011-2013 Ph.D Candidate

Shanghai Institute of Pharmaceutical Industry, Shanghai, China  
2007-2012 Ph.D

Huazhong University of science and technology, Wuhan, Hubei,  
China  
2003-2007 B Sc.

**Work Experience:** Research Assistant and Teaching Assistant  
University of Western Ontario, London, Ontario, Canada  
2011-2013

**Honors and Awards:** Graduate Student Scholarship, University of Western Ontario,  
Canada  
2011-2013

**Publications:** Zhang X, Ma Y, Zhang L, Zhu J, Jin F. The development of a  
novel dry powder inhaler, International Journal of Pharmaceutics.  
Volume 431, Issues 1–2, 15 July 2012, Pages 45–52.

Zhang X, Jin F. Progress of the powder filling and metering device  
of dry powder inhaler. WORLD CLINICAL DRUGS 2012, Vol.33  
NO.11

Zhang X, Ma Y, Zhu J. The Development and evaluation of a  
rotating fluidized bed fine powder dispenser for dry powder  
inhaler, ready to be submitted

Ma Yingliang, Zhu Jingxu, Zhang Xi, A new drug powder inhaler  
device, ready to apply for a Chinese patent.

